Universidade de Lisboa
Faculdade de Medicina de Lisboa

Deciphering the molecular role of DJ-1 in the etiology of Parkinson's and Huntington's disease

Maria Leonor Lemos Pereira Miller Fleming

Tese orientada por:
Prof. Doutor Tiago Outeiro
Prof. Doutor Flaviano Giorgini

Ramo das Ciências Biomédicas
Especialidade – Neurociências

A impressão desta dissertação foi aprovada pelo Conselho Cientifico da Faculdade de Medicina de Lisboa em reunião de (*15 de Outubro de 2013*)

Table of contents

Acknowledgements iii
Abstract v
Resumo vii
Abbreviations xi
Chapter 1. Introduction 1
Protein misfolding diseases 1
Huntington's disease 4
Parkinson's disease 9
Baker's yeast: a versatile "toolbox" for molecular biology studies 18
Modeling neurodegenerative diseases in yeast 19
Yeast models of HD 20
Yeast models of PD 21
References 23
Aims of the thesis 31
Chapter 2. Functional gene expression profiling in yeast implicates translational dysfunction in mutant huntingtin toxicity 35
Abstract 35
Introduction 35
Results 39
Yeast expressing a mutant Htt fragment differentially express genes involved in ribosome biogenesis and rRNA processing 39
Common mechanisms underlie mutant Htt toxicity suppression in gene deletion suppressor strains 40
Cis-regulatory domain analysis of DEGs identifies enriched elements 44
A unique subset of differential expressed, highly interconnected genes modulate mutant Htt toxicity 45
Discussion 49
Materials and Methods 52
Acknowledgments 56
References 56
Chapter 3. Yeast DJ-1 family members are required for diauxic-shift reprogramming and cell survival in stationary phase 61

Abstract 61
Introduction 61
Results 66
The *HSP31* mini-family is required for normal diauxic-shift and stationary phase. 66
Typical stationary phase characteristics are altered in *HSP31* mini-family knockout strains 73
Autophagic response is impaired during carbon starvation in *hsp31*Δ cells 74
TORC1 signaling is perturbed in *hsp31*Δ cells 77
Discussion 80
Materials and Methods 83
Acknowledgements 89
References 89
Chapter 4. DJ-1 modulates huntingtin aggregation and toxicity in models of Huntington's disease 97
Abstract 97
Introduction 97
Results 99
DJ-1 overexpression ameliorates mutant Htt toxicity in yeast and fruit flies 99
DJ-1 expression and its oxidation is increased in the HD brain and in cell and animal models of HD 100
DJ-1 directly modulates aggregation and toxicity of mutant Htt in an oxidation-sensitive manner 102
Discussion 108
Materials and Methods 109
Acknowledgements 114
References 114
Chapter 5. General discussion, future perspectives and conclusion 119
CONCLUSION 126
References 127
Chapter 6. Appendix 133

Acknowledgements

Esta tese é dedicada à minha querida avó Fátima.

(This PhD thesis is dedicated to my sweet grandmother Fátima.)

"To be is to do – Socrates
To do is to be – Sartre
Do Be Do Be Do – Sinatra"

Kurt Vonnegut

A PhD is a long and extremely challenging journey, during which I had the pleasure to meet many people who I am thankful for, in one way or another, contributing to the knowledge and scientific skills I have acquired.

I thank my supervisor Tiago Outeiro for his guidance and support throughout my PhD and for teaching me how to think as a scientist, work hard and stay focused. He introduced me to the world of yeast and opened for me the doors to one of my biggest scientific passions: neuroscience research. He gave me the opportunity to grow as a researcher in his lab, where I spent most of my PhD time.

I started my PhD in the lab of Flaviano Giorgini (Flav) – my co-supervisor – and had the privilege to be one of his first PhD students. Besides being a very intelligent scientist, Flav is a fantastic person, with a big heart and great sense of humor. His mentorship was a permanent source of inspiration. I thank Flav for always being very supportive and for giving me motivation and positive thinking. I will never forget once that I realized I had cloned a gene upside down. I was afraid of his reaction, but instead of being angry at me, he showed me the positive side: "Most people don't even realize they have made a mistake". I also thank him for the scientific discussions and for his scientific guidance.

I owe my sincere gratitude to Teresa Pais, my friend and wise colleague, the person with whom I had the longest and funniest scientific discussions. Teresa was the person who was always by my side; listening, teaching, criticizing, bearing my frustrations and sharing the joys of success, helping me to think and create hypotheses. Her smile, good mood and enthusiasm were always an inspiration. I also thank her for allowing me to expose my ideas and contribute to her work, which was a great experience.

Pedro Antas, a very special person who unfortunately only entered my life at the end of my PhD. He helped me to finish some experiments. I believe the last months of the PhD may be a stressful moment, but for me these were the best. I had lots of fun

with Pedro's jokes "night and day". Thanks Pedro for the help and hard work, for the nice suggestions and for making our work so much fun.

I am thankful to Federico Herrera (Fede), for proofreading my work many times and having taught me several rules of scientific writing. I also thank him for all the support and constructive - and sometimes hard – criticism throughout my PhD, which I really appreciated. I also thank Fede for giving me the opportunity to work with him.

It was great to share ideas and long hours in the lab with Sandra Jacinto, Oldriska Marques (Oli), Elisa Basso (Elisinha) and Patricia Guerreiro (Patricinha). I will miss those times.

I would like to thank all of my colleagues from Tiago's lab (UNCM) who in one way or another contributed to my work; especially Rita Oliveira and Hugo Miranda who were always very supportive and enriched my research with their questions and suggestions, to the present and former technicians of my lab, Tiago Mendes, Andreia Peixoto and Sónia Oliveira that always gave me help when they had time and to Sandra Tenreiro for always being helpful.

From Leicester, I am thankful to Rob Mason for teaching me the majority of the basic yeast molecular techniques I know, to Mahmut Ergoren, Rob Hardwick, Angelica Vittori, Raheleh Rahbari and Paul Ainsworth for receiving me in their homes during my short visits to Leicester and to all my friends in Leicester for always making me feel at home.

I would also like to thank Paula Ludovico for the fruitful discussions and constructive feedback, and Daniel Klionsky for spending some of his valuable time discussing some of my results and for kindly sharing material and protocols that were essential at a certain point of my PhD to move my work forward, and Marek Skoneczny for kindly providing several plasmids and strains - even more than I asked for.

I am grateful to all the collaborators, whose names are mentioned in the beginning of each chapter, for contributing to some of the experiments presented in this thesis.

Last but not least I want to thank my "Lisbon family", in particular Carolina and Francisco for making my life outside the lab really great, and all my friends in Porto, especially Joaninha, Joana Maranhas, Ana Inês and my cousin Sofia who, although far away, were closer than ever, and to my parents for always believing in me and encourageing me to pursue my goals.

Abstract

Neurodegenerative diseases are among the most complex and puzzling human disorders. These devastating disorders currently do not have any effective therapies or treatments, and thus are a social and economic burden for modern society. Intense efforts are being made to unravel the mechanisms underlying this group of diseases, however there is still much to be learnt and discovered. Therefore, it is of utmost importance to better understand the biological mechanisms involved in disease pathogenesis, and more importantly, to discover novel avenues for therapeutic intervention. Budding yeast have been successfully used to perform studies on these diseases that have resulted in the identification of several promising therapeutic drugs and targets. The ease of experimental manipulation, the high conservation in basic cellular mechanisms between yeast and humans, and the well defined genome are three of the numerous characteristics that make yeast so attractive to researchers studying neurodegenerative disorders. Here, we used the budding yeast to study the molecular basis of two neurodegenerative diseases: Huntington's (HD) and Parkinson's disease (PD).

HD is a fatal neurodegenerative disorder caused by a well defined genetic cause, which is an expansion of a polyglutamine tract in the huntingtin (Htt) protein. We have used a yeast HD model to find differentially expressed genes (DEGs) in wild-type yeast in response to mutant Htt toxicity, as well as in three Htt toxicity suppressor strains: *bna4*Δ, *mbf1*Δ, and *ume1*Δ. We found common DEGs in the suppressor strains involved in stress response, translation elongation, and mitochondrial transport. We then tested whether overexpression of the DEGs suppress mutant Htt toxicity. We identified 12 novel suppressors, including genes that play a role in stress response and rRNA processing. We have integrated the microarray and the genetic screening data that allowed us to generate a robust network that showed enrichment in genes involved in rRNA processing and ribosome biogenesis. Altogether, our results suggest that dysfunctional translation is implicated in HD. Ultimately pharmacological manipulation of translation may have therapeutic value in HD.

PD is the most common progressive neurodegenerative movement disorder. One of the proteins that when mutated leads to autosomal recessive forms of PD is DJ-1. The precise function of this protein and how this protein leads to PD is unclear. Yeast has four proteins that belong to the conserved DJ-1 superfamily: Hsp31, Hsp32, Hsp33 and Hsp34. Very little is known about their function. Here, we show that the yeast DJ-1

homologs are required for diauxic-shift, an important metabolic reprogramming stage in yeast that is triggered by glucose limitation. We found that the Hsp31 genes are strongly induced in diauxic-shift and in stationary phase, and that deletion of these genes leads to reduced chronological lifespan, an inability to reprogram gene transcription at diauxic-shift, and failure to acquire several typical characteristics of stationary phase, including defective autophagy induction. Furthermore, we showed that these proteins contribute to TORC1 regulation, a central signaling pathway involved in diauxic-shift reprogramming and, importantly, in autophagy. As dysregulation of both autophagy and TORC1 are associated with several disorders – including PD – our work may have broad relevance to understanding these processes in health and disease. These novel insights into the function of the yeast DJ-1 homologs contribute to the understanding of the normal function of both human DJ-1 and the remaining DJ-1 superfamily members, and may therefore bear therapeutic implications in various human diseases.

The human DJ-1 is thought to act as a redox-dependent chaperone by preventing the aggregation of misfolded proteins in oxidative stress conditions. One of the potential targets of DJ-1 is α-synuclein, which is the major component of Lewy bodies in PD. Oxidative stress is linked to several neurodegenerative diseases including HD. Here, we show that DJ-1 plays a potential role in the pathogenesis of HD, by modulating Htt aggregation and toxicity likely, by acting as a redox-dependent chaperone. We found that DJ-1 is upregulated and abnormally oxidized in the brains of HD patients, which is how DJ-1 is found in brains of patients with PD and Alzheimer's disease. Our results suggest a general role for DJ-1 as a redox-dependent chaperone that may have an impact in the pathogenesis of several protein misfolding diseases. Furthermore, it establishes DJ-1 as a potential therapeutic target for HD.

Overall, the work presented in this thesis opens novel avenues of research and therapeutics for HD and PD and proposes that DJ-1 has broad relevance in the pathogenesis of neurodegenerative diseases.

Keywords: Parkinson's disease, Huntington's disease, yeast, diauxic-shift, autophagy, translation, TORC1, protein misfolding

Resumo

As doenças neurodegenerativas estão entre as doenças humanas mais complexas e enigmáticas. As terapias e tratamentos actualmente existentes não são eficazes, causando um impacto negativo na sociedade moderna, tanto a nível social como económico. Apesar do esforço empregue na compreensão dos mecanismos patogénicos associados a este grupo de doenças, ainda há muito por explorar e aprender. É urgente investigar os mecanismos moleculares que levam a essas patologias e descobrir novos alvos terapêuticos. A levedura *Saccharomyces cerevisiae* tem sido usada com sucesso no estudo de doenças neurodegenerativas e já resultou na identificação de vários alvos terapêuticos bem como de compostos com potencial terapêutico bastante promissor. As leveduras, como modelo biológico, apresentam várias vantagens que as tornam atractivas para estudar estas doenças, incluindo a sua fácil manipulação laboratorial, a conservação dos mecanismos celulares básicos até aos humanos, e extensa caracterização do seu genoma. Nesta tese, as leveduras foram o modelo escolhido para estudar os mecanismos moleculares associados a duas doenças neurodegenerativas: a doença de Huntington (DH) e a doença de Parkinson (DP).

A DH é uma doença neurodegenerativa fatal, geneticamente bem caracterizada, causada por uma mutação genética no gene *IT15*, que consiste na repetição anormal da sequência de nucleotídeos CAG, originando a expansão de uma região rica em glutaminas na proteína huntingtina (Htt). O modelo de levedura para a DH foi usado para detectar genes diferencialmente expressos (GDE) em células a expressar a proteína Htt mutada, assim como em três estirpes supressoras de toxicidade de Htt: *bna4*Δ, *mbf1*Δ, e *ume1*Δ. Nestas estirpes supressoras da toxicidade foram encontrados GDE envolvidos na resposta ao stress, no alongamento durante a tradução do mRNA e no transporte mitocondrial. A sobre-expressão dos GDEs levou à identificação de 12 novos genes supressores da toxicidade provocada pela Htt, incluindo genes envolvidos na resposta ao stress e no processamento do rRNA. Pela integração dos resultados provenientes de microarrays e do screening genético, através de ferramentas informáticas, construiu-se uma rede de interacções que mostra um enriquecimento de genes envolvidos no processamento do rRNA e na biogénese de ribossomas associado à toxicidade da Htt. Estes resultados sugerem que a desregulação do processo de tradução está associado à DH e que novas terapias podem surgir pela modulação farmacológica deste processo.

A DP é a doença neurodenegerativa motora progressiva mais comum. Um dos genes geneticamente associados à DP, transmitida de uma forma autossómica recessiva, codifica a proteína DJ-1. A função normal desta proteína é ainda pouco clara e não se conhece ainda o papel da mutação desta proteína no desenvolvimento da DP. As leveduras têm quatro proteínas que pertencem à conservada superfamília da DJ-1: Hsp31, Hsp32, Hsp33 e a Hsp34, no entanto pouco se conhece sobre a sua função. Nesta tese, mostra-se que os homólogos da DJ-1 são necessários para a transição do metabolismo fermentativo para o respiratório, uma importante reprogramação metabólica nas leveduras originada pela falta de glucose. A deleção dos genes *HSP31-34* leva a um envelhecimento mais rápido de leveduras em fase estacionária e à ausência de várias características desta fase, que incluem a ausência de indução do processo autofágico. Em particular, mostramos que estas proteínas contribuem para a regulação da TORC1, uma via de sinalização envolvida nesta reprogramação, e mais importante ainda, na autofagia. Tendo em conta, que tanto a desregulação da TORC1 como da autofagia estão associadas a várias doenças, incluindo a DP, este trabalho pode ser relevante para a compreensão destes processos não só em condições normais, como também patológicas. Estas novas descobertas associadas à função dos homólogos em leveduras da DJ-1 contribuem para a compreensão da função da proteína humana e dos outros membros da superfamília DJ-1, podendo trazer implicações terapêuticas em várias doenças humanas.

Uma das funções propostas para a DJ-1 humana é a de actuar como uma *chaperone* dependente do estado redox, que previne a agregação de proteínas sem conformação definida em condições de stress oxidativo. Um dos potenciais alvos da DJ-1 é a α-sinucleína, o componente mais importante dos corpos de Lewy, na DP.

O stress oxidativo é um mecanismo molecular associado a diversas doenças neurodegenerativas, incluindo a DH. Neste estudo, demonstramos que a DJ-1 poderá ter um papel importante na patogénese da DH, pois consegue modular a agregação e toxicidade da Htt, possivelmente através da sua função como *chaperone*. Neste trabalho demonstramos que a DJ-1 está mais expressa e anormalmente oxidada em cérebros de doentes com DH, à semelhança do que acontece nos doentes com DP e doença de Alzheimer. Os nossos resultados sugerem que a DJ-1 apresenta um papel geral como *chaperone*, dependente do estado redox, e cujo impacto na patogénese de diversas doenças relacionadas com a agregação de proteínas não deve ser desvalorizado. Para além disso, determina a DJ-1 como um potencial alvo terapêutico para a DH.

O trabalho apresentado nesta tese abre novos campos de investigação e estratégias terapêuticas, sugerindo que a proteína DJ-1 está associada à patogénese de várias doenças neurodegenerativas como a DP e DH.

Palavras-chave: Doença de Parkinson, Doença de Huntington, leveduras, TORC1, tradução proteica

Abbreviations

α-syn – α-synuclein
3-HK – 3-hydroxykynurenine
AD - Alzheimer's disease
ATG – autophagy-related
ATP – adenosine triphosphate
BiFC - bimolecular fluorescence complementation
CMA – chaperone mediated autophagy
Cys106 – cysteine residue on position 106
DEG – differentially expressed gene
eIF2α – eukaryotic translation initiation factor 2, subunit 1 α
GFP – Green fluorescent protein
GPx – glutathione peroxidase
GO – gene ontology
HD – Huntington's disease
HDAC – histone deacetylase
Hsp – heat shock protein
Htt – huntingtin
IB – inclusion bodies
KMO – kynurenine 3-monooxygenase
KP – Kynurenine pathway
KYNA – kynurenic acid
Log – logarithmic phase
LRRK2 – Leucine-rich repeat kinase 2
MPP+ – 1-methyl-4-phenylpyridinium
MPTP – 1-methyl-4-phenyl-1,2,3,6-tetrahydropyridine
mRNA – messenger RNA
mtDNA – mitochondrial DNA
NMDA – N-methyl-D-aspartate
6-OHDA – 6- hydroxydopamine
ORF – open reading frame
PD – Parkinson's disease
PINK1 – PTEN-induced kinase 1
polyQ – polyglutamine
QC – Quality control
QUIN – quinolinic acid
RNS – reactive nitrogen species
ROS – reactive oxygen species

RPL – ribosomal protein, large subunit
RPS – ribosomal protein, small subunit
rRNA – ribosomal RNA
SEM – standard error of the mean
SNpc – substantia nigra pars compacta
TBP – TATA-binding protein
TORC1 – target of rapamycin complex 1
tRNA – transfer RNA
UCHL1 – ubiquitin C-terminal hydrolases L1
UPS – ubiquitin-proteasome system
WT – wild type
YOK – yeast open reading frame collection
YOC – yeast gene knockout collection

Chapter 1

Introduction

This chapter contains parts of the following publication:

Yeast as a model for studying human neurodegenerative disorders.

Miller-Fleming L, Giorgini F, Outeiro TF.
Biotechnol J. 2008 Mar;3(3):325–38.

Chapter 1. Introduction

Protein misfolding diseases

Protein aggregation disorders are a group of diseases characterized by the misfolding and aggregation of one or more proteins, which includes Alzheimer's disease (AD), Parkinson's disease (PD) and Huntington's disease (HD).

Proteins are constantly in risk of becoming unfolded, especially in stress conditions [1]. Intermediate folding species typically expose hydrophobic residues which have higher tendency to lead to aggregation. Once certain proteins are misfolded they can act as a seed, leading to the misfolding of others and ultimately resulting in the formation of aggregates [2] (Fig. 1.1).

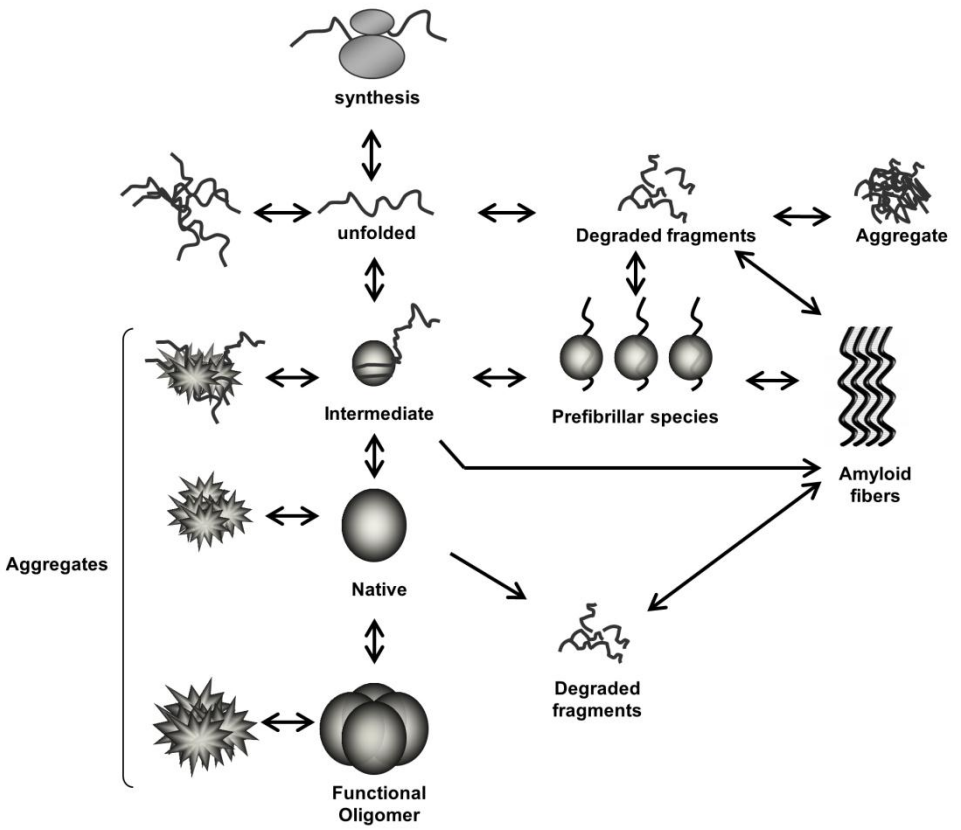

Figure 1.1. Schematic representation of protein folding/misfolding processes.

Following synthesis, each protein needs to adopt a specific three dimensional structure (native conformation) in order to become biologically functional. Proteins often acquire intermediate states before being completely folded. The different species may be prone to misfolding, leading to their accumulation and, in certain cases, to the formation of aggregates, which can be amorphous or amyloid-like. Some of the intermediates and/or aggregates are likely to be cytotoxic, and therapeutic intervention might be possible at different levels along these pathways to prevent their accumulation.

To deal with protein misfolding cells have developed a protein quality control (QC) system, which includes molecular chaperones, the ubiquitin proteasome system (UPS) and autophagy (Fig. 1.2). While chaperones help proteins to fold or refold, the UPS and autophagy are responsible for protein turnover. The degradation of proteins is critical not only to remove the damaged proteins and recycle amino acids but also to clear proteins that play essential roles in cellular processes such as signal transduction and cell division. Protein degradation by the UPS, the key mechanism to degrade short-lived proteins, consists in covalently linking the target proteins to multiple ubiquitin molecules (polyubiquitination) as a signal for degradation, which will subsequently be recognized and degraded by the 26S proteasome (Fig 1.2)[3]. Autophagy is a catabolic process essential to recycle cellular components that allows survival under nutrient-limited conditions. It is also required to eliminate dysfunctional organelles or other materials. Autophagy can be divided in three types: macroautophagy (hereafter autophagy), in which the cargo to be eliminated is engulfed by a double membrane vesicle, the autophagosome, and is transported to the vacuole, where it is degraded (Fig. 1.2); chaperone-mediated autophagy (CMA) which is characterized by selective translocation of the cargo across the lysosome through a specific receptor mediated by a chaperone (Fig. 1.2); and microautophagy, in which the material to be degraded directly enters the lysosome [4].

When the capacity of the protein QC system is exceeded or the system just fails, proteins may become toxic to the cell due to its accumulation and possible aggregation. Protein aggregation may be caused by additional factors, such as: mutations that increase the protein tendency to misfold and aggregate, errors in translation, environmental stresses such as oxidative stress and ageing (which is correlated with an increase in oxidation of proteins) [1]. The accumulation of abnormally folded proteins results, on one hand, in the loss of the normal biological role of the protein and, on the other hand, in a putative gain of cytotoxic function (Fig. 1.1). The ‘amyloid hypothesis’ (developed originally for AD) states that the aggregation of proteins into an ordered fibrillar structure is causally related to aberrant protein interactions that culminate in neuronal dysfunction and ultimately neurodegeneration [5–7]. However, it is still unclear which species correlate with toxicity, whether the aggregates or the intermediate species. It has been observed that cells can direct the aggregated proteins to specific cellular sites, which can be considered as the second line of protection against the potential toxic species upon failure of the QC system [1]. Nevertheless, the presence of large aggregates can still contribute for cellular toxicity.

Since neurons are post-mitotic cells and highly metabolic active they are more sensitive to the accumulation of misfolded proteins and this may explain the high number of brain diseases associated with protein misfolding.

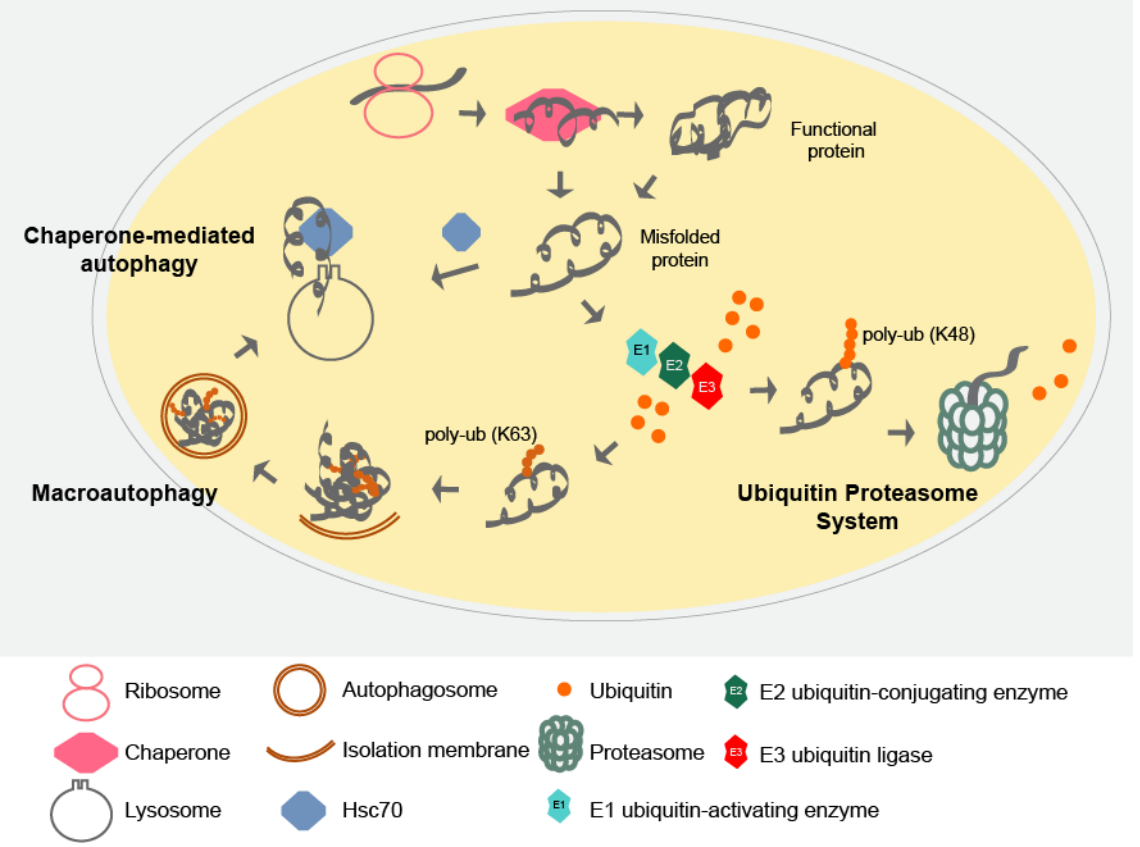

Figure 1.2. Protein quality control systems.

Following protein synthesis, chaperones help proteins to fold. If folding fails or the protein needs to be turned over, a chain of ubiquitin molecules is attached to the target protein by the action of a series of enzymes: ubiquitin activating (E1), conjugating (E2) and ligating (E3) enzymes. The ubiquitin molecules are usually linked between the terminal residue (G76) of one ubiquitin and a lysine of another ubiquitin molecule, usually lysine 48. The polyubiquitinated proteins are then recognized by the 26S proteasome and degraded. Ubiquitin molecules can instead be linked through the lysine 63, which promotes protein aggregation. Aggregates may be, engulfed by a double membrane – autophagosome – which will then fuse with the lysosome. Upon fusion, the cargo is degraded by the acidic lysosomal hydrolases (macroautophagy). Proteins can also be degraded by entering into the lysosome with the help of the chaperone Hsc70 through the receptor LAMP 2A (chaperone-mediated autophagy). poly-Ub – polyubiquitin chain.

Huntington's disease

HD is a fatal adult onset neurodegenerative disorder that has a worldwide prevalence of ~1 in 10,000 people. The onset of the symptoms is typically around 45-50 years old but there are also juvenile forms of the disease. Death usually occurs 10-15 years after the onset of the disease. This disorder is inherited in an autosomal dominant manner and is characterized by abnormal motor movements, personality changes and cognitive decline [8]. The neuropathology of HD is characterized by the loss of specific neuronal types in several brain regions, and can be related to specific symptoms and progression of the disease. However, neuronal loss can be detected before the clinical symptoms start to appear [9]. The most striking pathology in HD is the cell loss observed in the striatal region of the basal ganglia, of which medium spiny neurons are the most affected.

HD is caused by a mutation in the *IT15* gene (localized in exon 1) that consists in the expansion of CAG repeats beyond a critical length. This causes an expansion of the polyglutamine (polyQ) tract in the huntingtin (Htt) protein and consequently results in its misfolding. The CAG repeat in the *IT15* is polymorphic in the general population and expanded in individuals affected by HD, which have repeat lengths greater than 35 [10]. HD genes carrying expansions in the range of 36-39 CAG repeats show an increasing risk of developing HD, while expansions of 40 CAG repeats and higher are fully penetrant [11]. The length of the CAG repeat has also been found to be inversely correlated to the age of onset [12], with expansions of 70 CAG repeats or longer inevitably leading to juvenile onset HD [10,13]. Though increased size of the triplet repeat expansion correlates to an earlier age of onset, there is great variability in the age of onset of HD, even when controlling for repeat length. Indeed, work by the U.S.-Venezuela Collaborative Research Project with HD kindreds containing over 18,000 individuals has found that approximately 40% of variation in age of onset in HD patients is due to several genetic modifiers [14]. Although HD has a well-defined genetic cause, the molecular pathways that lead to neurodegeneration remain poorly understood and so far there is no therapy that prevents, delays or reverses this disease. However, the fact that several genetic modifiers can affect the HD age of onset suggest that many therapeutic targets may be available for treating progression of this devastating disorder.

Htt aggregation and inclusion bodies

The discovery of the polyQ expansion allowed the generation of several transgenic mice models expressing the first exon of the human Htt [15]. The most studied HD model is the R6/2 model that exhibits some characteristics of HD, such as progressive neurodegeneration, motor abnormalities and reduced lifespan [15]. The study of mouse models together with the analysis of HD brains led to discover the pathological hallmark of HD which consists in intraneuronal inclusion bodies (IB) containing aggregated Htt. IB are found in the nucleus, cytoplasm and neuronal processes [16–19]. Although these aggregates have been causally related to HD pathology, there is great debate as to their role in this disorder. Mutant Htt could lead to neuronal loss through sequestration of crucial proteins into IB, such as transcription factors, which could explain why transcription is dysregulated in HD [20–23]. On the other hand, sequestration into IB could also be biologically irrelevant [24,25], and soluble oligomeric species could be the actual cause of transcriptional dysregulation and mutant Htt neurotoxicity. Compelling evidence indicates that IB are not correlated with cell death. The cerebral cortex of HD patients has a high number of IB, whereas their striatum, which is where neuronal death is higher, shows only a few [16]. Formation of aggregates could be a protective mechanism to scavenge more neurotoxic Htt oligomeric species [26–28].

The most important intrinsic factor affecting the aggregation of mutant Htt is the length of the polyQ tract, but there are other factors, such as the amino acids flanking the polyQ stretch [29–31]. For instance, deleting the flanking proline rich region changes from non-toxic Htt to toxic one and it leads to changes in the aggregates shape and number [29,30]. The proteolytic cleavage of Htt is also thought to promote aggregation [17,32] and influence the localization of IB to the cytosol or nucleus [33]. Interestingly, transgenic mice expressing a caspase 6-resistant version of mutant Htt do not exhibit striatal degeneration [34], suggesting that proteolysis of Htt at the caspase-6 cleavage site is important for neurodegeneration in HD. Post translational modifications of Htt, such as ubiquitination, phosphorylation and sumoylation can influence Htt degradation and subsequently its aggregation [35].

Pathogenic mechanisms in HD

Since the cloning of the HD gene in 1993 [10], a great deal has been learned about the cellular dysfunction caused by mutant Htt expression, and several mechanisms have been uncovered that likely contribute to the selective

neurodegeneration observed in the disease. The Htt protein is a large cytoplasmic protein that is ubiquitously expressed [36] and is required for embryogenesis and development [37–39]. The precise function of this protein is still not clear, but it has been shown to be involved in several pathways and interact with multiple proteins that are involved in diverse mechanisms including intracellular transport, clathrin-mediated endocytosis, transcriptional regulation, RNA trafficking and cell survival [39–46]. Therefore, the loss of Htt interactions with binding partners or anomalous interactions may contribute to Htt neurotoxicity.

Neurodegeneration in HD occurs not only by dysregulation of intrinsic mechanisms of the vulnerable cells (cell-autonomous) (Fig. 1.3), but also by contribution of other cell types (non-cell-autonomous) (Fig. 1.4). The cell-autonomous mechanisms affected in HD include transcriptional dysregulation, mitochondrial dysfunction, defective vesicle trafficking in axons and impairment of ubiquitination and proteasomal function, whereas the non-cell-autonomous mechanims include excitotoxicity, perturbations in the kynurenine pathway (Chapter 2), and inflammation.

Transcriptional dysregulation has long been implicated in the pathogenesis of HD. Early studies on post mortem HD brains showed that several mRNAs of neurotransmitter receptors and signaling neuropeptides are decreased in striatal neurons [47–49]. The idea that transcription was affected by mutant Htt was further supported by the fact that wild-type Htt was mainly a cytosolic protein, while cleaved mutant Htt was strongly localized to the nucleus causing enhanced toxicity [32,50,51]. Mutant Htt can interact with transcription factors, such as SP1 and members of the core transcription machinery, and by this way affects transcription [52–55]. *BDNF* was one of the transcripts that was found reduced in the brains of HD patients [56]. BDNF (Brain-derived neurotrophic factor) is important for the survival of striatal neurons and was shown to have beneficial effects on mouse models of HD when overexpressed [57,58]. BDNF expression is regulated by the repressor element-1 transcription factor/neuron-restrictive silencer factor (REST/NRSF), which recognizes and binds to the neuron restrictive silencer element (NRSE) present in the BDNF promoter [59,60]. Wild-type Htt regulates BDNF transcription by sequestering REST/NRSF in the cytosol, preventing its translocation into the nucleus and binding to NRSE. In the presence of mutant Htt, the REST/NRSF is not sequestered anymore and enters into the nucleus leading to the repression of NRSE regulated genes, including BDNF [59,60], explaining why this gene is decreased in striatal neurons, and suggesting a mechanism for the unique sensitivity of these neurons in HD.

Compelling evidence from patients and several models of HD suggest that mitochondrial dysfunction contributes to the pathogenesis of HD. The weight loss that patients suffer at early stages of the disease is indicative of mitochondrial impairment [61]. The postmortem HD brain tissues show dysfunctional complex II, III, IV of the electron transport chain, mtDNA mutations [62–65], a reduced number of mitochondria and different morphology from controls [66]. Defects in calcium homeostasis in mitochondria from HD patients and HD transgenic mice has also been observed [67]. One hypothesis that explains how mutant Htt causes mitochondrial dysfunction is through its direct interaction with mitochondria[67–70]. Mutant Htt can also bind to the promoter of the Peroxisome proliferator-activated receptor gamma coactivator 1-alpha (PGC-1α) and repress its expression [71]. PGC-1α is a transcriptional coactivator of mitochondrial genes involved in respiration and mitochondrial biogenesis. The repression of PGC-1α can cause a defect in the energy homeostasis of the cell that may lead to cell death [71]. Interestingly, a correlation between the number of CAG repeats with the production of mitochondrial ATP has also been observed[72].

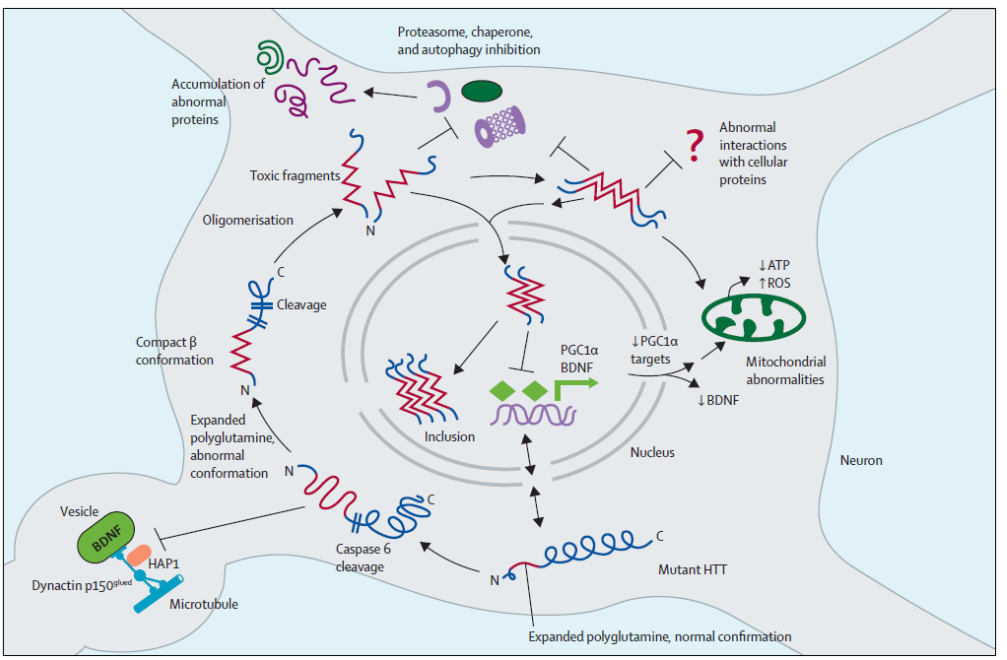

Figure 1.3. Cell autonomous mechanisms underlying HD.

Mutant huntingtin (HTT) can be cleaved by caspase-6 and interfere with essential neuronal processes, such as proteasomal function, autophagy and transcription. Moreover, it can lead to mitochondrial dysfunction and lead to an increase in oxidative stress.
Image from Ross et al., Lancet Neurology, 2011 [73].

Excitotoxicity, one of the non-cell-autonomous mechanisms implicated in HD, is caused by overstimulation of glutamate receptors, especially the ionotropic N-methyl-D-aspartate (NMDA) receptors, which leads to an increase in calcium influx and ultimately neuronal death (Fig. 1.4) [74]. Excitotoxicity is thought to be caused by reduced glutamate uptake by glutamate transporter 1 in astrocytes or increased glutamate release from cortical neurons [75,76]. Overactivation of NMDA receptors may also result from mitochondrial dysfunction and the consequent deficient energy production. The entry of calcium ions by NMDA receptors is blocked by Mg^{2+}, which is released by depolarization of the cell. Mitochondria are required to sustain the membrane potential. Upon its dysfunction, there is less energy to maintain the Na^{+}/K^{+} pump working, leading to cell depolarization, loss of Mg^{2+} and consequently entry of calcium into the cell [77].

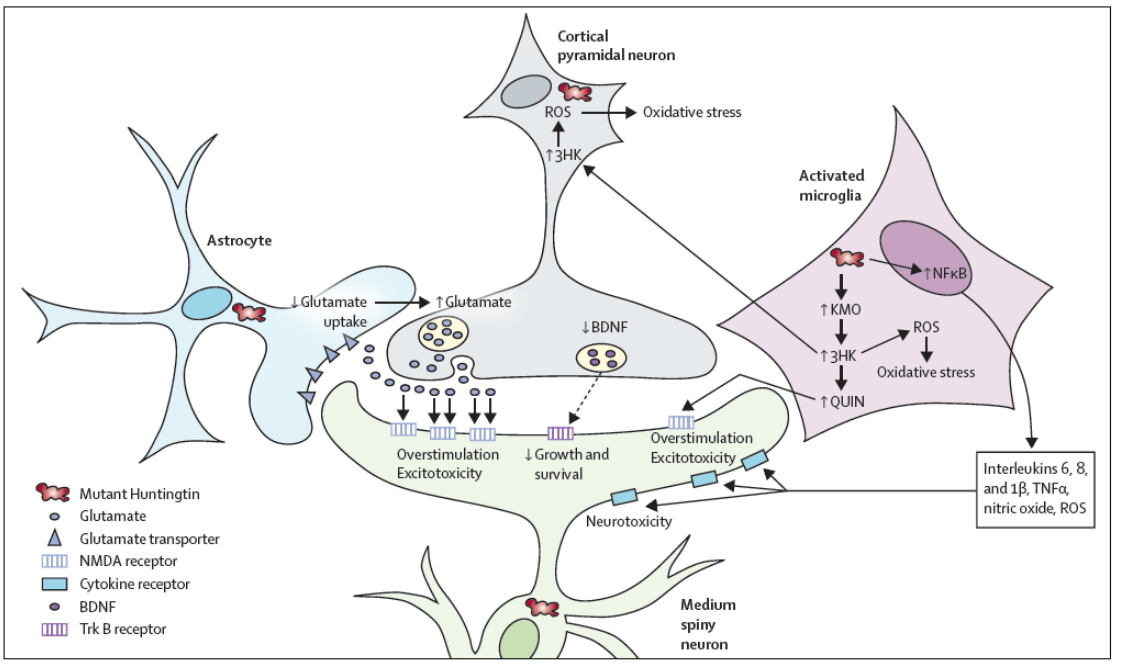

Figure 1.4. Non-cell-autonomous mechanisms underlying HD

Mutant huntingtin can lead to dysregulation of several mechanisms in different cell types, which will contribute for neuronal cell death. These mechanisms include excitotoxicity, perturbations in the kynurenine pathway and increase in neuroinflammation.
Image from Ross et al., Lancet Neurology, 2011 [73]

Parkinson's disease

PD is the second most common progressive neurodegenerative disorder, after AD. It affects about 2% of people over 65 years old and 4–5% of people over 85 [78]. PD was originally characterized in the monograph "An Essay on the Shaking Palsy" by James Parkinson in 1817, in which he described the major symptoms of PD: muscle rigidity, bradykinesia (slowness of voluntary movement), resting tremor and postural instability. Non-motor symptoms are also characteristic of the disease, such as hyposmia (reduced ability to smell), depression and rapid eye movement sleep behavior disorder. At later stages the patients can eventually suffer from dementia [79].

The major pathological hallmarks of PD are the presence of intraneuronal concentric hyaline cytoplasmic inclusions called Lewy bodies (LB) and loss of dopaminergic neurons in the *substantia nigra pars compacta* (SNpc). LBs contain fibrillar forms of α-synuclein (α-syn), as well as proteasomal and lysosomal subunits and molecular chaperones [80,81]. Curiously, LBs can also be found in patients with other neurodegenerative disorders, such as dementia with LBs and AD [82], and even in clinically normal people over 60 years old (10%), although in this case it is thought to be pre-symptomatic [83]. Surprisingly, LBs are not present in the brains of some patients with autosomal recessive PD. There is a great debate regarding whether LBs are cytotoxic or a protective mechanism to preclude the accumulation of the pathogenic intermediates, which have been proposed to be α-syn oligomers [84].

PD was first thought to affect essentially dopaminergic neurons, but nowadays is considered a multisystem disorder that affects several regions of the nervous system [79]. In the majority of idiopathic cases, it is possible to predict the spreading of LBs and thus it has been divided in 6 stages [85]. However, how exactly this pathology is spread is still unclear.

Despite the intense research on PD, there are still no effective therapies, neither a way to slow down the progression of the disease [86]. Dopamine replacement therapy (with the drug levodopa) ameliorates the motor symptoms (especially at the beginning), but generally causes severe secondary effects [87]. When the patients do not respond well to the drug treatment, they are candidates for an alternative procedure, deep brain stimulation, which consists in surgically inserting an electrode in the subthalamic nucleus or the internal global pallidus, both localized in basal ganglia. This electrode, by sending electric stimulus, can block the brain impulses that cause PD symptoms. However, it cannot slow the progression of the disease [87]. It is therefore of extreme

importance to understand the molecular mechanisms that underlie PD so that effective therapies can be discovered in a near future.

ETIOLOGY OF PD

The etiology of PD is complex and unclear and in many cases the cause is completely unknown (idiopathic). The majority of PD cases arise sporadically [88]. The major risk factor to develop this disease is clearly ageing, but there also some environmental factors associated to PD. For instance, subjects that continuously self-injected "synthetic heroin" with the contaminant MPTP (1-methyl-4-phenyl-1,2,3,6-tetrahydropyridine) developed typical symptoms of parkinsonism. Interestingly, although their brains showed nigrostriatal degeneration, LBs were not found [89]. In addition, chronic exposure to agricultural chemicals, such us rotenone, manganese ethylenebis(dithiocarbamate) (maneb) and paraquat, is considered a potential risk factor of PD [90]. Caffeine and nicotine have also been shown to be inversely correlated with the incidence of PD [91]. Until 1977, PD was considered to be a non-genetic disease, but today it is known that approximately 10% of PD cases are familial [88], and that genetics may also affect susceptibility to disease onset [92].

GENETICS OF PD

The first gene to be associated with PD was *SNCA,* the gene that encodes α-syn. Since then 18 loci named *PARK* have been genetically linked to PD. However, only 6 genes have been clearly found to cause monogenic PD: *SNCA* (*PARK1/4*), *LRRK2* (*PARK8*), *Parkin* (*PARK2*), *PINK1* (*PARK6*), *DJ-1* (*PARK7*), and *ATP13A2* (*PARK9*) [93] (Table 1.1). Mutations in these genes only explain around 30% of familial cases and 3% of sporadic [93].

Mutations in *SNCA* and *LRRK2* (Leucine-rich repeat kinase 2) are associated with autosomal dominant cases of PD. Although it is rare to find mutations in *SNCA*, five missense mutations (A53T, A30P, E46K, H50Q and G51D) have been identified in patients with familial PD or Dementia with LBs [94–98] as well as duplications and triplications of the genomic region of *SNCA* [99,100]. In addition, two genome-wide association studies showed that several single nucleotide polymorphisms in *SNCA* are risk factors to develop sporadic PD [101,102]. *LRRK2* mutations are the most frequent cause of familial and sporadic PD [103]. Patients with mutations in this gene present late-onset PD, clinically indistinguishable from sporadic cases [103].

Table 1.1. Loci associated with PD

Locus	Gene	Disorder	Inheritance	Status
PARK1	*SNCA*	EOPD	AD	Confirmed
PARK2	*Parkin*	EOPD	AR	Confirmed
PARK3	Unknown	Classical PD	AD	Unconfirmed; may represent a risk factor
PARK4	*SNCA*	EOPD	AD	Identical to Park1 (error)
PARK5	*UCHL1*	Classical PD	AD	Unconfirmed
PARK6	*PINK1*	EOPD	AR	Confirmed
PARK7	*DJ-1*	EOPD	AR	Confirmed
PARK8	*LRRK2*	Classical PD	AD	Confirmed
PARK9	*ATP13A2*	Kufor-Rakeb syndrome; atypical PD	AR	Confirmed
PARK10	Unknown	Classical PD	Risk factor	Confirmed
PARK11	Unknown	LOPD	AD	Possibly is a risk factor
PARK12	Unknown	Classical PD	Risk factor	Possibly is a risk factor
PARK13	*HTRA2*	Classical PD	AD or Risk factor	Unconfirmed
PARK14	*PLA2G6*	Early-onset dystonia-parkinsonism	AR	Confirmed
PARK15	*FBX07*	Early-onset parkinsonian-pyramidal syndrome	AR	Confirmed
PARK16	Unknown	Classical PD	Risk factor	Confirmed
PARK17	*VPS35*	Classical PD	AD	Confirmed
PARK18	*EIF4G1*	Classical PD	AD	Unconfirmed

Table adapted from Corti et al, Physiol Rev, 2011 [86] and Klein and Westenberger, Cold Spring Harbor Persp in Med, 2012 [93].

The remaining genes *Parkin*, *PINK1*, *DJ-1* and *ATP13A2* are associated with juvenile (≤ 20 years-old) and early-onset (≤ 45 years-old) autosomal recessive PD. Mutations in *Parkin* are the most frequent cause of autosomal recessive PD, followed by mutations in *PINK1* [104–106]. An intriguing aspect of the autosomal recessive cases is that LBs are absent in the majority of cases with *Parkin* mutations and so far only one case with mutations in PINK1 was reported to show LBs [107]. There are still no autopsy reports of patients with *DJ-1* or *ATP13A2* mutations. Additional genes have been linked to PD but need further confirmation: *UCHL1* (*PARK5*), *GYGYF2* (*PARK11*), *OMI/HTRA2* (*PARK13*), *PLA2G6* (*PARK14*), and *FBXO7* (*PARK15*) [93].

PATHOGENESIS OF PD

Although familial and sporadic forms of PD have certain differences, these likely share several pathogenic mechanisms. Therefore, intense research is focusing on investigating the proteins involved in familial PD, both in terms of their normal physiological role as well as their role in the disease. The discovery of PD genes and environmental factors such as MPTP have allowed the PD research community to

generate *in vivo* and *in vitro* models of the disease, which together with epidemiological studies and post-mortem analysis has already provided several insights into the molecular pathways and mechanisms that underlie PD. The fact that most genes linked to PD result in similar phenotypes, suggests that at least some of the proteins encoded by these may work in a single pathway (Fig. 1.5). Therefore, one of the goals of the PD research is to understand the relationship between these genes.

The key mechanisms that contribute for PD pathology are thought to be the loss of protein homeostasis and mitochondrial dysfunction (Fig. 1.5). These pathogenic factors do not act independently and it is not known exactly if their dysfunction is a cause or consequence of neurodegeneration.

α-synuclein and proteostasis imbalance

The fact that mutations in *SNCA* cause familial PD and that α-syn is the major component of LB strongly indicates that α-syn has a central role in the pathogenesis of PD. Therefore, much research attention is being devoted to this protein. α-syn is a small protein of 140 amino acids, enriched at presynaptic terminals [108]. The role of α-syn is still unclear, but it is thought to play a role in synaptic vesicle recycling, neurotransmission, and synaptic plasticity [109].

α-syn is natively unfolded with very little secondary structure and once it interacts with phospholipid membranes, its N-terminal region acquires an amphipathic α-helical structure [110]. The central region of α-syn contains a highly hydrophobic motif known as the non-amyloid-β component (NAC), which is highly aggregation prone [111]. A recent study reported that α-syn exists as an α-helical tetramer, suggesting that the protein can be stabilized by interacting with the neighboring subunits [112]. Nevertheless, it was further suggested that α-syn exists predominantly as an unfolded protein in the central nervous system [113]. Aggregation of α-syn starts by the formation of assembly intermediates, followed by oligomers, soluble protofibrils and amyloid fibrils that are deposited in LBs. The propensity of α-syn to aggregate increases with several factors, such as: familial point mutations, excess of α-syn caused by higher expression (gene duplications, triplications or polymorphisms) or defective clearance, oxidative stress or post-translational modifications [114].

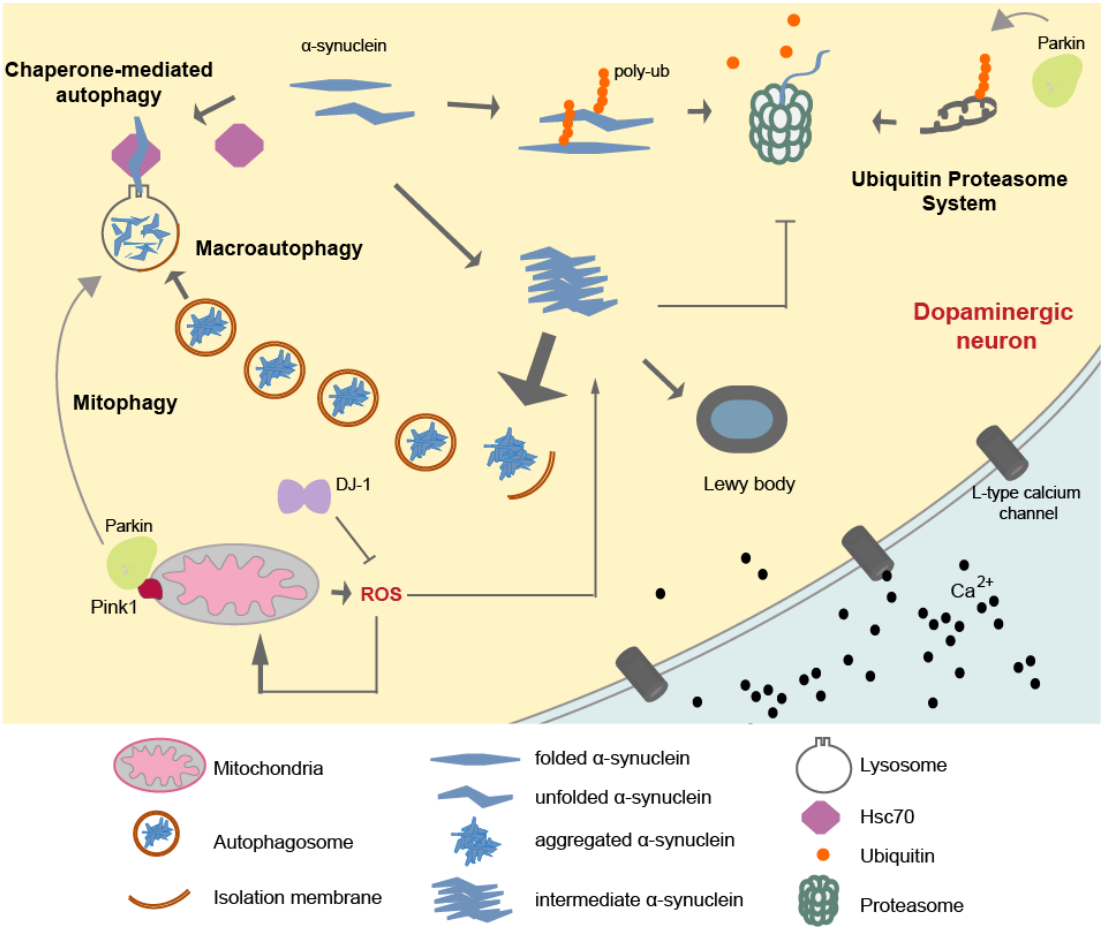

Figure 1.5. Pathogenic mechanisms that underlie Parkinson's disease.

The study of the genes associated with the familial forms of Parkinson's disease (PD) has been helping in elucidating the pathways that lead to neurodegeneration. Dysfunctional mitochondria, ubiquitin proteasome system or autophagy can promote the formation of intermediate α-synuclein species and aggregation, which in turn can impair the proteasome, mitochondria or autophagy. Dysfunctional mitochondria lead to higher generation of reactive oxygen species (ROS), which might cause further mitochondrial impairment and promote further aggregation.

Increasing evidence shows that the three protein QC systems – molecular chaperones, UPS and autophagy (especially macroautophagy and chaperone mediated autophagy) – are involved in α-syn homeostasis (Fig. 1.2) [115]. However, there are conflicting results regarding the exact mechanism by which α-syn is degraded and it is still unknown how the cell decides the route of protein degradation. The different results obtained in different labs seem to be dependent on the model system used and also on which kind of α-syn species the system has to deal with [116]. Nevertheless, several studies show that α-syn is degraded by both UPS and autophagy [116] and when one of these systems is inhibited causes α-syn accumulation and aggregation [116]. Conversely, the increase in α-syn and the consequent generation of toxic species may affect the QC systems and disturb cell homeostasis.

Ebrahimi-Fakhari and colleagues have proposed a model for α-syn degradation that hypothesizes that in non-pathological conditions, in which the levels of α-syn are maintained homeostatic, α-syn is degraded by both UPS and CMA; if the levels of α-syn increase in a way that exceeds the capacity of the QC system, toxic species may appear, blocking UPS and CMA (at initial stages of the disease). At this point, a vicious cycle begins, in which the dysfunction of UPS and CMA further increases the levels of toxic α-syn species (Fig 1.5). In order to cope with this dysfunction, cells upregulate macroautophagy, however in later stages of the disease, macroautophagy may also become impaired [117].

A strong indication that UPS and autophagy are implicated in PD pathogenesis and are responsible for α-syn degradation is the fact that among the genes linked to PD, three are strongly associated with these mechanisms: parkin, ATP13A2 and UCHL1. Parkin is an E3 ubiquitin ligase that is involved in UPS and more recently it was shown that it plays a role in mitochondria (discussed below). The role of an E3 ubiquitin ligase is to covalently link ubiquitin to a specific target protein. Parkin is capable of mediating either polyubiquitination through the ubiquitin lysine 48 (targets to the proteasome) or lysine 63 (targets to non degradative processes) or monoubiquitination (targets to non degradative processes) [118].

Mitochondria and PD

Mitochondria are essential organelles for the function and survival of neurons. These are the major energy suppliers and play a role in other critical mechanisms, such as calcium buffering and apoptosis. Importantly, mitochondria are the major source of reactive oxygen species (ROS). These are very mobile and dynamic organelles, constantly undergoing fission and fusion. These two mechanisms are required to maintain the mitochondrial network functional. While fusion is responsible for redistributing the mitochondrial components (which is a strategy of functional mitochondria to complement the damaged ones), fission occurs to create new mitochondria or remove the damaged components. When the damage is irreparable, mitochondria are removed by mitophagy.

Mounting evidence suggests that mitochondrial dysfunction is implicated in the pathogenesis of PD. However, whether it is a cause or consequence of neurodegeneration is still unclear. The first finding that led researchers to investigate the role of mitochondria in PD was that MPTP led to progressive and irreversible parkinsonism in humans [89,119]. Oxidation of MPTP in glial cells leads to formation of

MPP+ – an inhibitor of complex I – which is then released and selectively uptaken by dopaminergic neurons via the dopamine transporter. Within dopaminergic neurons this will inhibit complex I and thus impair the electron flux. As a consequence, ATP production decreases and both ROS and reactive nitrogen species (RNS) increase [119]. This finding raised the question whether complex I was impaired in idiopathic PD patients and in fact post-mortem analysis of the brains of PD patients showed reduced complex I activity in the SNpc [120]. The administration of MPTP and other complex I inhibitors, such as rotenone or paraquat, in rodents can also induce dopaminergic degeneration, further supporting that mitochondrial dysfunction has a central role in PD pathogenesis [121]. Additionally, many of the proteins encoded by the genes associated to PD (α-syn, PINK1, parkin, DJ-1, LRRK2) play a role directly or indirectly in mitochondrial functions and at least PINK1 and parkin act in a common pathway.

PINK1 (PTEN-induced kinase 1) is a nuclear encoded kinase that is localized in the outer mitochondrial membrane, with the kinase domain turned to the cytosol [122,123]. Mutations in PINK1 are thought to be loss of function; the majority of mutations are localized in the kinase domain and result in impairment of the kinase activity. So far, only three PINK1 substrates have been identified: the mitochondrial chaperone TNF-receptor-associated protein 1 (TRAP1), the mitochondrial serine protease Omi/HtrA2 and parkin [124–126]. Both TRAP1 and Omi/HtrA2 are involved in protecting cells against cell death in stress conditions [126,127]. Interestingly, the knockout mouse for Omi/HtrA2 develops a parkinsonian phenotype and dies after one month [127]. PINK1 and parkin were elegantly shown to function in the same pathway using *Drosophila* as a model system [128,129]. *Drosophila* deleted for *PINK1* or *Parkin* exhibit similar phenotypes due to mitochondrial defects, including male sterility, apoptotic muscle degeneration, higher sensitivity to several stresses and locomotive impairment [128,129]. The overexpression of parkin complements the phenotypes caused by deletion of *PINK1*, but not vice-versa, indicating that PINK1 is an upstream regulator of parkin. Compelling evidence shows that PINK1-parkin pathway is involved in maintaining the integrity of the mitochondrial network by modulating mitochondrial dynamics and promoting degradation of damaged mitochondria through mitophagy [130,131]. More recently it was shown that it can also induce the selective degradation of respiratory subunits [132]. It is not clear whether dysfunctional quality control of mitochondria is involved in the pathogenesis of sporadic PD, however parkin was found impaired even when it was not mutated [133,134], supporting this idea.

How DJ-1 is related to mitochondria is also unclear. DJ-1 is a cytosolic, nuclear and mitochondrial protein [135,136]. Localization of DJ-1 to mitochondria increases upon oxidative stress and is neuroprotective [137,138]. The precise cellular role of DJ-1 is unknown, but compelling evidence indicates that it is involved in cellular responses of oxidative stress (further discussed in Chapter 3). The link between mitochondria protection and DJ-1 may be in fact the protection against oxidative stress [139]. Nevertheless, multiple studies have shown that loss of DJ-1 leads to several mitochondrial defects, including mitochondria fragmentation [140–144]. Interestingly, fruit flies deleted for *DJ-1* (both orthologs *DJ-1a* and *DJ-1b*) exhibited similar phenotypes to flies deleted for *pink1* or *parkin* [145]*.* Overexpression of DJ-1 was able to complement the loss of PINK1, but not *parkin* [145]. These results suggest that DJ-1 acts in a parallel pathway or downstream PINK1, but likely is independent of PINK1-parkin pathway.

Finally, overexpression of wild-type or familial mutant forms of α-syn in transgenic mouse and cell culture models results in mitochondrial dysfunction [146–148].

Taking all this into account, it is clear that dissecting further the role of these proteins in the mitochondrial function will contribute for a better understanding of PD pathogenesis.

Oxidative stress

Oxidative stress occurs when the generation of ROS and RNS exceeds the cell antioxidant defense mechanisms. These reactive species have the capacity to chemically modify cell constituents such as proteins, lipids and nucleic acids, which may result in their irreversible damage and ultimately trigger neuronal injury [149]. High levels of ROS can even trigger apoptosis or autophagy leading to cell death [150]. Apart from its toxic effect in the cell, ROS have also an important signaling role under normal conditions [151]. Therefore, it is essential to control the levels of ROS and RNS in the cell.

Mitochondria are the major source of ROS. Electrons leak from the electron transport chain and partially reduce oxygen resulting in the formation of superoxide, which subsequently can be converted to hydrogen peroxide. Hydrogen peroxide by reacting with iron (Fenton reaction) results in the formation of the hydroxyl radical [150]. Superoxide can also be transformed into peroxynitrite by reacting with nitric oxide [152,153]. The accumulation of ROS in mitochondria leads a vicious cycle in which dysfunctional mitochondria result in higher production of ROS that in turn enhance mitochondrial impairment.

The brain is thought to be more susceptible to oxidative stress since is highly metabolically active and has a low capacity to regenerate the post mitotic neurons compared to other organs. Oxidative stress has been implicated as one of the mechanisms that contribute to the pathogenesis of several neurodegenerative diseases including PD, as well as one of the causes of ageing, proposed as the "free radical theory of ageing" [149,154].

Several observations indicate that dopaminergic neurons in SNpc are particularly exposed to oxidative stress, making them more vulnerable for cell death. As mentioned already, post mortem PD brains show decreased complex I activity in SNpc when compared with healthy controls, [120] as well as increased lipid peroxidation, protein carbonylation, DNA and RNA oxidation and decreased antioxidant defenses, such as glutathione [155–158]. Dopaminergic neurons in SNpc contain higher concentrations of iron, which can be toxic if iron reacts with hydrogen peroxide and the hydroxyl radical is generated [159–161]. In addition, these neurons contain dopamine, which oxidation products are potentially toxic [162]. An additional hypothesis that explains why nigral dopaminergic neurons have higher levels of oxidative stress is the presence of L-type calcium channels. These channels help to maintain the pacemaking activity which is characteristic of SNpc dopaminergic neurons and consists in maintaining neuronal activity autonomously, i.e. without any synaptic input [163]. L-type calcium channels are open frequently, since they open at relatively hyperpolarized state. This comes with an energetic cost, since the calcium concentration has to be under tight control and this is maintained by ATP dependent pumps. Since this is an energy dependent mechanism, mitochondria activity increases and subsequently the basal ROS also increase, turning the dopaminergic neurons more vulnerable for stressors [163].

In addition to the intracellular sources of ROS, these species can also come from activated microglial cells. Microglia are generally on a resting state, but become activated upon several insults, such as factors released by damaged neurons. Microglial cells are found activated in the brains of PD patients [164,165]. Activation of microglia may result in a vicious cycle, since these cells release neurotoxic factors (such as ROS) which will potentiate neuronal cell death [164]. Several studies have shown that neuroinflammation also contributes to the pathogenesis of PD [164]. Therefore, dissecting the mechanisms that control neuroinflammation may help in finding novel strategies to control PD. Excitingly, we have recently found that SIRT2 is a promising target to prevent sustained inflammation and neurotoxicity. We showed that reduction of SIRT2 expression in mouse models and microglial cell lines leads to enhanced

neuroinflammation and neurotoxicity induced by higher generation of ROS and RNS. Conversely, SIRT2 overexpression in microglial cell lines inhibits microglial activation[166]. The gene implicated in PD that predominantly supports the role of oxidative stress in the pathogenesis of PD is DJ-1 (see Chapter 3).

Baker's yeast: a versatile "toolbox" for molecular biology studies

Since ancient times the budding yeast *Saccharomyces cerevisiae* has been used in baking and brewing [167]. This unicellular eukaryotic organism is extremely useful for molecular biologists and our knowledge about fundamental cellular mechanisms has greatly benefited from the use of yeast as a model [168]. It has been extensively used in the study of numerous complex and devastating disorders, such as HD and PD and has provided insight into the molecular events underlying these disorders [169–171].

Multiple characteristics make this simple eukaryote a model system of choice. First of all, it is well defined genetically and genomically (*S. cerevisiae* was the first eukaryote organism to be fully sequenced). Of the 6000 genes predicted to be encoded by its 12,000-kilobase genome, ~80% are functionally characterized [172]. Since the electronic release of its genomic sequence several highly annotated online databases have become available, which provide multitudes of detailed information on yeast genes and proteins, such as protein-protein interactions, genetic interactions, protein function, and predicted orthologs in other organisms. The remarkably high degree of conservation between yeast and higher eukaryotes, with respect to basic processes such as cell cycle, intracellular transport, and cellular QC systems is another feature that makes yeast so attractive. Therefore, yeast studies may shed light into the conserved mechanisms involved in human diseases. In fact, yeast has been extensively used as an informative organism for human gene function, since approximately half of the genes involved in human heritable diseases are predicted to have yeast homologues [173].

Genetic and biochemical manipulations in yeast are extremely simple, rather quick, and inexpensive when compared to manipulations in other eukaryotes. Yeast is easy to grow on appropriate media, with a doubling time of approximately 90 minutes on rich medium, and survive indefinitely in frozen glycerol stocks. Strains can be maintained as stable haploids or diploids, allowing the study of lethal mutations in heterozygous diploids and recessive mutations in haploids. It is easy to mate the haploid strains and to sporulate diploid strains, making classical genetics extremely

facile. Other versatile characteristics of this organism are the ease of transformation and the ability to integrate genes by homologous recombination [167,174,175]. The experimental tractability of yeast has allowed the development of several sophisticated functional tools, such as yeast two-hybrid variants, affinity purification and mass-spectrometry identification providing substantial amounts of information about protein-protein interactions [176,177]. In addition, several yeast strain collections have been created, permitting rapid genomic systematic screenings and the identification of genetic interactions. These libraries include the yeast open reading frame (ORF) collection (YOC) and the yeast gene knock-out collection (YKO), which is available in haploid, homozygous diploid and heterozygous diploid strains [175]. So far, such screens have allowed the identification of several possible genetic modifiers (suppressors or enhancers) of amyloid diseases, the identification of new therapeutic targets, and the dissection of the pathogenic mechanisms and pathways involved in these diseases.

Although the simplicity of yeast is an advantage for experimental manipulation and interpretation of data, it does present a caveat of this model. For obvious reasons, several mechanisms and biological pathways present in higher eukaryotes are absent in yeast and, on the other hand, some pathways, such as cell wall biosynthesis, have no counterpart in mammals. Therefore, all findings in yeast related to human disease ultimately must be validated in more physiologically relevant systems prior to their trial in humans.

Modeling neurodegenerative diseases in yeast

Despite the obvious absence of a nervous system in yeast, basic mechanisms and pathways underlying neurodegenerative diseases, such as mitochondrial dysfunction, transcriptional dysregulation, trafficking defects and proteasomal dysfunction, are extremely well conserved between humans and yeast, enabling detailed studies of the molecular events involved in those conditions. In fact, several remarkable insights into the understanding of brain diseases have been recently achieved [171,178–180]. In order to develop disease models, it is essential that some relevant aspects of the disease phenotype are recapitulated. If the gene implicated in the disease has a yeast homolog, it is possible to study its function directly. If, on the other hand, the gene underlying the disease is absent in yeast but causes disease by a toxic gain-of-function mechanism in humans, it can still be modeled via the heterologous expression of the human gene in yeast cells.

Yeast models of HD

Several yeast models of HD have been developed to study the folding and behavior of mutant Htt as well as to dissect the underlying conserved mechanisms of mutant Htt-dependent toxicity [81,181–183]. Expression in yeast of an amino-terminal fragment of Htt fused to GFP results in polyQ length-dependent formation of cytoplasmic inclusions that can be visualized in cells via fluorescence microscopy [81,182]. A simple filter-retention assay has also been used to isolate detergent-insoluble aggregates formed by expression in yeast of a mutant Htt fragment [181]. One of these models exhibits polyQ length-dependent toxicity, such that expression of a Htt fragment with polyQ length in the pathogenic range (Htt103Q) produces cellular toxicity within yeast, while expression of the same construct containing a non-expanded polyQ tract (Htt25Q) shows no negative effect upon growth [182]. Recent work suggests that several factors are contributing to toxicity in this yeast model of HD, including perturbations in the kynurenine pathway (discussed in Chapter 2) [171], defects in endocytosis [184,185], apoptotic-like events [186], increased levels of ROS [171,187], and mitochondrial dysfunction [186,187]. Interestingly, the polyQ-length dependent toxicity observed in the Meriin et al. model requires the presence of the yeast prion Rnq1 in its prion conformation [182]. Several other glutamine-rich proteins play an additional role in modulating toxicity [29,171]. In addition, it was observed that the flanking amino acid sequences are required for modulating toxic conformations of these Htt fragments in yeast [29,30]. This conversion of benign species to toxic species (and vice-versa) can operate in *cis* or in *trans* [29].

The availability of yeast models of HD has facilitated the identification of candidate therapeutic targets for HD in the form of gene deletions that either enhance or suppress toxicity of a mutant Htt fragment [170,171,188]. Additionally, this model has allowed screening and individual testing of small molecules to identify novel candidate therapeutic compounds which have been validated in higher eukaryotes [189–191]. The YKO was screened for loss-of-function suppressors of the toxic Htt103Q construct [171,182]. Of the genes identified in this screen, 25% encode proteins that cluster into the functionally related categories of vesicular transport, vacuolar protein sorting, and vacuolar import; 25% encode proteins that are involved directly in transcription or in establishment/maintenance of chromatin architecture; and ~21% encode known yeast prions or proteins containing Q/N-rich regions that may mediate prion-like aggregation. Over half of the genes isolated are annotated as having one or more human orthologs. This suggests that there are conserved biological pathways associated to mutant Htt that ultimately may be relevant to HD. One of the identified suppressors was *BNA4*,

which encodes the yeast homolog of the mammalian kynurenine 3-monooxygenase (KMO) [171]. This enzyme functions in the conserved kynurenine pathway, which is activated in HD patients and in animal models of this disorder (discussed in further detail in Chapter 2) [192]. In humans this pathway is linked directly to HD by a mechanism that may involve ROS. It is intriguing that deletion or pharmacological inhibition of KMO activity reduces levels of ROS and strongly suppresses mutant Htt-mediated toxicity [171]. Excitingly, recent published trials of KMO inhibitors in HD model mice have found that treatment with these compounds significantly ameliorates several disease-relevant phenotypes in these mice [193]. Recently, a Htt suppressor screen was conducted in which 317 ORFs that protect yeast from Htt toxicity were identified [188]. Among these ORFs, two encode glutathione peroxidases (GPx), which are conserved cellular antioxidants. These results were further validated in *Drosophila* and mammalian model systems. Importantly, GPx mimetics were previously shown to be well tolerated in humans, further supporting the value of using yeast as a starting platform to identify novel therapeutic strategies for HD [188].

Yeast models of PD

To gain insight into the biology of α-syn a yeast model of PD was developed, which successfully reproduced several hallmarks of this disease [169]. Heterologous expression of the wild-type (WT) α-syn and the mutant A53T induces toxicity in yeast and formation of inclusion bodies in a concentration-dependent way. At moderate levels α-syn is initially associated with the plasma membrane, but when it is overexpressed the protein is recruited into cytoplasmic inclusions [169]. The toxicity of α-syn is consistent with the identification of duplications and triplications of the α-syn locus in PD patients [99,100] and with the observation that dopaminergic cells of mice and *Drosophila* die when α-syn is overexpressed [194,195]. It has also been found that WT and A53T α-syn are directed to the plasma membrane through the secretory pathway [196] and cause endoplasmic reticulum (ER) stress. In addition, it was found that A30P is directed to the vacuole, through the endocytic pathway, where it is proteolytically degraded [197]. The involvement of cellular QC systems was also investigated. While ubiquitination is dispensable for the formation of α-syn inclusion bodies in yeast, the proteasome activity is impaired [169]. The involvement of proteasome dysfunction in α-syn aggregates is further supported by the indication that mutations in proteasome 20S enhance toxicity [196]. It has been recently observed that α-syn toxicity in yeast leads to shorter chronological life span and induction of autophagy and mitophagy (mediated by Sir2)

[198]. Surprisingly, upon mitophagy impairment, α-syn toxicity is alleviated [198]. It was also shown that heterologous expression of α-syn also leads to impairment of endocytosis [169], mitochondria [199] and mitophagy [198] and to the accumulation of lipid droplets [169].The generation of ROS and apoptosis were also successfully reproduced in yeast [200], further validating these models. One important question in the PD field is whether phosphorylation of α-syn on the serine 129 is associated with α-syn aggregation and/or toxicity, since 90% of α-syn in LB is phosphorylated in this residue [201]. Interestingly, Basso et al. showed that phosphorylation of this residue mediated by the human PLK2 in yeast leads to an increase in cytotoxicity and higher number of α-syn inclusions. In addition, they showed that PLK2 in mammalian cell lines causes an increase in inclusions size [202], however, PLK3 despite phosphorylating α-syn in the same residue does not affect toxicity or the formation of foci, suggesting that phosphorylation of serine 129 is not modulating the formation of α-syn inclusions [202]. Interestingly, a recent study performed in yeast and validated in human cells demonstrated that α-syn leads to toxicity by impairing PLK2 function and consequently disrupting a stress response pathway [203].

The validation of these yeast α-syn models allowed performing several high-throughput studies. An overexpression screen identified genetic modifiers of α-syn. Genes inducing ER-Golgi transport were identified as suppressors, whereas genes that inhibit this transport were identified as enhancers of α-syn toxicity. Remarkably, Rab1 – the human homolog of *YPT1* – found among the suppressors, rescued the loss of dopaminergic neurons in animal models of PD [204].

Yeast has also been used as a model system to gain insights into the function of other PD-related genes: LRRK2 and ATP13A2. To investigate the role of LRRK2, a yeast model was developed which expresses the full length protein or only domain fragments [205]. It was found that LRRK2 toxicity in yeast depends on its GTPase activity and is related with impairment of endocytic vesicular trafficking and autophagy [205]. These results were further validated in mice primary neuronal cultures [205]. Ypk9, the yeast homolog of ATP13A2, was found to interact genetically with α-syn by suppressing its toxicity [206]. This result was conserved in higher complex models [206]. Ypk9 has a role in the homeostasis of manganese and other divalent heavy metal ions, which are environmental PD risk factors [206–208]. ATP13A2 is thus a potential link between genetic and environmental risk factors for PD.

References

1. Tyedmers, J., Mogk, A. & Bukau, B. Cellular strategies for controlling protein aggregation. Nat. Rev. Mol. Cell Biol. 11, 777–88 (2010).
2. Ben-Zvi, A. P. & Goloubinoff, P. Proteinaceous infectious behavior in non-pathogenic proteins is controlled by molecular chaperones. J. Biol. Chem. 277, 49422–7 (2002).
3. Hershko, A. & Ciechanover, A. The ubiquitin-proteasome system. 31, 137–155 (2006).
4. Yorimitsu, T. & Klionsky, D. J. Autophagy: molecular machinery for self-eating. Cell Death Differ. 12 Suppl 2, 1542–52 (2005).
5. Chiti, F. & Dobson, C. M. Protein misfolding, functional amyloid, and human disease. Annu. Rev. Biochem. 75, 333–66 (2006).
6. Ross, C. A. & Poirier, M. A. Protein aggregation and neurodegenerative disease. Nat. Med. 10 Suppl, S10–7 (2004).
7. Hardy, J. & Selkoe, D. J. The amyloid hypothesis of Alzheimer's disease: progress and problems on the road to therapeutics. Science 297, 353–6 (2002).
8. Martin, J. B. & Gusella, J. F. Huntington's disease. Pathogenesis and management. N. Engl. J. Med. 315, 1267–76 (1986).
9. Rosas, H. D. et al. Complexity and heterogeneity: what drives the ever-changing brain in Huntington's disease? Ann. N. Y. Acad. Sci. 1147, 196–205 (2008).
10. A novel gene containing a trinucleotide repeat that is expanded and unstable on Huntington's disease chromosomes. The Huntington's Disease Collaborative Research Group. Cell 72, 971–83 (1993).
11. Rubinsztein, D. C. et al. Phenotypic characterization of individuals with 30-40 CAG repeats in the Huntington disease (HD) gene reveals HD cases with 36 repeats and apparently normal elderly individuals with 36-39 repeats. Am. J. Hum. Genet. 59, 16–22 (1996).
12. Duyao, M. et al. Trinucleotide repeat length instability and age of onset in Huntington's disease. Nat. Genet. 4, 387–92 (1993).
13. Telenius, H. et al. Molecular analysis of juvenile Huntington disease: the major influence on (CAG)n repeat length is the sex of the affected parent. Hum. Mol. Genet. 2, 1535–40 (1993).
14. Wexler, N. S. et al. Venezuelan kindreds reveal that genetic and environmental factors modulate Huntington's disease age of onset. Proc. Natl. Acad. Sci. U.S.A. 101, 3498–503 (2004).
15. Mangiarini, L. et al. Exon 1 of the HD gene with an expanded CAG repeat is sufficient to cause a progressive neurological phenotype in transgenic mice. Cell 87, 493–506 (1996).
16. Gutekunst, C. A. et al. Nuclear and neuropil aggregates in Huntington's disease: relationship to neuropathology. J. Neurosci. 19, 2522–34 (1999).
17. DiFiglia, M. et al. Aggregation of huntingtin in neuronal intranuclear inclusions and dystrophic neurites in brain. Science 277, 1990–3 (1997).
18. Becher, M. W. et al. Intranuclear neuronal inclusions in Huntington's disease and dentatorubral and pallidoluysian atrophy: correlation between the density of inclusions and IT15 CAG triplet repeat length. Neurobiol. Dis. 4, 387–97 (1998).
19. Davies, S. W. et al. Formation of neuronal intranuclear inclusions underlies the neurological dysfunction in mice transgenic for the HD mutation. Cell 90, 537–48 (1997).
20. Suhr, S. T. et al. Identities of sequestered proteins in aggregates from cells with induced polyglutamine expression. J. Cell Biol. 153, 283–94 (2001).
21. Donaldson, K. M. et al. Ubiquitin-mediated sequestration of normal cellular proteins into polyglutamine aggregates. Proc. Natl. Acad. Sci. U.S.A. 100, 8892–7 (2003).
22. Nucifora, F. C. et al. Interference by huntingtin and atrophin-1 with cbp-mediated transcription leading to cellular toxicity. Science 291, 2423–8 (2001).
23. McCampbell, A. et al. CREB-binding protein sequestration by expanded polyglutamine. Hum. Mol. Genet. 9, 2197–202 (2000).
24. Bennett, E. J., Bence, N. F., Jayakumar, R. & Kopito, R. R. Global impairment of the ubiquitin-proteasome system by nuclear or cytoplasmic protein aggregates precedes inclusion body formation. Mol. Cell 17, 351–65 (2005).
25. Yu, Z.-X., Li, S.-H., Nguyen, H.-P. & Li, X.-J. Huntingtin inclusions do not deplete polyglutamine-containing transcription factors in HD mice. Hum. Mol. Genet. 11, 905–14 (2002).
26. Arrasate, M., Mitra, S., Schweitzer, E. S., Segal, M. R. & Finkbeiner, S. Inclusion body formation reduces levels of mutant huntingtin and the risk of neuronal death. Nature 431, 805–10 (2004).
27. Miller, J. et al. Quantitative relationships between huntingtin levels, polyglutamine length, inclusion body formation, and neuronal death provide novel insight into huntington's disease molecular pathogenesis. J. Neurosci. 30, 10541–50 (2010).

28. Truant, R., Atwal, R. S., Desmond, C., Munsie, L. & Tran, T. Huntington's disease: revisiting the aggregation hypothesis in polyglutamine neurodegenerative diseases. FEBS J. 275, 4252–62 (2008).
29. Duennwald, M. L., Jagadish, S., Muchowski, P. J. & Lindquist, S. Flanking sequences profoundly alter polyglutamine toxicity in yeast. Proc. Natl. Acad. Sci. U.S.A. 103, 11045–50 (2006).
30. Dehay, B. & Bertolotti, A. Critical role of the proline-rich region in Huntingtin for aggregation and cytotoxicity in yeast. J. Biol. Chem. 281, 35608–15 (2006).
31. Lakhani, V. V, Ding, F. & Dokholyan, N. V. Polyglutamine induced misfolding of huntingtin exon1 is modulated by the flanking sequences. PLoS Comput. Biol. 6, e1000772 (2010).
32. Martindale, D. et al. Length of huntingtin and its polyglutamine tract influences localization and frequency of intracellular aggregates. Nat. Genet. 18, 150–4 (1998).
33. Lunkes, A. et al. Proteases acting on mutant huntingtin generate cleaved products that differentially build up cytoplasmic and nuclear inclusions. Mol. Cell 10, 259–69 (2002).
34. Graham, R. K. et al. Cleavage at the caspase-6 site is required for neuronal dysfunction and degeneration due to mutant huntingtin. Cell 125, 1179–91 (2006).
35. Pennuto, M., Palazzolo, I. & Poletti, A. Post-translational modifications of expanded polyglutamine proteins: impact on neurotoxicity. Hum. Mol. Genet. 18, R40–7 (2009).
36. DiFiglia, M. et al. Huntingtin is a cytoplasmic protein associated with vesicles in human and rat brain neurons. Neuron 14, 1075–81 (1995).
37. Zeitlin, S., Liu, J. P., Chapman, D. L., Papaioannou, V. E. & Efstratiadis, A. Increased apoptosis and early embryonic lethality in mice nullizygous for the Huntington's disease gene homologue. Nat. Genet. 11, 155–63 (1995).
38. Nasir, J. et al. Targeted disruption of the Huntington's disease gene results in embryonic lethality and behavioral and morphological changes in heterozygotes. Cell 81, 811–23 (1995).
39. Gauthier, L. R. et al. Huntingtin controls neurotrophic support and survival of neurons by enhancing BDNF vesicular transport along microtubules. Cell 118, 127–38 (2004).
40. Singaraja, R. R. et al. HIP14, a novel ankyrin domain-containing protein, links huntingtin to intracellular trafficking and endocytosis. Hum. Mol. Genet. 11, 2815–28 (2002).
41. Metzler, M. et al. NMDA receptor function and NMDA receptor-dependent phosphorylation of huntingtin is altered by the endocytic protein HIP1. J. Neurosci. 27, 2298–308 (2007).
42. Borrell-Pagès, M., Zala, D., Humbert, S. & Saudou, F. Huntington's disease: from huntingtin function and dysfunction to therapeutic strategies. Cell. Mol. Life Sci. 63, 2642–60 (2006).
43. Savas, J. N. et al. A role for huntington disease protein in dendritic RNA granules. J. Biol. Chem. 285, 13142–53 (2010).
44. Zhang, Y. et al. Huntingtin inhibits caspase-3 activation. EMBO J. 25, 5896–906 (2006).
45. Leavitt, B. R. et al. Wild-type huntingtin protects neurons from excitotoxicity. J. Neurochem. 96, 1121–9 (2006).
46. Imarisio, S. et al. Huntington's disease: from pathology and genetics to potential therapies. Biochem. J. 412, 191–209 (2008).
47. Augood, S. J., Faull, R. L., Love, D. R. & Emson, P. C. Reduction in enkephalin and substance P messenger RNA in the striatum of early grade Huntington's disease: a detailed cellular in situ hybridization study. Neuroscience 72, 1023–36 (1996).
48. Augood, S. J., Faull, R. L. & Emson, P. C. Dopamine D1 and D2 receptor gene expression in the striatum in Huntington's disease. Ann. Neurol. 42, 215–21 (1997).
49. Arzberger, T., Krampfl, K., Leimgruber, S. & Weindl, A. Changes of NMDA receptor subunit (NR1, NR2B) and glutamate transporter (GLT1) mRNA expression in Huntington's disease--an in situ hybridization study. J. Neuropathol. Exp. Neurol. 56, 440–54 (1997).
50. Schilling, G. et al. Nuclear-targeting of mutant huntingtin fragments produces Huntington's disease-like phenotypes in transgenic mice. Hum. Mol. Genet. 13, 1599–610 (2004).
51. Saudou, F., Finkbeiner, S., Devys, D. & Greenberg, M. E. Huntingtin acts in the nucleus to induce apoptosis but death does not correlate with the formation of intranuclear inclusions. Cell 95, 55–66 (1998).
52. Li, X. et al. Targeting mitochondrial reactive oxygen species as novel therapy for inflammatory diseases and cancers. J Hematol Oncol 6, 19 (2013).
53. Zhai, W., Jeong, H., Cui, L., Krainc, D. & Tjian, R. In vitro analysis of huntingtin-mediated transcriptional repression reveals multiple transcription factor targets. Cell 123, 1241–53 (2005).
54. Li, S.-H. et al. Interaction of Huntington disease protein with transcriptional activator Sp1. Mol. Cell. Biol. 22, 1277–87 (2002).
55. Dunah, A. W. et al. Sp1 and TAFII130 transcriptional activity disrupted in early Huntington's disease. Science 296, 2238–43 (2002).
56. Ferrer, I., Goutan, E., Marín, C., Rey, M. . & Ribalta, T. Brain-derived neurotrophic factor in Huntington disease. Brain Res. 866, 257–261 (2000).

57. Simmons, D. A. et al. Up-regulating BDNF with an ampakine rescues synaptic plasticity and memory in Huntington's disease knockin mice. Proc. Natl. Acad. Sci. U.S.A. 106, 4906–11 (2009).
58. Gharami, K., Xie, Y., An, J. J., Tonegawa, S. & Xu, B. Brain-derived neurotrophic factor over-expression in the forebrain ameliorates Huntington's disease phenotypes in mice. J. Neurochem. 105, 369–79 (2008).
59. Zuccato, C. et al. Widespread disruption of repressor element-1 silencing transcription factor/neuron-restrictive silencer factor occupancy at its target genes in Huntington's disease. J. Neurosci. 27, 6972–83 (2007).
60. Zuccato, C. et al. Huntingtin interacts with REST/NRSF to modulate the transcription of NRSE-controlled neuronal genes. Nat. Genet. 35, 76–83 (2003).
61. Aziz, N. A. et al. Weight loss in Huntington disease increases with higher CAG repeat number. Neurology 71, 1506–13 (2008).
62. Mann, V. M. et al. Mitochondrial function and parental sex effect in Huntington's disease. Lancet 336, 749 (1990).
63. Gu, M. et al. Mitochondrial defect in Huntington's disease caudate nucleus. Ann. Neurol. 39, 385–9 (1996).
64. Benchoua, A. et al. Involvement of mitochondrial complex II defects in neuronal death produced by N-terminus fragment of mutated huntingtin. Mol. Biol. Cell 17, 1652–63 (2006).
65. Horton, T. M. et al. Marked increase in mitochondrial DNA deletion levels in the cerebral cortex of Huntington's disease patients. Neurology 45, 1879–83 (1995).
66. Kim, J. et al. Mitochondrial loss, dysfunction and altered dynamics in Huntington's disease. Hum. Mol. Genet. 19, 3919–35 (2010).
67. Panov, A. V et al. Early mitochondrial calcium defects in Huntington's disease are a direct effect of polyglutamines. Nat. Neurosci. 5, 731–6 (2002).
68. Trushina, E. et al. Mutant huntingtin impairs axonal trafficking in mammalian neurons in vivo and in vitro. Mol. Cell. Biol. 24, 8195–209 (2004).
69. Orr, A. L. et al. N-terminal mutant huntingtin associates with mitochondria and impairs mitochondrial trafficking. J. Neurosci. 28, 2783–92 (2008).
70. Choo, Y. S., Johnson, G. V. W., MacDonald, M., Detloff, P. J. & Lesort, M. Mutant huntingtin directly increases susceptibility of mitochondria to the calcium-induced permeability transition and cytochrome c release. Hum. Mol. Genet. 13, 1407–20 (2004).
71. Cui, L. et al. Transcriptional repression of PGC-1alpha by mutant huntingtin leads to mitochondrial dysfunction and neurodegeneration. Cell 127, 59–69 (2006).
72. Seong, I. S. et al. HD CAG repeat implicates a dominant property of huntingtin in mitochondrial energy metabolism. Hum. Mol. Genet. 14, 2871–80 (2005).
73. Ross, C. a & Tabrizi, S. J. Huntington's disease: from molecular pathogenesis to clinical treatment. Lancet Neurol 10, 83–98 (2011).
74. Thevandavakkam, M. A., Schwarcz, R., Muchowski, P. J. & Giorgini, F. Targeting Kynurenine 3-Monooxygenase Therapy in Huntington ' s Disease (KMO): Implications for. (2010).
75. Hassel, B., Tessler, S., Faull, R. L. M. & Emson, P. C. Glutamate uptake is reduced in prefrontal cortex in Huntington's disease. Neurochem. Res. 33, 232–7 (2008).
76. Zuccato, C., Valenza, M. & Cattaneo, E. Molecular Mechanisms and Potential Therapeutical Targets in Huntington ' s Disease. 905–981 (2010). doi:10.1152/physrev.00041.2009.
77. Hara, M. R. & Snyder, S. H. Cell signaling and neuronal death. Annu. Rev. Pharmacol. Toxicol. 47, 117–41 (2007).
78. De Lau, L. M. L. & Breteler, M. M. B. Epidemiology of Parkinson's disease. Lancet Neurol 5, 525–35 (2006).
79. Goedert, M., Spillantini, M. G., Del Tredici, K. & Braak, H. 100 years of Lewy pathology. Nat Rev Neurol 1–12 (2012). doi:10.1038/nrneurol.2012.242
80. Chernoff, Y. O., Lindquist, S. L., Ono, B., Inge-Vechtomov, S. G. & Liebman, S. W. Role of the chaperone protein Hsp104 in propagation of the yeast prion-like factor [psi+]. Science 268, 880–4 (1995).
81. Krobitsch, S. & Lindquist, S. Aggregation of huntingtin in yeast varies with the length of the polyglutamine expansion and the expression of chaperone proteins. Proc. Natl. Acad. Sci. U.S.A. 97, 1589–94 (2000).
82. Dauer, W. & Przedborski, S. Parkinson's disease: mechanisms and models. Neuron 39, 889–909 (2003).
83. Dickson, D. W. et al. Evidence that incidental Lewy body disease is pre-symptomatic Parkinson's disease. Acta Neuropathol. 115, 437–44 (2008).
84. Caine, J. et al. Alzheimer's Abeta fused to green fluorescent protein induces growth stress and a heat shock response. FEMS Yeast Res. 7, 1230–6 (2007).
85. Braak, H. et al. Stageing of brain pathology related to sporadic Parkinson's disease. Neurobiology of Ageing 24, 197–211 (2003).
86. Corti, O., Lesage, S. & Brice, A. What genetics tells us about the causes and mechanisms of Parkinson's disease. Physiol. Rev. 91, 1161–218 (2011).

87. Smith, K. Treatment frontiers. Nature 466, S15–8 (2010).
88. Thomas, B. & Beal, M. F. Parkinson's disease. Hum. Mol. Genet. 16 Spec No, R183–94 (2007).
89. Langston, J. W. et al. Evidence of active nerve cell degeneration in the substantia nigra of humans years after 1-methyl-4-phenyl-1,2,3,6-tetrahydropyridine exposure. Ann. Neurol. 46, 598–605 (1999).
90. Monte, D. A. Di, Lavasani, M. & Manning-bog, A. B. Environmental Factors in Parkinson ' s Disease. 23, 487–502 (2002).
91. Ross, G. W. et al. Association of coffee and caffeine intake with the risk of Parkinson disease. JAMA 283, 2674–9
92. Lesage, S. & Brice, A. Parkinson's disease: from monogenic forms to genetic susceptibility factors. Hum. Mol. Genet. 18, R48–59 (2009).
93. Klein, C. & Westenberger, A. Genetics of Parkinson's disease. Cold Spring Harbor perspectives in medicine 2, a008888 (2012).
94. Polymeropoulos, M. H. et al. Mutation in the alpha-synuclein gene identified in families with Parkinson's disease. Science 276, 2045–7 (1997).
95. Krüger, R. et al. Ala30Pro mutation in the gene encoding alpha-synuclein in Parkinson's disease. Nat. Genet. 18, 106–8 (1998).
96. Zarranz, J. J. et al. The new mutation, E46K, of alpha-synuclein causes Parkinson and Lewy body dementia. Ann. Neurol. 55, 164–73 (2004).
97. Proukakis, C. et al. A novel α-synuclein missense mutation in Parkinson disease. Neurology 80, 1062–4 (2013).
98. Lesage, S. et al. G51D α-synuclein mutation causes a novel parkinsonian-pyramidal syndrome. Ann. Neurol. (2013). doi:10.1002/ana.23894
99. Chartier-Harlin, M.-C. et al. Alpha-synuclein locus duplication as a cause of familial Parkinson's disease. Lancet 364, 1167–9
100. Singleton, A. B. et al. alpha-Synuclein locus triplication causes Parkinson's disease. Science 302, 841 (2003).
101. Simón-Sánchez, J. et al. Genome-wide association study reveals genetic risk underlying Parkinson's disease. Nat. Genet. 41, 1308–12 (2009).
102. Do, C. B. et al. Web-based genome-wide association study identifies two novel loci and a substantial genetic component for Parkinson's disease. PLoS Genet. 7, e1002141 (2011).
103. Haugarvoll, K. & Wszolek, Z. K. PARK8 LRRK2 parkinsonism. Current Neurology and Neuroscience Reports 6, 287–294 (2006).
104. Nuytemans, K., Theuns, J., Cruts, M. & Van Broeckhoven, C. Genetic etiology of Parkinson disease associated with mutations in the SNCA, PARK2, PINK1, PARK7, and LRRK2 genes: a mutation update. Hum. Mutat. 31, 763–80 (2010).
105. Kitada, T. et al. Mutations in the parkin gene cause autosomal recessive juvenile parkinsonism. Nature 392, 605–8 (1998).
106. Kawajiri, S., Saiki, S., Sato, S. & Hattori, N. Genetic mutations and functions of PINK1. Trends Pharmacol. Sci. 32, 573–80 (2011).
107. Poulopoulos, M., Levy, O. A. & Alcalay, R. N. The neuropathology of genetic Parkinson's disease. Mov. Disord. 27, 831–42 (2012).
108. Iwai, A. et al. The precursor protein of non-A beta component of Alzheimer's disease amyloid is a presynaptic protein of the central nervous system. Neuron 14, 467–75 (1995).
109. Cheng, F., Vivacqua, G. & Yu, S. The role of α-synuclein in neurotransmission and synaptic plasticity. J. Chem. Neuroanat. 42, 242–8 (2011).
110. Davidson, W. S. Stabilization of alpha -Synuclein Secondary Structure upon Binding to Synthetic Membranes. J. Biol. Chem. 273, 9443–9449 (1998).
111. HAN, H. The core Alzheimer's peptide NAC forms amyloid fibrils which seed and are seeded by ?-amyloid: is NAC a common trigger or target in neurodegenerative disease? Chemistry & Biology 2, 163–169 (1995).
112. Bartels, T., Choi, J. G. & Selkoe, D. J. α-Synuclein occurs physiologically as a helically folded tetramer that resists aggregation. Nature 477, 107–10 (2011).
113. Fauvet, B. et al. α-Synuclein in central nervous system and from erythrocytes, mammalian cells, and Escherichia coli exists predominantly as disordered monomer. J. Biol. Chem. 287, 15345–64 (2012).
114. Kalia, L. V, Kalia, S. K., McLean, P. J., Lozano, A. M. & Lang, A. E. α-Synuclein oligomers and clinical implications for Parkinson disease. Ann. Neurol. 73, 155–69 (2013).
115. Lynch-Day, M. A., Mao, K., Wang, K., Zhao, M. & Klionsky, D. J. The role of autophagy in Parkinson's disease. Cold Spring Harbor perspectives in medicine 2, a009357 (2012).
116. Xilouri, M., Brekk, O. R. & Stefanis, L. Alpha-synuclein and protein degradation systems: a reciprocal relationship. Mol. Neurobiol. 47, 537–51 (2013).
117. Ebrahimi-Fakhari, D., McLean, P. J. & Unni, V. K. Alpha-synuclein's degradation in vivo: opening a new (cranial) window on the roles of degradation pathways in Parkinson disease. Autophagy 8, 281–3 (2012).

118. Dawson, T. M. & Dawson, V. L. The role of parkin in familial and sporadic Parkinson's disease. Mov. Disord. 25 Suppl 1, S32–9 (2010).
119. Winklhofer, K. F. & Haass, C. Mitochondrial dysfunction in Parkinson's disease. Biochim. Biophys. Acta 1802, 29–44 (2010).
120. Schapira, A. H. et al. Mitochondrial complex I deficiency in Parkinson's disease. J. Neurochem. 54, 823–7 (1990).
121. Bové, J., Prou, D., Perier, C. & Przedborski, S. Toxin-induced models of Parkinson's disease. NeuroRx 2, 484–94 (2005).
122. Silvestri, L. et al. Mitochondrial import and enzymatic activity of PINK1 mutants associated to recessive parkinsonism. Hum. Mol. Genet. 14, 3477–92 (2005).
123. Zhou, C. et al. The kinase domain of mitochondrial PINK1 faces the cytoplasm. Proc. Natl. Acad. Sci. U.S.A. 105, 12022–7 (2008).
124. Kim, Y. et al. PINK1 controls mitochondrial localization of Parkin through direct phosphorylation. Biochem. Biophys. Res. Commun. 377, 975–80 (2008).
125. Plun-Favreau, H. et al. The mitochondrial protease HtrA2 is regulated by Parkinson's disease-associated kinase PINK1. Nat. Cell Biol. 9, 1243–52 (2007).
126. Pridgeon, J. W., Olzmann, J. A., Chin, L.-S. & Li, L. PINK1 protects against oxidative stress by phosphorylating mitochondrial chaperone TRAP1. PLoS Biol. 5, e172 (2007).
127. Martins, L. M. et al. Neuroprotective role of the Reaper-related serine protease HtrA2/Omi revealed by targeted deletion in mice. Mol. Cell. Biol. 24, 9848–62 (2004).
128. Park, J. et al. Mitochondrial dysfunction in Drosophila PINK1 mutants is complemented by parkin. Nature 441, 1157–61 (2006).
129. Clark, I. E. et al. Drosophila pink1 is required for mitochondrial function and interacts genetically with parkin. Nature 441, 1162–6 (2006).
130. Deas, E., Wood, N. W. & Plun-Favreau, H. Mitophagy and Parkinson's disease: the PINK1-parkin link. Biochim. Biophys. Acta 1813, 623–33 (2011).
131. Whitworth, A. J. & Pallanck, L. J. The PINK1/Parkin pathway: a mitochondrial quality control system? J. Bioenerg. Biomembr. (2009).
132. Vincow, E. S. et al. The PINK1-Parkin pathway promotes both mitophagy and selective respiratory chain turnover in vivo. Proc. Natl. Acad. Sci. U.S.A. 110, 6400–5 (2013).
133. LaVoie, M. J., Ostaszewski, B. L., Weihofen, A., Schlossmacher, M. G. & Selkoe, D. J. Dopamine covalently modifies and functionally inactivates parkin. Nat. Med. 11, 1214–21 (2005).
134. Wang, C. et al. Stress-induced alterations in parkin solubility promote parkin aggregation and compromise parkin's protective function. Hum. Mol. Genet. 14, 3885–97 (2005).
135. Zhang, L. et al. Mitochondrial localization of the Parkinson's disease related protein DJ-1: implications for pathogenesis. Hum. Mol. Genet. 14, 2063–73 (2005).
136. Miller, D. W. et al. L166P mutant DJ-1, causative for recessive Parkinson's disease, is degraded through the ubiquitin-proteasome system. J. Biol. Chem. 278, 36588–95 (2003).
137. Li, H.-M., Niki, T., Taira, T., Iguchi-Ariga, S. & Ariga, H. Association of DJ-1 with chaperones and enhanced association and colocalization with mitochondrial Hsp70 by oxidative stress. (2005).
138. Junn, E., Jang, W. H., Zhao, X., Jeong, B. S. & Mouradian, M. M. Mitochondrial localization of DJ-1 leads to enhanced neuroprotection. J. Neurosci. Res. 87, 123–9 (2009).
139. Cookson, M. R. Parkinsonism due to mutations in PINK1, parkin, and DJ-1 and oxidative stress and mitochondrial pathways. Cold Spring Harbor perspectives in medicine 2, a009415 (2012).
140. Wang, X. et al. Parkinson's disease-associated DJ-1 mutations impair mitochondrial dynamics and cause mitochondrial dysfunction. J. Neurochem. 121, 830–9 (2012).
141. Krebiehl, G. et al. Reduced basal autophagy and impaired mitochondrial dynamics due to loss of Parkinson's disease-associated protein DJ-1. PLoS ONE 5, e9367 (2010).
142. Irrcher, I. et al. Loss of the Parkinson's disease-linked gene DJ-1 perturbs mitochondrial dynamics. Hum. Mol. Genet. 19, 3734–46 (2010).
143. Larsen, N. J., Ambrosi, G., Mullett, S. J., Berman, S. B. & Hinkle, D. A. DJ-1 knock-down impairs astrocyte mitochondrial function. Neuroscience 196, 251–64 (2011).
144. Giaime, E., Yamaguchi, H., Gautier, C. A., Kitada, T. & Shen, J. Loss of DJ-1 does not affect mitochondrial respiration but increases ROS production and mitochondrial permeability transition pore opening. PLoS ONE 7, e40501 (2012).
145. Hao, L.-Y., Giasson, B. I. & Bonini, N. M. DJ-1 is critical for mitochondrial function and rescues PINK1 loss of function. Proc. Natl. Acad. Sci. U.S.A. 107, 9747–52 (2010).
146. Song, D. D., Shults, C. W., Sisk, A., Rockenstein, E. & Masliah, E. Enhanced substantia nigra mitochondrial pathology in human alpha-synuclein transgenic mice after treatment with MPTP. Exp. Neurol. 186, 158–72 (2004).
147. Martin, L. J. et al. Parkinson's disease alpha-synuclein transgenic mice develop neuronal mitochondrial degeneration and cell death. J. Neurosci. 26, 41–50 (2006).
148. Hsu, L. J. et al. alpha-synuclein promotes mitochondrial deficit and oxidative stress. Am. J. Pathol. 157, 401–10 (2000).

149. Wang, X. & Michaelis, E. K. Selective neuronal vulnerability to oxidative stress in the brain. Front Ageing Neurosci 2, 12 (2010).
150. Finkel, T. Signal transduction by mitochondrial oxidants. J. Biol. Chem. 287, 4434–40 (2012).
151. D'Autréaux, B. & Toledano, M. B. ROS as signalling molecules: mechanisms that generate specificity in ROS homeostasis. Nat. Rev. Mol. Cell Biol. 8, 813–24 (2007).
152. Adam-Vizi, V. & Chinopoulos, C. Bioenergetics and the formation of mitochondrial reactive oxygen species. Trends Pharmacol. Sci. 27, 639–45 (2006).
153. Trushina, E. & McMurray, C. T. Oxidative stress and mitochondrial dysfunction in neurodegenerative diseases. Neuroscience 145, 1233–48 (2007).
154. Harman, D. Free radical theory of ageing. Mutat. Res. 275, 257–66 (1992).
155. Zhang, J. et al. Parkinson's disease is associated with oxidative damage to cytoplasmic DNA and RNA in substantia nigra neurons. Am. J. Pathol. 154, 1423–9 (1999).
156. Alam, Z. I. et al. A generalised increase in protein carbonyls in the brain in Parkinson's but not incidental Lewy body disease. J. Neurochem. 69, 1326–9 (1997).
157. Alam, Z. I. et al. Oxidative DNA damage in the parkinsonian brain: an apparent selective increase in 8-hydroxyguanine levels in substantia nigra. J. Neurochem. 69, 1196–203 (1997).
158. Perry, T. L., Godin, D. V & Hansen, S. Parkinson's disease: a disorder due to nigral glutathione deficiency? Neurosci. Lett. 33, 305–10 (1982).
159. Hirsch, E. C., Brandel, J. P., Galle, P., Javoy-Agid, F. & Agid, Y. Iron and aluminum increase in the substantia nigra of patients with Parkinson's disease: an X-ray microanalysis. J. Neurochem. 56, 446–51 (1991).
160. Dexter, D. T. et al. Increased nigral iron content and alterations in other metal ions occurring in brain in Parkinson's disease. J. Neurochem. 52, 1830–6 (1989).
161. Oakley, A. E. et al. Individual dopaminergic neurons show raised iron levels in Parkinson disease. Neurology 68, 1820–5 (2007).
162. Graham, D. G., Tiffany, S. M., Bell, W. R. & Gutknecht, W. F. Autoxidation versus covalent binding of quinones as the mechanism of toxicity of dopamine, 6-hydroxydopamine, and related compounds toward C1300 neuroblastoma cells in vitro. Mol. Pharmacol. 14, 644–53 (1978).
163. Chan, C. S. et al. "Rejuvenation" protects neurons in mouse models of Parkinson's disease. Nature 447, 1081–6 (2007).
164. Block, M. L., Zecca, L. & Hong, J.-S. Microglia-mediated neurotoxicity: uncovering the molecular mechanisms. Nat. Rev. Neurosci. 8, 57–69 (2007).
165. McGeer, P. L., Itagaki, S., Boyes, B. E. & McGeer, E. G. Reactive microglia are positive for HLA-DR in the substantia nigra of Parkinson's and Alzheimer's disease brains. Neurology 38, 1285–91 (1988).
166. Pais, T. F. et al. The NAD-dependent deacetylase sirtuin 2 is a suppressor of microglial activation and brain inflammation. The EMBO Journal advance on, (2013).
167. Botstein, D. & Fink, G. Yeast: an experimental organism for modern biology. Science (80-) 240, 1439–1443 (1988).
168. Fields, S. & Johnston, M. Cell biology. Whither model organism research? Science 307, 1885–6 (2005).
169. Outeiro, T. F. & Lindquist, S. Yeast cells provide insight into alpha-synuclein biology and pathobiology. Science 302, 1772–5 (2003).
170. Willingham, S., Outeiro, T. F., DeVit, M. J., Lindquist, S. L. & Muchowski, P. J. Yeast genes that enhance the toxicity of a mutant huntingtin fragment or alpha-synuclein. Science 302, 1769–72 (2003).
171. Giorgini, F., Guidetti, P., Nguyen, Q., Bennett, S. C. & Muchowski, P. J. A genomic screen in yeast implicates kynurenine 3-monooxygenase as a therapeutic target for Huntington disease. Nat. Genet. 37, 526–31 (2005).
172. Peña-Castillo, L. & Hughes, T. R. Why are there still over 1000 uncharacterized yeast genes? Genetics 176, 7–14 (2007).
173. Lecture, N. & Hutchinson, F. Yeast and cancer. 246–265 (2001).
174. Sherman, F. Getting started with yeast. Meth. Enzymol. 194, 3–21 (1991).
175. Giorgini, F. & Muchowski, P. J. Screening for genetic modifiers of amyloid toxicity in yeast. Meth. Enzymol. 412, 201–22 (2006).
176. Stagljar, I. Finding partners: emerging protein interaction technologies applied to signaling networks. Sci. STKE 2003, pe56 (2003).
177. Kumar, A. & Snyder, M. Emerging technologies in yeast genomics. Nat. Rev. Genet. 2, 302–12 (2001).
178. Cavadini, P., Gellera, C., Patel, P. I. & Isaya, G. Human frataxin maintains mitochondrial iron homeostasis in Saccharomyces cerevisiae. Hum. Mol. Genet. 9, 2523–30 (2000).
179. Lindquist, S., Krobitsch, S., Li, L. & Sondheimer, N. Investigating protein conformation-based inheritance and disease in yeast. Philos. Trans. R. Soc. Lond., B, Biol. Sci. 356, 169–76 (2001).

180. Knight, S. A., Kim, R., Pain, D. & Dancis, A. The yeast connection to Friedreich ataxia. Am. J. Hum. Genet. 64, 365–71 (1999).
181. Muchowski, P. J. et al. Hsp70 and hsp40 chaperones can inhibit self-assembly of polyglutamine proteins into amyloid-like fibrils. Proc. Natl. Acad. Sci. U.S.A. 97, 7841–6 (2000).
182. Meriin, A. B. et al. Huntington toxicity in yeast model depends on polyglutamine aggregation mediated by a prion-like protein Rnq1. J. Cell Biol. 157, 997–1004 (2002).
183. Hughes, R. E. et al. Altered transcription in yeast expressing expanded polyglutamine. Proc. Natl. Acad. Sci. U.S.A. 98, 13201–6 (2001).
184. Meriin, A. B. et al. Aggregation of expanded polyglutamine domain in yeast leads to defects in endocytosis. Mol. Cell. Biol. 23, 7554–65 (2003).
185. Meriin, A. B. et al. Endocytosis machinery is involved in aggregation of proteins with expanded polyglutamine domains. FASEB journal : official publication of the Federation of American Societies for Experimental Biology 21, 1915–25 (2007).
186. Sokolov, S., Pozniakovsky, A., Bocharova, N., Knorre, D. & Severin, F. Expression of an expanded polyglutamine domain in yeast causes death with apoptotic markers. Biochim. Biophys. Acta 1757, 660–6 (2006).
187. Solans, A., Zambrano, A., Rodríguez, M. & Barrientos, A. Cytotoxicity of a mutant huntingtin fragment in yeast involves early alterations in mitochondrial OXPHOS complexes II and III. Hum. Mol. Genet. 15, 3063–81 (2006).
188. Mason, R. P. et al. Glutathione peroxidase activity is neuroprotective in models of Huntington's disease. Nat. Genet. 1–8 (2013). doi:10.1038/ng.2732
189. Zhang, X. et al. A potent small molecule inhibits polyglutamine aggregation in Huntington's disease neurons and suppresses neurodegeneration in vivo. Proc. Natl. Acad. Sci. U.S.A. 102, 892–7 (2005).
190. Bodner, R. a et al. Pharmacological promotion of inclusion formation: a therapeutic approach for Huntington's and Parkinson's diseases. Proc. Natl. Acad. Sci. U.S.A. 103, 4246–51 (2006).
191. Ehrnhoefer, D. E. et al. Green tea (-)-epigallocatechin-gallate modulates early events in huntingtin misfolding and reduces toxicity in Huntington's disease models. Hum. Mol. Genet. 15, 2743–51 (2006).
192. Schwarcz, R. The kynurenine pathway of tryptophan degradation as a drug target. Curr Opin Pharmacol 4, 12–7 (2004).
193. Zwilling, D. et al. Kynurenine 3-monooxygenase inhibition in blood ameliorates neurodegeneration. Cell 145, 863–74 (2011).
194. Masliah, E. et al. Dopaminergic loss and inclusion body formation in alpha-synuclein mice: implications for neurodegenerative disorders. Science 287, 1265–9 (2000).
195. Feany, M. B. & Bender, W. W. A Drosophila model of Parkinson's disease. Nature 404, 394–8 (2000).
196. Dixon, C., Mathias, N., Zweig, R. M., Davis, D. a & Gross, D. S. Alpha-synuclein targets the plasma membrane via the secretory pathway and induces toxicity in yeast. Genetics 170, 47–59 (2005).
197. Flower, T. R. et al. YGR198w (YPP1) targets A30P alpha-synuclein to the vacuole for degradation. J. Cell Biol. 177, 1091–104 (2007).
198. Sampaio-Marques, B. et al. SNCA (α-synuclein)-induced toxicity in yeast cells is dependent on sirtuin 2 (Sir2)-mediated mitophagy. Autophagy 8, 1494–509 (2012).
199. Su, L. J. et al. Compounds from an unbiased chemical screen reverse both ER-to-Golgi trafficking defects and mitochondrial dysfunction in Parkinson's disease models. Dis Model Mech 3, 194–208
200. Flower, T. R., Chesnokova, L. S., Froelich, C. a, Dixon, C. & Witt, S. N. Heat shock prevents alpha-synuclein-induced apoptosis in a yeast model of Parkinson's disease. J. Mol. Biol. 351, 1081–100 (2005).
201. Anderson, J. P. et al. Phosphorylation of Ser-129 is the dominant pathological modification of alpha-synuclein in familial and sporadic Lewy body disease. J. Biol. Chem. 281, 29739–52 (2006).
202. Basso, E. et al. PLK2 Modulates α-Synuclein Aggregation in Yeast and Mammalian Cells. Mol. Neurobiol. (2013). doi:10.1007/s12035-013-8473-z
203. Wang, S. et al. α-Synuclein disrupts stress signaling by inhibiting polo-like kinase Cdc5/Plk2. Proc. Natl. Acad. Sci. U.S.A. 109, 16119–24 (2012).
204. Cooper, A. A. et al. Alpha-synuclein blocks ER-Golgi traffic and Rab1 rescues neuron loss in Parkinson's models. Science 313, 324–8 (2006).
205. Xiong, Y. et al. GTPase activity plays a key role in the pathobiology of LRRK2. PLoS Genet. 6, e1000902 (2010).
206. Gitler, A. D. et al. Alpha-synuclein is part of a diverse and highly conserved interaction network that includes PARK9 and manganese toxicity. Nat. Genet. 41, 308–15 (2009).
207. Chesi, A., Kilaru, A., Fang, X., Cooper, A. A. & Gitler, A. D. The role of the Parkinson's disease gene PARK9 in essential cellular pathways and the manganese homeostasis network in yeast. PLoS ONE 7, e34178 (2012).

208. Schmidt, K., Wolfe, D. M., Stiller, B. & Pearce, D. A. Cd2+, Mn2+, Ni2+ and Se2+ toxicity to Saccharomyces cerevisiae lacking YPK9p the orthologue of human ATP13A2. Biochem. Biophys. Res. Commun. 383, 198–202 (2009).

Aims of the thesis

Neurodegenerative diseases are among the most complex and puzzling of human disorders. These devastating illnesses currently do not have any effective therapies or treatments, and are thus a social and economic burden for modern society. Intense efforts are being made to unravel the mysteries underlying this group of diseases, however there is still much to be learnt and discovered. Therefore, it is of utmost importance to better understand the biological mechanisms involved in disease pathogenesis, and more importantly, to discover novel avenues for therapeutic intervention. Budding yeast have been successfully used to perform studies on these diseases that have resulted in the identification of several promising therapeutic drugs and compounds. The ease of experimental manipulation, the high conservation in basic cellular mechanisms between yeast and humans, and the well-defined genome are three of the numerous characteristics that make yeast so attractive to study neurodegenerative disorders.

The work described in this thesis has taken advantage of this simple organism to achieve the following goals:

1. Identify critical genes and major pathways or networks involved in suppression of mutant huntingtin toxicity using yeast as a model system (Chapter 2)
    1.1. Identify the genes that are differentially expressed in wild-type yeast cells and gene deletion suppressor strains expressing mutant huntingtin protein
    1.2. Find novel suppressor genes of mutant huntingtin toxicity
    1.3. Find novel pathways or networks that underlie mutant Htt toxicity suppression

2. Provide novel insights into the function of the yeast DJ-1 homologues (Chapter 3)
    2.1. Characterize the phenotypes associated with the lack of DJ-1 homologues
    2.2. Identify and characterize the pathways and biological processes that are affected by the loss of the yeast DJ-1 homologues.

3. Investigate whether DJ-1 plays a role in HD
    3.1. Characterize the levels of DJ-1 and its oxidation state in HD brains and R6/2 mouse model of HD
    3.2. Investigate the effect of DJ-1 on Htt toxicity and aggregation

Chapter 2

Functional gene expression profiling in yeast implicates translational dysfunction in mutant huntingtin toxicity

This chapter contains parts of the following publication:

Functional gene expression profiling in yeast implicates translational dysfunction in mutant huntingtin toxicity.

Eran Tauber[1*], Leonor Miller-Fleming[1,2*], Robert P. Mason[1*], Wanda Kwan[3], Jannine Clapp[1], Nicola J. Butler[1], Tiago F. Outeiro[2,4], Paul J. Muchowski[3], and Flaviano Giorgini[1]

J. Biol. Chem. 2011 Jan 7;286(1):410–9.

*Contributed equally to the work.

[1]Department of Genetics, University of Leicester, Leicester LE1 7RH, UK,
[2]Cell and Molecular Neuroscience Unit, Instituto de Medicina Molecular, Av. Prof. Egas Moniz, 1649-028, Lisboa, Portugal,
[3]Gladstone Institute of Neurological Disease, Departments of Biochemistry and Biophysics, and Neurology, University of California, San Francisco, California, 94158, USA,
[4]Instituto de Fisiologia, Faculdade de Medicina da Universidade de Lisboa, Av. Prof. Egas Moniz, 1649-028 Lisboa, Portugal

Chapter 2. Functional gene expression profiling in yeast implicates translational dysfunction in mutant huntingtin toxicity

Abstract

Huntington's disease (HD) is a neurodegenerative disorder caused by the expansion of a polyglutamine tract in the huntingtin (Htt) protein. To uncover candidate therapeutic targets and networks involved in pathogenesis we integrated gene expression profiling and functional genetic screening to identify genes critical for mutant Htt toxicity in yeast. Using mRNA profiling we have identified genes differentially expressed in wild-type yeast in response to mutant Htt toxicity, as well as in three toxicity suppressor strains: *bna4*Δ, *mbf1*Δ, and *ume1*Δ. *BNA4* encodes the yeast homolog of kynurenine 3-monooxygenase (KMO), a promising drug target for HD. Intriguingly, despite playing diverse cellular roles, these three suppressors share common differentially expressed genes involved in stress response, translation elongation, and mitochondrial transport. We then systematically tested the ability of the differentially expressed genes to suppress mutant Htt toxicity when overexpressed, and have thereby identified 12 novel suppressors, including genes that play a role in stress response, Golgi to endosome transport, and rRNA processing. Integrating the mRNA profiling data and the genetic screening data we have generated a robust network which shows enrichment in genes involved in rRNA processing and ribosome biogenesis. Strikingly, these observations implicate dysfunction of translation in the pathology of HD. Recent work has shown that regulation of translation is critical for lifespan extension in *Drosophila* and that manipulation of this process is protective in Parkinson's disease models. In total these observations suggest that pharmacological manipulation of translation may have therapeutic value in HD.

Introduction

Since the cloning of the HD disease gene in 1993, several transgenic models of HD have been generated in a variety of organisms, including yeast, *Caenorhabditis elegans*, *Drosophila*, and mice. These models have allowed researchers to explore the underlying mechanisms of HD pathogenesis, as well as to perform genetic screens and to test candidate therapeutic compounds. Yeast models have proven to be particularly powerful and facile for high-throughput approaches as well as for molecular genetic manipulations [1]. While not all aspects of pathogenesis can be studied in a single-cell

organism like yeast, expression of a mutant Htt fragment in yeast produces several HD-relevant phenotypes such as formation of mutant Htt-containing aggregates, transcriptional dysregulation, cellular toxicity, perturbations in kynurenine pathway metabolites, increased levels of reactive oxygen species (ROS), mitochondrial dysfunction, defects in endocytosis, and apoptotic events [2].

In a genome-wide screen we identified 28 gene deletions that suppress toxicity of a mutant Htt fragment (Htt103Q) in yeast [3]. We focus on three of these suppressor genes in this study: *BNA4*, *UME1 and MBF1.*

The suppressor BNA4

BNA4 encodes the yeast homolog of the mammalian enzyme kynurenine 3-mononygenase (KMO), a promising therapeutic target for HD. KMO is an enzyme that catalyzes the hydroxylation of kynurenine in the kynurenine pathway (KP), the major route for tryptophan degradation (Fig. 2.1) [4]. In the brain, KMO is predominantly expressed in microglia [5]. The KP is implicated in several other diseases, including cerebral malaria and Alzheimer's disease (AD) [6].

Three KP metabolites are known to be neuroactive: quinolinic acid (QUIN), 3-hydroxykynurenine (3-HK), and kynurenic acid (KYNA). Increased levels of 3-HK and QUIN, which are downstream of KMO, have both been shown to be neurotoxic and have been implicated in the pathophysiology of HD (reviewed in [5]). QUIN is a weak, though specific agonist of NMDA receptors, present in low concentrations in brain tissue (Fig. 1.4). It exerts an excitatory effect when levels are elevated, and it has been observed in high levels in the brain of patients with initial stages of HD [7]. Interestingly, intrastriatal injection of QUIN in rodents recapitulates some of the cardinal features of the disease [8]. In addition to the activation of NMDA receptors, QUIN is thought to cause toxicity by the generation of free radicals [9]. Unlike QUIN, 3-HK is not known to bind directly to any receptor, but it leads to the production of reactive oxygen species and potentiates QUIN-induced neurotoxicity [10]. In contrast, the kynurenic acid (KYNA) is neuroprotective, acting as an NMDA receptor antagonist [11].

The KP metabolites and enzymes are well conserved between yeast and humans, and the genetics of the pathway has been extensively characterized in yeast (Fig. 2.1) [4]. This pathway has been dissected in yeast with regards to its influence on mutant Htt toxicity, and it was found that much like in HD patients the levels of 3-HK and QUIN are increased in cells expressing a toxic mutant Htt fragment [3,12]. It was found that genetic or pharmacological inhibition of Bna4 in yeast lowers the levels of these

metabolites and ameliorates disease-relevant phenotypes. These results were further validated in a HD Drosophila model [13] and, excitingly, it was shown that the oral administration of a prodrug which releases a KMO inhibitor leads to neuroprotection in HD and AD mouse models [14].

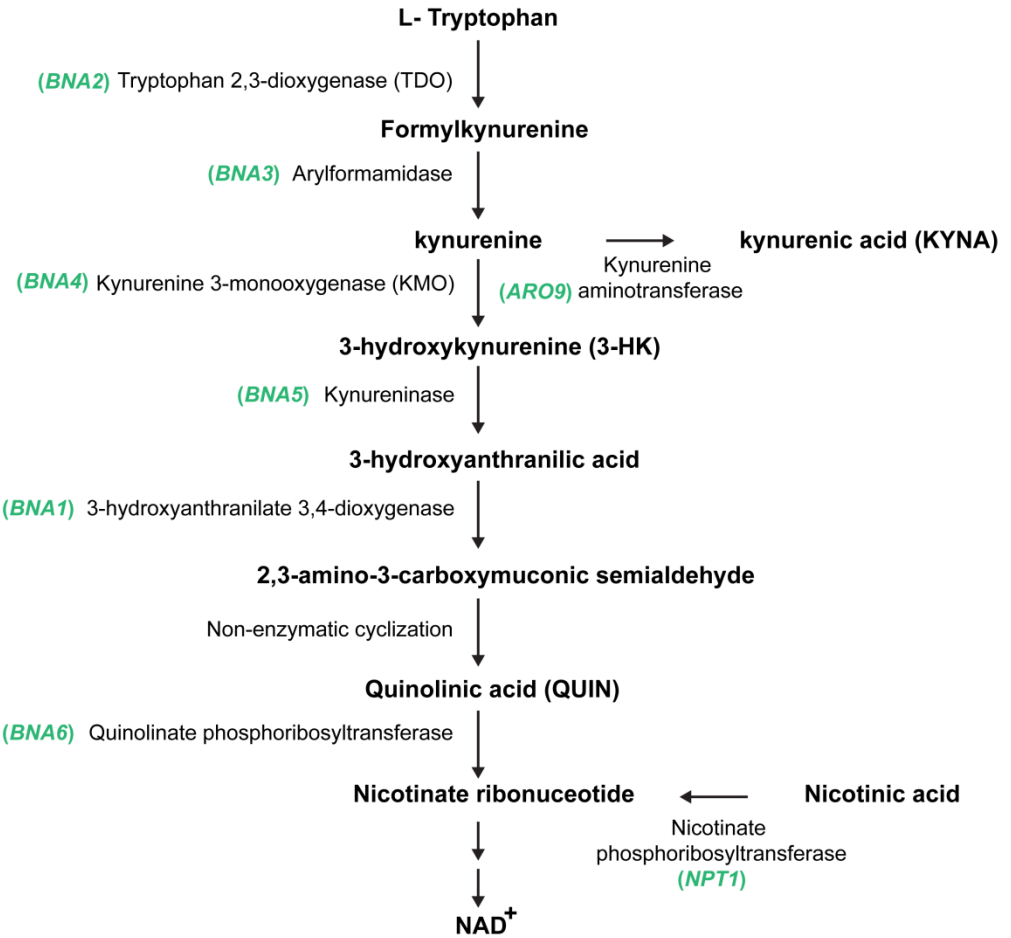

Figure 2.1. Kynurenine pathway in mammalian and yeast.
The enzymes playing a role in kynurenine pathway are represented on the left side of the arrows. In green is shown the yeast gene that encodes the respective enzyme.

The suppressor UME1

Ume1 is a component of the Rpd3 histone deacetylase (HDAC) complex in yeast. Several studies in fly and mouse models of HD have shown that inhibition of HDAC function either pharmacologically or genetically ameliorates HD-relevant phenotypes [15]. In addition, HDAC inhibitors decrease the levels of 3-HK and KMO activity in R6/2 HD model mice and in primary microglia cultured from these animals [16]. Interestingly, HDAC5 expression is increased in the cerebellum of HD patients, whereas several acetylated core histones are decreased, suggesting that indeed acetylation and

consequently transcription are dysregulated in patients [17]. Ume1 is required for full transcriptional repression of a subset of genes in yeast, in a mechanism requiring Rpd3 and Sin3 [18], suggesting that genetic inhibition of the yeast Rpd3 HDAC complex relieves polyQ toxicity in a mechanism similar to that observed in fly and mouse polyQ disease models. It was previously found that in *ume1*Δ cells expressing Htt103Q both kynurenine pathway genes (*BNA1*, *BNA2*, *BNA4*, *BNA5*) and kynurenine pathway metabolites (3-HK and QUIN) are downregulated as compared to wild-type cells expressing the same construct [8]. Interestingly, the genes downregulated in wild-type cells expressing Htt103Q cells are enriched for Rpd3-target genes. These observations directly link transcriptional dysregulation and perturbations in the kynurenine pathway in HD [8].

The suppressor MBF1

MBF1 encodes a transcriptional coactivator conserved from yeast to humans that bridges the DNA-binding region of transcriptional activator Gcn4 and TATA-binding protein (TBP) Spt15, a general transcription factor required for transcription by the three nuclear RNA polymerases (I, II, III) [19,20]. Interestingly, a polyQ expansion in TBP in humans leads to Spinocerebellar ataxia 17, which in many patients has phenotypes indistinguishable from HD [21]. Gcn4 is considered to be the master regulator of amino acid metabolism in yeast. It is a member of the AP-1 family of transcription factors, and regulates the expression of genes involved in 19 out of 20 amino acid biosynthetic pathways, purine biosynthesis, autophagy (*ATG1*, *ATG13*, *ATG14*), and multiple stress responses [22]. In addition, it has been observed that ~90 *RPL* (Ribosomal Protein, Large subunit) and *RPS* (Ribosomal Protein, Small subunit) genes which encode ribosomal proteins are repressed by activation of Gcn4 under stress conditions [22].

Here, we expand on our previous studies by using a unique combination of functional approaches and differential gene expression analysis on a genome-wide scale. In order to identify critical genes/pathways/networks involved in suppression of mutant Htt toxicity, we employ oligonucleotide microarray analysis to identify genes differentially expressed in mutant Htt expressing cells compared to controls, as well as in three suppressor deletion strains expressing a toxic mutant Htt fragment: *bna4*Δ, *mbf1*Δ, and *ume1*Δ. We next functionally interrogate 380 of these differentially expressed genes (DEGs) by testing the effect of overexpression of the respective ORFs on mutant Htt toxicity in yeast, and thereby identify 14 DEGs that modulate mutant Htt

toxicity. In total this work identifies ribosomal biogenesis and rRNA processing as critical cellular processes modulated in eukaryotic cells expressing a mutant Htt fragment, which suggests these processes are likely relevant to HD pathophysiology and therapy.

Results

Yeast expressing a mutant Htt fragment differentially express genes involved in ribosome biogenesis and rRNA processing

We recently performed oligonucleotide microarray hybridization assays to compare mRNA expression profiles of isogenic parental yeast (BY4741, MAT a) expressing either a wild-type or mutant Htt fragment (Htt25Q or Htt103Q, respectively) [16]. Here we re-analysed the data from this experiment using the limma package implemented in R/Bioconductor [23,24].This analysis showed that in Htt103Q-expressing cells, expression of 226 genes was up-regulated when compared to Htt25Q-expressing cells, whereas expression of 244 genes was down-regulated (q value < 0.2) (Fig. 2.2). A subset of these DEGs were analysed and confirmed via quantitative real-time PCR (QPCR) (Appendix 2.1).

We used the DAVID Bioinformatics Resources Functional Annotation Tool (http://david.abcc.ncifcrf.gov) to test whether the DEGs were enriched by known or predicted function using gene ontology (GO) [25]. In a manner similar to our previous analysis, functional groups upregulated significantly in the Htt103Q expressing cells included genes involved in protein folding ($p < 1.0 \times 10^{-3}$) and response to stress ($p < 0.01$) (Appendix 2.2) [16]. In addition, the new analysis found enrichment in the GO terms of response to unfolded protein ($p < 1.0 \times 10^{-5}$), ubiquitin cycle ($p < 0.01$), post-translational protein modification ($p < 0.01$), and vacuolar protein catabolic process ($p < 0.05$). We previously described that downregulated genes in Htt103Q-expressing cells were involved in the functional groups of ribosome biogenesis ($p < 1.0 \times 10^{-39}$) and rRNA processing and metabolism ($p < 1.0 \times 10^{-20}$) [16], and we have confirmed those observations in our new analyses (Appendix 2.3). These data suggest that yeast cells expressing Htt103Q mount a response to deal with this toxic, misfolded protein, via upregulation of proteins involved with protein misfolding, protein degradation, autophagy, and stress response. At the same time, in a manner similar to classic heat

shock response, the presence of Htt103Q in yeast cells causes a dramatic reduction in expression of genes involved in rRNA metabolism and ribosome biogenesis, suggesting that general protein synthesis in these cells is significantly repressed, ultimately contributing to Htt103Q-dependent toxicity.

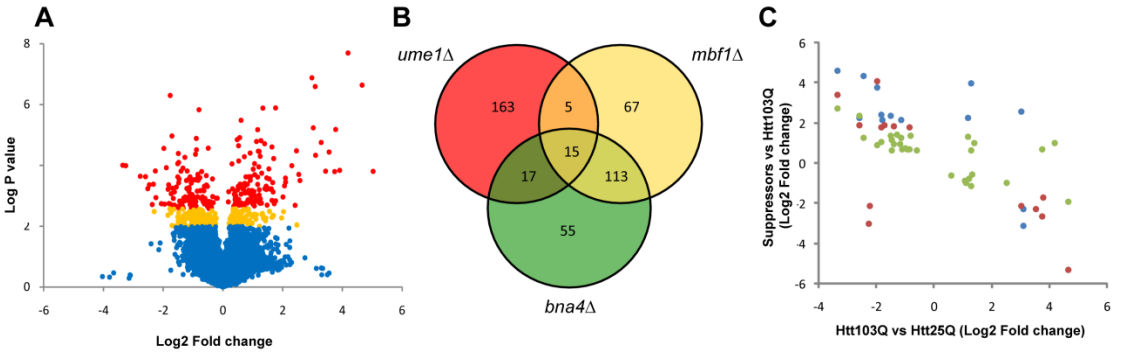

Figure 2.2. Identification of DEGs in wild-type and gene deletion suppressor strains expressing Htt103Q.

(**A**) Volcano plot of DEGs. The log2 of the fold change (Htt103Q versus Htt25Q) is represented on the x-axis and the negative log of P-values from t-test analyses is represented on the y-axis. Upregulated genes due to Htt103Q have positive fold-changes. Red indicates DEGs at the FDR of q < 0.1, orange indicates 0.1 < q < 0.2, and blue indicates q > 0.2. (**B**) Venn diagram indicating the overlap in DEGs between *bna4*Δ *mbf1*Δ, and *ume1*Δ strains expressing Htt103Q compared to the parental BY4741 strain expressing Htt103Q. 15 DEGs are shared among the three deletion strains. (**C**) Inverse correlation of log fold change (M) in DEGs in suppressors expressing Htt103Q on the y-axis and in a wild-type strain expressing Htt103Q (compared with Htt25Q-expressing cells) on the x-axis. Blue: *bna4*Δ (r=-0.77, t = -4.19, df = 12, P < 0.01), Red: *mbf1*Δ (r= -0.74, t = -4.10, df = 14, P = 0.01), Green: *ume1*Δ (r=-0.67, t = -4.84, df = 29, P < 0.0001).

Common mechanisms underlie mutant Htt toxicity suppression in gene deletion suppressor strains

In order to discern if there are common mechanisms underlying toxicity suppression in mutant Htt suppressor strains, we next monitored gene expression perturbations in three gene deletion Htt103Q suppressor strains: *bna4*Δ, *mbf1*Δ, and *ume1*Δ [3]. Thus, we performed microarray experiments to identify DEGs in *bna4*Δ, *mbf1*Δ, or *ume1*Δ yeast expressing Htt103Q versus parental wild-type cells expressing Htt103Q. We tested the 200 DEGs which showed the highest fold change (and q < 0.1) from each deletion suppressor for enrichment of GO terms. We found that in *bna4*Δ cells expressing Htt103Q there is an enrichment of several GO terms as compared to control cells, including carboxylic acid metabolism ($p < 1.0 \times 10^{-4}$), translation elongation ($p < 1.0 \times 10^{-3}$), nitrogen compound metabolism ($p < 1.0 \times 10^{-3}$), water-soluble vitamin

biosynthesis ($p < 0.01$), and vesicle organization and biogenesis ($p < 0.05$)(Appendix 2.4). DEGs in *mbf1*Δ cells showed enrichment in many GO term categories, including amino acid metabolism ($p < 1.0 \times 10^{-11}$), nitrogen compound metabolism ($p < 1.0 \times 10^{-9}$), carboxylic acid metabolism ($p < 1.0 \times 10^{-7}$), and urea cycle intermediate metabolic process ($p < 1.0 \times 10^{-4}$) (Appendix 2.5). The *ume1*Δ suppressor strain exhibited DEGs with enrichment in GO term categories of water-soluble vitamin biosynthesis ($p < 0.01$), NAD biosynthesis ($p < 0.01$), nitrogen compound metabolism ($p < 0.01$), carboxylic acid metabolism ($p < 0.05$), among others (Appendix 2.6). The four genes present within the NAD biosynthesis GO group are the central kynurenine pathway genes of *BNA1*, *BNA2*, *BNA4*, and *BNA5*, confirming our original analysis with this data set [16]. It is critical to note that while some of the GO groups enriched in these data are specific to individual suppressors, several categories are common amongst these suppressors, such as nitrogen compound metabolism and carboxylic acid metabolism.

As full levels of Htt103Q toxicity are dependent upon the presence of the Rnq1 yeast prion [RNQ^+] [26], we analysed Rnq1 prion status in the three gene deletion strains to ensure that the DEGs identified above are independent of Rnq1 prion. To this end, we analysed Rnq1 by sedimentation analysis in all three suppressor strains (Fig. 2.3A,B). We found that in all three strains Rnq1 was present in the pellet fraction of cells expressing Htt103Q or carrying empty vector (pYES2), indicating that Rnq1 is present in its prion form independent of Htt103Q expression. Interestingly, in the case of the *bna4*Δ strain, we observed that Rnq1 is also present in the soluble fraction, suggesting that this population of cells contains both prion and non-prion forms of Rnq1 (Fig. 2.3B). A similar phenotype has been described with other deletion strains from this library(30). Treatment with the prion curing agent GuHCl shifted Rnq1 from the pellet fraction to the soluble fraction, providing further support that Rnq1 status is “mixed” in the *bna4*Δ strain (Fig. 2.3B). To test whether prion status was directly altered by the deletion of *BNA4* we analysed a second *bna4*Δ strain, and consistent with previously published work [27], we found that Rnq1 was entirely in prion form, indicating that the “mixed” prion phenotype is independent of *BNA4* deletion (Fig. 2.3C). In total this data suggests that DEGs identified in the *mbf1*Δ and *ume1*Δ strains are independent of Rnq1 prion status, while a subset of DEGs from the BY4741 *bna4*Δ strain may arise from [RNQ^+]-dependent modulation of Htt103Q.

In order to filter out DEGs dependent upon modulation of Rnq1 prion status, and to ascertain if common genes/mechanisms underlie suppression in the three suppressor strains, we cross-compared the three sets of DEGs identified above (Fig.

2.2B). Strikingly, we found that 15 annotated genes were common among these three groups, seven of which are also differentially expressed in wild-type cells expressing Htt103Q (Table 2.1). Assuming independence, the probability of finding 15 genes shared amongst these three groups is < 1.0×10^{-13}, which supports the notion that the suppressors share common mechanisms of mutant Htt suppression. The genes shared among the suppressor strains function in a variety of cellular processes, including translation elongation (*ANB1*), stress response (*DAK2*), amino acid transport (*DIP5*), lactate metabolism (*DLD3*), and mitochondrial transport (*YMC2*). Interestingly, 3 of the 15 genes are predicted to encode tRNAs, all of which are down-regulated in the suppressor strains. Of these genes, 2 encode tRNAs for tRNA-Pro and one encodes tRNA-Lys (Table 2.1). In 13/15 cases the genes are differentially expressed in the same direction in all three suppressor strains, reinforcing the notion that the shared DEGs represent common underlying mechanisms involved in mutant Htt toxicity. Intriguingly, of these 13 genes, 5 are differentially expressed in the opposite direction in Htt103Q-expressing cells (*AQR1*, *DAK2*, *YGR035C*, *YMC2*, *YOR338W*)(Table 2.1 and Appendix 2.7).

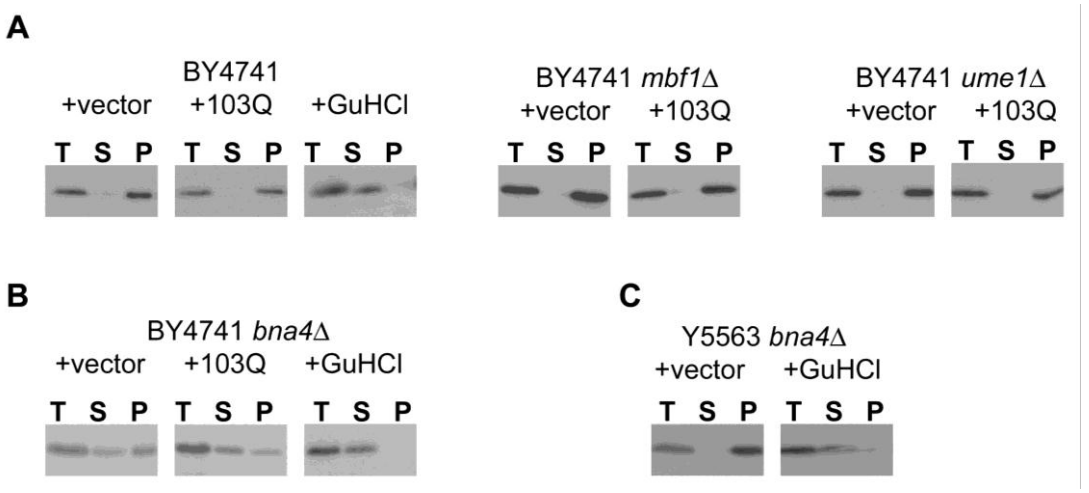

Figure 2.3. Rnq1p is present in prion conformation in gene deletion suppressor strains.

[RNQ^+] prion status in wild-type yeast and deletion suppressors (BY4741 parental strain) carrying the pYES2 empty vector or expressing Htt103Q was determined by a combination of high-speed centrifugation and immunoblotting. "T" indicates total extract for each yeast strain, while "S" indicates supernatant fraction (soluble form of Rnq1), and "P" indicates pellet fraction (prion form of Rnq1, [RNQ^+]). (**A**) Immunoblotting with α-Rnq1 antibody showed that Rnq1 is found exclusively in the pellet fraction of the BY4741 wild-type strain, as well as the *mbf1*Δ and *ume1*Δ strains, indicating the protein is in the prion conformation. (**B**) In the BY4741 *bna4*Δ strain, [RNQ^+] prion status is "mixed", with protein present in both pellet and supernatant fractions. Treatment of BY4741 *bna4*Δ and parental cells carrying pYES2 with guanidine hydrochloride (GuHCL) cures [RNQ^+] prion, shifting Rnq1p from the pellet fraction to the supernatant fraction. (**C**) [RNQ^+] prion status is independent of *BNA4* deletion. In Y5563 *bna4*Δ

cells all Rnq1 is found in the pellet fraction. Treatment of Y5563 *bna4*Δ cells with GuHCL cured [RNQ^{+}] prion present in the pellet fraction of untreated cells carrying pYES2, moving Rnq1 to the supernatant fraction.

This observation led us to compare the DEGs from the individual suppressor strains to the top 200 DEGs from Htt103Q expressing cells to ascertain if a negative correlation exists in expression between these groups of DEGs. Strikingly, in all three comparisons we found a significant negative correlation in differential expression of the overlapping genes (Fig. 2.2C). This suggests that the differential expression observed in the parental wild-type strain due to expression of Htt103Q is relieved in the three deletion suppressor strains. Though it is likely that these changes in expression profiles directly contribute to mutant Htt toxicity, we cannot exclude the possibility that the changes are simply a downstream consequence of cellular toxicity.

Table 2.1. Common DEGs between *bna4*Δ, *mbf1*Δ, and *ume1*Δ suppressor strains expressing Htt103Q as compared to the parental BY4741 wild-type strain expressing Htt103Q.

Gene	Htt103Q	*bna4*Δ	*mbf1*Δ	*ume1*Δ	Function
ANB1	n/c	Up	Up	Up	Translation elongation factor eIF-5A
AQR1	Down	Up	Up	Up	Plasma membrane multidrug transporter
COS7	Up	Up	Up	Down	Mitochondrial protein of unknown function
DAK2	Up	Down	Down	Down	Dihydroxyacetone kinase
DIP5	n/c	Up	Up	Up	Dicarboxylic amino acid permease
DLD3	n/c	Up	Up	Up	D-lactate dehydrogenase
LYS20	n/c	Up	Up	Up	Homocitrate synthase isozyme
MMP1	n/c	Up	Up	Up	High-affinity S-methylmethionine permease
SPG4	Up	Up	Down	Down	Protein required for survival at high temperatures
SUF2	n/c	Down	Down	Down	tRNA-Pro, 1 of 3 nuclear tRNAs; anticodon AGG
SUF10	n/c	Down	Down	Down	tRNA-Pro, 1 of 3 nuclear tRNAs; anticodon AGG
tK(CUU)J	n/c	Down	Down	Down	tRNA-Lys, imported into mitochondria; AAG
YGR035C	Down	Up	Up	Up	Protein of unknown function, Cdc28 substrate
YMC2	Down	Up	Up	Up	Mitochondrial inner membrane transporter
YOR338W	Down	Up	Up	Up	Protein of unknown function; regulated by Azf1

Shaded areas indicate genes differentially expressed in all three suppressor strains, as well as in Htt103Q-expressing parental cells (in the opposite direction). Htt103Q differential expression is related to Htt25Q-expressing parental cells ($q < 0.2$). DEGs in the three suppressor strains expressing Htt103Q (*bna4*Δ, *mbf1*Δ, and *ume1*Δ are relative to parental cells expressing Htt103Q (top 200 annotated genes, $q < 0.1$).

Cis-regulatory domain analysis of DEGs identifies enriched elements

To clarify whether common regulatory mechanisms were affected in Htt103Q-expressing cells as compared to Htt25Q controls, the DEGs with local false discovery rate (FDR) < 2%, as estimated by the Rank product algorithm (n=46), were analysed for shared regulatory motifs using the MUSA algorithm. This analysis revealed 14 families of *de novo* motifs that were significantly over-represented in these sequences [28] (Table 2.2). Aligning the Position Weight Matrix (PWM) of each family with the PWM of known transcription factors revealed several matches. Interestingly, Gcn4 was among the transcription factors identified, suggesting a link between response to Htt103Q-dependent toxicity and this transcription factor. The list of transcription factors identified includes several zinc transcription factors such as Hap1 (which responds to heme and oxygen levels), Azf1 (responds to glucose) and Zap1 (responds to zinc levels).

Table 2.2. Families of over-represented motifs in promoter regions of genes differentitally expressed in Htt103Q versus Htt25Q yeast cells

Family	Count*	P-value	Transcription factors**
TTTATAT	26	1.77e-06	Mig2p, Hap1p, Fzf1p, Zap1p
TTCTTTTC	17	3.59e-06	Azf1p, Cup2p, Zap1p, Ime1p
AAAAGAAA	22	9.24e-06	Azf1p, Zap1p, Cup2p, Tec1p
CATCGC	22	3.33e-05	Hap1p, Rfx1p, Ime1p, Rox1p,
GCGATG	22	3.33e-05	Hap1p, Rfx1p, Ime1p, Rox1p
CGCACA	21	0.000104	Crz1p, Hap1p, Aft2p, Stp2p
TGTGCG	21	0.000104	Crz1p, Aft2p, Stp2p, Hap1p
AAGAAG	39	0.000146	Tec1p, Azf1p, Zap1p, Azf1p
ATATTAT	24	0.000166	Arg81p, Arr1p, Mig1p,Mig3p
TTCTTC	39	0.000257	Tec1p, Zap1p, Abf1p, Ime1p
GCACGT	18	0.000573	Gcn4p, Met4p, Mig3p, Pho4p
ACGTGC	18	0.000573	Gcn4p, Pho4p, Met4p, Mig1p
GCGGCT	16	0.000988	Ume6p, Abf1p, Mig2p, Mig3p
AGCCGC	16	0.000988	Ume6p, Stp1p, Mig1p, Stp2p

* Count represents the number of sequences containing at least one motif in the family (out of 46).
** Only top four matches are listed for each family.

Other candidate transcription factors include Cup2, a copper-binding transcription factor which responds to copper levels, and Ime1, which is the master regulator of meiosis, and activates early meiotic genes through interactions with Ume6 [29], another transcription factor whose binding site was over-represented in the DEGs (Table 2.2).

Ume6 recruits the Rpd3-Sin3 HDAC complex during mitosis to repress early meiosis-specific genes via hypoacetylation of histones H3 and H4 [30]. Critically, Ume6 has been shown by affinity mass spectrometry to be a component of the Rpd3-Sin3 corepressor complex along with the loss-of-function Htt103Q suppressors Ume1 and Rxt3 [3,31]. Thus, this observation further implicates transcriptional dysregulation in mutant Htt toxicity and HDACs as candidate therapeutic targets.

A unique subset of differential expressed, highly interconnected genes modulate mutant Htt toxicity

In order to ascertain the potential role of the DEGs in mutant Htt toxicity, we individually tested the ability of these genes to suppress toxicity of Htt103Q when individually overexpressed in yeast. The genes available as ORFs constructs from the Yeast ORF Collection (380/470, 80.9%) were individually tested via growth assays for suppression of Htt103Q toxicity. We found that 12 of the DEGs suppressed toxicity of Htt103Q when overexpressed (Fig. 2.4A, Table 2.3). To eliminate the possibility that the DEGs suppressed toxicity by silencing Htt103Q expression, we analysed expression levels by Western and dot blotting, and found that Htt103Q expression was unchanged (Fig. 2.4B,C). However, an increase in soluble Htt103Q-GFP is observed in suppressor strains (Fig. 2.3B), suggesting decreased levels of aggregated Htt103Q-GFP. In addition, we confirmed that Rnq1 remains in its prion conformation when expression of a DEG is induced (Fig. 2.4D).

Interestingly, these overexpression suppressors include genes whose expression is upregulated as well as genes whose expression is downregulated in cells expressing Htt103Q, indicating two different models for overexpression protection: 1) ORF overexpression mimics upregulation of genes exerting a protective role against mutant Htt toxicity, or 2) ORF overexpression is rescuing a depletion of a critical factor (Table 2.3). Excitingly, these overexpression suppressors are potential candidate therapeutic targets for HD. Of the 12 novel suppressors, 7 (~ 58%) have human orthologs as determined by Ensembl Genome Browser (http://www.emsembl.org).

We next compared our list of DEGs with our previously published gene deletion enhancers and suppressors of mutant Htt toxicity, and identified another two common genes (*MBF1*, *APJ1*) [3,32]. Thus, in total we identified 14 DEGs that modify mutant Htt toxicity when overexpressed or deleted (Table 2.3). Amongst these 14 genes, we observed enrichment of genes within seemingly unrelated functional groups. Approximately half of the genes (*BUD23*, *DBP2, IPI3, NSA2*, *RRP9, UTP9*) are involved

in the processing of rRNAs. Interestingly, these were all significantly downregulated. The remaining genes are involved in stress/heat shock response (*APJ1*, *JJJ3*), and transcription (*CSE2* and *MBF1*) (Table 2.3). Aside from rRNA processing, all of these functional groups have been extensively implicated in HD pathology.

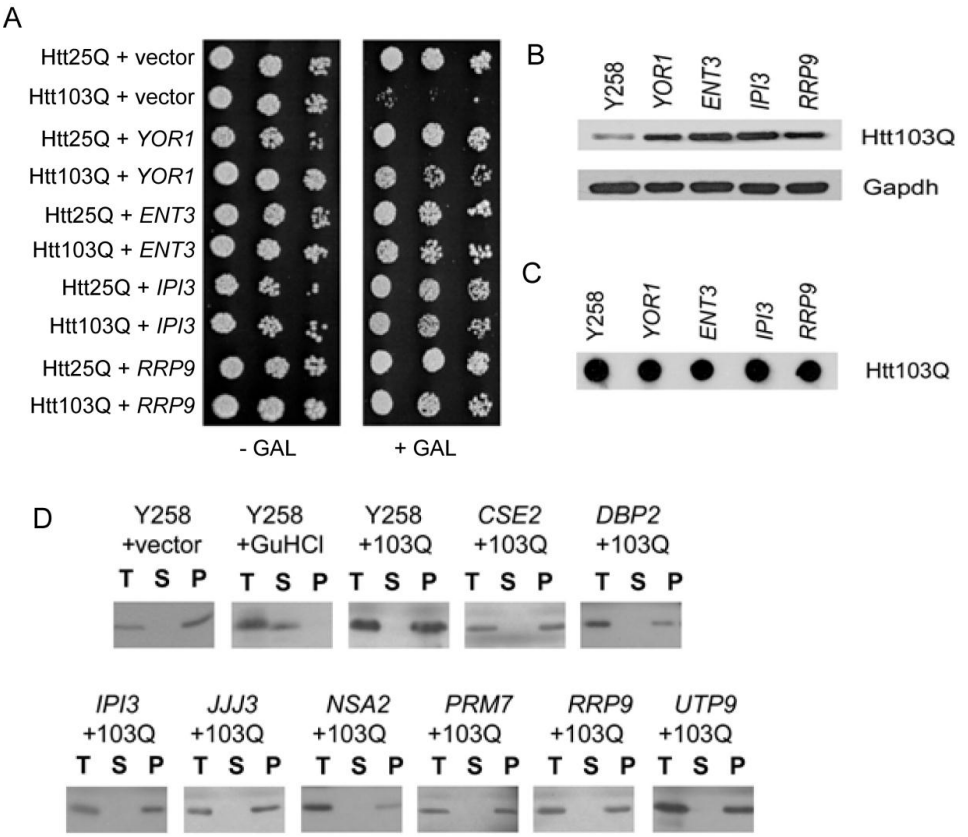

Figure 2.4. Suppression of Htt103Q toxicity in yeast overexpression strains.
(A) Wild-type Y258 strain overexpressing YOR1, ENT3, IPI3 and RRP9 were independently transformed with p425-Htt25Q and p425-Htt103Q. Cellular viability was determined by growth assays. Five-fold serial dilutions starting with equal number of cells are shown. Expression of Htt and the indicated yeast ORF was induced by galactose. (B) Expression levels of soluble Htt103Q-GFP in the wild-type strain expressing the indicated ORFs or carrying an empty vector (p425) were analysed by immunoblotting with a GFP antibody. GAPDH levels, detected with a GAPDH antibody, were used as loading control. (C) Equal amounts of the extracts in panel B were analysed by dot immunoblotting to quantify total levels of Htt103Q-GFP (soluble and aggregated), which showed no change in total Htt103Q-GFP expression levels in the suppressor strains (D) Rnq1 prion status with ORF suppressors (Y258 parental strain) expressing Htt103Q was determined by a combination of high-speed centrifugation and immunoblotting. “T” indicates total extract for each yeast strain, while “S” indicates supernatant fraction (soluble form of Rnq1), and “P” indicates pellet fraction (prion form of Rnq1). Immunoblotting with α-Rnq1 antibody showed that Rnq1 is found in the pellet fraction for all suppressors, indicating the protein is in the prion conformation. The Y258 strain carrying empty vector (p425) or Htt103Q serve as a positive control, and treatment of cells carrying p425 with guanidine hydrochloride (GuHCL) cures Rnq1 prion, shifting this protein from the pellet fraction to the supernatant fraction.

Table 2.3. DEGs in Htt103Q expressing cells modulate mutant Htt toxicity

Suppressor	Ortholog(s)*	Expression**	Function
BUD23	+	Down	rRNA processing
CSE2	-	Up	RNA pol II transcription
DBP2	+	Down	rRNA processing
ENT3	+	Up	Golgi-endosome transport
IPI3	-	Down	rRNA processing
JJJ3	-	Down	HSP40 chaperone
NSA2	+	Down	rRNA processing
PRM7	-	Down	pheromone response
RAS1	+	Down	G-protein signaling
RRP9	+	Down	rRNA processing
UTP9	-	Down	rRNA processing
YOR1	+	Down	ABC transporter
Deletion Suppressor			
*mbf1*Δ	+	Up	transcriptional coactivator
Deletion Enhancer			
*apj1*Δ	+	Up	HSP40 chaperone

*Human orthologs determined via the Ensembl Genome Browser. Orthologs may be either 1-to-1, 1-to-many, or many-many. *BUD23*, *ENT3*, *NSA2*, *RRP9*, and *MBF1* have 1-to-1 orthologs in humans which could potentially be targeted for therapeutics. **Refers to direction of differential expression in Htt103 versus Htt25Q cells.

To clarify the functional connectivity amongst this functionally validated list of DEGs we performed network analysis using the Osprey Network Visualization System (Version 1.2.0), which allows visualization of complex interaction networks [33]. This software is powered by the BioGRID database (http://www.thebiogrid.org), which houses and distributes data collections of protein and genetic interactions of model organisms, including yeast via the *Saccharomyces* Genome Database (http://www.yeastgenome.org). Via these databases, Osprey allows insertion of all known interactions for each "node" (gene of interest). The interactions types (or "edges") include data from affinity capture experiments, two-hybrid screens, and synthetic lethality analyses, among others. Here, we have used Osprey to investigate all the known genetic and physical interactions of the 14 functionally validated DEGs. As an initial test, we asked for all the interactions within these 14 nodes. Interestingly, we found only one interaction amongst these nodes, a physical interaction between Rrp9 and Utp9, both of which are components of the small ribosomal subunit (SSU) processome involved in pre-rRNA processing, as determined by affinity capture/mass spectroscopy studies [34–36] (data not shown). This result highlights our observations from

the GO analysis that showed enrichment in genes from disparate functional groups. In order to determine if the above 14 genes function indirectly in the same network, we explored all of the interactions for these functionally validated nodes, and we found a total of 538 interactions among 464 nodes (data not shown). In order to select genes with higher level relationships, we processed the network data with an iterative minimum filter of two, which identified all of the nodes within this group which have a minimum of two interactions with other genes within the group, and then sorted the remaining nodes by GO function (Fig. 2.5). This analysis uncovered a highly interconnected network of genes, which surprisingly included 11/14 of the original functionally validated genes. Critically, this network of 81 nodes (with 156 edges) reinforced and expanded the GO groups enriched in the mutant Htt toxicity interaction network: ribosome biogenesis and assembly (71.6%, $p = 1.2 \times 10^{-49}$), rRNA processing (55.6%, $p = 4.7 \times 10^{-43}$), nuclear transport (12.3%, $p = 1.5 \times 10^{-4}$), and G-protein signaling (2.5%, $p = 4.5 \times 10^{-2}$). When a more stringent iterative minimum filter of three is applied, 5/14 modifiers are still present in the network (11 nodes; 23 edges), all of which are involved in ribosome biogenesis and assembly ($p = 2.6 \times 10^{-12}$), rRNA processing ($p = 1.2 \times 10^{-8}$), and related processes (data not shown). In total, this work suggests that though these modifiers of mutant Htt toxicity play roles in disparate functional groups, they function within a highly-interrelated network.

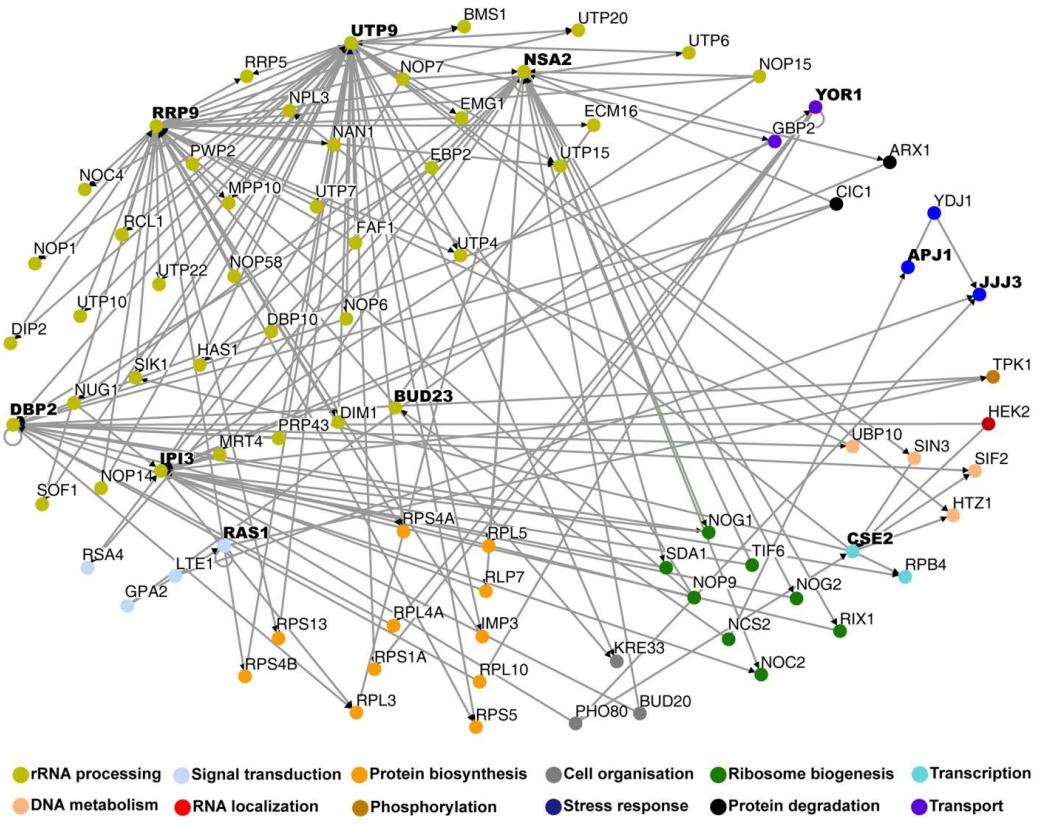

Figure 2.5. Network analysis uncovers a high degree of interconnectivity amongst functionally validated DEGs.
(see previous page for figure) Osprey network analysis of 14 DEGs (indicated in bold) which suppress toxicity of Htt103Q when overexpressed. All interactions for these genes (both physical and genetic) were included in the analysis. Genes described by the same significantly enriched GO terms are color-coded and grouped together. Network data analysed with an iterative minimum filter of 2 (minimum of 2 interactions with other network genes). A total of 81 nodes and 156 edges define this network, which contains 11 of the original 14 functionally validated genes.

Discussion

In this study we utilized a novel functional approach to gene profiling experiments in order to dissect the underlying mechanisms of mutant Htt toxicity in yeast. This work has not only highlighted the central role of rRNA processing and ribosome biogenesis in mutant Htt toxicity in yeast, but has also identified several novel suppressors of this toxicity which are candidate therapeutic targets for HD. Several gene profiling experiments with mammalian models of HD support our observations. Gene expression profiling in PC12 cells and rat striatal cells expressing mutant Htt fragments has found an enrichment in genes encoding ribosomal proteins and RNA processing proteins [37,38]. In addition, analysis of gene expression in the striatum of R6/2 HD model mice has found an enrichment in genes encoding ribosomal proteins as compared to wild-type controls [39]. Recently, microarray profiling using a primary rat neuron model of HD found enrichment in genes involved in RNA splicing/RNA processing [40]. Finally, an RNAi screen in *Drosophila* cells identified several modifiers of mutant Htt aggregation which play a role in RNA processing [41]. In total, these observations suggest that the results described here are not likely to be yeast-specific, but may reflect cellular perturbations conserved in mammalian cells. In addition, in this study we identified DEGs from *bna4*Δ, *mbf1*Δ, and *ume1*Δ strains expressing Htt103Q versus control cells to learn more about underlying mechanisms contributing to Htt103Q toxicity suppression. Analysis of prion status in these strains found that in the *bna4*Δ strain Rnq1 is present in both prion and soluble forms, suggesting that a subset of these DEGs may arise from modulation of [RNQ^+] status. Thus, in order to reduce [RNQ^+]-dependent effects we focused on the cross-section of these DEGs with the DEGs from the *mbf1*Δ and *ume1*Δ strains. By this approach we identified 15 common DEGs amongst these three gene deletion suppressor strains. These genes include 3 tRNA-encoding genes, as well as genes involved in a variety of cellular pathways. What is

unclear in the examples above is the mechanism of these changes, and how these changes contribute to mutant Htt toxicity, and ultimately to HD pathology. These yeast studies will serve as a strong starting point for future studies elucidating these underlying mechanisms.

A critical finding from this study is the identification of a robust network of interactions derived from 14 differentially expressed genes (nodes) that modulate toxicity of a mutant Htt fragment. Despite the original nodes playing roles in diverse cellular processes, the resulting network contains 11 of these nodes within a network of 81 nodes and 156 edges, and has an enrichment of genes involved in rRNA processing and ribosome biogenesis. Intriguingly, several of the functionally validated nodes appear to be highly interconnected in the network (nodes indicated in bold in Figure 2.5), underscoring the importance of these nodes within the context of the network.

Several of our observations above implicate Gcn4 in mutant Htt toxicity in yeast. First, we found that Gcn4 binding sequences are over-represented in the upstream regions of genes differentially expressed in Htt103Q-expressing cells. Second, *MBF1*, which is a deletion suppressor of Htt103Q toxicity, encodes a transcriptional coactivator which can bridge Gcn4 and TBP. Third, expression of Htt103Q in yeast leads to downregulation of genes involved in ribosome biogenesis, and under stress conditions Gcn4 is known to repress transcription of ~90 *RPL* and *RPS* genes which encode ribosomal proteins [22]. In total this work suggests that expression of Htt103Q in yeast may downregulate expression of ribosomal genes via induction of Gcn4 expression. As Mbf1 expression is required for Gcn4 function, these observations collectively suggest that deletion of *MBF1* may suppress mutant Htt toxicity by impairing Gcn4 function. It must also be noted that induction of Gcn4 leads to upregulation of three kynurenine pathway genes, *BNA1* (3-hydroxyanthranilate 3,4-dioxygenase), *BNA4* (which encodes KMO), and *BNA6* (quinolinate phosphoribosyl transferate) [22]. Intriguingly, deletions of either *BNA1* or *BNA4* suppresses toxicity of Htt103Q [3]. These observations also support a hypothesis in which Gcn4 induction due to Htt103Q expression contributes to toxicity. We did not, however, see differential expression of *GCN4* in our present study in Htt103Q-expressing cells (data not shown). This is not particularly surprising as *GCN4*, which is under strict transcriptional control, is also under translational control, via four small upstream ORFs (uORFs) in the 5' leader region of the *GCN4* mRNA [42]. Induction of translation occurs primarily under environmental stresses [43]. In addition, as recruitment of TBP via Mbf1 is the rate-limiting step in Gcn4 activation [19], and *MBF1* expression is upregulated in Htt103Q-expressing yeast (Table 2.3), it is possible that

increased levels of Mbf1 alone may be sufficient to increase Gcn4 activity, without induction of Gcn4 expression. Interestingly, lifespan extension in yeast due to depletion of 60s ribosomal subunits, dietary restriction, or TOR inhibition appears to require induction of Gcn4 [44]. Thus, in the case of mutant Htt expression, Gcn4 induction may reflect a cellular coping mechanism gone awry. This pathway may play a similar role in humans as ATF4, the functional ortholog of Gcn4 in mammals [45], is regulated via a similar translational mechanism and activation of Gcn4 is analogous to the mammalian integrated stress response [46].

In a related note, the yeast eIF4E-associated protein Eap1, which inhibits cap-dependent translation initiation via the TOR signaling cascade, attenuates induction of Gcn4 translation [47]. Recent work has shown that overexpression of eIF4E-BP, the Eap1 functional equivalent in *Drosophila*, rescues parkinsonian phenotypes in fly models of PD by inhibiting cap-dependent translation, and thereby inducing expression of genes involved in stress response [48]. It has also been seen that during dietary restriction in *Drosophila* 4E-BP promotes lifespan extension by activation of nuclear-encoded mitochondrial protein translation [49]. Interestingly, in the present study we have found that the gene encoding eIF5A, a translation elongation factor, is upregulated in all three suppressor strains expressing Htt103Q, as compared to controls. Taken together, these data suggest that altered regulation of translation may be contributing to mutant Htt toxicity, and that pharmacological modulation of this process may have therapeutic relevance. Supporting this, it has been shown that rapamycin treatment of mouse embryonic fibroblast cells expressing mutant Htt abrogates HD-relevant phenotypes by inhibition of translation, independent of effects on autophagy [50]. It has also been observed that normal Htt localizes to neuronal RNA granules – cellular structures involved in mRNA transport and storage [51]. A recent study showed that mutant Htt interact with several ribosomal proteins and translation initiation factors and moreover that wild-type and mutant Htt impair the translation of a mRNA reporter [52]. It is also important to note that while much interest in the HD community has been focused on transcriptional dysregulation in pathogenesis and as a target for therapeutics, our study suggests that the effect of mutant Htt on translational processes in the cell may also be critical.

As most basic cellular mechanisms are conserved in yeast to higher eukaryotes, the work presented here will likely inform future studies on disease pathogenesis in HD. Due to the ease and rapidity of genetic screening in yeast, this organism is particularly amenable for integrated approaches to functional gene expression profiling. Yeast will

therefore likely provide an important platform for future analyses of disease genes, further evidenced by a recent study dissecting α-synuclein toxicity in yeast [53]. It is important to mention that we have identified 12 novel suppressors of mutant Htt toxicity in yeast, 7 of which have human orthologs as determined by the Ensembl Genome Browser. Four of these yeast genes (*BUD23*, *ENT3*, *NSA2*, and *RRP9*) have clear 1-to-1 orthologs in humans which could potentially be targeted for therapy if validated in other model systems. Interestingly, *ENT3* has recently been identified as a suppressor of α-synuclein toxicity in yeast [54].

In summary, our study has provided new insights into the mechanisms associated with mutant Htt toxicity in yeast which may be relevant to HD pathogenesis and has also identified novel candidate targets for therapeutic intervention in this disorder. Clearly it is now critical to test the above hypotheses and to validate the candidate HD targets identified in order to ascertain how our observations are linked to mutant Htt toxicity in yeast and how they may inform therapeutic strategies in HD patients. Finally, the power of using yeast to clarify mechanisms involved in HD pathogenesis and to identify candidate drug targets is underscored by the recent validation of KMO as a promising therapeutic target in HD model mice [14].

Materials and Methods

Yeast strains and DNA constructs

The strains used for microarray experiments were from the yeast gene deletion set in the MATa (BY4741) [*MAT*a *his3*Δ1 *leu2*Δ0 *met15*Δ0 *ura3*Δ0] strain background (Open Biosystems). The Y258 strain background [*MAT*a *pep*4-3, *his*4-580, *ura*3-53, *leu*2-3,112] was used for the overexpression studies (Open Biosystems). The constructs pYES2-Htt25Q-GFP and pYES2-Htt103Q-GFP [55] were used for the microarray studies. Htt103Q is a galactose (GAL)-inducible, FLAG- and GFP-tagged construct encoding the first 17 amino acids of Htt fused to a polyQ tract of 103 glutamines. The constructs p425*GALL*-Htt25Q-GFP and p425*GALL*-Htt103Q-GFP were used in the yeast overexpression studies and were generated by amplifying the huntingtin constructs from pYES2-Htt25Q-GFP and pYES2-Htt103Q-GFP and cloning into the *Spe*I and *Xho*I sites of p425*GALL*(17).

Yeast total RNA preparation

SC –Ura galactose (2%) cultures (12 ml) were inoculated at OD_{600} 0.2 and incubated with shaking at 30º C until reaching an OD_{600} of ~1.0. Cells were harvested and lysed with acid-washed glass beads. Total RNA was isolated with Qiagen RNeasy Midi kits, following standard protocols.

Gene expression analysis by DNA oligonucleotide arrays

Double-stranded cDNA was synthesized from total RNA, amplified as cRNA, labeled with biotin, and hybridized to Affymetrix Yeast Genome S98 Array GeneChips, which were washed and scanned at the University of Washington Center for Expression Arrays and at the J. David Gladstone Institutes Genomics Core Laboratory, University of California, San Francisco according to manufacturer protocols. Images were processed with Affymetrix Microarray Suite 5.0 (MAS-5). The quality of hybridization and overall chip performance were determined from the MAS-5 generated report file.

Analysis of Microarray Data

The statistical computing language R [56] was used for quality controls, pre-processing and analyses of the data. The quality of the microarrays was assessed by inspecting pseudo-images of the arrays, MA scatter plots of the arrays versus a pseudo-median reference chip, and histogram and boxplot of raw log intensities. Expression data are available through the Gene Expression Omnibus (GEO) database, accession number GSE18644. The data were analysed using the R bioconductor package affylmGUI (version 1.8.0), the graphic interface to limma (version 2.9.17) [24]. Data were normalized and summarised using the GCRMA method [57] DEGs were identified by using a moderated t-test (limma). To correct for multiple comparison we have estimated the false-discovery rate (FDR) using the QVALUE package [58] with a typical FDR threshold (q) of 10%. Gene ontology searches were performed with the DAVID Functional Annotation Tool (http://david.abcc.ncifcrf.gov/home.jsp). Network visualization was performed using the Osprey Network Visualization System (Version 1.2.0), which is powered by the BioGRID database (http://www.thebiogrid.org) [33]. Cis-regulatory elements of the DEGs were identified using the MUSA algorithm [28] in the YEASTRACT suite [59]. The Position Weight Matrix of each family was used to search for known transcription factor binding sites in the YEASTRACT database using the Smith-Waterman local alignment algorithm (using the sum of the squared distances metric).

Real-Time Quantitative PCR

The BY4741 yeast strain was transformed independently with pYES2-Htt103Q-GFP and pYES2-Htt25Q [55] by standard procedures. Yeast cells were grown overnight in complete media lacking uracil (SC-URA) containing glucose (2%) as a carbon source. Cultures were diluted back to optical density 0.4 and grown in SC-URA containing galactose (2%) to induce protein expression. Cells were harvested after growing until mid-log phase, pelleted and stored at -80ºC until needed. RNA was extracted using the Qiagen RNeasy Midi kits following manufacturer instructions. Genomic DNA contamination was removed from RNA using Turbo DNAse according to the manufacturer's protocol. 500 ng of RNA was used as a template to synthesize cDNA with the Qiagen QuantiTect® Reverse Transcription kit. To ensure that RNA had no genomic DNA contamination a control reaction was included in which no reverse transcription was carried out. 17 genes were selected to analyse the mRNA expression levels by quantitative PCR and actin-1 was chosen as a reference. Reactions were carried out in a LightCycler Real-Time PCR System (Roche). cDNA was quantified using 5 ul of Sybr Green (Fermentas) and 0.3 uM of forward and reverse primers. Primers were analysed for specificity and efficiency by melting curve analysis. The efficiency was calculated at the end of each amplification reaction via relative standard curves. PCR efficiencies ranged from 0.80 to 1.0. Standard curves were calculated using the amplification of 5 serial dilutions of genomic DNA in triplicate. At least three independent cDNA samples were analysed. PCR reactions were run in duplicate. Relative quantification was performed using LightCycler® 480 Relative Quantification Software. The crossing points were calculated by the second derivative method and relative expression was calculated by the available advanced relative quantification. Further analysis and statistical tests were performed using the Relative Expression Software 2008 (REST) [60,61]. The relative quantification was corrected for PCR efficiency via both methods.

Functional Testing of DEGs

Yeast strains containing plasmids for the overexpression of selected genes were obtained from the yeast ORF collection in the Y258 strain background. The relevant yeast strains were grown overnight in 96 well plates containing 100 µl of SC-URA supplemented with 2% glucose per well and transformed with either p425*GALL*-Htt25Q-GFP or p425*GALL*-Htt103Q-GFP using a high throughput transformation method [1]. Transformants were grown to stationary phase in complete media lacking

uracil and leucine (SC–Ura–Leu) containing 2% glucose, serial diluted, and spotted onto SC-Ura-Leu media supplemented with either 2% glucose or 2% galactose and 2% raffinose. Plates were incubated at 30˚C for 3-5 days and yeast strains scored for growth.

Determination of RNQ prion status

20 ml cultures of suppressor strains were grown to approximately an OD_{600} 1.0 in SC – Ura GAL/RAF media, at which point cells were harvested by centrifugation at 3000 rpm for 5 min. Cell pellets were washed with 10 ml water and spun as above. The cell pellets were resuspended in 200 µl lysis buffer (100 mM Tris pH 7.0, 200 mM NaCl, 1mM EDTA, 5% glycerol, 0.5 mM DTT, 1X protease inhibitor cocktail) and transferred to microfuge tubes. The cells were lysed by addition of ~200 µl of acid washed glass beads (425-600 µm, Sigma, St. Louis, MO), vortexing for 1 min, addition of 200 µl of RIPA buffer (50 mM Tris pH 7.0, 200 mM NaCl, 1% Triton, 0.5 % Na-deoxycholate, 0.1% SDS), and further vortexing for 10 sec. Samples were then centrifuged at 3000 rpm for 15 sec to pellet the glass beads and cell debris. 60 µl of supernatant was used as the “Total” sample, while 200 µl of the supernatant was centrifuged for 30 min at 80,000 rpm in the Beckman TLA 100 Ultracentrifuge. 60 µl of the supernatant from this step was isolated and used at the “Soluble” fraction, while the “Pellet” fraction was prepared by resuspending the pellet in 100 µl of lysis buffer and 100 µl of RIPA buffer, adding 67 µl of 4X protein sample buffer (SB), and boiling for 5 minutes. 20 µl of 4X SB was added to the “Total” and “Soluble” fractions, and boiled for 5 min. The samples were resolved by SDS-PAGE and immunoblotting as described above. Curing yeast strains of endogenous prion cells was performed by growth for 5 passages on YPD supplemented with 5 mM guanidine hydrochloride (GuHCl) [62].

Htt103Q Expression Levels

In order to analyse the level of Htt103Q protein expression in the yeast strains, protein extracts were analysed by immunoblotting. SC –Ura -Leu GAL yeast cultures were inoculated from overnight SC –Ura -Leu raffinose (RAF) cultures to an OD600 ~0.4, and were grown under inducing conditions for 5-6 hours. Cells were lysed by mechanical disruption with acid washed glass beads (425-600 µm, Sigma, St. Louis, MO) and lysis buffer (50 mM Tris pH 7.5; 1X protease inhibitor cocktail, Roche), vortexing seven times for 30 sec each, with 1 min incubations on ice in between. Glass beads and cell debris were removed by centrifugation and protein extracts were quantified using the BioRad

Protein Assay (BioRad, Hercules, CA). For SDS-PAGE, extracts were mixed with 4x Protein Sample Buffer (200mM Tris-HCl, 8% SDS, 40% glycerol, 0.4% bromophenol blue, 6% β-mercaptoethanol), boiled 10 min, and subjected to electrophoresis in 12% SDS-polyacrylamide gel. The proteins were transferred to nitrocellulose membranes. For dot blots, extracts were mixed with 2% SDS and captured in nitrocellulose membrane by vacuum. Htt103Q-GFP was identified by a monoclonal α-GFP antibody (Santa Cruz Biotechnology, Inc), used at a 1:1000 dilution while the GAPDH loading control was detected using α-GAPDH antibody (Ambion) at 1:4000 dilution. These incubations were followed by a α-Mouse Ig horseradish peroxidase conjugated antibody (Amersham Bioscience, Piscataway, NJ) at 1:10000 dilution. Detection was done by enhanced chemiluminescence (ECL) (Amersham Bioscience, Piscataway, NJ) and exposure to X-ray film.

Acknowledgments

F.G. is supported by the Medical Research Council, the CHDI Foundation, and the Huntington's Disease Association. P.J.M. is supported by National Institute of Neurological Disease Grant NS47237. T.F.O. is supported by EMBO and Marie Curie IRG. L.M. is supported by the Fundação para a Ciência e a Tecnologia (FCT). We would like to thank M. Sherman and A. Meriin for the pYES2-Htt25Q and pYES2-Htt103Q constructs.

References

1. Giorgini, F. & Muchowski, P. J. Screening for genetic modifiers of amyloid toxicity in yeast. Meth. Enzymol. 412, 201–22 (2006).
2. Giorgini, F. & Muchowski, P. J. Exploiting yeast genetics to inform therapeutic strategies for Huntington's disease. Methods Mol. Biol. 548, 161–74 (2009).
3. Giorgini, F., Guidetti, P., Nguyen, Q., Bennett, S. C. & Muchowski, P. J. A genomic screen in yeast implicates kynurenine 3-monooxygenase as a therapeutic target for Huntington disease. Nat. Genet. 37, 526–31 (2005).
4. Panozzo, C. et al. Aerobic and anaerobic NAD+ metabolism in Saccharomyces cerevisiae. FEBS Lett. 517, 97–102 (2002).
5. Thevandavakkam, M. A., Schwarcz, R., Muchowski, P. J. & Giorgini, F. Targeting Kynurenine 3-Monooxygenase Therapy in Huntington ' s Disease (KMO): Implications for. (2010).
6. Schwarcz, R. The kynurenine pathway of tryptophan degradation as a drug target. Curr Opin Pharmacol 4, 12–7 (2004).
7. Guidetti, P., Luthi-Carter, R. E., Augood, S. J. & Schwarcz, R. Neostriatal and cortical quinolinate levels are increased in early grade Huntington's disease. Neurobiol. Dis. 17, 455–61 (2004).
8. Schwarcz, R., Whetsell, W. & Mangano, R. Quinolinic acid: an endogenous metabolite that produces axon-sparing lesions in rat brain. Science (80-) 219, 316–318 (1983).
9. Santamaría, A. et al. Copper blocks quinolinic acid neurotoxicity in rats: contribution of antioxidant systems. Free Radic. Biol. Med. 35, 418–27 (2003).
10. Guidetti, P. & Schwarcz, R. 3-Hydroxykynurenine potentiates quinolinate but not NMDA toxicity in the rat striatum. Eur. J. Neurosci. 11, 3857–63 (1999).

11. Foster, A. C., Vezzani, A., French, E. D. & Schwarcz, R. Kynurenic acid blocks neurotoxicity and seizures induced in rats by the related brain metabolite quinolinic acid. Neurosci. Lett. 48, 273–8 (1984).
12. Giorgini, F. et al. Histone deacetylase inhibition modulates kynurenine pathway activation in yeast, microglia, and mice expressing a mutant huntingtin fragment. J. Biol. Chem. 283, 7390–400 (2008).
13. Campesan, S. et al. The kynurenine pathway modulates neurodegeneration in a Drosophila model of Huntington's disease. Curr. Biol. 21, 961–6 (2011).
14. Zwilling, D. et al. Kynurenine 3-monooxygenase inhibition in blood ameliorates neurodegeneration. Cell 145, 863–74 (2011).
15. Kazantsev, A. G. & Thompson, L. M. Therapeutic application of histone deacetylase inhibitors for central nervous system disorders. Nat Rev Drug Discov 7, 854–68 (2008).
16. Giorgini, F. et al. Histone deacetylase inhibition modulates kynurenine pathway activation in yeast, microglia, and mice expressing a mutant huntingtin fragment. J. Biol. Chem. 283, 7390–400 (2008).
17. Yeh, H. H. et al. Histone deacetylase class II and acetylated core histone immunohistochemistry in human brains with Huntington's disease. Brain Res. 1504, 16–24 (2013).
18. Mallory, M. J. & Strich, R. Ume1p represses meiotic gene transcription in Saccharomyces cerevisiae through interaction with the histone deacetylase Rpd3p. J. Biol. Chem. 278, 44727–34 (2003).
19. Takemaru, K., Harashima, S., Ueda, H. & Hirose, S. Yeast coactivator MBF1 mediates GCN4-dependent transcriptional activation. Mol. Cell. Biol. 18, 4971–6 (1998).
20. Takemaru, K. i, Li, F. Q., Ueda, H. & Hirose, S. Multiprotein bridging factor 1 (MBF1) is an evolutionarily conserved transcriptional coactivator that connects a regulatory factor and TATA element-binding protein. Proc. Natl. Acad. Sci. U.S.A. 94, 7251–6 (1997).
21. Stevanin, G. et al. Huntington's disease-like phenotype due to trinucleotide repeat expansions in the TBP and JPH3 genes. Brain 126, 1599–603 (2003).
22. Natarajan, K. et al. Transcriptional profiling shows that Gcn4p is a master regulator of gene expression during amino acid starvation in yeast. Mol. Cell. Biol. 21, 4347–68 (2001).
23. Reimers, M. & Carey, V. J. Bioconductor: an open source framework for bioinformatics and computational biology. Meth. Enzymol. 411, 119–34 (2006).
24. Wettenhall, J. M., Simpson, K. M., Satterley, K. & Smyth, G. K. affylmGUI: a graphical user interface for linear modeling of single channel microarray data. Bioinformatics 22, 897–9 (2006).
25. Huang, D. W., Sherman, B. T. & Lempicki, R. a. Systematic and integrative analysis of large gene lists using DAVID bioinformatics resources. Nat Protoc 4, 44–57 (2009).
26. Meriin, A. B. et al. Aggregation of expanded polyglutamine domain in yeast leads to defects in endocytosis. Mol. Cell. Biol. 23, 7554–65 (2003).
27. Manogaran, A. L., Fajardo, V. M., Reid, R. J. D., Rothstein, R. & Liebman, S. W. Most, but not all, yeast strains in the deletion library contain the [PIN(+)] prion. Yeast 27, 159–66 (2010).
28. Mendes, N. D. et al. MUSA: a parameter free algorithm for the identification of biologically significant motifs. Bioinformatics 22, 2996–3002 (2006).
29. Kassir, Y. et al. Transcriptional regulation of meiosis in budding yeast. Int. Rev. Cytol. 224, 111–71 (2003).
30. Kadosh, D. & Struhl, K. Repression by Ume6 involves recruitment of a complex containing Sin3 corepressor and Rpd3 histone deacetylase to target promoters. Cell 89, 365–71 (1997).
31. Carrozza, M. J. et al. Stable incorporation of sequence specific repressors Ash1 and Ume6 into the Rpd3L complex. Biochim. Biophys. Acta 1731, 77–87; discussion 75–6 (2005).
32. Willingham, S., Outeiro, T. F., DeVit, M. J., Lindquist, S. L. & Muchowski, P. J. Yeast genes that enhance the toxicity of a mutant huntingtin fragment or alpha-synuclein. Science 302, 1769–72 (2003).
33. Breitkreutz, B.-J., Stark, C. & Tyers, M. Osprey: a network visualization system. Genome Biol. 4, R22 (2003).
34. Collins, S. R. et al. Toward a comprehensive atlas of the physical interactome of Saccharomyces cerevisiae. Mol. Cell Proteomics 6, 439–50 (2007).
35. Gavin, A.-C. et al. Proteome survey reveals modularity of the yeast cell machinery. Nature 440, 631–6 (2006).
36. Grandi, P. et al. 90S pre-ribosomes include the 35S pre-rRNA, the U3 snoRNP, and 40S subunit processing factors but predominantly lack 60S synthesis factors. Mol. Cell 10, 105–15 (2002).
37. Wyttenbach, A. et al. Polyglutamine expansions cause decreased CRE-mediated transcription and early gene expression changes prior to cell death in an inducible cell model of Huntington ' s disease. 10, 1829–1845 (2001).
38. Sipione, S. et al. Early transcriptional profiles in huntingtin-inducible striatal cells by microarray analyses. Hum. Mol. Genet. 11, 1953–65 (2002).
39. Crocker, S. F., Costain, W. J. & Robertson, H. A. DNA microarray analysis of striatal gene expression in symptomatic transgenic Huntington's mice (R6/2) reveals neuroinflammation and insulin associations. Brain Res. 1088, 176–86 (2006).

40. Runne, H. et al. Dysregulation of gene expression in primary neuron models of Huntington's disease shows that polyglutamine-related effects on the striatal transcriptome may not be dependent on brain circuitry. J. Neurosci. 28, 9723–31 (2008).
41. Doumanis, J., Wada, K., Kino, Y., Moore, A. W. & Nukina, N. RNAi screening in Drosophila cells identifies new modifiers of mutant huntingtin aggregation. PLoS ONE 4, e7275 (2009).
42. Hinnebusch, A. G. Evidence for translational regulation of the activator of general amino acid control in yeast. Proc. Natl. Acad. Sci. U.S.A. 81, 6442–6 (1984).
43. Hinnebusch, A. G. Translational regulation of yeast GCN4. A window on factors that control initiator-trna binding to the ribosome. J. Biol. Chem. 272, 21661–4 (1997).
44. Steffen, K. K. et al. Yeast life span extension by depletion of 60s ribosomal subunits is mediated by Gcn4. Cell 133, 292–302 (2008).
45. Lu, P. D., Harding, H. P. & Ron, D. Translation reinitiation at alternative open reading frames regulates gene expression in an integrated stress response. J. Cell Biol. 167, 27–33 (2004).
46. Mascarenhas, C. et al. Gcn4 is required for the response to peroxide stress in the yeast Saccharomyces cerevisiae. Mol. Biol. Cell 19, 2995–3007 (2008).
47. Matsuo, R. et al. The yeast eIF4E-associated protein Eap1p attenuates GCN4 translation upon TOR-inactivation. FEBS Lett. 579, 2433–8 (2005).
48. Tain, L. S. et al. Rapamycin activation of 4E-BP prevents parkinsonian dopaminergic neuron loss. Nat. Neurosci. 12, 1129–35 (2009).
49. Zid, B. M. et al. 4E-BP extends lifespan upon dietary restriction by enhancing mitochondrial activity in Drosophila. Cell 139, 149–60 (2009).
50. King, M. A. et al. Rapamycin inhibits polyglutamine aggregation independently of autophagy by reducing protein synthesis. Mol. Pharmacol. 73, 1052–63 (2008).
51. Savas, J. N. et al. A role for huntington disease protein in dendritic RNA granules. J. Biol. Chem. 285, 13142–53 (2010).
52. Culver, B. P. et al. Proteomic analysis of wild-type and mutant huntingtin-associated proteins in mouse brains identifies unique interactions and involvement in protein synthesis. J. Biol. Chem. 287, 21599–614 (2012).
53. Yeger-Lotem, E. et al. Bridging high-throughput genetic and transcriptional data reveals cellular responses to alpha-synuclein toxicity. Nat. Genet. 41, 316–23 (2009).
54. Liang, J. et al. Novel suppressors of alpha-synuclein toxicity identified using yeast. Hum. Mol. Genet. 17, 3784–95 (2008).
55. Meriin, A. B. et al. Huntington toxicity in yeast model depends on polyglutamine aggregation mediated by a prion-like protein Rnq1. J. Cell Biol. 157, 997–1004 (2002).
56. Index, R., Development, T. R. & Team, C. R : A Language and Environment for Statistical Computing. 1, (2010).
57. Wu, Z., Irizarry, R. A., Gentleman, R., Martinez-Murillo, F. & Spencer, F. A Model-Based Background Adjustment for Oligonucleotide Expression Arrays. J Am Stat Assoc 99, 909–917 (2004).
58. Storey, J. D. & Tibshirani, R. Statistical significance for genomewide studies. Proc. Natl. Acad. Sci. U.S.A. 100, 9440–5 (2003).
59. Monteiro, P. T. et al. YEASTRACT-DISCOVERER: new tools to improve the analysis of transcriptional regulatory associations in Saccharomyces cerevisiae. Nucleic Acids Res. 36, D132–6 (2008).
60. Pfaffl, M. W. A new mathematical model for relative quantification in real-time RT-PCR. Nucleic Acids Res. 29, e45 (2001).
61. Pfaffl, M. W., Horgan, G. W. & Dempfle, L. Relative expression software tool (REST) for group-wise comparison and statistical analysis of relative expression results in real-time PCR. Nucleic Acids Res. 30, e36 (2002).
62. Derkatch, I. L., Bradley, M. E., Zhou, P., Chernoff, Y. O. & Liebman, S. W. Genetic and environmental factors affecting the de novo appearance of the [PSI+] prion in Saccharomyces cerevisiae. Genetics 147, 507–19 (1997).

Chapter 3

Yeast DJ-1 family members are required for diauxic-shift reprogramming and survival in stationary phase

This chapter contains parts of the following publication (under revision):

Yeast DJ-1 family members are required for diauxic-shift reprogramming and cell survival in stationary phase

Leonor Miller-Fleming[1,2], Pedro Antas[1], Teresa F Pais[1], Joshua J Smalley[3], Flaviano Giorgini[2*] and Tiago F Outeiro[1,4,5*]

* co-corresponding authors

[1]Cell and Molecular Neuroscience Unit, Instituto de Medicina Molecular, Lisboa, Portugal
[2]Department of Genetics, University of Leicester, Leicester, UK
[3]Systems Toxicology Group Medical Research Council Toxicology Unit, University of Leicester, UK.
[4]Instituto de Fisiologia, Faculdade de Medicina, Universidade de Lisboa, Lisboa, Portugal
[5]Department of Neurodegeneration and Restorative Research, University Medical Center Göttingen, Göttingen, Germany

Chapter 3. Yeast DJ-1 family members are required for diauxic-shift reprogramming and cell survival in stationary phase

Abstract

The yeast Hsp31 mini-family – comprised of the four homologous proteins Hsp31, Hsp32, Hsp33 and Hsp34 – belongs to the conserved DJ-1 superfamily. Proteins from this superfamily are predominantly involved in protecting cells against various forms of cellular stress. DJ-1, the human homolog, is associated with autosomal recessive forms of Parkinson's disease (PD) and is thought to be involved in oxidative stress response. Despite great interest in these proteins, the function of the Hsp31 mini-family members remains unclear. In this study, we show that the Hsp31 mini-family has a role in diauxic-shift, which is characterized by metabolic reprogramming due to glucose limitation. We found that the Hsp31 genes are strongly induced in diauxic-shift and in stationary phase, and that deletion of these genes leads to reduced chronological lifespan, an inability to reprogram gene transcription at diauxic-shift, and failure to acquire several typical characteristics of stationary phase, including defective autophagy induction. In addition, carbon starvation of the gene deletion strains impaired autophagy and led to abnormal Atg13 phosphorylation mediated by TORC1. Repression of this kinase by rapamycin in the gene deletion strains completely reversed their sensitivity to heat shock. Altogether our data indicate the Hsp31 mini-family is required for diauxic-shift reprogramming and cell survival in stationary phase, and plays a role upstream of TORC1. The enhanced understanding of the cellular function of these genes sheds light on the biological role of other members of the family, including DJ-1, which is an attractive target for therapeutic intervention in cancer and in PD.

Introduction

The DJ-1 superfamily includes a vast number of conserved proteins with similar three dimensional structures distributed across Archaea, Bacteria, and Eukaryota [1–10]. Special attention has been given to the members of this family, since it includes DJ-1, a human protein that has been implicated in two major global health problems: cancer and Parkinson's disease (PD) [11–13]. Other known members of the DJ-1 superfamily include the *Escherichia coli* proteins Hsp31 (EcHsp31), YajL and YhbO, the archeal *Pyrococcus horikoshii* protein PH1704 and four orthologs in the yeast *Saccharomyces cerevisiae* (Hsp31-34). These proteins have disparate functions however they are all implicated in cellular stress response. EcHsp31 is a chaperone [14–16] that has peptidase

[17] and glyoxalase activities [18]. YajL, which shares the highest homology with human DJ-1 [8], functions as a chaperone [19], while YbhO is required for stress protection [20] and PH1704 functions as protease [3].

The human DJ-1 protein

The human protein DJ-1 – the most extensively studied protein from the DJ-1 superfamily – is a small protein of 189 amino acids that was first discovered as an oncogene that transformed NIH3T3 in association with H-Ras [13]. DJ-1 expression is found elevated in several types of cancer, including leukemia, breast cancer, primary lung cancer, prostate cancer, cervical cancer and pancreatic cancer [21–29]. The oncogenic potential is thought to be related to its role as regulator of the tumor suppressor phosphate and tensin homolog (PTEN) [22,30].

DJ-1 was first implicated in neurodegeneration when it was found that mutations in the gene *PARK7* cause autosomal-recessive early onset cases of PD [11]. Mutations in DJ-1 are thought to destabilize its structure, which results in its degradation or to affect the normal homodimerization, which is critical for its function [31]. DJ-1 is ubiquitously expressed in the body, including in the brain. It is localized mostly in the cytoplasm, but also in mitochondria and nucleus [32–36]. Interestingly, DJ-1 is secreted by different cell types [21,37,38] and it may be a potential biomarker not only for PD [39], but also for several cancer types [40–42]. In the brain, DJ-1 expression is increased in reactive astrocytes in sporadic PD patients as well as in reactive astrocytes that are under oxidative stress conditions [43,44]. DJ-1 is not present in Lewy bodies but intriguingly it is found in Pick bodies, which are a hallmark of Pick's disease that contain the tau protein [45,46].

DJ-1 has three cysteine residues C46, C56 and C106. C106 is the most conserved residue among the members of DJ-1 superfamily and it has been proposed to regulate the function and localization of DJ-1 [36,47]. It is highly susceptible to oxidation and can be oxidized to cysteine-sulfenic (SOH) or to the irreversibly oxidized cysteine-sulfinic (SO_2H) or cysteine-sulfonic acid (SO_3H); the oxidation of C106 to the SO_3H form is thought to inactivate the protein function [36,48,49]. Interestingly, DJ-1 is found oxidatively damaged in the brains of patients with idiopathic PD and Alzheimer's disease (AD) [50]. Recently, we found that DJ-1 is also highly oxidized and overexpressed in HD brains (Chapter 4) [51]. These findings suggest that oxidatively damaged DJ-1 may contribute to the pathogenesis not only of the genetic DJ-1 linked PD cases but also of idiopathic PD cases, as well as AD and HD. To study DJ-1, several models have been generated, including DJ-1 knockout mice, DJ-1 knockdown zebrafish (*Danio rerio*) and double or

single knockout fruit flies (*Drosophila melanogaster;* has two DJ-1 orthologs: DJ-1α and DJ-1β). The DJ-1 null mouse does not present observable neurodegeneration, oxidative damage, or inclusion bodies, which shows that loss of DJ-1 does not cause higher oxidative stress in basal conditions [52–54]. However, some abnormalities were observed, including increased levels of mitochondrial reactive oxygen species (ROS) in the SN and whole brain, higher vulnerability of dopaminergic neurons to MPTP and impaired dopamine signaling [52,55,56]. The DJ-1 zebrafish knockdown and *Drosophila* knockout models although do not exhibit dopaminergic neurodegeneration under basal conditions, they are more sensitive to oxidative insults, indicating that DJ-1 has a role in the antioxidants defense mechanisms [57–61]. The precise role of DJ-1 in the cell is not clear, however compelling evidence indicates that DJ-1 is a multifunctional protein associated with protection of cells from oxidative stress [62]. It has been proposed that DJ-1 acts as a redox-dependent chaperone preventing α-syn aggregation [48,63], however contradictory data raises the question of whether DJ-1 is in fact a chaperone. For instance, while one study showed that DJ-1 is able to inhibit heat-induced aggregation of citrate synthase and luciferase [64], another study employing similar experimental conditions did not replicate these results [65]. Using different cellular models it was shown that DJ-1 suppresses the toxicity of α-syn wild-type or A53T but required the heat shock protein 70 (Hsp70) activity, suggesting that the putative DJ-1 chaperone activity is weak [47]. DJ-1 was also shown to scavenge directly ROS [52], although it is not clear whether this capacity is relevant to reduce the load of ROS in the cell. Since the oxidation of DJ-1 may be irreversible, new protein would need to be synthesized in order to scavenge more ROS and therefore this function does not seem physiologically relevant [66]. Similar to the archaeal cysteine protease PH1704 from *Pyrococcus horikoshii,* several reports showed that DJ-1 is a cysteine protease [65,67,68], however others failed to detect this activity [63,69]. The comparison between the crystal structures of human DJ-1 and the archaeal protein showed that DJ-1 has an additional α-helix at the C-terminal that blocks the putative catalytic domain of protease [70]. However, it has been suggested that this helix is opened in vivo, allowing DJ-1 to act as a protease, namely on transthyretin – the protein associated with familial amyloidotic polyneuropathy [68,71]. DJ-1 has also been identified as regulator of survival and oxidative stress signaling pathways. For instance, it negatively regulates the survival pathway PTEN/PI3K pathway by direct binding to PTEN inhibiting its activity [30,72]. In addition, there are studies suggesting that DJ-1 positively regulates the nuclear factor erythroid 2-related factor 2 (Nrf2) [73–75], which is a major antioxidant transcription factor and would explain why loss of DJ-1 leads to

increased sensitivity to oxidative stress. However, contradictory results were obtained by another group that showed no physiological relation between DJ-1 and Nrf2, although the authors suggest that this interaction may be cell specific [76]. Interestingly, DJ-1 was further suggested to play a role in regulating RNA, by binding several mRNAs that encode proteins involved in several processes such as glutathione metabolism, PTEN/PI3K pathway and mitochondrial function, which are released upon oxidative stress [77,78]. This observation, if further confirmed, may explain the diversity in DJ-1 functions in just one.

Since there are many contradictory results regarding the function of DJ-1 as well as multiple proposed functions, further clarification is needed to fully understand the function of such a complex protein.

The yeast Hsp31 mini-family

The yeast *Saccharomyces cerevisiae* Hsp31 gene mini-family is comprised of Hsp31 (*YDR533C*), Hsp32 (*YMR322C*), Hsp33 (*YOR391C*), and Hsp34 (*YPL280W*). Among the four yeast DJ-1 family members, Hsp31 is the most divergent and likely gave rise to the other three paralogous proteins by genome duplication [7] (Fig. 3.1). Hsp32, Hsp33 and Hsp34 share strong sequence homology of over 90%. While *HSP32*, *HSP33* and *HSP34* localize within subtelomeric regions (within large blocks of conserved DNA that includes other genes), *HSP31* is an interstitial gene.

The name of these proteins was given after resolving the crystal structure of Hsp31. The Hsp31 standard name was based on the structural similarity it shares with the *E. coli* EcHsp31. The other three proteins were renamed due to the homology shared with Hsp31. The crystal structure of Hsp33 was later resolved and showed striking similarities with Hsp31 [4,79].

Though little is known about the function of these proteins, Hsp31 may play a role in cellular stress response as it is upregulated in oxidative stress conditions [80]. Furthermore, *hsp31*Δ cells are more sensitive to oxidative stress and exhibit increased levels of reactive oxygen species (ROS) compared with the parental cells [80]. Proteomic and transcriptomic studies have shown that *HSP31* expression increases after exposure to misfolded proteins [7], sorbic acid [81], the pro-oxidant and neurotoxic fungicide mancozeb [82] and high pressure conditions [83].

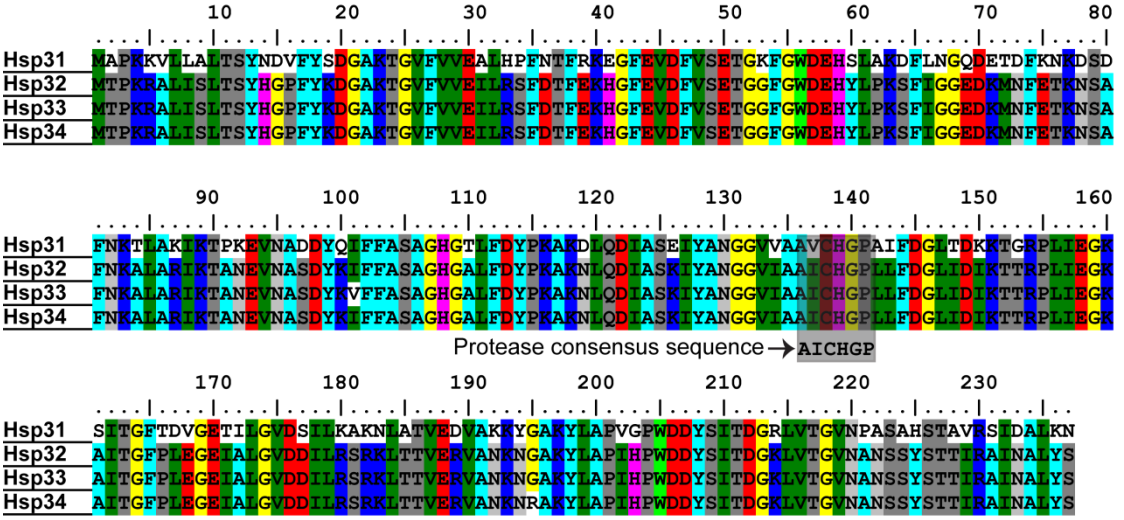

Figure 3.1. Alignment of the protein sequences of the yeast DJ-1 superfamily members: Hsp31, Hsp32, Hsp33 and Hsp34.

Hsp32, Hsp33 and Hsp34 share the highest homology amongst the family members. Hsp32 shares ~99.6% protein identity with Hsp33, as they differ by only one amino acid. Hsp33 has two differing amino acids from Hsp34 (~ 99.2% amino acid identity) and Hsp34 differs in only one amino acid from Hsp32 (~99.6% identity). These three proteins are most diverged from Hsp31, sharing ~69% identity.

Here, we show that the Hsp31 mini-family is required for normal transition from logarithmic (log) growth phase to post-diauxic phase and for the acquisition of typical hallmark features of stationary phase. In their absence, yeast cells lose the capacity to survive in stationary phase conditions and display TORC1 (target of rapamycin complex 1) signaling dysfunction. Altogether, we provide novel insights into the function of the DJ-1-related Hsp31 mini-family, which may contribute to the understanding of the general function of the DJ-1 superfamily, opening novel perspectives for intervention in cancer, PD and, more generally, in lifespan extension.

Results

The HSP31 mini-family is required for normal diauxic-shift and stationary phase

As Hsp31 expression is induced in post-diauxic phase [80], we started by characterizing the expression levels of *HSP31*, *HSP32* and *HSP33* throughout the different phases of yeast growth in liquid medium (Fig. 3.2). Due to the extremely-high sequence similarity between *HSP32*, *HSP33* and *HSP34* (Fig. 3.1) it was not possible to design primers that distinguished *HSP34* from the other two genes, and thus we excluded *HSP34* from these analyses. In parallel, we determined the expression profile of *GIS1,* a transcription factor required for gene expression during nutrient limitation [84].

A

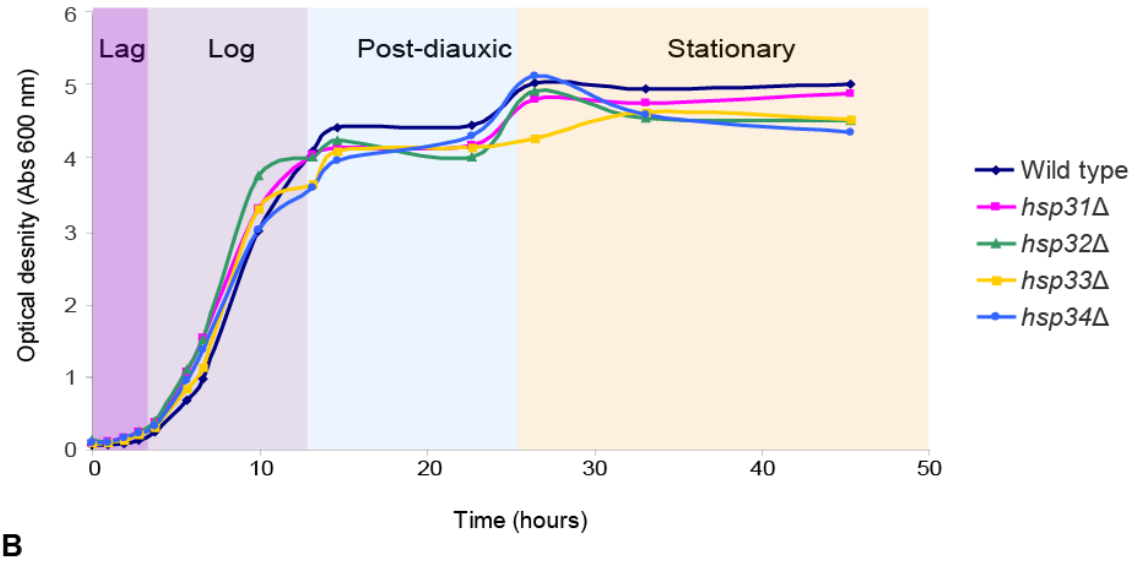

B

Log phase	Post-diauxic phase	Post-diauxic/Stationary phase
Fermentation of glucose Cells produce ethanol Glycogen starts to accumulate	Aerobic respiration Cells consume ethanol	Stress response Trehalose accumulation Decrease in translation Thick cell wall Autophagy induction

Figure 3.2. Yeast growth in glucose-rich liquid culture.
(**A**) Representative growth curves of wild-type and *hsp31*Δ, *hsp32*Δ, *hsp33*Δ and *hsp34*Δ. (**B**) Main characteristics of yeast growth. Yeast cells grown in glucose-rich media exhibit exponential division, known as logarithmic growth (Log phase). In this phase, cells obtain energy through fermentation and produce ethanol. When glucose becomes limiting (known as diauxic-shift) cells enter post-diauxic phase, in which growth rate decreases. Cells readjust their metabolism to aerobic respiration and consequently exhibit higher levels of reactive oxygen species. In parallel, cells upregulate stress response genes, induce autophagy, acquire thicker cell walls, accumulate trehalose and exhibit decreased protein translation. Upon exhaustion of the available carbon source, cells stop proliferating by arresting their cell cycle in G0 and enter stationary phase.

Our results showed that *HSP31-33* and *GIS1* had similar expression patterns (Fig. 3.3): the expression of these genes was highly induced when cells shifted from log phase to post-diauxic phase, and the levels were maintained in stationary phase. We detected slight differences in the timing and levels of expression between the members of the Hsp31 mini-family. *HSP31* and *HSP33* mRNAs reached maximum levels in early stationary phase, whereas *HSP32* mRNA levels peaked at diauxic-shift (Fig. 3.3).

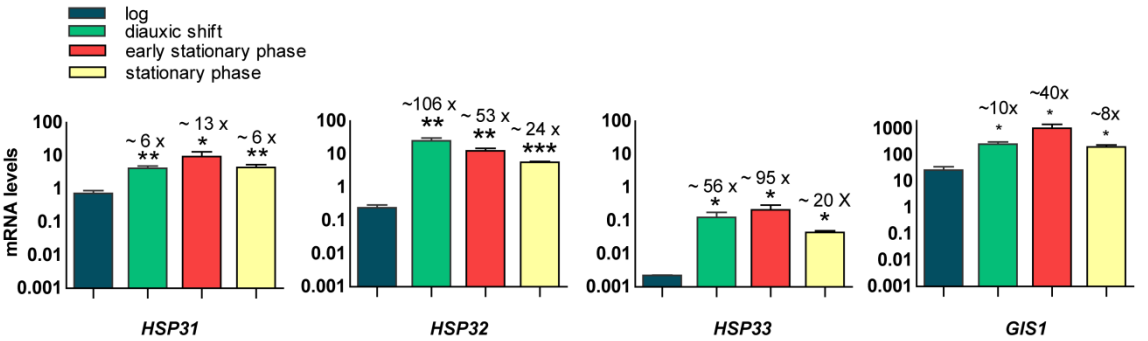

Figure 3.3. *HSP31, HSP32* and *HSP33* expression is induced at diauxic-shift and is maintained in stationary phase.

Gene expression quantification was performed via quantitative real time PCR in mid-log, diauxic-shift, early stationary phase (1 day in culture) and stationary phase (2 days in culture). Expression levels of *HSP31*, *HSP32* and *HSP33* were normalized by *TAF10* and *UBC6*. Error bars represent standard deviation (SD) of the mean (n=3). Fold induction is indicated on top of each bar. Pair-wise statistical analysis was performed using Student's t-test (*** p<0.001; ** p<0.01; * p<0.05).

As previously shown for *hsp31*Δ cells [80], we observed that deletion of *HSP32, HSP33* and *HSP34* had no effect on yeast growth in normal conditions, but resulted in higher sensitivity to oxidative stress (Fig. 3.4A), reduced thermotolerance (Fig. 3.4B), and accumulation of higher levels of ROS (Fig. 3.4C-D).

Given that the expression of *HSP31*, *HSP32* and *HSP33* significantly increased at diauxic-shift, we tested whether the absence of these genes, as well as *HSP34*, would affect yeast survival in stationary phase – chronological lifespan (CLS). We included *gis1*Δ cells for comparison as it has a shortened chronological lifespan versus wild-type [85]. Deletion of *HSP31* family genes resulted in reduced CLS, although to a lesser extent than deletion of *GIS1* (Fig. 3.5A). Re-introduction of Hsp genes in knockout strains reverted this phenotype (Fig. 3.5B-C).

The fact that *HSP31, HSP32* and *HSP33* were highly upregulated at diauxic-shift, together with the loss of cell viability in aged cultures of knockout strains, prompted us to further investigate the role of these genes during diauxic-shift. We

performed gene expression microarrays of *hsp31*Δ, *hsp32*Δ, *hsp33*Δ and wild-type strains at diauxic-shift, which was determined based upon growth rate and glucose consumption. The microarray analyses were validated by testing selected differentially expressed genes (DEGs) by quantitative real-time PCR (QPCR) (Appendix 3.1). The expression profiles of knockout strains were independently compared to that of the wild-type strain, and only genes differently expressed more than two fold ($p \leq 0.05$) were considered for subsequent analyses.

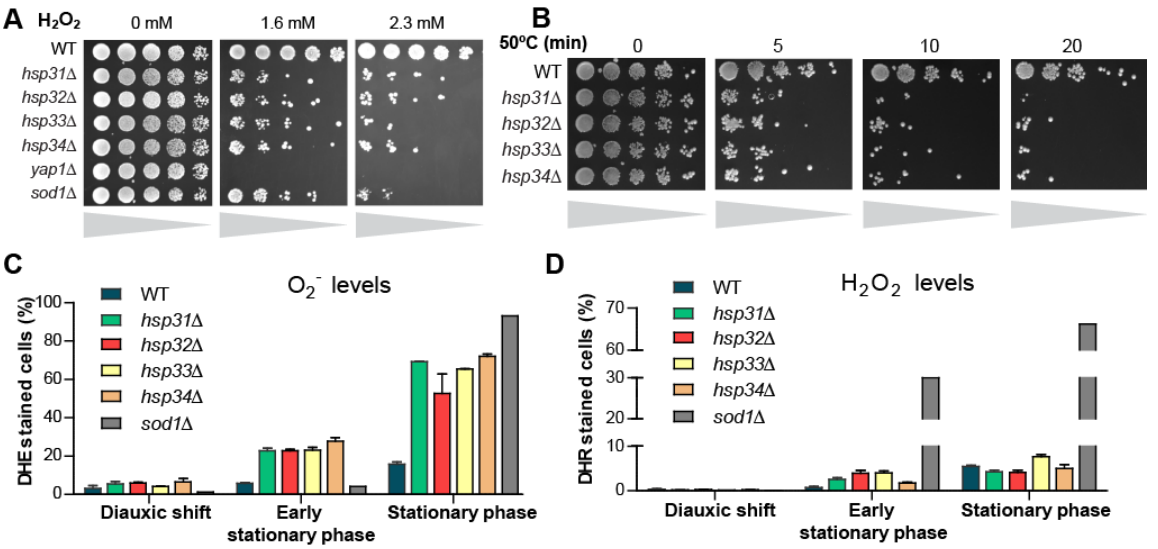

Figure 3.4. *hsp31*Δ, *hsp32*Δ, *hsp33*Δ and *hsp34*Δ are more sensitive to oxidative and heat stress and accumulate higher levels of ROS.

(**A**) Mid-log phase cultures were normalized to an optical density at 600 nm of 0.2, serially diluted (five-fold), and spotted onto solid media containing various concentrations of hydrogen peroxide (H_2O_2), as shown. (**B**) Cultures were subjected to a heat shock of 50ºC for 5, 10 or 20 minutes and subsequently spotted onto YPD plates. (**C**) Superoxide levels were measured using the oxidation sensitive dye dihydroethidium (DHE), (**D**) while hydrogen peroxide levels were measured using the dye dihydrorhodamine 123 (DHR 123). Stained cells were scored by flow cytometry. (**D**) Dead cells were excluded prior to analysis based upon propidium iodide staining.

Among the three pair-wise comparisons, *hsp32*Δ showed the highest number of differentially expressed genes with alterations in approximately one quarter of the yeast genome (Fig. 3.6). To identify overlapping DEGs between the three knockout strains we performed a separate comparison of upregulated (Fig. 3.6A) and downregulated genes (Fig. 3.6B). *hsp32*Δ and *hsp33*Δ strains shared a high number of DEGs that did not overlap with *hsp31*Δ, *which* is in agreement with the high conservation between Hsp32 and Hsp33 protein sequences (Fig. 3.6A-B). For further analysis we selected DEGs common to the three knockout strains and clustered these overlapping genes using gene ontology (GO) analysis based upon biological process annotation (Fig. 3.7A-B; Appendix 3.2 and 3.3).

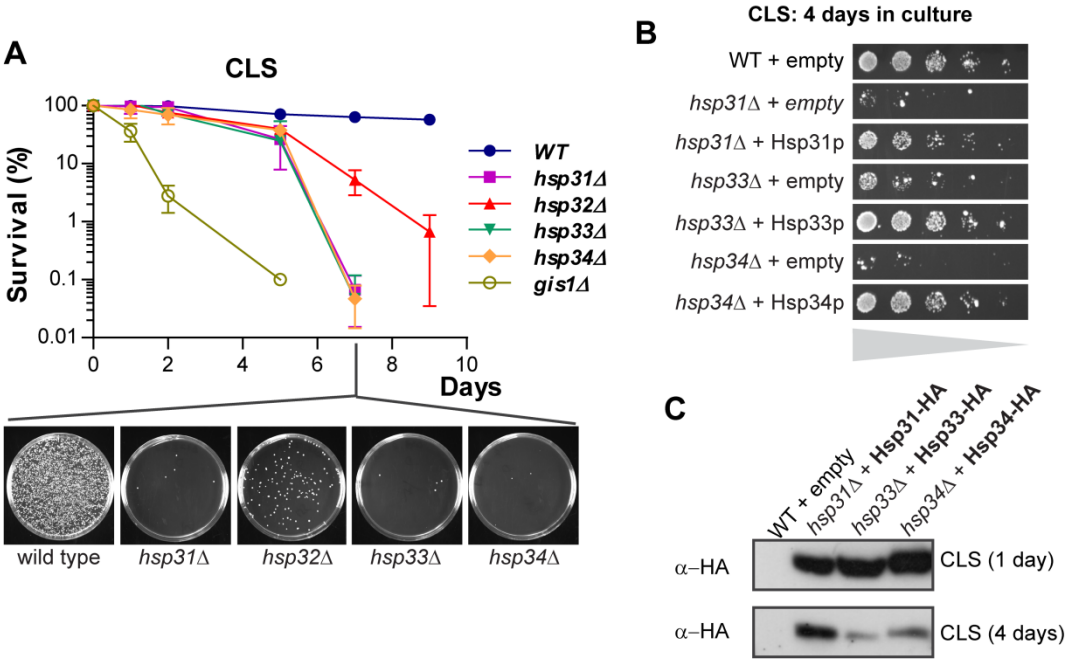

Figure 3.5. Hsp31-34 are required for normal lifespan in stationary phase.
(**A**) Strains were monitored for chronological lifespan (CLS) by counting colony-forming units. Day zero is defined as the time when cultures reached stationary phase (survival = 100%). Mean and standard deviation (n=3) are indicated in the graph. Images below are representative plates of the lowest dilution to score CFUs at day 7. (**B**) Overexpression of Hsp31, Hsp33 and Hsp34 complements reduced chronological lifespan in Hsp gene deletion strains. *hsp31*Δ, *hsp33*Δ and *hsp34*Δ cells were transformed with an empty vector (p416GPD) or with a vector encoding an HA-tagged version of the respective deleted protein (p416GPD/Hsp31-HA, p416GPD/Hsp33-HA and p416GPD/Hsp34-HA). Cultures were grown on selective rich media (SC-URA) until reaching stationary phase – considered day zero. An aliquot of each culture was serially diluted (5 fold) and spotted onto solid YPD media. A representative spotting plate after 4 days in culture is depicted. (**C**) Hsp31, Hsp33, Hsp34 expression was confirmed after 1 and 4 days of growth in stationary phase using an antibody against the HA tag.

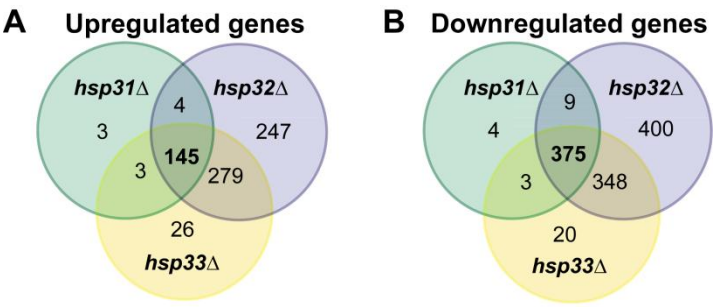

Figure 3.6. Venn diagrams representing the overlap between up- (A) or downregulated (B) genes in *hsp31*Δ, *hsp32*Δ and *hsp33*Δ versus wild-type cells at diauxic-shift.
Differentially expressed genes with greater than 2 fold differences ($p<0.05$) were selected for analysis.

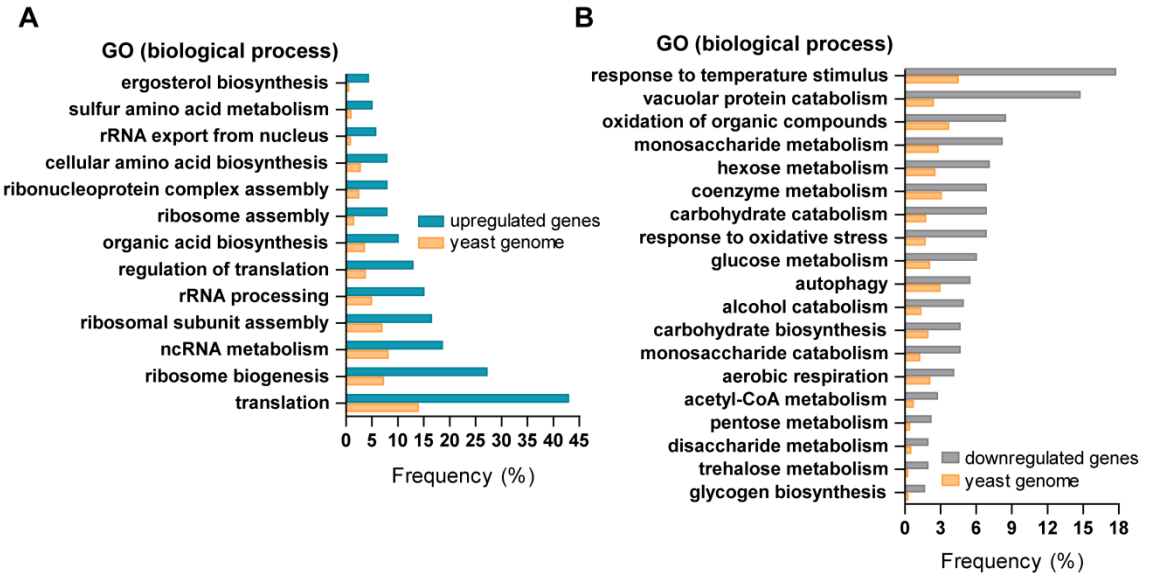

Figure 3.7. Gene ontology analyses of expression profiles of *hsp31*Δ, *hsp32*Δ and *hsp33*Δ.

Overlapping Up- (**D**) or downregulated (**E**) genes obtained by venn diagrams (Fig. 3.6) were grouped in terms of gene ontology (GO). The most significant gene clusters are shown. Frequency is the percentage of overlapping genes that are clustered in a given ontology group, while the yeast genome frequency is the total percentage of genes annotated for that term in the parental strain.

Table 3.1. Gluconeogenesis genes downregulated in *hsp31*Δ, *hsp32*Δ and *hsp33*Δ vs wild-type cells

Standard Name	Systematic Name	SGD description (summarized)
TDH3	YGR192C	Glyceraldehyde-3-phosphate dehydrogenase, isozyme 3; involved in glycolysis and gluconeogenesis
TDH1	YJL052W	Glyceraldehyde-3-phosphate dehydrogenase, isozyme 1; involved in glycolysis and gluconeogenesis
TDH2	YJR009C	Glyceraldehyde-3-phosphate dehydrogenase, isozyme 2; involved in glycolysis and gluconeogenesis
PCK1	YKR097W	Phosphoenolpyruvate carboxykinase, key enzyme in gluconeogenesis
FBP1	YLR377C	Fructose-1,6-bisphosphatase, key regulatory enzyme in the gluconeogenesis pathway
MDH2	YOL126C	Cytoplasmic malate dehydrogenase, involved in the glyoxylate cycle and gluconeogenesis during growth on two-carbon compounds

In order to further confirm that the DEGs found in our gene expression analyses overlap with the reprogrammed genes at diauxic-shift, we compared our results to existing gene expression data available at ArrayExpress [89]. We first compared existing log-phase expression profiles with diauxic-shift profiles, allowing us to determine which genes change in diauxic-shift (data not shown). Next, we compared this dataset to our "overlapping" dataset. This analysis revealed that ~62% of the genes in our dataset overlapped with the reprogrammed genes (Table 3.3). However, ~59% of these genes were anti-correlated, indicating that normal diauxic transition is impaired in the knockout

strains (Table 3.3). Log and diauxic-shift expression profiles were downloaded from ArrayExpress (E-TABM-496) and subsequently analysed to calculate the fold change between these two conditions. DEGs higher than 2 fold ($p<0.05$) were divided in up- and downregulated groups and where compared to the overlapping genes obtained in (Fig. 3.6). Due to glucose limitation at diauxic-shift genes that are under glucose repression are derepressed. Indeed, we found that several DEGs are involved in glucose transport and metabolism, including *MIG2, NRG2* and *HXT5* (Table 3.4). *MIG2* and *NRG2*, which are involved in glucose repression, were upregulated in the knockout strains, whereas *HXT5* – a glucose transporter induced at diauxic-shift [90] – was highly downregulated. Interestingly, expression of *HXT4*, another glucose transporter induced at diauxic-shift, was upregulated in the knockout strains, which may represent a compensatory mechanism due to reduced expression of *HXT5*.

Table 3.2. Reserve carbohydrate biosynthesis genes downregulated in *hsp31*Δ, *hsp32*Δ and *hsp33*Δ vs wild-type cells

Standard Name	Systematic Name	SGD description (summarized)
Glycogen biosynthetic process		
GLC3	YEL011W	Glycogen branching enzyme, involved in glycogen accumulation
GLG2	YJL137C	Glycogenin glucosyltransferase; self-glucosylating initiator of glycogen synthesis
GSY2	YLR258W	Glycogen synthase; expression induced by glucose limitation, nitrogen starvation, heat shock, and stationary phase
PGM2	YMR105C	Phosphoglucomutase; catalyzes the conversion from glucose-1-phosphate to glucose-6-phosphate
GAC1	YOR178C	Regulatory subunit for Glc7p type-1 protein phosphatase (PP1), tethers Glc7p to Gsy2p glycogen synthase
GDB1	YPR184W	Glycogen debranching enzyme; contains glucanotranferase and alpha-1,6-amyloglucosidase activities; required for glycogen degradation
Trehalose biosynthetic process		
ATH1	YPR026W	Acid trehalase required for utilization of extracellular trehalose
HSP104	YLL026W	Disaggregase; heat shock protein that cooperates with Ydj1p (Hsp40) and Ssa1p (Hsp70)
NTH1	YDR001C	Neutral trehalase, degrades trehalose
NTH2	YBR001C	Putative neutral trehalase, required for thermotolerance
PGM2	YMR105C	Phosphoglucomutase; catalyzes the conversion from glucose-1-phosphate to glucose-6-phosphate
TPS1	YBR126C	Synthase subunit of trehalose-6-P synthase/phosphatase complex; synthesizes the storage carbohydrate trehalose
TSL1	YML100W	Large subunit of trehalose 6-phosphate synthase/phosphatase complex; Tps1p-Tps2p complex converts uridine-5'-diphosphoglucose and glucose 6-phosphate to trehalose

Table 3.3. Comparison of the overlapping DEGs obtained in this study with diauxic-shift expression profile

	Overlapping genes (wt vs hsp31Δ, hsp32Δ and hsp33Δ)	
Log vs Diauxic shift	**Correlated**	**Anti-correlated**
	2.5 %	59%

Table 3.4. DEGs involved in glucose transport and metabolism

Gene	Saccharomyces Genome Database description	*hsp31*Δ vs WT (fold change)	*hsp32*Δ vs WT (fold change)	*hsp33*Δ vs WT (fold change)
HXT1	Low-affinity glucose transporter; induced by Hxk2p in the presence of glucose and repressed by Rgt1p when glucose is limiting	-	2,07	-
HXT3	Low-affinity glucose transporter; induced in low or high glucose conditions	3,19	3,44	4,29
HXT4	High-affinity glucose transporter, induced by low levels of glucose and repressed by high levels of glucose	5,74	5,7	5,17
HXT5	Moderate affinity for glucose, induced in the presence of non-fermentable carbon sources, induced by a decrease in growth rate	-3,8	-11,4	-6,33
MIG2	Zinc finger transcriptional repressor; cooperates with Mig1p in glucose-induced repression of many genes	6,49	8,38	7,94
HXK2	catalyzes phosphorylation of glucose in the cytosol; predominant hexokinase during growth on glucose; functions in the nucleus to repress expression of HXK1 and GLK1 and to induce expression of its own gene	5,46	6,08	6,66
GLK1	Glucokinase, catalyzes the phosphorylation of glucose at C6 in the first irreversible step of glucose metabolism; one of three glucose phosphorylating enzymes; expression regulated by non-fermentable carbon sources	-	-5	-3,34
RGT1	Glucose-responsive transcription factor that regulates expression of HXT genes in response to glucose; binds to promoters and acts both as a transcriptional activator and repressor	-	-2,61	-2,13
NRG2	Transcriptional repressor that mediates glucose repression and negatively regulates filamentous growth	3,32	2,82	3,32
SKS1	Putative serine/threonine protein kinase; involved in the adaptation to low concentrations of glucose independent of the SNF3 regulated pathway	3,24	6,89	3,78
STD1	Protein involved in control of glucose-regulated gene expression; interacts with kinase Snf1p, glucose sensors Snf3p and Rgt2p, TATA-binding Spt15p; regulator of transcription factor Rgt1p	-	3	2,22
SNF3	Plasma membrane low glucose sensor that regulates glucose transport; contains 12 predicted transmembrane segments and a long C-terminal tail required for induction of hexose transporters; also senses fructose and mannose; similar to Rgt2p	-	-2,36	-

To confirm whether glucose repression is enhanced in the knockout strains, we next transformed both wild-type and *hsp31*Δ strains with a vector containing *LEU2* under the control of the *GAL1* promoter. We found that while expression of Leu2 increased progressively over time upon galactose induction in the wild-type strain, *hsp31*Δ cells exhibited lower levels of Leu2 which did not increase over the timeframe of the experiment (Fig. 3.8). This suggests that glucose repression is enhanced in *hsp31*Δ in comparison to the wild-type strain, confirming that Hsp31 is required for glucose derepression.

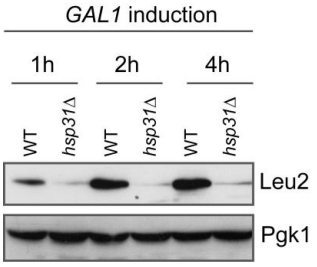

Figure 3.8. *GAL1* promotor repression is stronger in *hsp31Δ*.
BY4741 and *hsp31*Δ cells were transformed with a vector expressing Leu2 under control of the GAL1 promoter (BG1805). The strains were grown until mid-log phase in media containing glucose (GAL1 repression) and then shifted to media containing galactose (GAL1 induction). Cultures were retrieved after 1, 2 and 4 hours of growth in galactose.

Typical stationary phase characteristics are altered in HSP31 mini-family knockout strains

Several changes that occur in post-diauxic phase are maintained in stationary phase [87]. Therefore, we next evaluated whether typical characteristics of stationary phase were altered in the knockout strains. We first tested the thermotolerance of the strains to a 50ºC heat shock, which is an indicator of cellular steady-state defenses. Consistently, the knockout strains were less thermotolerant than the wild-type strain, exhibiting decreased viability within 10 minutes of heat shock (Fig. 3.9A). The thickness of the cell wall, known to increase in cells in stationary phase, was evaluated by resistance to the lytic enzyme zymolyase. Cells in stationary phase were incubated with zymolyase in a non-osmotic environment and monitored for optical density (OD) over time. As the cell wall is digested, cells burst and the OD decreases. We observed that the cell walls of *HSP31* mini-family and *GIS1* knockout strains were digested faster than those of the wild-type strain, indicating that the cell wall of the knockout strains was less resistant to zymolyase and therefore thinner (Fig. 3.9B).

We next evaluated autophagy in the knockout strains at stationary phase by monitoring *ATG8*, which is among the autophagy genes downregulated in the knockout strains. Atg8 is involved in the formation of autophagosomes and during this process is degraded in the vacuole [91]. We investigated autophagy using a GFP-Atg8 reporter construct under control of *ATG8* promoter, which permits monitoring of both autophagy induction and autophagic flux as Atg8 is rapidly degraded in the vacuole while GFP is not [92]. Anti-GFP immunoblot analysis allows detection of two protein bands, the higher molecular weight band corresponding to cytosolic GFP-Atg8 and the lower band corresponding to GFP-Atg8 degraded in the vacuole [93]. We analysed autophagy in wild-type, *hsp31*Δ, *hsp33*Δ and *hsp34*Δ strains in both stationary and log phase. Strikingly, we observed impaired induction of autophagy in the knockout strains during stationary phase and reduced levels of basal autophagy during log phase (Fig. 3.9C). These

results indicate that autophagy is impaired in the absence of at least one of the Hsp31 family members.

Finally, we evaluated cell cycle progression in the knockout strains. To measure DNA content, we stained cells with propidium iodide and performed flow cytometry analyses and found a higher percentage of cells that failed to enter G0 in knockout cells (Fig. 3.9D).

Autophagic response is impaired during carbon starvation in hsp31Δ cells

As it was previously shown that *HSP31* is induced in oxidative stress conditions [80] and that levels of ROS increase at diauxic-shift, we considered the possibility that ROS might trigger the observed upregulation of *HSP31*, *HSP32* and *HSP33* at diauxic-shift (Fig. 3.3). Intriguingly, oxidative stress induced by hydrogen peroxide failed to increase expression of *HSP32* and *HSP33*, and only the highest concentration – 2mM – was able to induce *HSP31* (Fig. 3.10A). Yeast viability decreased beyond this concentration so we did not exceed this concentration in our experiments (data not shown).

Next, we tested whether the *HSP31* mini-family was induced by starvation, another hallmark of diauxic-shift and stationary phase. *HSP32* and *HSP33* expression was highly induced by both nitrogen and carbon starvation, but it was higher in carbon starvation conditions (Fig. 3.10B). On the other hand, *HSP31* was significantly upregulated only by nitrogen depletion (Fig. 3.10B). These results suggest that expression of the Hsp31 mini-family members during diauxic-shift and stationary phase is mainly regulated by starvation rather than oxidative stress. We next assessed whether the autophagy impairment that we observed in the knockout strains during stationary phase was also observed under nutrient (nitrogen or carbon) starvation or upon rapamycin treatment, which is a compound widely-used to induce autophagy via TORC1 inactivation [94]. Cells expressing GFP-Atg8 were analysed before treatment and 1, 3 and 5 hours post-treatment. As the autophagy phenotypes of the knockout strains were identical, we primarily focused our efforts on the *hsp31*Δ strain for the subsequent experiments. After one hour of rapamycin treatment we observed induction of autophagy which increased over time in both wild-type and *hsp31*Δ cells (Fig. 3.11A). We found that nitrogen depletion also induced autophagy in *hsp31*Δ cells, while autophagic induction and flux were maintained at basal levels during carbon starvation (Fig. 3.11A).

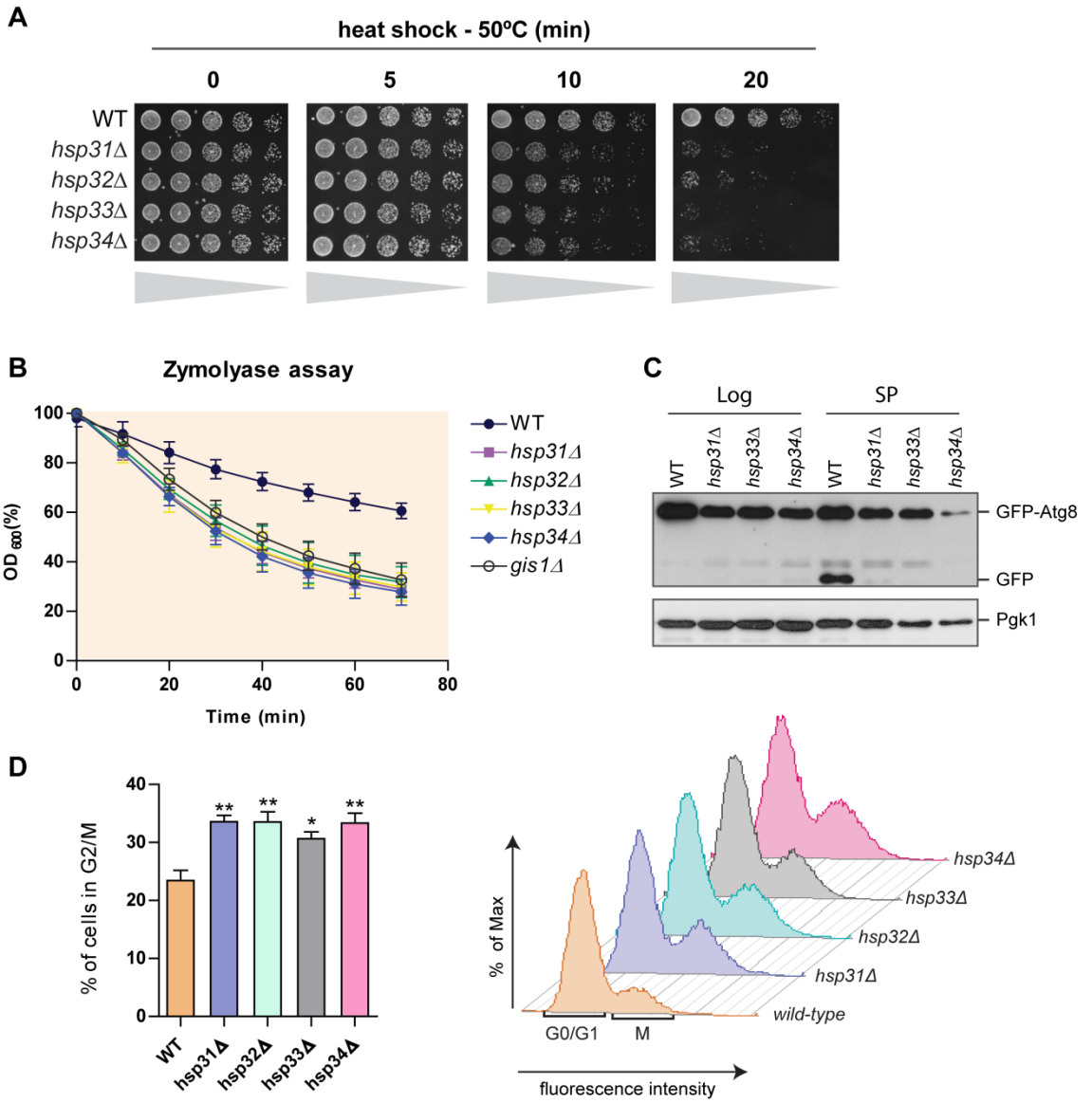

Figure 3.9. *hsp31*Δ, *hsp32*Δ, *hsp33*Δ and *hsp34*Δ cells fail to acquire typical stationary phase characteristics.

Wild-type and gene deletion strains were analysed for resistance to heat stress (A), cell wall integrity (B), autophagy flux (C) and cell cycle (D). (A) Yeast cultures were grown in liquid media until stationary phase and subjected to a 50ºC heat shock for the specified time. Cultures were normalized to an OD600 of 0.3 and spotted onto solid media to measure viability. (B) Stationary phase cultures (48 hours growth) were incubated with zymolyase and cell wall digestion was monitored by measuring the OD600 every 10 minutes. (C) Mid-log (Log) and stationary phase (SP) cells expressing GFP-Atg8 under its endogenous promoter were lysed and analysed by immunoblotting. The presence of free GFP is an indicator of autophagic flux. (D) To quantify DNA content, cells in stationary phase were stained with propidium iodide and analysed by flow cytometry. The histogram shows propidium iodide fluorescence intensity of wild-type and knockout strains. Error bars represent standard deviation of the mean for each assay (n=3). Statistical analysis was performed using Student's t-test (** p<0.01; * p<0.05).

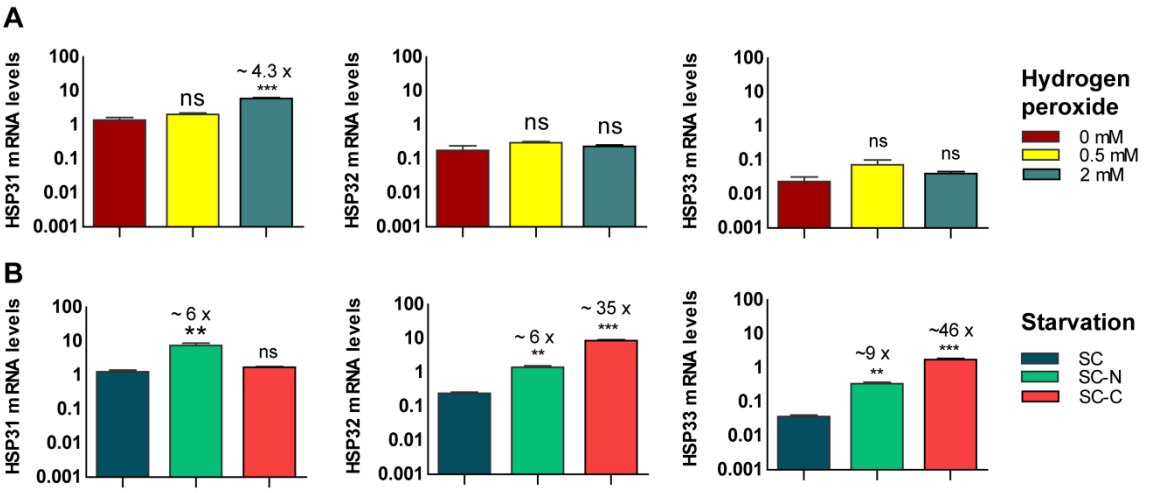

Figure 3.10. Expression levels of *HSP31*, *HSP32* and *HSP33* under oxidative stress and starvation conditions.

Parental strain BY4741 was grown until mid-log phase on synthetic complete media (SC) and was incubated with hydrogen peroxide at two different concentrations or washed and starved for carbon (SC-C) or nitrogen (SC-N). mRNA was isolated and gene expression levels were quantified via QPCR and normalized relative to *TAF10* and *UBC6* expression. Error bars represent standard deviation of three independent experiments. Statistical analysis was performed using Student's t-test (*** P<0.001; ** P<0.01; NS, not significant).

Next, we confirmed these findings by fluorescence microscopy and found that while *hsp31*Δ cells displayed faint GFP-ATG8 fluorescence signal in cytoplasm in the absence of glucose, wild-type cells displayed strong GFP-Atg8 signal localized to the vacuole (Fig. 3.11B*)*. On the other hand, upon nitrogen starvation or rapamycin treatment GFP-Atg8 was localized to the vacuole in both wild-type and *hsp31*Δ cells (Fig. 3.11B). Similar immunoblot results were obtained in *hsp33*Δ and *hsp34*Δ (Fig. 3.11C).

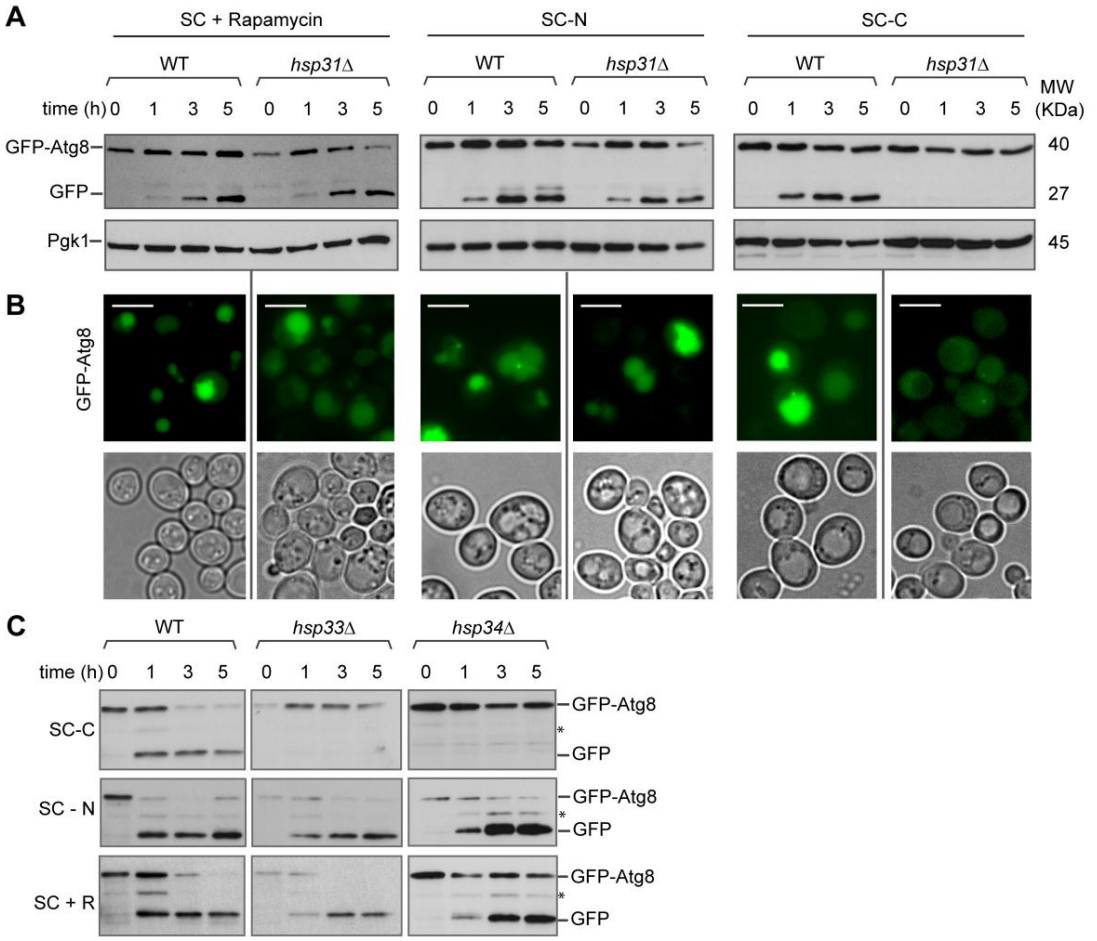

Figure 3.11. Autophagic response in *hsp31*Δ, *hsp33*Δ and *hsp34*Δ strains is impaired in carbon starvation conditions.
(**A-C**) Wild-type and deletion strains expressing pr^{ATG8}-GFP-Atg8 were grown until mid-log phase and treated with rapamycin or starved for carbon (SC-C) or nitrogen (SC-N) for the specified time. (**A,C**) Total lysates were analysed by immunoblotting using antibodies against GFP or a housekeeping control Pgk1p. (**B**) After 5 hours of incubation with rapamycin or starvation, GFP-Atg8 localization was analysed by fluorescence and light microscopy. Scale bar represents 5 µm.

TORC1 signaling is perturbed in hsp31Δ cells

Entry into post-diauxic phase and progression into stationary phase is orchestrated by nutrient-sensing signaling pathways. Two of the major signaling pathways associated with this transition are the TOR complex 1 (TORC1) and protein kinase A (PKA) [87,95–97]. These two kinases, in addition to playing a role in cellular growth via translation and stress response repression, also negatively regulate autophagy [98–101]. Due to the dramatic gene expression changes observed in the knockout strains at diauxic-shift, we next asked whether one of these signaling pathways were

dysregulated in *hsp31*Δ strains by using Atg13 as a reporter. Atg13 is a key player in autophagy and is regulated via direct phosphorylation by PKA and TORC1 [98,102,103]. As TORC1 hyperphosphorylates Atg13, we monitored phospho-status based upon Atg13 mobility in SDS-polyacrylamide gels [98,99,104].

In stationary phase TORC1 is repressed and therefore the levels of Atg13 phosphorylation decrease. As expected for the wild-type, Atg13 migrated faster in stationary phase (Fig. 3.12A). In *hsp31*Δ cells, the difference in Atg13 migration between log and stationary phase was reduced (Fig. 3.12A). This suggests that Atg13 is more highly phosphorylated in *hsp31*Δ cells, possibly due to TORC1 hyperactivity. To confirm that the differences observed in migration were caused by phosphorylation, and not by other posttranslational modifications, we treated stationary phase Atg13 with ʎ-phosphatase (Ppase). After Ppase treatment we observed that Atg13 from *hsp31*Δ cells migrated side by side with Atg13 from wild-type cells confirming that migrational differences in stationary phase were caused by phosphorylation (Fig. 3.12B). We further analysed the phosphorylation status of Atg13 under carbon and nitrogen starvation conditions. These conditions led to Atg13 dephosphorylation in both the parental and *hsp31*Δ strains. However, Atg13 migration in *hsp31*Δ was slower in all the conditions tested (Fig. 3.12C-D), suggesting a difference in phosphorylation-status between the strains, which was more pronounced under carbon starvation than nitrogen starvation. To investigate the activity of PKA we immunoprecipitated Atg13 and analysed phosphorylation by immunoblotting using a PKA substrate antibody [α-(P)PKA]. The levels of PKA-mediated Atg13 phosphorylation were similar between wild-type and *hsp31*Δ cells in the conditions tested (stationary phase, carbon and nitrogen starvation) (Fig. 3.12E-F), indicating that this process is not affected in the knockout strain.

In total, these results suggest that TORC1 is dysregulated upon *HSP31* deletion, which is more evident in stationary phase conditions. As heat shock also leads to TORC1 inactivation [105,106], we next assessed whether blocking TORC1 using rapamycin reverts *hsp31*Δ lack of thermotolerance. Using growth assays we observed that knockout cells treated with rapamycin exhibited decreased sensitivity to heat shock, indicating that TORC1 inhibition restores normal heat shock response in these cells (Fig. 3.13), further supporting the hypothesis that absence of *HSP31* affects the normal upstream regulation of TORC1.

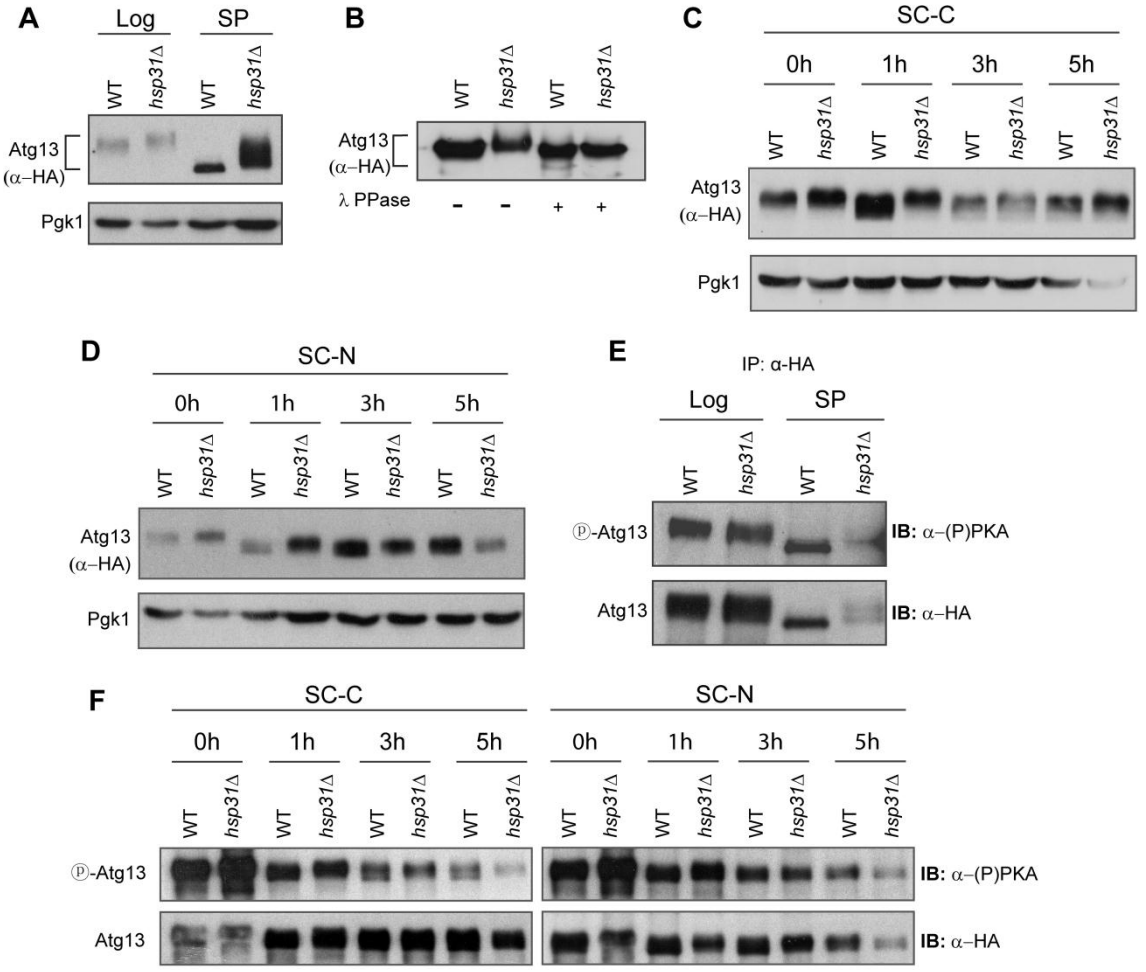

Figure 3.12. Atg13 phosphorylation is altered in *hsp31*Δ.

(**A**) Protein extracts were collected from cultures at mid-log phase (Log) and stationary phase (SP). Migration of HA-Atg13 in SDS-polyacrylamide gels was assessed using an antibody against HA. An antibody for Pgk1 was used as control for protein loading. (**B**) HA-Atg13 from SP cell lysates was immunoprecipitated with α-HA and treated with ʎ-phosphatase (Ppase) and then run on SDS-polyacrylamide gel to analyse its migration. (**C, D**) Atg13 migration from cell lysates of cultures that were starved for carbon (SC-C) or nitrogen (SC-N) was analysed. (**E, F**) Atg13 from Log and SP cultures (**E**) or from mid-log phase cultures that were starved for carbon (SC-C) or nitrogen (SC-N) (**F**) was immunoprecipitated with α-HA and analysed for PKA mediated phosphorylation using phospho-(Ser/Thr) PKA substrate antibody (α-(P)PKA).

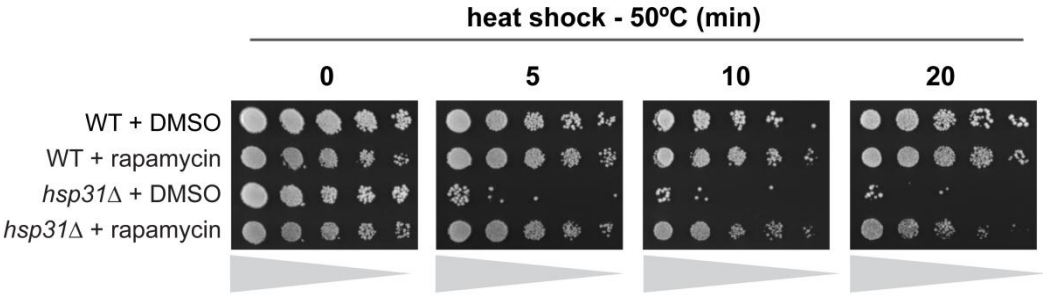

Figure 3.13. Rapamycin reverts the lack of *hsp31*Δ thermotolerance.
Yeast strains in mid-log phase were treated with DMSO or rapamycin for 3 hours and subjected to a 5, 10 and 20 minute heat shock at 50ºC. Cultures were serial diluted and spotted on media plates to analyse cell survival.

Discussion

This study provides novel insights into the function of *HSP31* and, to our knowledge, provides the first functional analysis of the remaining members of the DJ-1 superfamily in yeast: *HSP32*, *HSP33* and *HSP34.* Our findings reveal that *HSP31* and its orthologs are required for the transition from the log phase to post-diauxic phase. Cells enter diauxic-shift when glucose becomes limiting in liquid cultures, which leads to extensive metabolic and transcriptional reprogramming. Some of the changes that occur at this shift include induction of genes involved in aerobic respiration and stress protection and repression of genes involved in mRNA translation [86–88]. We showed that *HSP31*, *HSP32* and *HSP33* expression strikingly increased when cells entered post-diauxic phase and was maintained at high levels in stationary phase. The lack of these genes led to shorter chronological lifespan, revealing an important role of this mini gene family at diauxic-shift. Expression microarray profiling indicated that *hsp31*Δ, *hsp32*Δ and *hsp33*Δ have an abnormal expression profile at diauxic-shift. Gene ontology clustering of the microarray data showed that the knockout strains were incapable of entering diauxic-shift; knockout cells were maintained in the glucose repressed state even though glucose was absent from the media. Functionally, the absence of one of the *HSP31* mini-family members led to the inability of cells to acquire several characteristics of stationary phase, such as induction of autophagy and acquisition of a thick cell wall.

We also found that nutrient starvation induces the expression of the Hsp31 mini-family: nitrogen starvation induced all three genes tested (*HSP31*, *HSP32* and *HSP33*), while carbon starvation only led to *HSP32* and *HSP33* upregulation. Although *HSP31* was not upregulated at mRNA level under carbon starvation, we cannot exclude that it is induced at the protein level. Consistent with our results, the *E. coli* EcHsp31 (the

closest *HSP31* homologue in the DJ-1 superfamily) is also induced in stationary phase and when this gene is deleted, cell survival decreases during this phase [15]. In addition, the *Caenorhabditis elegans* DJ-1 homologue DJR-1.2 is induced upon starvation and dauer stage (starvation-induced alternative developmental stage) [107]. Interestingly, human leukemia cell lines depleted for DJ-1 have reduced viability in serum starvation conditions [22].

One of the major signaling pathways implicated in diauxic-shift and further progression into stationary phase is TORC1 [87,95,96,108]. TORC1 is a nutrient sensitive kinase very well conserved from yeast to humans, and has been associated with ageing and when dysregulated in humans (mTORC1 – mechanistic TORC1) is implicated in several pathologies including cancer and neurodegeneration [109]. TORC1 controls yeast growth by promoting processes such as transcription, protein translation and mRNA stability and repressing stress responses and autophagy [110]. TORC1 signaling pathway has been extensively studied, but due to its complexity, there are still many unanswered questions, such as how the availability of carbon is signaled to TORC1 [110]. The study of this particular question is likely difficult due to the crosstalk with other signaling pathways like PKA (another key kinase that signals the entry into diauxic shift) and also due to their overlapping readouts. Much of what is known about the role of TORC1 is based upon the inhibition of its activity by rapamycin, which has enabled the understanding of the downstream actions of TORC1, independently of the upstream effectors. Nevertheless, rapamycin treatment revealed that TORC1 controls glucose metabolic pathways [111]. Our data revealed for the first time that *HSP31* mini-family members are potential TORC1 upstream effectors. We initially observed a dramatic transcriptional effect due to deletion of the Hsp31 mini-family members and the consequent absence of typical stationary phase characteristics. Interestingly, some of the phenotypes caused by deletion of *HSP31* mini-family members, such as deficient G0 arrest and reduced thermotolerance, are similar to the ones observed by deletion of *RIM15. RIM15* encodes a protein kinase that integrates signals from Sch9, PKA and TORC1 [112] and transduces it to Gis1 (the transcription factor responsible for expression of post-diauxic-shift (PDS) genes [84]) and to Msn2/Msn4 – transcription factors responsible for expression of stress-induced genes. Next, by monitoring GFP-Atg8 processing, we found that autophagy in the knockout strains was completely blocked when the carbon source was depleted from the media, but it was identical to the wild-type response upon rapamycin treatment and nitrogen starvation. This is consistent with the impairment observed in stationary phase, since the entry in this phase is

characterized by the depletion of any carbon source. These results indicate that Hsp31 is involved in transducing the carbon starvation signal that leads to autophagy induction. It also shows that the autophagic machinery is working properly and importantly, that Hsp31 has no role downstream of TORC1.

To further explore autophagy and dissect the pathway that is affected in the knockout strains, we assessed the kinase activity of TORC1 and PKA using Atg13 as a reporter. Atg13 is a key protein in autophagy that is a substrate for both kinases, and phosphorylation of Atg13 mediated by one of these kinases represses autophagy. Our results showed striking differences in terms of Atg13 phosphorylation levels mediated by TORC1 in stationary phase between the parental strain and *hsp31*Δ cells, suggesting that TORC1 is hyperactive in the knockout strain. We also found differences in TORC1 mediated phosphorylation in carbon starvation conditions and, unexpectedly, in nitrogen starvation as well, although to a smaller degree. Interestingly, the differences in phosphorylation levels were detected in log-phase cells growing in rich media, suggesting that deleting *HSP31* not only blocks TORC1 inactivation upon carbon starvation and during stationary phase, but also that the basal activation state of TORC1 is higher. Furthermore, we confirmed that phosphorylation of Atg13 mediated by PKA is not affected by *HSP31* deletion. Importantly, we found that the sensitivity of *hsp31*Δ cells to heat shock was decreased after TORC1 inactivation via rapamycin, supporting our genetic data. Altogether, our findings suggest that the Hsp31 mini-family modulates TORC1 activity in yeast, likely playing a role as negative regulators (Fig. 3.13). Therefore, these proteins are likely required to regulate autophagy, a process that needs to be tightly controlled. Human DJ-1 has already been associated with autophagy, however the precise mechanisms underlying this are still unclear. In agreement with our data, it was found that loss of human DJ-1 leads to lower levels of basal autophagy [113]. In contrast, loss of DJ-1 induces autophagy, whereas overexpression represses it [114,115]. Further studies will be required to further elucidate the role of DJ-1 in autophagy.

Overall, this study describes a novel role for the Hsp31 mini-family members at diauxic-shift. Deletion of these proteins led to impaired transcriptional reprogramming at diauxic-shift and an inability to acquire normal stationary phase characteristics, in addition to reduced chronological lifespan and a striking impairment of autophagy in stationary phase. Altogether, our study provides important insight into the function of DJ-1 family members, opening novel avenues for intervention in pathways that are

related both to normal ageing as well as disease, such as cancer and neurodegeneration.

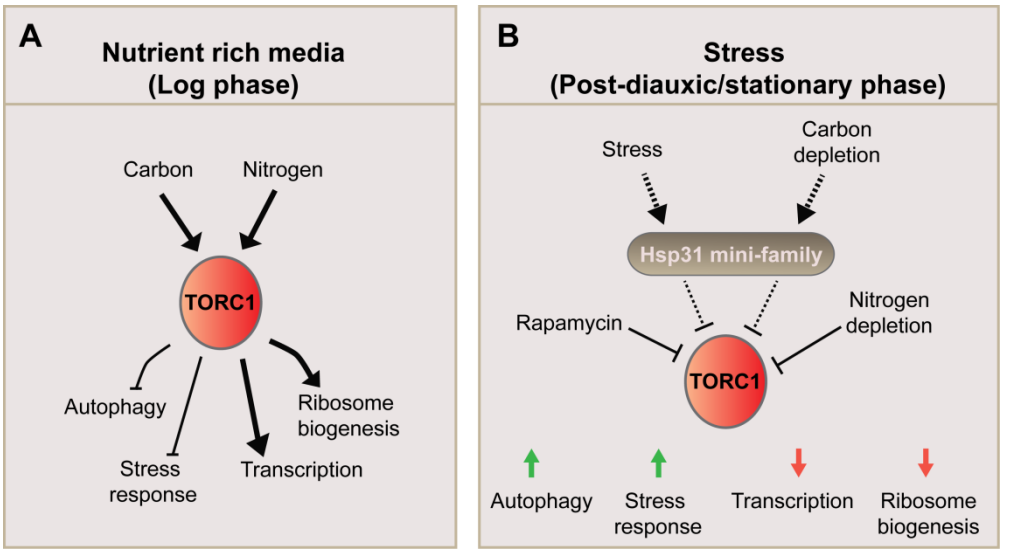

Figure 3.13. Hsp31 mini-family members modulate TORC1 activity.
(**A**) Yeast cells grow exponentially (Logarithmic - log phase) in the presence of nutrient-rich media containing glucose. TORC1, a conserved kinase, positively regulates processes that contribute to growth, such as ribosome biogenesis and transcription, and represses processes related to stress, including autophagy. (B) Upon stress, treatment with rapamycin, or nutrient depletion (post-diauxic or stationary phase), TORC1 decreases its activity and, therefore, autophagy and stress genes are induced. In parallel, ribosome biogenesis and transcription are repressed. Our data suggest that Hsp31 mini-family members have a role in controlling the repression of TORC1 upon stress or carbon starvation.

Materials and Methods

Strains and genotyping

All strains used in this study were derived from the parental BY4741, BY4742 or BY4743 strains (Appendix 3.4). The *hsp31*Δ strain was a kind gift from Marek Skoneczny (Institute of Biochemistry and Biophysics) and *hsp32*Δ was obtained by sporulation of the BY4743 strain heterozygous for the *HSP32* deletion (Thermo Scientific Open Biosystems). *hsp33*Δ and *hsp34*Δ strains (in the BY4742 background) were generated by PCR-based gene disruption as previously described [116]. Since the flanking regions of these genes are identical, the same pair of primers was used to amplify the MX cassettes and delete the genes. The primers used are listed on (Appendix 3.5). The strategy for gene deletion verification is represented in (Figure 3.14) and consisted in performing the following PCR reactions: 1) Amplification of

HSP32 and *HSP33* – forward primer complementary to *HSP32, HSP33* and *HSP34* (*HSP32*/33/34F) together with a reverse primer that hybridizes with *HSP32* and *HSP33* 3' flanking regions (*HSP32*/33R); 2) Amplification of *HSP34* – forward primer *HSP32*/33/34 and a reverse primer specific to *HSP34* 3' flanking region (*HSP34*R); 3) Amplification of the cassette integrated either on *HSP32* or *HSP33* locus (forward primer complementary to the cassette (MX4F) and *HSP32*/33R); 4) Amplification of the cassette integrated in *HSP34* locus (MX4F + *HSP34*R).

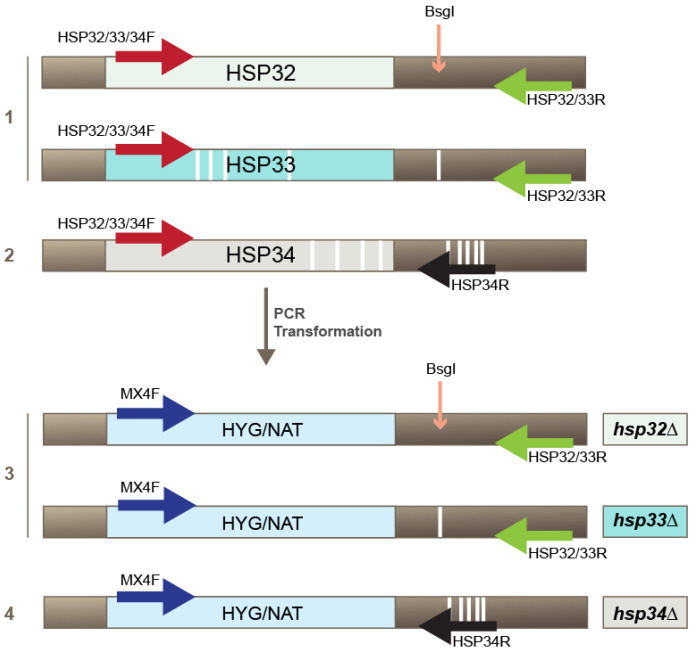

Figure 3.14. Schematic representation of the PCR strategy to screen for *hsp32*Δ *hsp33*Δ and *hsp34*Δ clones.
HSP32, *HSP33, HSP34* and flanking regions are represented. White bars indicate the presence of non-conserved nucleotides between the sequences of the three genes. When either *HSP32* or *HSP33* is deleted, amplification is positive for PCR reaction 1, 2 and 3 and negative for reaction 4. When *HSP34* is deleted an amplicon is obtained in reactions 1 and 4, while the other two are negative. To differentiate between *HSP32* or *HSP33* deletion, the PCR products obtained in reactions 1 and 3 were digested with Bsg1, as this restriction site is only present in *HSP32* 3' flanking region.

To distinguish between *HSP32* and *HSP33*, the 3' flanking region was amplified and digested with *BsgI*, which had a unique restriction digestion site on *HSP32* flanking region. To further confirm the knockout strains, the flanking regions of the deleted genes were analysed by DNA sequencing and real time quantitative PCR (QPCR). The knockout strains were crossed to generate a heterozygous diploid quadruple knockout. By sporulation and tetrad dissection of the diploid strain, wild-type and single knockouts strains were selected (Lx strains). Experiments were performed on the original strains and repeated with Lx strains with no differences observed among the phenotypes

analysed. Microarrays were performed with RNA retrieved from Lx strains. The remaining knockout strains used: *gis1Δ*, *sod1*Δ and *yap1*Δ were obtained from EUROSCARF (Appendix 3.4).

Plasmids

HSP31, *HSP32, HSP33* and *HSP34* open reading frames (ORFs) were subcloned using the Gateway® Cloning technology. ORFs were moved from entry clones (kindly provided by Tony Hazbun, Purdue University) into the expression vector pAG416GPD-ccdB-HA (Addgene). The plasmid pRS316 GFP-Atg8 [117] was kindly given by Yoshinori Ohsumi (Tokyo Institute of Technology) and pRS315 HA-Atg13 by Daniel Klionsky (University of Michigan) [118]. Both genes are under control of their endogenous promoters. The plasmid BG1805 (encoding the Leu2-His6-HA-protease-3Csite-ZZ domain) was obtained from the ORF library (Thermo Scientific Open Biosystems). The protein is expressed under control of the *GAL1* promoter.

Media and growth conditions

Yeast strains were grown on standard media: YPD (2%), synthetic complete media containing all the amino acids (SC) or lacking uracil (SC-URA) or leucine (SC-LEU). SC contains yeast nitrogen base (YNB), 2% glucose and a mixture of all the amino acids or a URA or LEU drop out powder. For starvation experiments, cultures were grown until mid-log phase in SC, SC-URA or SC-LEU, washed once with water and then were resuspended either on carbon starvation media (SC-C), which is the respective synthetic complete media without any carbon source, or resuspended on nitrogen starvation media (SC-N) that contains of 0.17% of YNB without amino acids and ammonium sulfate and glucose at 2%. Rapamycin (Sigma) was added to mid-log phase cultures growing on SC-URA at a final concentration of 200 ng/ml. For *GAL1* induction analysis, cultures were grown in SC-URA with 2% glucose until mid-log phase, washed and resuspended in SC-URA with 2% galactose. Cultures were harvested for protein extraction at the indicated time points. Optical densities at wavelength 600 nm (OD_{600}) were measured on a microplate reader (Tecan Infinite M200^{TM}).

Quantitative real-time PCR (QPCR)

For oxidative stress treatments, liquid cultures of cells in mid-log phase were treated with hydrogen peroxide (0.5 mM and 2 mM) for one hour. Starvation was performed as described above for one hour. After treatment, cells were harvested, pelleted and stored

at -80ºC until needed. RNA was extracted using Qiagen Rneasy Midi kits following manufacturer instructions. Genomic DNA contamination was removed from RNA using Turbo DNAse (Ambion®) according to the manufacturer's protocol. 500 ng of total RNA was used as a template to synthesize cDNA with the Qiagen QuantiTect® Reverse Transcription kit. To insure that RNA had no genomic DNA contamination a control reaction was included in which no reverse transcription was carried out. Primers used for QPCR are listed in Table S5. Reactions were carried out using a LightCycler Real-Time PCR System (Roche) with the Thermo Scientific Maxima SYBR Green/ROX qPCR Master Mix (Thermo Fisher Scientific Inc.). Primers were analysed for specificity and efficiency. PCR efficiencies ranged from 0.80 to 1.0. Specificity was assessed by melting curve profile analysis; for *HSP32* and *HSP33* primers, due to their high homology, specificity was ensured by the absence of amplification when cDNA of the respective knockout strain was used as template. The crossing thresholds (CT) were calculated by the second derivative method using the LightCycler® Relative Quantification Software. The relative quantification was corrected for PCR efficiency. *TAF10* and *UBC6* were used as housekeeping genes to normalize the cDNA input between samples. Three independent cDNA samples were analysed. Statistical significance was determined using Student's *t*-test.

Microarray analysis and validation

Wild-type, *hsp31*Δ, *hsp32*Δ and *hsp33*Δ were harvested when cultures reached diauxic-shift. RNA was obtained as described above for QPCR. Three independent RNA samples of each strain were used. RNA integrity was determined on the Agilent 2100 bioanalyser. cDNA was synthetized from total RNA and amplified as fluorescent cRNA (cyanine 3-labeled CTP) using Agilent's Low Input Quick Amp Labeling Kit (one color label) following manufacturer instructions. Labeled cRNA was purified and hybridized to Agilent yeast gene expression microarrays (containing 6256 60-mer probes). Scanning was done on GenePix 4200A and normalization was performed in ArrayTrackTM using mean median scaling without background subtraction. wild type expression profiles were compared individually to each knockout strain profile. Statistical significance was obtained using the Welch's t-test in ArrayTrack^{TM}. Technical validation of the microarrays was performed by relative quantification of the expression of 11 genes by QPCR, using as a template cDNA obtained from the RNA used for the microarrays. The QPCR primers are listed in Table S5. Gene ontology was analysed using the online DAVID Functional Annotation Tool [119] (http://david.abcc.ncifcrf.gov/).

Survival assays

Sensitivity to oxidative stress or thermotolerance was evaluated by spotting assays. Fresh colonies were grown in liquid YPD overnight, serially diluted, normalized to an OD_{600} of 0.1 and spotted on solid SC media containing hydrogen peroxide at different concentrations (1.6 mM and 2.3 mM). For heat shock, cultures were normalized for the number of cells and incubated at 50ºC at the indicated time points. For chronological lifespan determination, cultures were grown on SC media containing 2% glucose, diluted back to synchronize their growth and allowed to grow until cultures cease dividing (beginning of stationary phase). This time point was considered as day zero. Survival was measured by counting colony forming units (CFUs) or by spotting assays, considering 100% survival, the number of CFU or the spots growth at day zero. CFU or spotting assays were performed by taking an aliquot of each culture at the indicated time points, serial diluting and plating or spotting the dilutions on YPD plates.

Zymolyase assay

Cells were collected by centrifugation and resuspended on Tris-HCl (10mM) containing β-mercaptoethanol (40 mM) and 50ug/ml of zymolyase-20T (Seikagaku) and incubated at 30ºC. OD_{600} was measured every 10 minutes.

Cell cycle analysis

Cells in early stationary phase were fixed and stained with propidium iodide (PI) as previously described [120]. Briefly, cells were pelleted and resuspended by vortexing in cold 70% ethanol. After fixation, they were washed and resuspended on sodium citrate pH 7, containing RNAse A (Sigma) to a final concentration of 0.1 mg/ml. After 2 hours of incubation at 37ºC, cells were stained with propidium iodide (final concentration 4 µg/ml) and analysed by flow cytometry on a BD LSR Fortessa™ and detected on the 575/26 nm channel. DNA content was quantified on FlowJo™ v9.6.2.

Immunoblotting, immunoprecipitation and kinase assays

At the indicated time points, the volume of cells equivalent to OD_{600}=1.5 was collected and precipitated with TCA. For precipitation with TCA, cells were resuspended in 1 ml of media and TCA was added to a final concentration of 10%. The samples were incubated 20 minutes at -20ºC and subsequently were centrifuged at 15000 g for 3 min. The pellet was washed twice with 500 ul of acetone and air dried. The pellet was resuspended in MURB (50 mM sodium phosphate, 25 mM MES, pH 7.0, 1% SDS, 3 M

urea, 0.5% 2-mercaptoethanol, 1 mM sodium azide) and disrupted by vortex with glass beads. Before loading the samples into the SDS-polyacrylamide gel, the samples are incubated 10 min at 70ºC and centrifuged at 10000 for 5 minutes to pellet unlysed cells. Protein extracts were separated by SDS-polyacrylamide gel electrophoresis, transferred to nitrocellulose membranes (Bio-Rad) followed by immunoblotting with α-GFP (UC Davis/NIH NeuroMab Facility), α-HA (Santa Cruz Biotechnology Inc.) or α-Pgk1 (Invitrogen) antibodies overnight depending on the protein of interest. α-GFP was used at a dilution of 1:1000 followed by incubation with α-Mouse Ig horseradish peroxidase conjugated antibody (Amersham Bioscience, Piscataway, NJ). For HA-Atg13 immunoprecipitation, the volume corresponding to an OD_{600}=7 was harvested and lysed. The resulting protein extract was incubated with α-HA (Roche Applied Science) for 3 hours followed by one hour incubation with Protein G agarose beads (Invitrogen) with rotatory agitation at 4ºC. Beads were washed 6 times, resuspended on 2x loading buffer (200mM Tris-HCl, 8% SDS, 40% glycerol, 0.4% bromophenol blue, 6% β-mercaptoethanol), boiled at 95ºC for 10 minutes and loaded on an SDS-polyacrylamide gel. After protein separation, the protein extracts were transferred to nitrocellulose membranes and blotted for phospho-(Ser/Thr) PKA substrate antibody (Cell Signaling) at the diltution 1:500 overnight followed by incubation at room temperature with α-Rabbit Ig horseradish peroxidase conjugated antibody (Amersham Bioscience, Piscataway, NJ). After incubation with the secondary antibody and exposure to X-ray film, the membrane was washed with a stripping solution (25 nM glycine hydrochloride, SDS 1%, pH 2) and incubated with α-HA (Santa Cruz Biotechnology, Inc). For phosphatase treatment, HA-Atg13 was immunoprecipitated and incubated with 200 units of ʎ phosphatase (New England Biolabs) for one hour at 30ºC and subsequently run on SDS-polyacrylamide gel electrophoresis followed by immunoblotting as described above.

Fluorescence microscopy

After 5 hours of starvation or rapamycin treatment, GFP-Atg8 expressing cells were observed on a Zeiss Axiovert 200M microscope, either to generate bright field or fluorescence images using a 100X objective. Images were further processed on ImageJ software (http://rsbweb.nih.gov/ij/index.html).

Measurement of ROS

To quantify ROS, $5x10^6$ cells/ml cells were incubated in the dark at 30ºC with 5 µM dihydroethidium (DHE)(Molecular Probes) for 10 minutes and washed 3 times with PBS, or incubated with dihydrorhodamine 123 (DHR 123) (Molecular Probes) at 15 µM for 90 minutes and washed 1 time with PBS, followed by staining with propidium iodide (500ug/ml) to exclude dead cells for 10 minutes and washed 3 times with PBS. Positive cells were counted by flow cytometry.

Acknowledgements

We thank Dr. Federico Herrera for critical reading of the manuscript, Prof. Paula Ludovico for helpful discussions and Prof. Claudina Rodrigues for access to her group's tetrad dissection microscope. We also thank Dr. Nicolas Sylvius and the NUCLEUS facility (Department of Genetics, University of Leicester, UK) for assistance in the gene expression microarrays. We are also grateful to Profs. Daniel Klionsky, Tony Hazbun and Marek Skoneczny for kindly providing plasmids and strains.

References

1. Wilson, M. A., Collins, J. L., Hod, Y., Ringe, D. & Petsko, G. A. The 1.1-A resolution crystal structure of DJ-1, the protein mutated in autosomal recessive early onset Parkinson's disease. Proc. Natl. Acad. Sci. U.S.A. 100, 9256–61 (2003).
2. Cookson, M. R. Crystallizing ideas about Parkinson's disease. Proc. Natl. Acad. Sci. U.S.A. 100, 9111–3 (2003).
3. Du, X. et al. Crystal structure of an intracellular protease from Pyrococcus horikoshii at 2-A resolution. Proc. Natl. Acad. Sci. U.S.A. 97, 14079–84 (2000).
4. Guo, P. C., Zhou, Y. Y., Ma, X. X. & Li, W. F. Structure of Hsp33/YOR391Cp from the yeast Saccharomyces cerevisiae. Acta Crystallogr. Sect. F Struct. Biol. Cryst. Commun. 66, 1557–61 (2010).
5. Quigley, P. M., Korotkov, K., Baneyx, F. & Hol, W. G. J. The 1.6-A crystal structure of the class of chaperones represented by Escherichia coli Hsp31 reveals a putative catalytic triad. Proc. Natl. Acad. Sci. U.S.A. 100, 3137–42 (2003).
6. Tao, X. & Tong, L. Crystal structure of human DJ-1, a protein associated with early onset Parkinson's disease. J. Biol. Chem. 278, 31372–9 (2003).
7. Wilson, M. a, St Amour, C. V, Collins, J. L., Ringe, D. & Petsko, G. a. The 1.8-A resolution crystal structure of YDR533Cp from Saccharomyces cerevisiae: a member of the DJ-1/ThiJ/PfpI superfamily. Proc. Natl. Acad. Sci. U.S.A. 101, 1531–6 (2004).
8. Wilson, M. a, Ringe, D. & Petsko, G. a. The atomic resolution crystal structure of the YajL (ThiJ) protein from Escherichia coli: a close prokaryotic homologue of the Parkinsonism-associated protein DJ-1. J. Mol. Biol. 353, 678–91 (2005).
9. Lucas, J. I. & Marín, I. A new evolutionary paradigm for the Parkinson disease gene DJ-1. Mol. Biol. Evol. 24, 551–61 (2007).
10. Bandyopadhyay, S. & Cookson, M. R. Evolutionary and functional relationships within the DJ1 superfamily. BMC Evol. Biol. 4, 6 (2004).
11. Bonifati, V. et al. Mutations in the DJ-1 gene associated with autosomal recessive early-onset parkinsonism. Science 299, 256–9 (2003).
12. Abou-Sleiman, P. M., Healy, D. G., Quinn, N., Lees, A. J. & Wood, N. W. The role of pathogenic DJ-1 mutations in Parkinson's disease. Ann. Neurol. 54, 283–6 (2003).

13. Nagakubo, D. et al. DJ-1, a novel oncogene which transforms mouse NIH3T3 cells in cooperation with ras. Biochem. Biophys. Res. Commun. 231, 509–13 (1997).
14. Choi, D., Ryu, K.-S. & Park, C. Structural alteration of Escherichia coli Hsp31 by thermal unfolding increases chaperone activity. Biochim. Biophys. Acta 1834, 621–8 (2013).
15. Mujacic, M. & Baneyx, F. Regulation of Escherichia coli hchA, a stress-inducible gene encoding molecular chaperone Hsp31. Mol. Microbiol. 60, 1576–89 (2006).
16. Sastry, M. S. R., Korotkov, K., Brodsky, Y. & Baneyx, F. Hsp31, the Escherichia coli yedU gene product, is a molecular chaperone whose activity is inhibited by ATP at high temperatures. J. Biol. Chem. 277, 46026–34 (2002).
17. Malki, A. et al. Peptidase activity of the Escherichia coli Hsp31 chaperone. J. Biol. Chem. 280, 14420–6 (2005).
18. Subedi, K. P., Choi, D., Kim, I., Min, B. & Park, C. Hsp31 of Escherichia coli K-12 is glyoxalase III. Mol. Microbiol. 81, 926–36 (2011).
19. Le, H.-T. et al. YajL, prokaryotic homolog of parkinsonism-associated protein DJ-1, functions as a covalent chaperone for thiol proteome. J. Biol. Chem. 287, 5861–70 (2012).
20. Abdallah, J., Caldas, T., Kthiri, F., Kern, R. & Richarme, G. YhbO protects cells against multiple stresses. J. Bacteriol. 189, 9140–4 (2007).
21. Le Naour, F. et al. Proteomics-based identification of RS/DJ-1 as a novel circulating tumor antigen in breast cancer. Clin. Cancer Res. 7, 3328–35 (2001).
22. Liu, H. et al. Expression and role of DJ-1 in leukemia. Biochem. Biophys. Res. Commun. 375, 477–83 (2008).
23. He, X. et al. DJ-1 promotes invasion and metastasis of pancreatic cancer cells by activating SRC/ERK/uPA. Carcinogenesis 33, 555–62 (2012).
24. Arnouk, H. et al. Characterization of Molecular Markers Indicative of Cervical Cancer Progression. Proteomics Clin Appl 3, 516–527 (2009).
25. Chen, Y. et al. DJ-1, a novel biomarker and a selected target gene for overcoming chemoresistance in pancreatic cancer. J. Cancer Res. Clin. Oncol. 138, 1463–74 (2012).
26. Lee, H., Choi, S. K. & Ro, J. Y. Overexpression of DJ-1 and HSP90α, and loss of PTEN associated with invasive urothelial carcinoma of urinary bladder: Possible prognostic markers. Oncol Lett 3, 507–512 (2012).
27. Zong, M., Jia, L. & Li, L. Expression of novel tumor markers of pancreatic adenocarcinomas in intrahepatic cholangiocarcinomas. Onco Targets Ther 6, 19–23 (2013).
28. Wei, W., Tang, C., Zhan, X., Yi, H. & Li, C. [Effect of DJ-1 siRNA on biological behavior of human lung squamous carcinoma SK-MES-1 cells]. Zhong Nan Da Xue Xue Bao Yi Xue Ban 38, 7–13 (2013).
29. Kahle, P. J., Waak, J. & Gasser, T. DJ-1 and prevention of oxidative stress in Parkinson's disease and other age-related disorders. Free Radic. Biol. Med. 47, 1354–61 (2009).
30. Kim, R. H. et al. DJ-1, a novel regulator of the tumor suppressor PTEN. Cancer Cell 7, 263–73 (2005).
31. Repici, M. et al. Parkinson's disease-associated mutations in DJ-1 modulate its dimerization in living cells. J. Mol. Med. (2012). doi:10.1007/s00109-012-0976-y
32. Blackinton, J. et al. Effects of DJ-1 mutations and polymorphisms on protein stability and subcellular localization. Brain Res. Mol. Brain Res. 134, 76–83 (2005).
33. Li, H. M., Niki, T., Taira, T., Iguchi-Ariga, S. M. M. & Ariga, H. Association of DJ-1 with chaperones and enhanced association and colocalization with mitochondrial Hsp70 by oxidative stress. Free Radic. Res. 39, 1091–9 (2005).
34. Zhang, L. et al. Mitochondrial localization of the Parkinson's disease related protein DJ-1: implications for pathogenesis. Hum. Mol. Genet. 14, 2063–73 (2005).
35. Miller, D. W. et al. L166P mutant DJ-1, causative for recessive Parkinson's disease, is degraded through the ubiquitin-proteasome system. J. Biol. Chem. 278, 36588–95 (2003).
36. Canet-Avilés, R. M. et al. The Parkinson's disease protein DJ-1 is neuroprotective due to cysteine-sulfinic acid-driven mitochondrial localization. Proc. Natl. Acad. Sci. U.S.A. 101, 9103–8 (2004).
37. Yoshida, K. et al. Immunocytochemical localization of DJ-1 in human male reproductive tissue. Mol. Reprod. Dev. 66, 391–7 (2003).
38. Tsuboi, Y. et al. DJ-1, a causative gene product of a familial form of Parkinson's disease, is secreted through microdomains. FEBS Lett. 582, 2643–9 (2008).
39. Devic, I. et al. Salivary α-synuclein and DJ-1: potential biomarkers for Parkinson's disease. Brain 134, e178 (2011).
40. Pardo, M. et al. The characterization of the invasion phenotype of uveal melanoma tumour cells shows the presence of MUC18 and HMG-1 metastasis markers and leads to the identification of DJ-1 as a potential serum biomarker. Int. J. Cancer 119, 1014–22 (2006).
41. Oda, M. et al. High levels of DJ-1 protein in nipple fluid of patients with breast cancer. Cancer Sci. 103, 1172–6 (2012).
42. Tian, M. et al. Proteomic analysis identifies MMP-9, DJ-1 and A1BG as overexpressed proteins in pancreatic juice from pancreatic ductal adenocarcinoma patients. BMC Cancer 8, 241 (2008).

43. Yanagida, T. et al. Oxidative stress induction of DJ-1 protein in reactive astrocytes scavenges free radicals and reduces cell injury. Oxid Med Cell Longev 2, 36–42
44. Bandopadhyay, R. et al. The expression of DJ-1 (PARK7) in normal human CNS and idiopathic Parkinson's disease. Brain 127, 420–30 (2004).
45. Rizzu, P. et al. DJ-1 colocalizes with tau inclusions: a link between parkinsonism and dementia. Ann. Neurol. 55, 113–8 (2004).
46. Neumann, M. et al. Pathological properties of the Parkinson's disease-associated protein DJ-1 in alpha-synucleinopathies and tauopathies: relevance for multiple system atrophy and Pick's disease. Acta Neuropathol. 107, 489–96 (2004).
47. Wilson, M. A. The Role of Cysteine Oxidation in DJ-1 Function and Dysfunction. 15, (2011).
48. Zhou, W., Zhu, M., Wilson, M. A., Petsko, G. A. & Fink, A. L. The oxidation state of DJ-1 regulates its chaperone activity toward alpha-synuclein. J. Mol. Biol. 356, 1036–48 (2006).
49. Blackinton, J. et al. Formation of a stabilized cysteine sulfinic acid is critical for the mitochondrial function of the parkinsonism protein DJ-1. J. Biol. Chem. 284, 6476–85 (2009).
50. Choi, J. et al. Oxidative damage of DJ-1 is linked to sporadic Parkinson and Alzheimer diseases. J. Biol. Chem. 281, 10816–24 (2006).
51. U. Sajjad, M. et al. DJ-1 modulates aggregation and pathogenesis in models of Huntington's disease. Human molecular genetics (In revision) (2013).
52. Andres-Mateos, E. et al. DJ-1 gene deletion reveals that DJ-1 is an atypical peroxiredoxin-like peroxidase. Proc. Natl. Acad. Sci. U.S.A. 104, 14807–12 (2007).
53. Yamaguchi, H. & Shen, J. Absence of dopaminergic neuronal degeneration and oxidative damage in aged DJ-1-deficient mice. Mol Neurodegener 2, 10 (2007).
54. Chen, L. et al. Age-dependent motor deficits and dopaminergic dysfunction in DJ-1 null mice. J. Biol. Chem. 280, 21418–26 (2005).
55. Kim, R. H. et al. Hypersensitivity of DJ-1-deficient mice to 1-methyl-4-phenyl-1,2,3,6-tetrahydropyrindine (MPTP) and oxidative stress. Proc. Natl. Acad. Sci. U.S.A. 102, 5215–20 (2005).
56. Manning-Boğ, A. B. et al. Increased vulnerability of nigrostriatal terminals in DJ-1-deficient mice is mediated by the dopamine transporter. Neurobiol. Dis. 27, 141–50 (2007).
57. Bretaud, S., Allen, C., Ingham, P. W. & Bandmann, O. p53-dependent neuronal cell death in a DJ-1-deficient zebrafish model of Parkinson's disease. J. Neurochem. 100, 1626–35 (2007).
58. Baulac, S. et al. Increased DJ-1 expression under oxidative stress and in Alzheimer's disease brains. Mol Neurodegener 4, 12 (2009).
59. Park, J. et al. Drosophila DJ-1 mutants show oxidative stress-sensitive locomotive dysfunction. Gene 361, 133–9 (2005).
60. Menzies, F. M., Yenisetti, S. C. & Min, K.-T. Roles of Drosophila DJ-1 in survival of dopaminergic neurons and oxidative stress. Curr. Biol. 15, 1578–82 (2005).
61. Meulener, M. et al. Drosophila DJ-1 mutants are selectively sensitive to environmental toxins associated with Parkinson's disease. Curr. Biol. 15, 1572–7 (2005).
62. Cookson, M. R. Parkinsonism due to mutations in PINK1, parkin, and DJ-1 and oxidative stress and mitochondrial pathways. Cold Spring Harbor perspectives in medicine 2, a009415 (2012).
63. Shendelman, S., Jonason, A., Martinat, C., Leete, T. & Abeliovich, A. DJ-1 is a redox-dependent molecular chaperone that inhibits alpha-synuclein aggregate formation. PLoS Biol. 2, e362 (2004).
64. Lee, S.-J. et al. Crystal structures of human DJ-1 and Escherichia coli Hsp31, which share an evolutionarily conserved domain. J. Biol. Chem. 278, 44552–9 (2003).
65. Olzmann, J. a et al. Familial Parkinson's disease-associated L166P mutation disrupts DJ-1 protein folding and function. J. Biol. Chem. 279, 8506–15 (2004).
66. Duan, X., Kelsen, S. G. & Merali, S. Proteomic analysis of oxidative stress-responsive proteins in human pneumocytes: insight into the regulation of DJ-1 expression. J. Proteome Res. 7, 4955–61 (2008).
67. Chen, J., Li, L. & Chin, L.-S. Parkinson disease protein DJ-1 converts from a zymogen to a protease by carboxyl-terminal cleavage. Hum. Mol. Genet. 19, 2395–408 (2010).
68. Koide-Yoshida, S. et al. DJ-1 degrades transthyretin and an inactive form of DJ-1 is secreted in familial amyloidotic polyneuropathy. Int. J. Mol. Med. 19, 885–93 (2007).
69. Wilson, M. A., Collins, J. L., Hod, Y., Ringe, D. & Petsko, G. A. The 1 . 1-Å resolution crystal structure of DJ-1 , the protein mutated in autosomal recessive early onset Parkinson ' s disease. (2003).
70. Honbou, K. et al. The crystal structure of DJ-1, a protein related to male fertility and Parkinson's disease. J. Biol. Chem. 278, 31380–4 (2003).
71. Mitsugi, H. et al. Identification of the recognition sequence and target proteins for DJ-1 protease. FEBS Lett. 587, 2493–9 (2013).
72. Kim, Y.-C., Kitaura, H., Taira, T., Iguchi-Ariga, S. M. M. & Ariga, H. Oxidation of DJ-1-dependent cell transformation through direct binding of DJ-1 to PTEN. Int. J. Oncol. 35, 1331–41 (2009).

73. Malhotra, D. et al. Decline in NRF2-regulated antioxidants in chronic obstructive pulmonary disease lungs due to loss of its positive regulator, DJ-1. Am. J. Respir. Crit. Care Med. 178, 592–604 (2008).
74. Clements, C. M., McNally, R. S., Conti, B. J., Mak, T. W. & Ting, J. P.-Y. DJ-1, a cancer- and Parkinson's disease-associated protein, stabilizes the antioxidant transcriptional master regulator Nrf2. Proc. Natl. Acad. Sci. U.S.A. 103, 15091–6 (2006).
75. Im, J.-Y., Lee, K.-W., Woo, J.-M., Junn, E. & Mouradian, M. M. DJ-1 induces thioredoxin 1 expression through the Nrf2 pathway. Hum. Mol. Genet. 21, 3013–24 (2012).
76. Gan, L., Johnson, D. A. & Johnson, J. A. Keap1-Nrf2 activation in the presence and absence of DJ-1. Eur. J. Neurosci. 31, 967–77 (2010).
77. Van der Brug, M. P. et al. RNA binding activity of the recessive parkinsonism protein DJ-1 supports involvement in multiple cellular pathways. Proc. Natl. Acad. Sci. U.S.A. 105, 10244–9 (2008).
78. Hod, Y., Pentyala, S. N., Whyard, T. C. & El-Maghrabi, M. R. Identification and characterization of a novel protein that regulates RNA-protein interaction. J. Cell. Biochem. 72, 435–44 (1999).
79. Liu, W., Zhou, Y.-Y., Teng, M.-K. & Zhou, C.-Z. Purification, crystallization and preliminary X-ray analysis of Hsp33 from Saccharomyces cerevisiae. Acta Crystallogr. Sect. F Struct. Biol. Cryst. Commun. 63, 114–6 (2007).
80. Skoneczna, A., Miciałkiewicz, A. & Skoneczny, M. Saccharomyces cerevisiae Hsp31p, a stress response protein conferring protection against reactive oxygen species. Free Radic. Biol. Med. 42, 1409–20 (2007).
81. De Nobel, H. et al. Parallel and comparative analysis of the proteome and transcriptome of sorbic acid-stressed Saccharomyces cerevisiae. Yeast 18, 1413–28 (2001).
82. Santos, P. M., Simões, T. & Sá-Correia, I. Insights into yeast adaptive response to the agricultural fungicide mancozeb: a toxicoproteomics approach. Proteomics 9, 657–70 (2009).
83. Miura, T., Minegishi, H., Usami, R. & Abe, F. Systematic analysis of HSP gene expression and effects on cell growth and survival at high hydrostatic pressure in Saccharomyces cerevisiae. Extremophiles 10, 279–84 (2006).
84. Pedruzzi, I., Bürckert, N., Egger, P. & De Virgilio, C. Saccharomyces cerevisiae Ras/cAMP pathway controls post-diauxic shift element-dependent transcription through the zinc finger protein Gis1. EMBO J. 19, 2569–79 (2000).
85. Wei, M. et al. Life span extension by calorie restriction depends on Rim15 and transcription factors downstream of Ras/PKA, Tor, and Sch9. PLoS Genet. 4, e13 (2008).
86. DeRisi, J. L., Iyer, V. R. & Brown, P. O. Exploring the metabolic and genetic control of gene expression on a genomic scale. Science 278, 680–6 (1997).
87. Galdieri, L., Mehrotra, S., Yu, S. & Vancura, A. Transcriptional regulation in yeast during diauxic shift and stationary phase. OMICS 14, 629–38 (2010).
88. De Virgilio, C. The essence of yeast quiescence. FEMS Microbiol. Rev. 36, 306–39 (2012).
89. Rustici, G. et al. ArrayExpress update--trends in database growth and links to data analysis tools. Nucleic Acids Res. 41, D987–90 (2013).
90. Verwaal, R. et al. HXT5 expression is under control of STRE and HAP elements in the HXT5 promoter. Yeast 21, 747–57 (2004).
91. Xie, Z., Nair, U. & Klionsky, D. J. Atg8 controls phagophore expansion during autophagosome formation. Mol. Biol. Cell 19, 3290–8 (2008).
92. Klionsky, D. J., Cuervo, A. M. & Seglen, P. O. Methods for monitoring autophagy from yeast to human. Autophagy 3, 181–206
93. Klionsky, D. J. For the last time, it is GFP-Atg8, not Atg8-GFP (and the same goes for LC3). Autophagy 7, 1093–4 (2011).
94. Heitman, J., Movva, N. R. & Hall, M. N. Targets for cell cycle arrest by the immunosuppressant rapamycin in yeast. Science 253, 905–9 (1991).
95. Zaragoza, D., Ghavidel, a, Heitman, J. & Schultz, M. C. Rapamycin induces the G0 program of transcriptional repression in yeast by interfering with the TOR signaling pathway. Mol. Cell. Biol. 18, 4463–70 (1998).
96. Gray, J. V et al. " Sleeping Beauty ": Quiescence in Saccharomyces cerevisiae †. 68, 187–206 (2004).
97. Dechant, R. & Peter, M. Nutrient signals driving cell growth. Curr. Opin. Cell Biol. 20, 678–87 (2008).
98. Kamada, Y. et al. Tor directly controls the Atg1 kinase complex to regulate autophagy. Mol. Cell. Biol. 30, 1049–58 (2010).
99. Yorimitsu, T., Zaman, S., Broach, J. R. & Klionsky, D. J. Protein Kinase A and Sch9 Cooperatively Regulate Induction of Autophagy in Saccharomyces cerevisiae. 18, 4180–4189 (2007).
100. Sampaio-Marques, B., Felgueiras, C., Silva, A., Rodrigues, F. & Ludovico, P. Yeast chronological lifespan and proteotoxic stress: is autophagy good or bad? Biochem. Soc. Trans. 39, 1466–70 (2011).

101. Stephan, J. S., Yeh, Y.-Y., Ramachandran, V., Deminoff, S. J. & Herman, P. K. The Tor and PKA signaling pathways independently target the Atg1/Atg13 protein kinase complex to control autophagy. Proc. Natl. Acad. Sci. U.S.A. 106, 17049–54 (2009).
102. Kamada, Y. & Funakoshi, T. Tor-mediated induction of autophagy via an Apg1 protein kinase complex. The Journal of cell … 150, 1507–1513 (2000).
103. Stephan, J. S., Yeh, Y.-Y., Ramachandran, V., Deminoff, S. J. & Herman, P. K. The Tor and PKA signaling pathways independently target the Atg1/Atg13 protein kinase complex to control autophagy. Proc. Natl. Acad. Sci. U.S.A. 106, 17049–54 (2009).
104. Ramachandran, V. & Herman, P. K. Antagonistic interactions between the cAMP-dependent protein kinase and Tor signaling pathways modulate cell growth in Saccharomyces cerevisiae. Genetics 187, 441–54 (2011).
105. Takahara, T. & Maeda, T. Transient sequestration of TORC1 into stress granules during heat stress. Mol. Cell 47, 242–52 (2012).
106. Urban, J. et al. Sch9 is a major target of TORC1 in Saccharomyces cerevisiae. Mol. Cell 26, 663–74 (2007).
107. Lee, J.-Y., Kim, C., Kim, J. & Park, C. DJR-1.2 of Caenorhabditis elegans is induced by DAF-16 in the dauer state. Gene (2013). doi:10.1016/j.gene.2013.04.032
108. Powers, R. W., Kaeberlein, M., Caldwell, S. D., Kennedy, B. K. & Fields, S. Extension of chronological life span in yeast by decreased TOR pathway signaling. Genes Dev. 20, 174–84 (2006).
109. Laplante, M. & Sabatini, D. M. mTOR signaling in growth control and disease. Cell 149, 274–93 (2012).
110. Loewith, R. & Hall, M. N. Target of rapamycin (TOR) in nutrient signaling and growth control. Genetics 189, 1177–201 (2011).
111. Hardwick, J. S., Kuruvilla, F. G., Tong, J. K., Shamji, a F. & Schreiber, S. L. Rapamycin-modulated transcription defines the subset of nutrient-sensitive signaling pathways directly controlled by the Tor proteins. Proc. Natl. Acad. Sci. U.S.A. 96, 14866–70 (1999).
112. Swinnen, E. et al. Rim15 and the crossroads of nutrient signalling pathways in Saccharomyces cerevisiae. Cell Div 1, 3 (2006).
113. Krebiehl, G. et al. Reduced basal autophagy and impaired mitochondrial dynamics due to loss of Parkinson's disease-associated protein DJ-1. PLoS ONE 5, e9367 (2010).
114. Irrcher, I. et al. Loss of the Parkinson's disease-linked gene DJ-1 perturbs mitochondrial dynamics. Hum. Mol. Genet. 19, 3734–46 (2010).
115. Ren, H. et al. DJ-1, a cancer and Parkinson's disease associated protein, regulates autophagy through JNK pathway in cancer cells. Cancer Lett. 297, 101–8 (2010).
116. Wach, A. PCR-synthesis of marker cassettes with long flanking homology regions for gene disruptions in S. cerevisiae. Yeast 12, 259–65 (1996).
117. Suzuki, K. et al. The pre-autophagosomal structure organized by concerted functions of APG genes is essential for autophagosome formation. EMBO J. 20, 5971–81 (2001).
118. Cheong, H., Nair, U., Geng, J. & Klionsky, D. J. The Atg1 kinase complex is involved in the regulation of protein recruitment to initiate sequestering vesicle formation for nonspecific autophagy in Saccharomyces cerevisiae. Mol. Biol. Cell 19, 668–81 (2008).
119. Huang, D. W., Sherman, B. T. & Lempicki, R. a. Systematic and integrative analysis of large gene lists using DAVID bioinformatics resources. Nat Protoc 4, 44–57 (2009).
120. Costello, G., Rodgers, L. & Beach, D. Fission yeast enters the stationary phase G0 state from either mitotic G1 or G2. Curr. Genet. 11, 119–125 (1986).

Chapter 4

DJ-1 modulates huntingtin aggregation and toxicity in models of Huntington's disease

This chapter includes the most relevant results obtained in collaboration with the group of Andreas Wyttenbach (University of Southampton, UK) that are part of the following publication:

U. Sajjad, M., Green, W., E., Miller-Fleming, L., Hands, S., Herrera, F., Outeiro, T. F., Giorgini, F., Wyttenbach, A. DJ-1 modulates aggregation and pathogenesis in models of Huntington's disease. Human Molecular Genetics (September 2013).

Chapter 4. DJ-1 modulates huntingtin aggregation and toxicity in models of Huntington's disease

Abstract

Neurodegenerative diseases such as Parkinson's (PD) and Huntington's disease (HD) share common pathogenic mechanisms including the misfolding and aggregation of proteins. Molecular chaperones are the first line of defense against misfolded proteins and thus are potential drug targets against neurodegeneration. Mutations in the DJ-1 protein are associated to familial PD. DJ-1 has been proposed to function as a redox-regulated chaperone that prevents α-synuclein aggregation. Here, we investigated whether DJ-1 also plays a role in HD. Overexpression of DJ-1 in yeast and *Drosophila* suppressed the toxicity of mutant huntingtin (Htt). DJ-1 expression levels and oxidation state were abnormally increased in brains of HD patients and various experimental models of HD. DJ-1 directly interacted with mutant Htt and modulated polyglutamine aggregation and toxicity in a redox-dependent manner. Altogether, our findings support a general role for DJ-1 as a redox-regulated chaperone and provide the basis for further studies into the protective effect of DJ-1 in neurodegenerative disorders and other human pathologies involving protein misfolding and aggregation.

Introduction

Huntington's disease (HD) is caused by the expansion of a CAG repeat in the *IT-15* gene, which encodes a polyglutamine (polyQ) tract in the N-terminal region of the huntingtin (Htt) protein [1]. The CAG repeat number is polymorphic in the general population, with repeat lengths ranging from 6 to 35. When the polyQ tract exceeds 35 glutamines, Htt becomes prone to misfold and aggregate, and individuals develop HD. The length of the polyQ expansion correlates directly with Htt aggregation *in vitro* and with severity of the disease in HD patients, and inversely with age of disease onset [2].

The first line of defense against misfolded proteins is represented by molecular chaperones that have the ability to help proteins in the folding process [3]. Molecular chaperones are able to modulate polyQ aggregation and toxicity *in vitro* and *in vivo* [4–6]. Therefore, they are considered as potential therapeutic targets for HD [5]. Redox-regulated chaperones are a specific class of chaperones that are activated by oxidation instead of ATP. These are particularly important in stress conditions in which the levels

of ATP are low and the intracellular space becomes more oxidative, such as Parkinson´s disease (PD), HD and other neurodegenerative disorders [7,8].

DJ-1 is a protein which mutation has been associated with Parkinson's disease (PD) [9,10]. It is thought to play a role as a redox-dependent chaperone [11,12], as well as numerous functions generally related with protection against oxidative stress (described in further detail on Chapter 3). Mild oxidation of DJ-1 has been associated with its activation, whereas extensive oxidation is thought to cause its dysfunction (Fig. 4.1) [13]. Interestingly, ageing causes overoxidation of DJ-1 in different models and human brain samples [14]. Moreover, DJ-1 is irreversibly oxidized at Cys106 in the brains of patients with PD and Alzheimer's disease (AD), suggesting that DJ-1 may be not only linked to familial PD but also may contribute for the pathogenesis of AD and idiopathic PD [15].

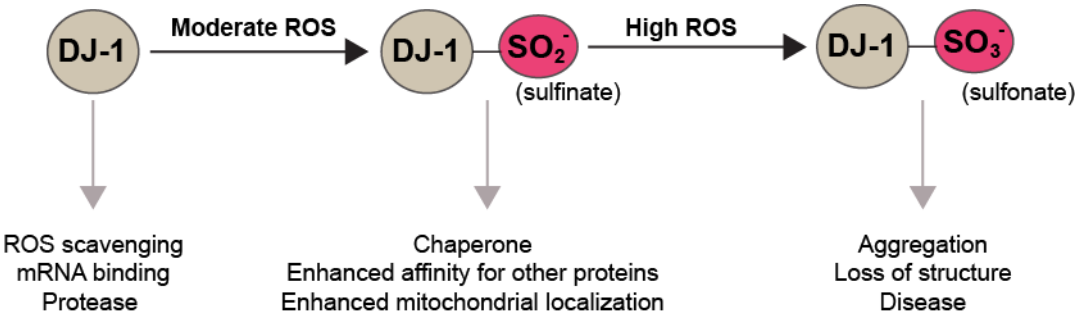

Figure 4.1. Proposed functions for human DJ-1 associated with the major oxidized forms of cysteine 106.
The human DJ-1 can be oxidized in several cysteine and methione residues. Different oxidation status of the cysteine residue 106 is likely related with different roles played by DJ-1. Cysteine 106 can be oxidized to cysteine-sulfenic (SOH) to cysteine-sulfinic (SO_2H) or cysteine-sulfonic acid (SO_3H). Scheme adapted from [13].

Here, we provide data that support DJ-1 as a potential therapeutic target for HD. We demonstrate that DJ-1 expression and oxidation is abnormally increased in the human HD brain, in the brain of an HD mouse model and in various HD cell models. Importantly, DJ-1 overexpression conferred protection against toxicity in Drosophila and yeast models of HD. Furthermore, we found that DJ-1 directly interacted with an expanded fragment of Htt exon 1 in the test tube and in cell models, providing a basis for the effects of DJ1 in Htt aggregation and toxicity. Our work serves as the base for future studies to elucidate the precise mode of action of DJ-1 during HD, as well as to confirm its validity as a therapeutical target for HD.

Results

DJ-1 overexpression ameliorates mutant Htt toxicity in yeast and fruit flies

To test whether DJ-1 plays a role in HD pathogenesis, we first interrogated its potential function in *Saccharomyces cerevisiae* and *Drosophila melanogaster* models of HD. As already mentioned in Chapter 1, expression of a mutant Htt fragment with an expanded polyQ stretch (Htt72Q) leads to Htt aggregation and cellular toxicity in yeast (Fig. 4.2A). We found that overexpression of Hsp31 – one of the yeast DJ-1 homologues – suppresses Htt72Q toxicity (Fig. 4.2A), which correlated with a reduction in aggregated mutant Htt protein (Fig. 4.2B). Information about the yeast DJ-1 homologues can be found on Chapter 3. In contrast, overexpression of DJ-1 led to an increase in Htt72Q aggregation and did not prevent Htt toxicity. We could not determine whether DJ-1 enhanced Htt toxicity, as Htt72Q completely suppresses the yeast growth.

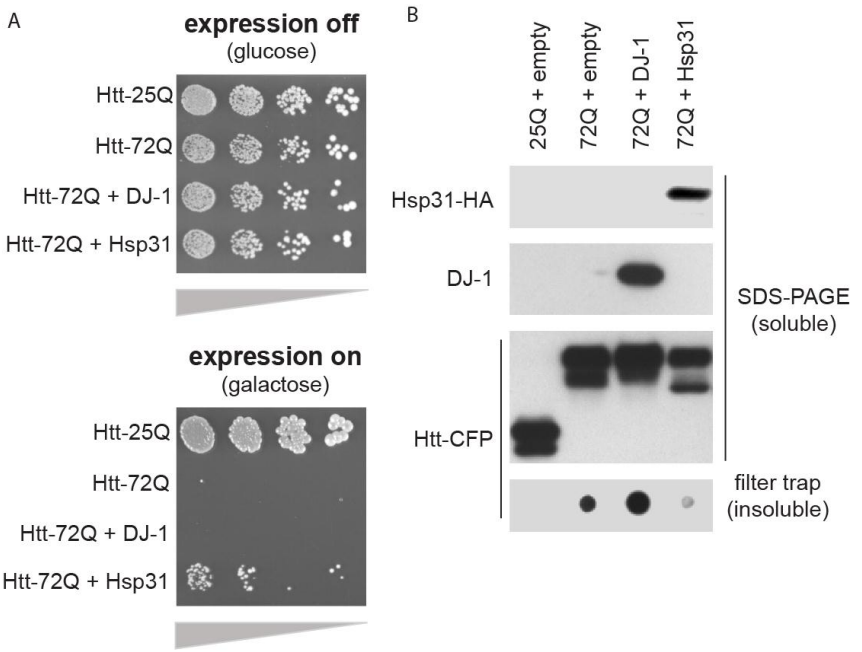

Figure 4.2. Modulation of mutant Htt aggregation and toxicity by human DJ-1 and its yeast homologue Hsp31.

(A) Hsp31 overexpression protects yeast against Htt72Q toxicity. Yeast cells expressing Htt72Q were independently transformed with DJ-1, Hsp31 or an empty vector. Equal numbers of cells were serially diluted five-fold and plated on media containing glucose to assess cell numbers and galactose to induce expression of Htt72Q. Control cells carrying empty vector and expressing Htt25Q were used as reference for normal cell growth. (B) Human DJ-1 and Hsp31 modulate mutant Htt aggregation. Protein extracts were subjected to SDS-PAGE for detection of soluble Htt72Q or filter trap to detect SDS-insoluble Htt, followed by immunoblotting using an anti-GFP antibody.

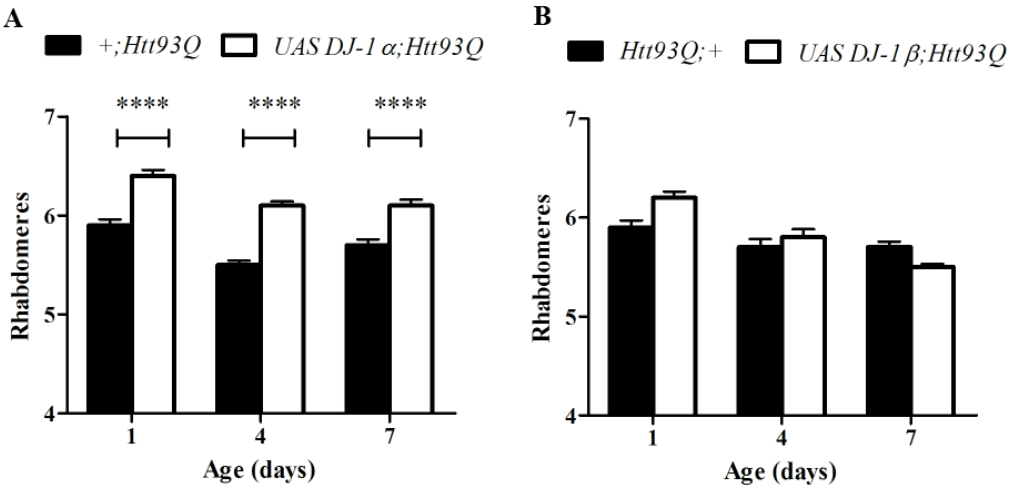

Figure 4.3. Overexpression of DJ-1α ameliorates neurodegeneration in HD model flies.

Quantification of mean rhabdomeres (± SEM) per ommatidum in flies pan-neuronally expressing both Htt93Q and either DJ-1α or DJ-1β under the control of the *elavGAL4* driver. Overexpression of DJ-1α at day 1, 4, and 7 post eclosion ($F_{1,48}$ = 88.52, p < 0.0001) (A), and DJ-1β ($F_{1,47}$ = 1.59, P = 0.2138) (B) Statistical significance was assessed by a one-way ANOVA followed by a Bonferroni post hoc test. n = 5–13 samples per genotype (****p < 0.0001). Error bars represent standard deviation.

DJ-1 expression and its oxidation is increased in the HD brain and in cell and animal models of HD

Human HD frontal cortex (Vonsattel Grade 2), but not the cerebellum of the same patients, showed a significant increase in DJ-1 levels versus age-matched controls (Fig. 4.4 A-F). Seventeen weeks-old R6/2 HD mice (overexpressing mutant Htt exon 1) also showed higher levels of DJ-1 in the frontal cortex, but not in the cerebellum (Fig. 4.4 G-L). At this age, HD behavioural and pathological features are already present. These results were confirmed in three different cell models of HD, also expressing Htt exon 1 under different types of promoters (data not shown).

Irreversible oxidation of DJ-1 at Cys106 (sulfonate) was significantly increased in the frontal cortex (Fig. 4.5) of HD patients, consistent with previous reports on DJ-1 oxidation in PD and AD patients brains [15].

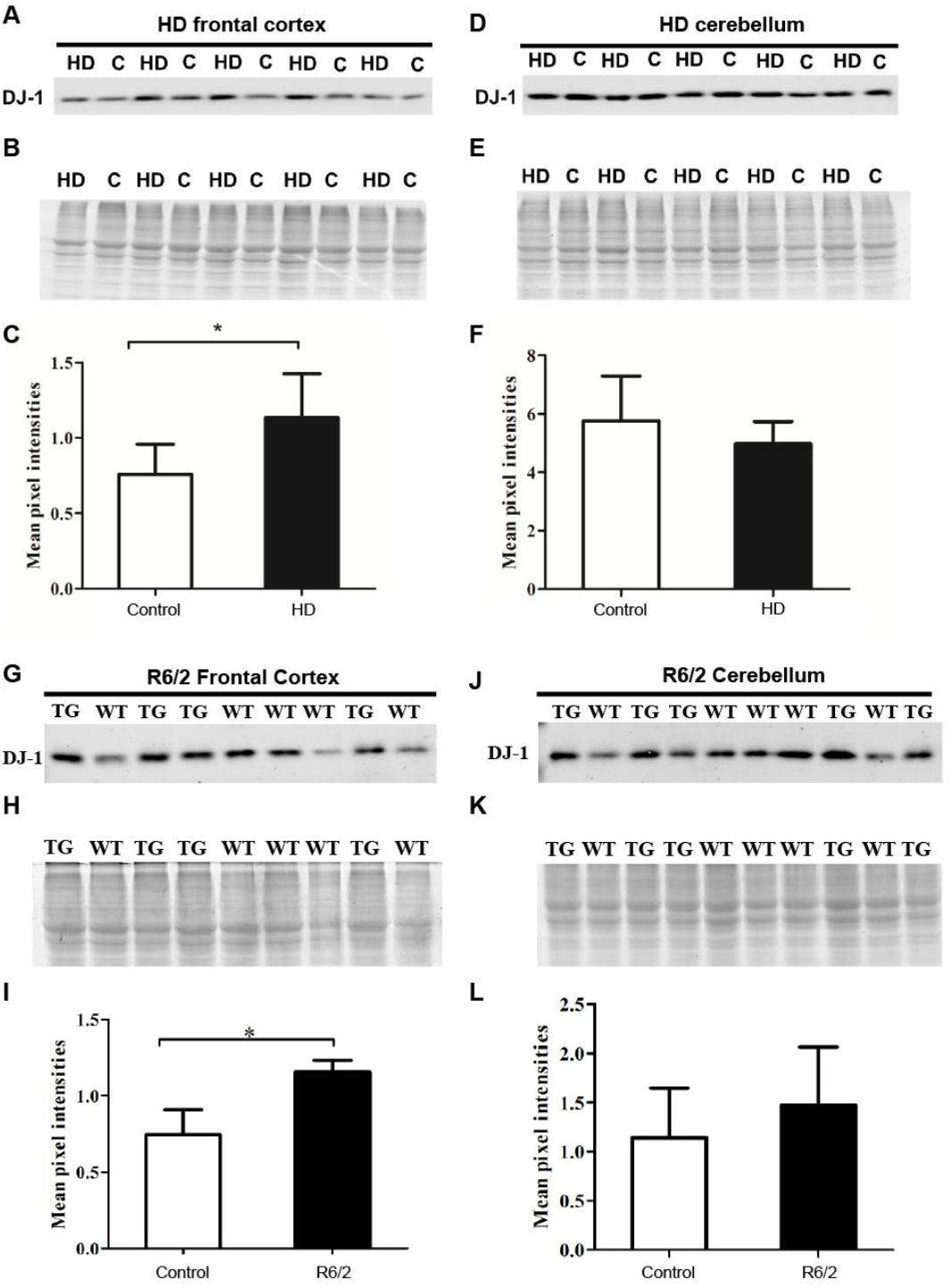

Figure 4.4. DJ-1 expression is increased in the frontal cortex of HD patients and R6/2 mouse tissue.

Immunoblot analysis showing expression levels of DJ-1 in the frontal cortex (A,G) and cerebellum (D,J) of brains of HD patients (A-F) and R6/2 mouse model (G-L). Their respective loading controls (coomassie gels B,H and E,K) and band intensity quantification (C,I and F,L) (DJ-1 bands were normalized versus loading control signals) are shown. Error bars represent standard deviation. Statistical significance was determined by means of an unpaired t-test (*P < 0.05, n = 5, frontal cortex and cerebellum, HD = Huntington's disease patient tissue and C = age matched control tissue).

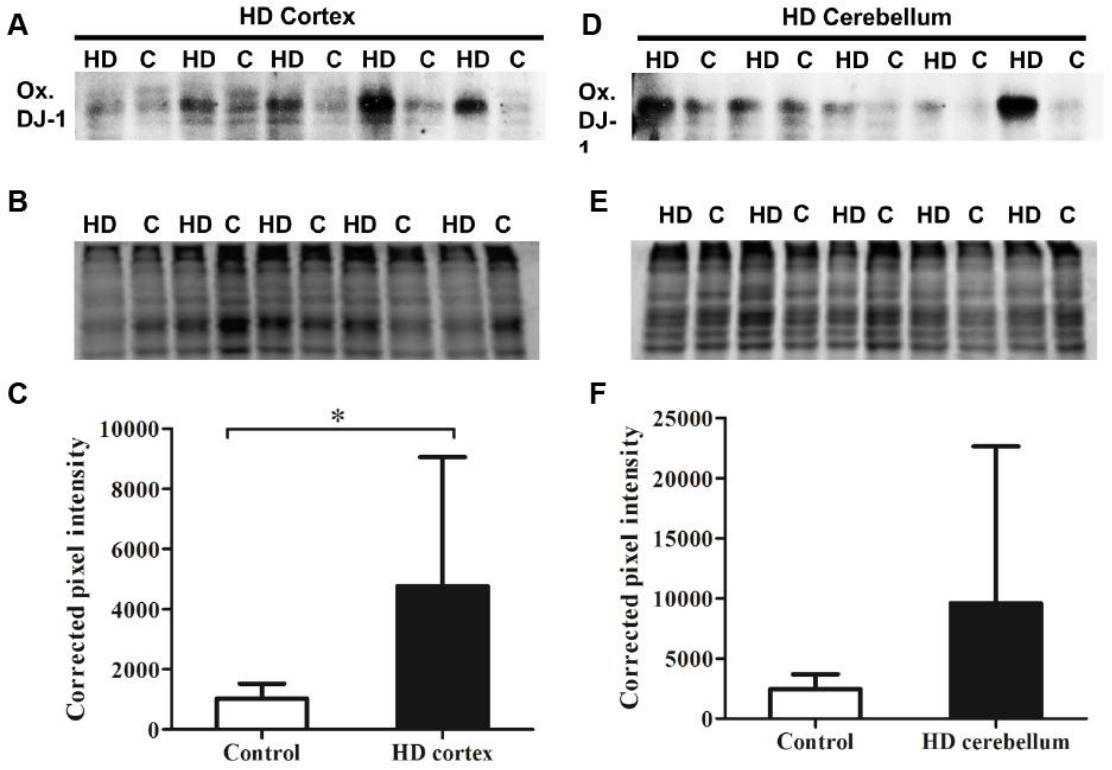

Figure 4.5. Enhanced DJ-1 oxidation in the frontal cortex of HD brain tissue.
Immunoblot analysis of frontal cortex (A) and cerebellum (D) tissues using an antibody against DJ-1 oxidised at cysteine 106. (C, D) Corresponding coomassie gels (loading control) and the respective graph showing the quantification of the bands intensity normalized versus the loading control. (F) Error bars represent standard deviation. Statistical significance was determined by means of an unpaired t-test (n=5 patients and control samples, *P< 0.05 for frontal cortex and P= 0.13 for cerebellum).

DJ-1 directly modulates aggregation and toxicity of mutant Htt in an oxidation-sensitive manner

We next evaluated whether DJ-1 modulated mutant Htt toxicity and aggregation in mammalian systems. Surprisingly, in contrast to the results obtained in yeast and flies, DJ-1 significantly increased the toxicity and the number of cells with Htt97Q-mRFP aggregates in HeLa cells (Fig. 4.6A and C) and astrocytes (Fig. 4.6B and D). These results were further supported by filter trap assays, which indicated a trend towards an increase in SDS-insoluble Htt aggregates. Although it did not reach statistical significance, higher levels of Htt97Q-mRFP were retained in a filter when co-expressed with DJ-1 in HeLa cells (Fig. 4.6E). DJ-1 transfection was confirmed by immunoblotting analysis (data not shown).

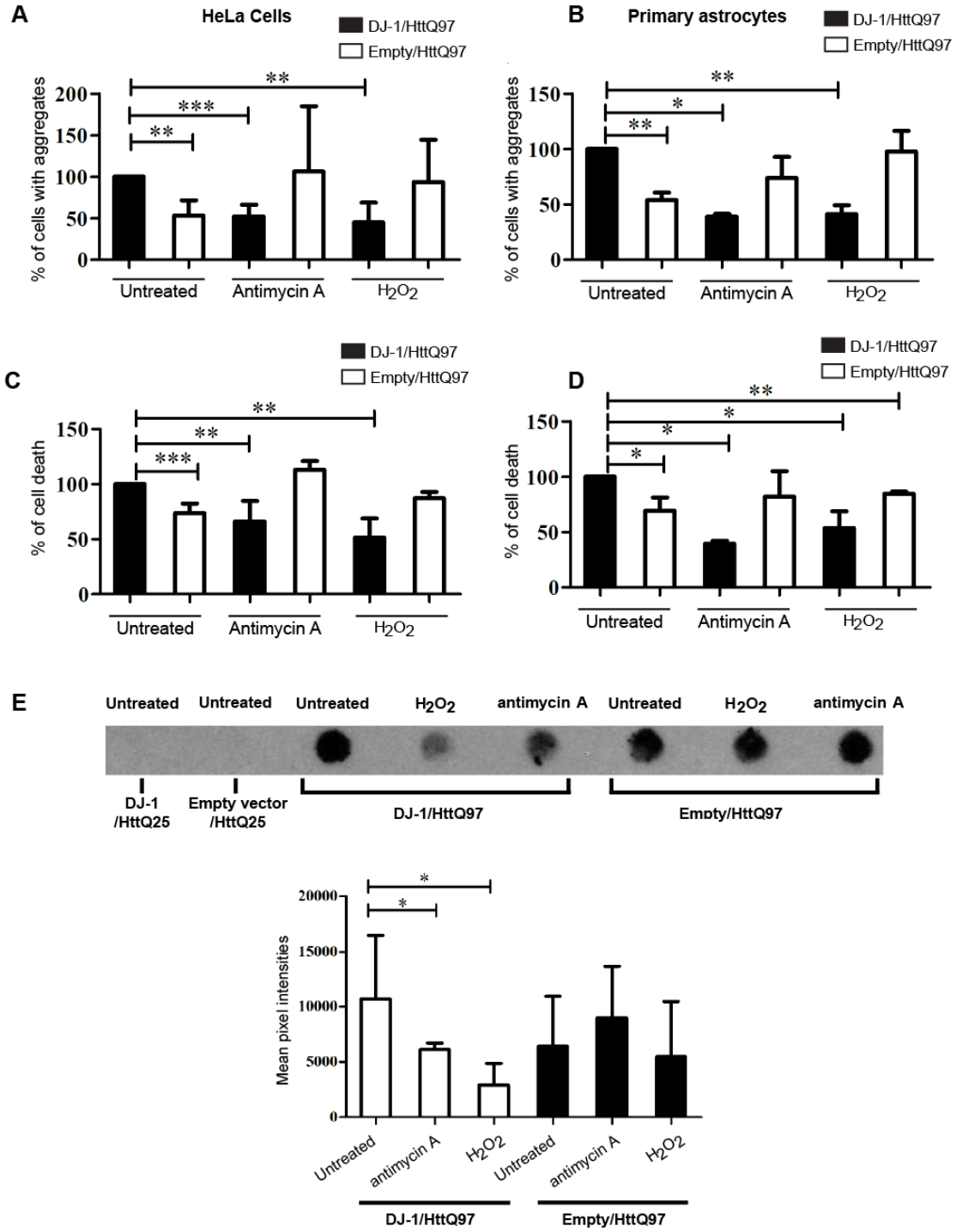

Figure 4.6. DJ-1 increases mutant Htt aggregation and toxicity in an oxidation-dependent manner.

HeLa cells (A,C,E) and primary astrocytes (B,D) were transfected with Htt93Q in combination with either an empty vector or a vector containing DJ-1. Cells were treated with 5 μM of the pro-oxidant antimycin A or 100μM hydrogen peroxide (H_2O_2) or left untreated as a control. After 3 days of transfection, cells were analysed by microscopy to score aggregate-positive cells (% of cells with aggregates), (A,B) or were analysed for toxicity (C,D). Cell death was measured by scoring abnormal nuclear morphology of cells co-transfected with DJ-1 or control vector and HttQ97-mRFP. The % of cell death was normalized by the cell death of untreated cells

transfected with DJ-1 and Htt97Q.(A-D) Error bars represent standard deviation. One sample t-test was used for statistical analysis (*p < 0.05, **p <0.01 and ***p <0.001). (E) DJ-1 overexpression under mild oxidative stress decreases the SDS insoluble aggregates detected on a filter trap assay. Immunoblot analyses were performed with an anti-Htt antibody. The graph represents the mean of three independent experiments and the error bars represent the standard deviation. Statistical analysis was performed using One-sample t-test.

We next asked whether this effect of DJ-1 on Htt was due to direct interaction between the two proteins. We found that endogenous or exogenous DJ-1 co-localized with Htt in HeLa cells (Fig. 4.7B-D) and occasionally surrounded Htt97Q aggregates in a ring-like pattern (Fig. 4.7C and D), which were found more frequently when DJ-1 was overexpressed. To assess whether this interaction occurred in living cells we used the bimolecular fluorescence complementation (BiFC) assay, which we had previously developed to visualize Htt oligomerization and aggregation [18]. We transfected constructs encoding either a Htt exon1 fragment (with either 25Q or 103Q tracts) or DJ-1 fused to two non-fluorescent halves of the Venus fluorescent reporter into human neuroglioma H4 cells (Fig. 4.8A). If DJ-1 and Htt interact, the non-fluorescent halves are brought together and reconstitute the functional Venus fluorophore. Confirming our previous results, DJ-1 not only interacted directly with both Htt25Q and Htt103Q (Fig. 4.8B,C), but also DJ-1 co-aggregated with Htt103Q. While DJ-1 did not modify the number of aggregates per cell (Fig. 4.8D) or the percentage of small- and medium-size aggregates (<3 µm), it produced a significant increase in the percentage of large aggregates (>3 µm) (Fig. 4.8E).

Consistent with the results obtained in HeLa cells and primary astrocytes, Htt103Q toxicity was significantly increased upon co-expression of DJ-1 Htt103Q BiFC constructs. Interestingly, DJ-1 expression also increased Htt25Q toxicity.

Our results strongly suggest that DJ-1 interacts with Htt and enhances its aggregation in mammalian cell models, whereas overexpression of the organism-specific DJ-1 homologs in yeast and fly models of HD is protective. We hypothesized that DJ-1 exerted different functions depending on its oxidation status, since it is well established that oxidation affects directly the chaperone function of DJ-1 [13]. HeLa cells or primary astrocytes (co-transfected with Htt97Q and an empty vector or a DJ-1 plasmid) were exposed to sub-lethal doses of oxidative stressors: hydrogen peroxide (H_2O_2) or antimycin A. The higher levels of Htt97Q aggregation and toxicity caused by DJ-1 overexpression were reduced back to basal levels upon treatment with H_2O_2 or antimycin A (Fig. 4.8A-D). Filter trap assays further supported these results (Fig. 4.8E).

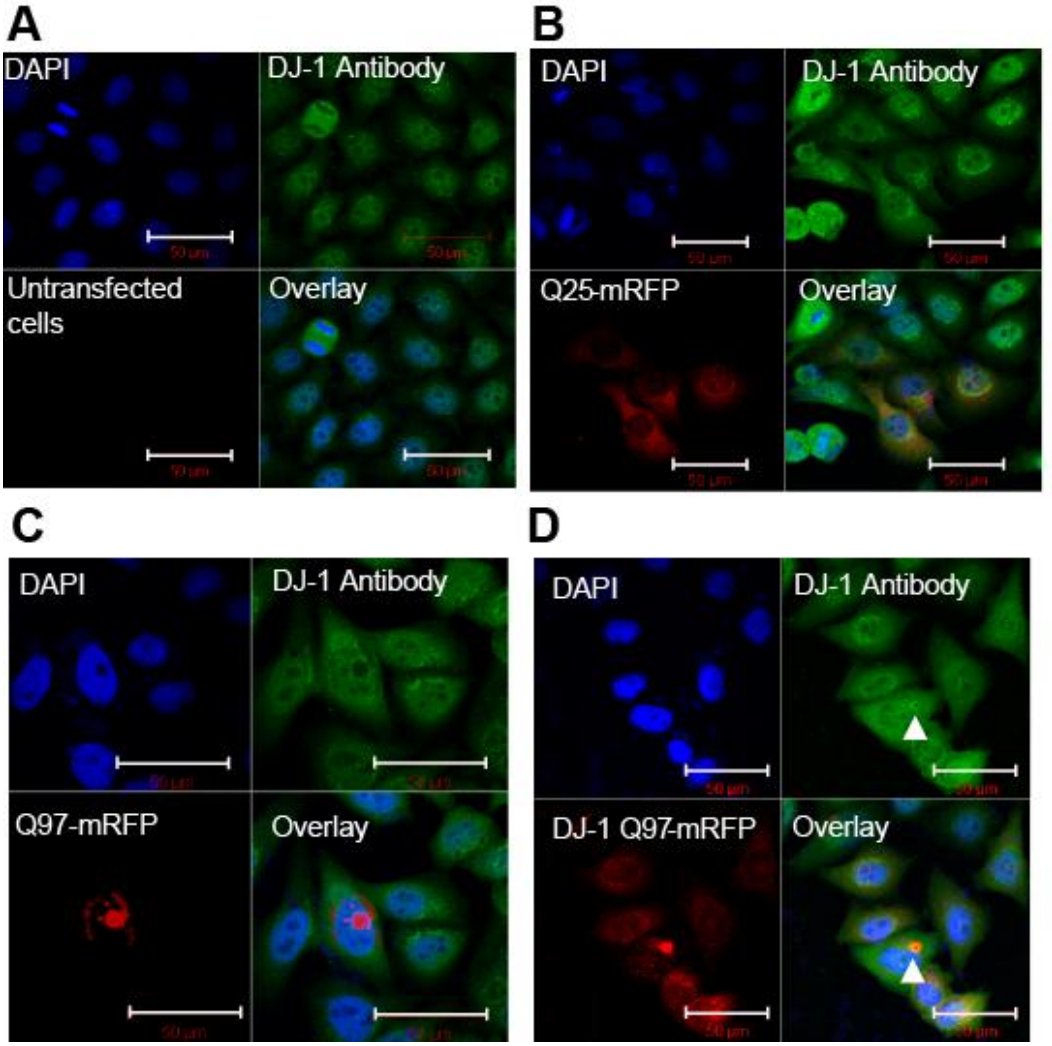

Figure 4.7. Endogenous and exogenous DJ-1 occasionally co-localize with HttQ97 inclusion bodies in HeLa cells.

(A) Untransfected control HeLa cells after staining with a DJ-1 antibody. (B) DJ-1 staining after co-transfection with HttQ25-mRFP and the empty vector. (C) DJ-1 staining after co-transfection with HttQ97-mRFP and the empty vector. (D) DJ-1 staining after co-transfection with HttQ97-mRFP and DJ-1 vector. White arrowhead points to DJ-1 surrounding an aggregate in a ring-like structure. Scale bar represents 50 µm.

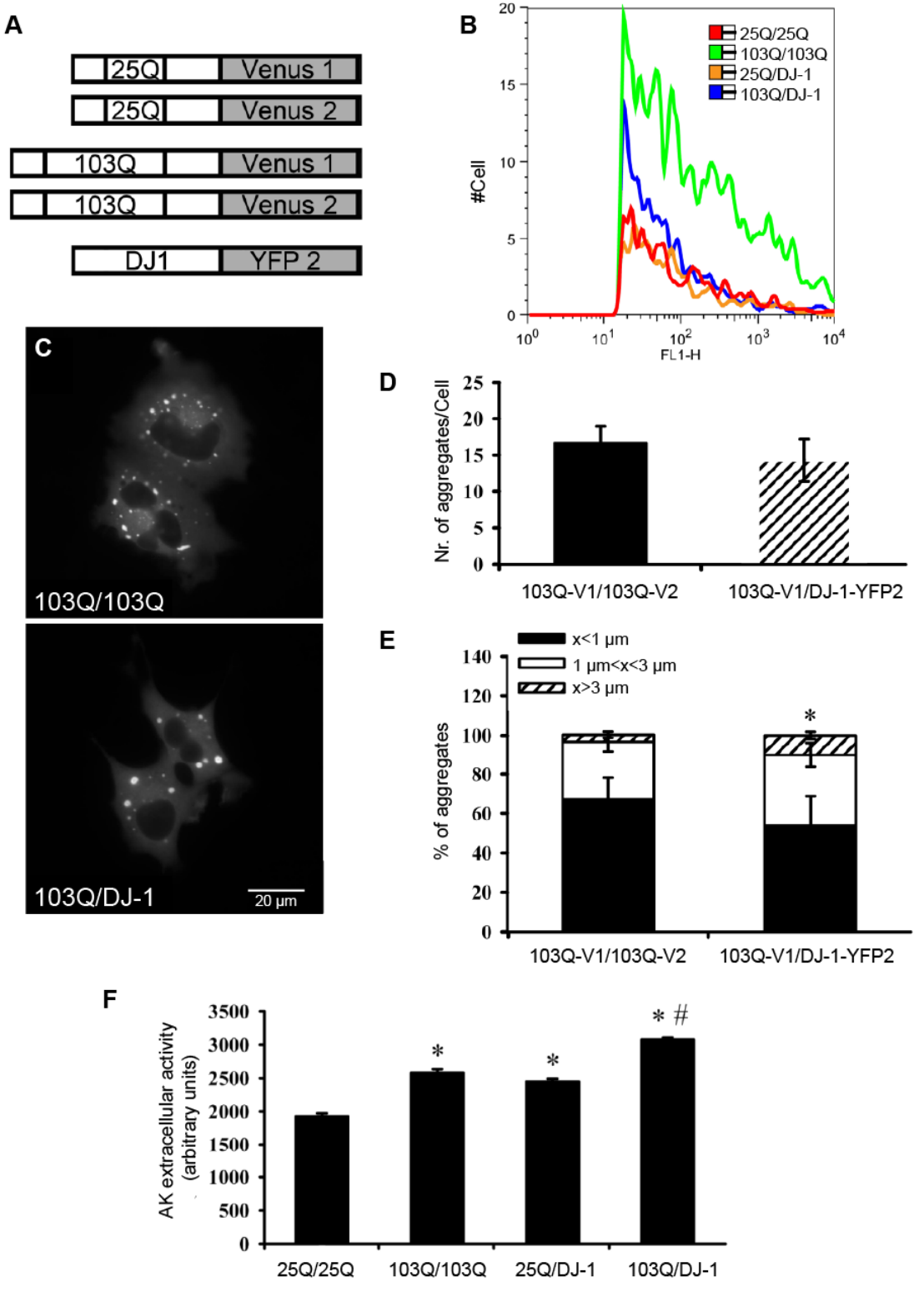

Figure 4.8. DJ-1 interacts with mutant Htt and potentiates its toxicity in mammalian cells.

(A) Representation of Htt and DJ-1 BiFC constructs. (B-F) H4 cells were transfected with Htt25Q-Venus1 together with Htt25Q-Venus2 or DJ-1-YFP2 (B and F) or Htt103Q-Venus1 in combination either with Htt103Q-Venus2 or DJ-1-YFP2 BiFC constructs (B-F). After 24 hours, cells were analysed by flow cytometry (B) and widefield fluorescence microscopy (C-E). (D,E)

The number of aggregates per cell was counted and classified according to their longer diameter in three classes: smaller than 1 µm, larger than 1 µm but smaller than 3 µm, and larger than 3 µm. Scale bar, 20 µm. Statistical significance was determined by means of Student *t*-test. Results depicted are the mean ± SEM of 3 independent experiments (*p < 0.05). (F) Cell toxicity after 24 hours determined by the levels of extracellular adenylate kinase activity. Statistical significance was assessed by means of a one-way ANOVA followed by a Student-Newman-Keuls post hoc test. Results depicted are the mean ± SEM of 3 independent experiments (* p < 0.05 vs 25Q/25Q; # p < 0.05 vs 103Q/103Q).

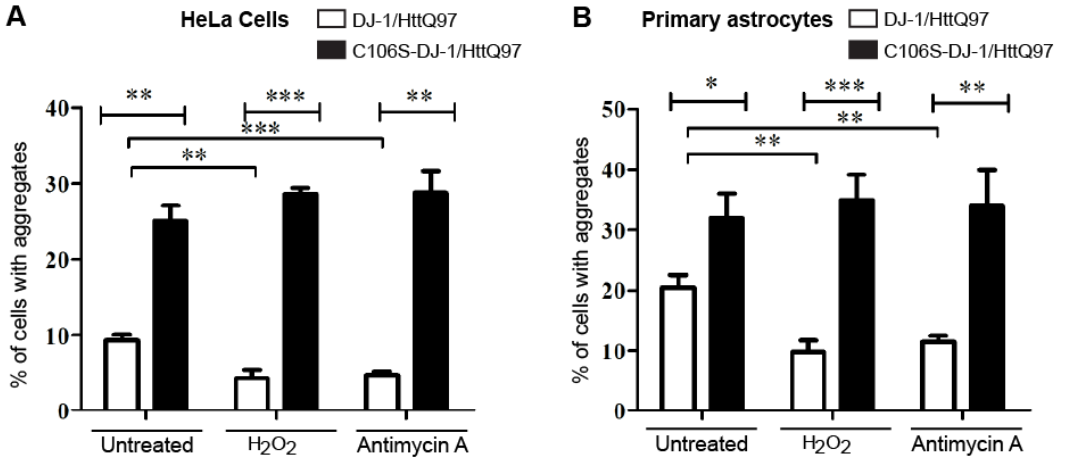

Figure 4.9. Modulation of Htt aggregation by DJ-1 is regulated by cysteine 106 redox status.

HeLa cells (A) and primary astrocytes (B) were co-transfected with HttQ97-mRFP and wild-type DJ-1 or C106S-DJ-1 constructs. Transfected cells were treated with 100 µM of H_2O_2 or 5 µM of antimycin A or left untreated. The number of cells with aggregates was counted after 3 days of transfection. Error bars represent standard deviation. Unpaired t-test was performed for statistical analysis (*P < 0.05, **P <0.01 and ***P <0.001, n = 3-6)

As mentioned above, oxidation of DJ-1 has been shown to have an important role in the activation of DJ-1 function, specially the oxidation of the cysteine residue 106 (Cys106) [13]. Co-expression of HttQ97-mRFP with a mutant version of DJ-1, in which Cys106 was replaced by a serine (C106S-DJ-1) that cannot be oxidized, increased the formation of aggregates compared to cells co-transfected with wild-type DJ-1 both in HeLa cells (Fig. 4.9A) and primary astrocytes (Fig. 4.9B). In addition, it increased cellular toxicity and the number of aggregates per cell (data not shown). As expected, Htt97Q-mRFP aggregation and toxicity were not changed upon exposure to H_2O_2 or antimycin (Fig. 4.9A, B). Altogether, our results indicate that modulation of Htt aggregation and toxicity by DJ-1 depends on its oxidation state.

We next tested whether DJ-1 was able to modulate Htt oligomerization and fibril formation *in vitro.* For that, we incubated recombinant DJ-1 (both oxidized and non-oxidized forms) in the presence of Htt53Q and analysed the formation of oligomers and

fibers by atomic force microscopy (data not shown). We found that non-oxidized DJ-1 significantly enhanced Htt53Q oligomerization and fibril formation. The oxidized form of DJ-1 had no effect on Htt oligomerization, but slightly decreased its fibrillization. These results further support that DJ-1 modulates Htt aggregation in a redox-dependent manner.

Discussion

In our study, we identified a potential novel role for DJ-1 in modulating aggregation and toxicity of polyQ-expanded Htt in a redox-dependent manner. We found that DJ-1 homologs in yeast and *Drosophila* (Hsp31 and DJ-1α, respectively) suppress mutant Htt toxicity. Hsp31 not only suppressed Htt toxicity but also caused a reduction in the levels of SDS-insoluble Htt. In contrast, heterologous expression of human DJ-1 in yeast resulted in increased levels of SDS-insoluble Htt. One possible explanation for this intriguing result is that human DJ-1 might be dysfunctional in yeast, possibly due to aberrant folding, defects in essential post-translational modifications, abnormal interactions with yeast proteins or even because of its oxidation state.

We found that DJ-1 was significantly more abundant and more oxidized in the frontal cortex of HD patients and in several HD models, including R6/2 HD mice. Interestingly, DJ-1 has already been shown to be upregulated and oxidatively damaged in the brains of patients with other neurodegenerative diseases, such as PD and Alzheimer's disease [15,19,20]. It is still unclear why DJ-1 levels are elevated in these diseases.

We showed that DJ-1 physically interacts with Htt (both WT and mutant forms) and co-aggregates with the mutant form. In contrast to what we observed with Hsp31 overexpression in yeast, DJ-1 exacerbated Htt aggregation. This aggregation-enhancing action likely does not contribute to eliminate toxic misfolded protein species or to shift the balance to less toxic Htt species, since we observed an increase in toxicity. DJ-1 effects on Htt were dependent on cys106 oxidation state, consistent with a redox-dependent chaperone function of DJ-1 [12].

Although our results strongly suggest that DJ-1 modulates Htt toxicity and aggregation via a direct interaction, possibly as a redox-dependent chaperone, it is unclear why DJ-1 did not protect mammalian cells against mutant Htt toxicity. It is also unclear why DJ-1 interacted with Htt in the absence of mild oxidative stress, since we were expecting that DJ-1 would bind to Htt only after Cys106 oxidation, as redox-dependent chaperones need to be oxidized in order to bind to their targets [7].

Nevertheless, we hypothesize that in the initial stages of HD, in which ROS are likely high [21], DJ-1 is upregulated and oxidized in cys106 as a protective response. With the progression of the disease, and further increase in the generation of ROS, DJ-1 becomes irreversibly oxidized and dysfunctional, which may contribute to the pathogenesis in HD. It is noteworthy that DJ-1 is mainly expressed in astrocytes [22], which are cells that play a crucial role in providing protection against oxidative stress [23,24]. Thus, in late stages of HD, the loss of DJ-1 function may be especially deleterious for astrocytes. Since we did not evaluate exactly the oxidation state of DJ-1, we cannot exclude the hypothesis that DJ-1 in the normal experimental conditions used was already oxidized and therefore interacted with Htt. The addition of an oxidant to the media would cause further DJ-1 oxidation, leading to its inactivation. In these conditions DJ-1 no longer would bind to Htt and therefore no enhanced toxicity would be observed.

Our results altogether suggest that it will be critical to further elucidate the mechanistic underpinnings of how DJ-1 modulates the pathogenesis of HD and other neurodegenerative disorders involving oxidative stress, protein misfolding and aggregation. Such studies could lay the groundwork for the development of effective treatments for these devastating and currently incurable disorders.

Materials and Methods

Plasmids, cell culture and transfection experiments

The chemicals used in this study were purchased from Sigma unless otherwise stated. Plasmids (pcDNA3.1) contained the sequence for Htt exon 1 (HttEx1) with either 25 or 97 glutamine repeats fused to monomeric Red Fluorescent Protein (mRFP) at the C-terminus were used for transfections or adenoviral infections (MOI 10-20) as described previously [25]. HeLa cells were cultured in DMEM with 2 mM L-glutamine, 10% fetal bovine serum (FBS) and 100U/ml penicillin with 100µg/ml streptomycin at 37°C, 10% CO2. After 24 hours of seeding, HeLa cells were exposed to the appropriate DNA construct/s and lipofectamine (Invitrogen) for 5 hours in serum-free medium (OPTI-MEM, Invitrogen) for both transfection and co-transfection procedures as described previously [26,27]Mouse primary astrocytes were cultured by dissecting P0 mouse cortices and meninges were removed. Cortices were cut into small cubes (<1mm^3), suspended in 20ml of DMEM (maximum of 5 brains) and subsequently vortexed at maximum speed for 90 seconds in a 50ml centrifuge tube (Greiner Bio One) and then the cell suspension

was sieved through a 40µm cell strainer (BD Falcon). Cell filtrate was mixed with DMEM supplemented by 10% Hybond FBS (characterised, Hyclone) and 100 U/ml penicillin with 100 µg/ml streptomycin (Sigma, UK) and seeded in a 1x T75cm2 laminin (20µg/ml, Sigma, UK) coated flask. 24 hours after seeding, the cells were washed twice with 1x PBS (GIBCO, UK) and the media was replaced. Cell media was changed every 3 days and cells reached confluency after 9-12 days. Confluent flasks lids were sealed with parafilm, and shaken for 15 hours at 180 rpm in a 37ºC heated incubator. After 15 hours the media was removed and cells were washed with PBS. Cells were then trypsinised with 0.025% trypsin/EDTA (GIBCO, UK) and seeded in a 6 well poly-L-lysine coated plate with/without coverslips (200,000 cells per well for 6 well plate). These secondary cultures were then used after 3-4 days of seeding for transfection- and other studies (final age of astrocyte were normally between 15-20 days). Cells in astrocyte cultures were >80% GFAP positive and >99% cells were connexin 43 positive hence suggesting a high astrocyte purity. No oligodendrocyes or microgial cells could be detected by ICC (data not shown).

Protein extraction, Immunoblot and dot blot analysis

Cells transiently transfected and primary astrocytes were collected at different time points. Samples were lysed in SDS containing lysis buffer (65.2mM Tris-HCl (pH 6.8), 2% (w/v) SDS and 10% sucrose and complete protease inhibitor cocktail) followed by a 20 minutes incubation on ice and then stored at -20°C. 17 weeks old R6/2 [28] and WT littermates were sacrificed and cortex and cerebellum brain regions were collected. Samples were extracted initially with 10% W/V homogenisation buffer (20mM Hepes and 100mM KCl (pH 7.4) with complete protease inhibitors). Subsequently, total SDS soluble protein extraction was then performed by boiling the samples (both soluble and insoluble material) at 95°C for 4 minutes with 2% SDS. Samples were then spin at 6000 rpm for 3 minutes to remove the SDS insoluble material. Supernatants were collected and stored at -80°C until further needed.

Pre-dissected brain regions (cortex and cerebellum) from human HD patients and control groups were extracted with an ice-cold lysis buffer (40mM β-glycerolphosphate, 1 mM EDTA, 1mM NaF, 50 mM Tris-HCl (pH 7.5), 1% (v/v) NP-40, 120 mM NaCl, 1mM Benzamidine, antifoam (1:1000, Sigma) and complete protease inhibitors (Roche)). Human HD patients and control samples were then re-extracted using 2% SDS. Samples were stored until further required. Samples were thawed and Bio-Rad DC protein assay was performed to quantify total soluble protein. Western blot was

performed as described previously [26,29]. Membranes were incubated with primary antibodies, rabbit anti-DJ-1 antibody (1:2500; Neuromics, USA), rabbit anti-DJ-1 antibody (1:1000; cell signaling), human anti-oxidised DJ-1 (1:50; Serotec, UK), for 1 hour at room temperature, unless otherwise stated. Membranes were washed 3 x 10 minutes with 1x TBS-T followed by incubation with secondary antibodies (sheep anti-rabbit 800 (1:10000) Rockland, USA; Goat anti-rabbit HRP (1:10000), Vector, UK and Human F(ab')2 HRP (1:5000), Jackson Immunoresearch, USA). Fluorescent secondary antibody labeled membranes were scanned with a Li-COR scanner at 800nm and quantified by using odyssey v1.2 while HRP labeled secondary antibodies were analysed by using ECL detection kit (GE Healthcare Life Sciences, UK).

For dot blot analysis, HeLa cells were co-transfected with HttQ25/Q97-mRFP and DJ-1/EV (1:3) and treated with 5μM antimycin A and 100 μM H2O2 as mentioned earlier. Cells lysates were collected after 72 hours of transfection and processed as described previously [29]. Dot blot lysates were normalized for total protein and filtered through a 2% SDS pre-equilibrated cellulose acetate membrane with a pore size of 0.2 μm andhese samples. Membranes were washed twice with 0.2% SDS followed by incubation with 3% skimmed milk in 1x TBS. The membranes were then incubated with sheep anti-HttEx1 (S830, Gilian Bates, Kings College London, London) antibody at a concentration of 1:5000 for 1 hour at room temperature followed by an incubated with anti-sheep HRP (1:10000, Jackson Immunoresearch, USA) secondary antibody. Finally membranes were developed by using Enhanced Chemiluminescence (ECL) kit. Dot blot quantification was performed by using image J software.

Analysis of cellular HttEx1 polyQ-aggregation and interaction studies, toxicity and immunocytochemistry

For the Bimolecular fluorescent complementation (BiFC) interaction analysis the Htt-Venus BiFC constructs were used and have been previously described [18]. The DJ-1 BiFC construct was generated by PCR-based subcloning of DJ-1 and either the N-terminal or C-terminal fragment of the fluorescent protein into the NheI and XhoI sites of pcDNA3.1. H4 human neuroglioma cells were transfected with complementary pairs of BiFC constructs using the Xtremegene reagent (Roche diagnostics, Mannheim, Germany). After 24 hours of incubation, cell cultures were processed and analysed by flow cytometry, microscopy and toxicity assays as previously described [18,30]. Briefly, 5 μl of cell culture medium were collected for determination of toxicity following manufacturer´s instructions (Toxilight, Lonza Rockland Inc., Rockland, ME, USA).

Cultured cells were either collected by trypsinization for flow cytometry analyses (10000 cells per group) or left on plates for bioimageing. Microscopy pictures were acquired from live cultures using an Axiovert 200M widefield fluorescence microscope equipped with a CCD camera (Carl Zeiss MicroImageing GmbH, Germany) and a stage incubator. A total of 150 cells per group (from 3 independent experiments) were analysed, and images were processed using ImageJ software (http://rsbweb.nih.gov/ij/). Aggregates were counted and classified according to their largest diameter in three classes for some experiments: smaller than 1 µm, larger than 1 µm but smaller than 3 µm, and larger than 3 µm. Aggregates were scored by counting the total number of cells positive for aggregates. Similarly, cellular toxicity was measured by counting the cells expressing HttEx1Q25/Q97-mRFP with fragmented nuclei as described previously [25] or using the MTS assay (Promega). Cell death endpoints were analysed by scoring the proportion of HttEx1mRFP/EGFP-expressing cells with fragmented or pyknotic nuclei, showing that both apoptotic and non-apoptotic types of death can be detected. IB and toxicity counts analyses were performed in parallel.

For immunocytochemistry (ICC) cells on coverslips were washed with 1× PBS, fixed with 4% paraformaldehyde in 1× PBS for 20 minutes and then processed for ICC or mounted in Fluoromount G medium (SouthernBiotech) supplemented with 1 µg/ml 4',6-diamidino-2-phenylindole (DAPI) to allow visualization of nuclear morphology. ICC was performed as described [26]. Cells were counted as aggregate-positive if one/several IB were visible. We counted 200–300 mRFP/EGFP-positive cells in multiple random visual fields per coverslip in duplicate for independent experiments. Cells were incubated with primary antibody (polyclonal rabbit anti-DJ-1) at a concentration of 1:200 for 1 hour at room temperature. Subsequently, cells were washed with dH2O and allowed to dry then mounted on glass slides with Fluoromount G (Southern Biotech, USA). Cells were finally imaged using a Zeiss LSM 510 Meta Axioscope-2 confocal microscope.

Analysis of mutant Htt toxicity and aggregation in yeast

Yeast strains used in this study are in the W303 (*MATa can1-100 ade2-1 his3-11*, *15 trp1-1 ura3-1 leu23*,*112*) genetic background and carry an integrated human Htt fragment construct, encoding either 25Q or 72Q glutamines [3132]. Yeast were transformed independently with pYX212/DJ-1, pBG1805/*HSP31* [Open Biosystems [33]] or an empty vector control. Yeast cultures were grown overnight in complete media lacking uracil (SC-URA), containing yeast nitrogen base and glucose (2%). Yeast growth was synchronized by diluting the cultures to an optical density (OD_{600}) of 0.1.

After reaching mid log phase, cultures were normalized for the same OD_{600}, serially diluted (5-fold), and spotted onto SC-URA solid media containing glucose (2%) or galactose (2%) as carbon sources. These carbon sources were used to repress or induce Htt and Hsp31p expression, respectively. DJ-1 was under control of the *TPI* constitutive promoter.

For protein extraction, mid-log phase cultures were washed twice to remove glucose from the media and were diluted to an OD_{600} of 0.1 in SD-URA containing 2% of galactose. Cells were harvested after 8 hours of induction and lysed by mechanical disruption with acid-washed glass beads (425-600 nm, Sigma, St. Louis, MO) in lysis buffer (50 mM Tris pH 7.5; 1X protease inhibitor cocktail, Roche), vortexing three times for 30 sec each in a mini-bead beater (Biospec), with 1 min incubations on ice in between. Glass beads and cell debris were removed by centrifugation and protein extracts were quantified using the BCA protein assay kit (Pierce Biotechnology, Inc). For SDS-PAGE, extracts were mixed with 4X Protein Sample Buffer (200mM Tris-HCl, 8% SDS, 40% glycerol, 0.4% bromophenol blue, 6% β-mercaptoethanol), boiled 10 min, and subjected to electrophoresis using a 12% SDS-polyacrylamide gel. The proteins were transferred to nitrocellulose membranes and detected by immunoblotting. Htt tagged with CFP was identified by a monoclonal α-GFP antibody (Santa Cruz Biotechnology, Inc), used at a 1:1000 dilution. Hsp31p, tagged with HA, was detected with a polyclonal α-HA antibody (Santa Cruz) diluted 1:500. DJ-1 was detected with a polyclonal α-DJ-1 (Chemicon), used at 1:5000. α-CFP detection was done by an α-Mouse Ig horseradish peroxidase conjugated antibody (Amersham Bioscience, Piscataway, NJ) at 1:10000, whereas α-DJ-1 and α-HA were done by an α-Rabbit Ig horseradish peroxidase conjugated antibody (Amersham Bioscience, Piscataway, NJ) also at 1:10000. Immunoblots were developed by ECL (Millipore, Billerica, MA, USA) and exposed to X-ray films. For filter trap experiments, cell lysates were obtained as described above and mixed with 1% SDS. A total of 100 ug of protein extract was loaded in a dot blotting apparatus and filtered by vacuum in acetate cellulose membranes (0.22 μ pore; GE Water & Process Technologies, Fairfield, CT, USA). Slots were washed two times with PBS 1% SDS. Detection of Htt in the filter was performed by immunoblotting as described above.

Analysis of mutant Htt-mediated neurodegeneration in fruit flies

Flies were raised on maize media, in LD12:12 at 25°C. The elav-GAL4^{c155} driver, and the DJ-1α$^{\Delta 72}$ and DJ-1β$^{\Delta 93}$ deficiency lines [described in [34]] were obtained from the Bloomington Stock Centre, Indiana. The *w;+;UAS Htt93Q* exon 1 flies were a gift from

Larry Marsh and Leslie Thompson (University of California, Irvine) [16]. The UAS DJ-1α and DJ-1β over-expression lines were a gift from Alex Whitworth, and are described in [35]. Neurodegeneration was assayed using the pseudopupil assay. Briefly, the number of visible rhabdomeres per ommatidium was scored for 50-200 ommatidia per fly, with 5-13 flies examined per genotype at day 1, 4 or 7 post-eclosion. Heads from appropriately aged flies were fixed to glass slides using clear fingernail polish and rhabdomeres were examined at 500X magnification using an Olympus BH2 microscope.

Acknowledgements

We would like to thank Richard Faull (University of Auckland, New Zealand) for provision of the human brain tissue and express our appreciation to the Huntington's disease families of New Zealand for the generous bequest of tissue for research purposes. The human brain tissue was obtained from the New Zealand Neurological Foundation Human Brain Bank with ethical approval from the University of Auckland Human Participants Ethical Committee. We also thank A. J. Morton (University of Cambridge, UK) for provision of the mouse tissue and L. Jones (Cardiff University, UK) for help with the storage and extraction of the human brain tissue. Thanks also go to Charalambos P. Kyriacou (University of Leicester, UK) for advice with the Drosophila work. Many thanks go to Vincent O'Connor (University of Southampton, UK) for constant intellectual support and stimulation and fruitful discussions on the DJ-1 project.

References

1. A novel gene containing a trinucleotide repeat that is expanded and unstable on Huntington's disease chromosomes. The Huntington's Disease Collaborative Research Group. Cell 72, 971–83 (1993).
2. Chen, S., Ferrone, F. A. & Wetzel, R. Huntington's disease age-of-onset linked to polyglutamine aggregation nucleation. Proc. Natl. Acad. Sci. U.S.A. 99, 11884–9 (2002).
3. Meriin, a B. & Sherman, M. Y. Role of molecular chaperones in neurodegenerative disorders. Int J Hyperthermia 21, 403–19 (2005).
4. Nagai, Y., Fujikake, N., Popiel, H. A. & Wada, K. Induction of molecular chaperones as a therapeutic strategy for the polyglutamine diseases. Curr Pharm Biotechnol 11, 188–97 (2010).
5. Sajjad, M. U., Samson, B. & Wyttenbach, A. Heat shock proteins: therapeutic drug targets for chronic neurodegeneration? Curr Pharm Biotechnol 11, 198–215 (2010).
6. Wyttenbach, A. Role of heat shock proteins during polyglutamine neurodegeneration: mechanisms and hypothesis. J. Mol. Neurosci. 23, 69–96 (2004).
7. Kumsta, C. & Jakob, U. Redox-regulated chaperones. Biochemistry 48, 4666–76 (2009).
8. Graf, P. C. F. & Jakob, U. Redox-regulated molecular chaperones. Cell. Mol. Life Sci. 59, 1624–31 (2002).
9. Bonifati, V. et al. Mutations in the DJ-1 gene associated with autosomal recessive early-onset parkinsonism. Science 299, 256–9 (2003).
10. Abou-Sleiman, P. M., Healy, D. G., Quinn, N., Lees, A. J. & Wood, N. W. The role of pathogenic DJ-1 mutations in Parkinson's disease. Ann. Neurol. 54, 283–6 (2003).
11. Shendelman, S., Jonason, A., Martinat, C., Leete, T. & Abeliovich, A. DJ-1 is a redox-dependent molecular chaperone that inhibits alpha-synuclein aggregate formation. PLoS Biol. 2, e362 (2004).
12. Zhou, W., Zhu, M., Wilson, M. A., Petsko, G. A. & Fink, A. L. The oxidation state of DJ-1 regulates its chaperone activity toward alpha-synuclein. J. Mol. Biol. 356, 1036–48 (2006).
13. Wilson, M. A. The Role of Cysteine Oxidation in DJ-1 Function and Dysfunction. 15, (2011).

14. Meulener, M. C. et al. Mutational analysis of DJ-1 in Drosophila implicates functional inactivation by oxidative damage and ageing. Proc. Natl. Acad. Sci. U.S.A. 103, 12517–22 (2006).
15. Choi, J. et al. Oxidative damage of DJ-1 is linked to sporadic Parkinson and Alzheimer diseases. J. Biol. Chem. 281, 10816–24 (2006).
16. Steffan, J. S. et al. Histone deacetylase inhibitors arrest polyglutamine-dependent neurodegeneration in Drosophila. Nature 413, 739–743 (2001).
17. Menzies, F. M., Yenisetti, S. C. & Min, K.-T. Roles of Drosophila DJ-1 in survival of dopaminergic neurons and oxidative stress. Curr. Biol. 15, 1578–82 (2005).
18. Herrera, F., Tenreiro, S., Miller-Fleming, L. & Outeiro, T. F. Visualization of cell-to-cell transmission of mutant huntingtin oligomers. PLoS Curr 3, RRN1210 (2011).
19. Baulac, S. et al. Increased DJ-1 expression under oxidative stress and in Alzheimer's disease brains. Mol Neurodegener 4, 12 (2009).
20. Neumann, M. et al. Pathological properties of the Parkinson's disease-associated protein DJ-1 in alpha-synucleinopathies and tauopathies: relevance for multiple system atrophy and Pick's disease. Acta Neuropathol. 107, 489–96 (2004).
21. Hands, S., Sajjad, M. U., Newton, M. J. & Wyttenbach, A. In vitro and in vivo aggregation of a fragment of huntingtin protein directly causes free radical production. J. Biol. Chem. 286, 44512–20 (2011).
22. Bandopadhyay, R. et al. The expression of DJ-1 (PARK7) in normal human CNS and idiopathic Parkinson's disease. Brain 127, 420–30 (2004).
23. Vargas, M. R. & Johnson, J. A. The Nrf2-ARE cytoprotective pathway in astrocytes. Expert Rev Mol Med 11, e17 (2009).
24. Bélanger, M. & Magistretti, P. J. The role of astroglia in neuroprotection. Dialogues Clin Neurosci 11, 281–95 (2009).
25. Hands, S. L., Mason, R., Umar Sajjad, M., Giorgini, F. & Wyttenbach, A. Metallothioneins and copper metabolism are candidate therapeutic targets in Huntington's disease. Biochem. Soc. Trans. 38, 552–8 (2010).
26. Hands, S., Sajjad, M. U., Newton, M. J. & Wyttenbach, A. In vitro and in vivo aggregation of a fragment of huntingtin protein directly causes free radical production. J. Biol. Chem. 286, 44512–20 (2011).
27. Wyttenbach, A. et al. Effects of heat shock, heat shock protein 40 (HDJ-2), and proteasome inhibition on protein aggregation in cellular models of Huntington's disease. Proc. Natl. Acad. Sci. U.S.A. 97, 2898–2903 (2000).
28. Mangiarini, L. et al. Exon 1 of the HD gene with an expanded CAG repeat is sufficient to cause a progressive neurological phenotype in transgenic mice. Cell 87, 493–506 (1996).
29. King, M. A. et al. Rapamycin inhibits polyglutamine aggregation independently of autophagy by reducing protein synthesis. Mol. Pharmacol. 73, 1052–63 (2008).
30. Herrera, F. & Fleming, T. a -Synuclein modifies huntingtin aggregation in living cells. FEBS Lett. 586, 7–12 (2011).
31. Duennwald, M. L., Jagadish, S., Muchowski, P. J. & Lindquist, S. Flanking sequences profoundly alter polyglutamine toxicity in yeast. Proc. Natl. Acad. Sci. U.S.A. 103, 11045–50 (2006).
32. Meriin, A. B. et al. Aggregation of expanded polyglutamine domain in yeast leads to defects in endocytosis. Mol. Cell. Biol. 23, 7554–65 (2003).
33. Gelperin, D. M. et al. Biochemical and genetic analysis of the yeast proteome with a movable ORF collection. Genes development 19, 2816–2826 (2005).
34. Meulener, M. et al. Drosophila DJ-1 mutants are selectively sensitive to environmental toxins associated with Parkinson's disease. Curr. Biol. 15, 1572–7 (2005).
35. Yang, Y. et al. Inactivation of Drosophila DJ-1 leads to impairments of oxidative stress response and phosphatidylinositol 3-kinase/Akt signaling. Proc. Natl. Acad. Sci. U.S.A. 102, 13670–5 (2005).

Chapter 5

General discussion, future perspectives and conclusion

Chapter 5. General discussion, future perspectives and conclusion

Protein misfolding and aggregation are key molecular features shared by a large family of human pathologies known as protein misfolding diseases. This diverse group includes the majority of neurodegenerative disorders, such as Alzheimer's (AD), Parkinson's (PD) and Huntington's disease (HD). In general, each disease is associated with a different misfolded protein, a different affected brain region and different clinical symptoms. Despite extensive research on these diseases, the exact molecular mechanisms underlying neurodegeneration are still poorly understood. In the work described in this thesis, we used yeast as a model system to investigate the molecular mechanisms underlying HD, to find novel insights into the general function of the yeast DJ-1 homologues, which may have relevance to PD, and to characterize the potential role of DJ-1 in HD.

Translational dysfunction is associated with HD

Although HD is genetically well defined, the disease progression is influenced by several genetic modifiers [1], indicating that several potential therapeutic targets may be available. These genetic modifiers and the mechanisms of how mutant huntingtin (Htt) leads to neurodegeneration are still poorly characterized. Yeast has been successfully used to unravel the molecular mechanisms underlying HD as well as other neurodegenerative diseases. In addition, it has led to the identification of several potential therapeutic targets and drugs with therapeutic application for many diseases [2].

In Chapter 2 we suggest that translational dysfunction contributes to mutant Htt toxicity and we identify several candidate therapeutic targets for HD. Translation is a fundamental molecular mechanism that needs to be tightly controlled. Dysregulation of this process can be extremely deleterious for cells and thus the number of diseases associated with this process is continuously rising. These include cancer [3–5], neurological diseases [6] and metabolic diseases [7]. Several studies suggest that translational dysfunction may also underlie neurodegeneration [8,9]. Reduced translation fidelity (due to mischarged tRNAs or increased translation speed) leads to an increased rate of missense translation errors, which could affect protein folding and lead to the accumulation of misfolded proteins in neurons. Ultimately, this accumulation could cause neurodegeneration [8,9]. Compelling evidence, although still scarce, supports that translational dysregulation is implicated in HD (discussed in Chapter 2).

We found that expression of several genes encoding ribosome biogenesis proteins, including proteins involved in rRNA processing are downregulated in Htt103Q-expressing cells. Repression of ribosome biogenesis is a typical response to stress, which leads to a reduction in general translation and protein synthesis [10]. Repression of general protein synthesis is a strategy that cells use to save energy [11,12] and to release the burden of the quality control system, which becomes more available to degrade misfolded/aggregated proteins allowing cells to recover. However, if the stress (in this case mutant Htt expression) is sustained, the decrease in protein synthesis may be deleterious for cells, since protein synthesis is fundamental for cell growth and survival. Interestingly, a recent study showed that persistent inhibition of protein synthesis through phosphorylation of eukaryotic translation initiation factor 2, subunit 1 α (eIF2α) contributes to neurodegeneration in prion infected mice [13] and that inhibition of this phosphorylation prevents it. High levels of eIF2α phosphorylation have also been observed in hippocampal neurons from AD patients [14] and differentiated dopaminergic cells treated with MPP+ and 6-hydroxydopamine (6-OHDA) (Parkinsonism-inducing neurotoxins) [15], suggesting translational dysfunction. Whether this process is indeed involved in neurodegeneration in AD or PD is unknown. In addition, inhibition of eIF2α phosphorylation enhances cortex-dependent memory consolidation, which deteriorates with ageing [16].

We showed that rRNA processing genes that were downregulated in Htt-expressing yeast cells are able to suppress Htt toxicity. Among these genes, several have human homologues, and we propose that these rRNA processing proteins are potential therapeutic targets for HD. It is unclear and surprising that overexpression of just one of these proteins is sufficient to suppress Htt toxicity. We could speculate that single overexpression of these proteins may lead to an increase of general translation and consequently an increase in protein synthesis, which would be beneficial. However, unless overexpression of these proteins causes a feedback loop which would lead to upregulation of other genes encoding essential players in translation, overexpression of a single gene should be limited by the expression of the remaining genes downregulated upon Htt expression. Moreover, many of these suppressors, such as Rrp9 and Utp9 [17,18], belong to large protein complexes, and thus it is surprising that overexpression of only one of the components could have an effect. Upon stress cells require a fast way to attenuate translation, thus besides repressing ribosome biogenesis at the transcriptional level, cells suppress translational initiation by mechanisms that affect mainly the activity of the initiation factors eIF2α, eIF4E, and eIF4A [12]. Therefore,

overexpression of these proteins involved in rRNA processing should also be able to bypass these inhibitory mechanisms. However, it is still unknown whether cells expressing mutant Htt repress translation initiation. Indeed, increased phosphorylation of eIF2 was not observed in HeLA cells expressing mutant Htt when compared to wt Htt [19]. It would be interesting to evaluate the phosphorylation of this factor in other HD models. We hypothesize that although translation is not totally reverted to its basal levels – which in fact could be deleterious for cells due to the increase in energy consumption, higher burden in UPS and likely decreased translation of stress related genes – it is slightly increased and this supports cell survival and promotes growth.

Downregulation of a subset of genes involved in translation could be also caused by transcriptional dysregulation via GCN4. Gcn4 is a transcriptional coactivator that requires MBF1, a deletion suppressor of Htt toxicity, to become activated [20]. We hypothesize that deletion of *MBF1* suppress mutant Htt toxicity by impairing Gcn4 function (further discussed in Chapter 2). To test whether translation is affected through Gcn4 we could delete this gene and analyse its effect on Htt toxicity. We expect this deletion to be protective as it is observed upon deleting *MBF1.* Again, this hypothesis does not explain why overexpressing only one gene involved in rRNA processing is enough to suppress Htt toxicity. We cannot exclude the hypothesis that the suppressor genes identified have a protective function independent of rRNA processing.

As we identified common differentially expressed genes in three toxicity suppressor strains expressing mutant Htt (*bna4*Δ, *mbf1*Δ, and *ume1*Δ), these genes may also be considered candidate therapeutic targets for HD. Therefore, in the future, we could test whether these can rescue mutant Htt toxicity (by modulating their expression), first in yeast and later in mammalian HD models.

Recently, the connection between translation and HD was suggested to be via direct binding of Htt with components of the translation machinery [19]. Further studies should be carried out to confirm the effect of mutant Htt in translation and its relevance in HD pathogenesis, since our findings were mainly at the transcriptional level. To assess translation directly, we could perform ribosome profiling, which is a powerful technique based on deep sequencing of ribosome protected mRNA fragments [21]. It can be used to quantify gene expression at the level of protein synthesis, since each mRNA fragment corresponds to a translating ribosome, and the number of fragments is proportional to the amount of protein being synthetized and the time required to produce it. In addition, this method can also be used to identify which genes are being translated and where the ribosomes are positioned at the mRNA. We could also use reporter-

based assays for translation efficiency/fidelity in various HD models to ascertain the role of translational dysfunction and the impact of the identified genes in this process.

Overall, our work shows that translation is impaired in HD and contributes to the pathogenesis of this disease. Therefore, we propose that targeting translation is an attractive therapeutic approach for this devastating disease, which is critical as there are still no treatments for onset or progression of symptoms.

Yeast DJ-1 homologues are involved in diauxic-shift

PD is not as well defined genetically as HD. Indeed, only ~10% of the PD cases are associated to genetic mutations, which are found in different genes [22]. DJ-1 is encoded by *PARK7*, one of the genes associated with this disease [23,24]. *S. cerevisiae* has four proteins that belong to the DJ-1 superfamily – the Hsp31 mini-family: Hsp31, Hsp32, Hsp33 and Hsp34. The function of both human and yeast members of the DJ-1 superfamily is unclear, but it has been associated with protection against stress.

In Chapter 3, we provide a significant advance in our understanding of the function of the Hsp31 mini-family. We showed that the proteins of this family have a role in the metabolic reprogramming that occurs in diauxic-shift. The transition from log phase to post-diauxic and stationary phase, in terms of global mRNA expression and several physiological mechanisms, is abolished upon deleting individually the members of the Hsp31-mini family, suggesting that cells fail to respond to glucose deprivation. The absence of this reprogramming caused knockout strains to age faster in stationary phase. Our results led us to propose a novel function for these proteins in regulating the activity of TORC1, one of the kinases responsible for this transition [25–28].

Since TORC1 negatively regulates autophagy, we monitored this process as readout of TORC1 activity. We found that the members of the Hsp31 mini-family are required to maintain the basal levels of autophagy and to induce autophagy upon glucose starvation, via regulation of TORC1 activity. The number of diseases associated with mTORC1 dysfunction is continuously rising, and include cancer, type 2 diabetes and neurodegeneration [29]. Autophagy has been implicated in several neurodegenerative diseases, including PD [30]. Indeed, conditional neuronal knockout mice for essential genes for autophagy (Atg5 or Atg7) exhibited striking neurodegeneration, formation of inclusion bodies and importantly locomotion deficits [31,32], showing that autophagy is a critical process for neuronal cell survival. Dysregulation of autophagy also has an impact on α-synuclein (α-syn) homeostasis, which consequently accumulates in the cytoplasm and causes toxicity [30,33]. Several

proteins genetically linked to PD were shown to have a role in autophagy, such as PINK1 and Parkin, which were shown to be particularly involved in mitophagy (degradation of mitochondria) [34]. Compelling evidence suggest that DJ-1 also plays a role in autophagy, however the mechanism remains unclear and some findings are controversial [35–37]. Consistent with our results, mouse embryonic fibroblasts (MEFs) depleted for DJ-1 and fibroblast from patients with the DJ-1 mutation E64D showed reduced basal autophagy [35]. In addition, the absence of DJ-1 led to accumulation of dysfunctional mitochondria, which may be due to impaired autophagy [35]. In contrast, another study that also used MEFs from DJ-1 knockout mice showed enhanced autophagic flux, but also mitochondrial defects [36].

mTORC1 is considered an attractive therapeutic target for neurodegenerative diseases, since the use of rapamycin, which inhibits the activity of mTORC1, has already been shown to be neuroprotective in models of AD, PD and HD [38–42]. Besides increasing autophagy, rapamycin showed beneficial effects by modulating other mechanisms regulated by mTORC1, such as translation [42]. Rapamycin is already used as an immunosuppressant to prevent tissue rejection [43], but since neurodegenerative diseases need prolonged treatment, it may cause deleterious effects [42]. Ideally, autophagy should be correctly balanced and therefore the mechanisms involved in this process should be thoroughly dissected. The role of DJ-1 in mTORC1 should therefore be further investigated, so that this pathway can be specifically modulated.

Dysfunctional mTOR signaling is also associated with several cancers [44]. Indeed, the oncogenic properties of DJ-1 may be mediated by the PI3K/AKT pathway, which positively regulates mTORC1 [45]. Curiously, DJ-1 levels increased in response to high levels of glucose and led to the activation of AKT and mTORC1, resulting in mesangial cell hypertrophy [46]. These results support our hypothesis that DJ-1 plays a role upstream TORC1, likely by transducing carbon signaling, however it suggests that DJ-1 is an activator rather than a repressor as shown for yeast proteins. One question that arises from these contrasting results is whether human DJ-1 behaves differently in different types of cells, as different effectors could lead to different responses. Although TORC1 pathway is a conserved pathway in eukaryotes, it has changed and diverged throughout evolution [47]. Moreoever, it should be noted that the pathways associated with glucose starvation in mammalian cells are not very well studied and there are some controversies for instance whether glucose deprivation leads to inhibition or activation of autophagy [48].

Future studies should be performed to provide further mechanistic insights into how the Hsp31 family is playing its role in the diauxic shift through TORC1. We could address several questions: What is the level of function overlap of the members of the Hsp31 mini-family? Can overexpression of one protein compensate the absence of another? Since individual deletion of each family member leads to similar phenotypes, do they form a complex and upon the deletion of one protein does the complex become dysfunctional? What is the intracellular localization of these proteins? Does the localization change in stationary phase or in conditions of glucose starvation? Do these proteins interact with known upstream effectors of the TORC1 pathway? In parallel, the role of the human DJ-1 as a regulator of mTORC1 could be further explored.

Altogether, our results open a new window for research in PD by showing a new perspective on the role of DJ-1. Moreover, it provides novel insights into the function of the yeast Hsp31 mini-family, which were not characterized in detail until now.

A novel role for DJ-1 in HD

The work described in Chapter 4 shows that DJ-1 interacts with Htt and modulates its aggregation and toxicity. As already described in patients with PD and AD, DJ-1 was found more abundant and hyperoxidized in cys106 in the brains of patients with HD [49], although it is unclear why DJ-1 is upregulated and whether its upregulation is protective.

We found that Hsp31 and one of the fly homologues of DJ-1 suppressed Htt toxicity, and that Hsp31 reduced Htt aggregation. Surprisingly, overexpression of DJ-1 in mammalian cells was not protective against mutant Htt and actually enhanced Htt toxicity and aggregation. Upon rendering the environment of cultured cells more oxidative, DJ-1 no longer enhanced Htt toxicity and aggregation. We further showed that this effect was mediated by oxidation of the cys106 residue. Oxidation of this residue is required to activate the protein for certain functions, namely to act as a redox-dependent chaperone and prevent α-syn aggregation [50]. It is unclear why DJ-1 in mammalian cells is not protective against mutant Htt, while its yeast and fly homologues are. A possible explanation is that the overexpression of Htt in these two models induces enough ROS to trigger DJ-1 oxidation, while in mammalian cells it does not. However, if the redox state of the yeast cell is enough to trigger the activation of Hsp31, it is still unanswered why human DJ-1 did not suppress Htt toxicity in yeast. Although human DJ-1 was actually expressed in yeast (detected by immunoblotting) it might be dysfunctional, due to abnormal folding, differences in post-translational modifications or

even by abnormal interactions with yeast proteins. Another possibility is that human DJ-1 is sufficiently diverged from the yeast orthologs that it responds to different levels of cellular ROS.

To further understand the role of DJ-1 in modulating mutant Htt toxicity and aggregation, it is important to clarify what is the exact redox status of cys106 in each experimental condition. In our basal experimental conditions was cys106 reduced or already mildly-oxidized (active) (Fig. 4.1)? And in an oxidizing environment, did cys106 become mildly-oxidized (active) or hyperoxidized (inactive)? The oxidation status of cys106 could be measured by mass spectrometry [50]. Alternatively, we could complement the experiments done with C106S DJ-1 (mutation that prevents oxidation), with a C106DD DJ-1 construct in which cys106 is replaced by two aspartates to mimic DJ-1 active form [51]. In addition, we could also complement the experiment in which we increased the oxidative environment and use an antioxidant compound such as N-acetylcysteine, to guarantee that the effects observed are caused by reduced DJ-1 and not by mild-oxidized DJ-1. It would also be important to verify the redox state of the corresponding cys106 in the DJ-1 homologues in yeast and fly upon mutant Htt expression, which could help us to understand why in these organisms DJ-1 homologues suppress Htt toxicity. Furthermore, it would be interesting to verify whether DJ-1 still interacts with Htt upon mild oxidative stress and whether mutant DJ-1 C106S, which cannot be oxidized in this residue, also interacts with mutant Htt. This would inform us whether modulation of cys106 redox state is required for mutant Htt and DJ-1 interaction.

To further study the role of cys106 oxidation we can use available compounds that bind to the cys106 region when it is reduced or partially oxidized [52–55]. These compounds are thought to activate DJ-1 or prevent its excessive oxidation [53,56], and have been shown to inhibit ROS production and toxicity induced by oxidative stress in SH-SY5Y cells and primary neurons [52–55]. Importantly, they also prevented 6-hydroxydopamine- and rotenone-induced dopaminergic cell death in vivo and reduced the infarct size in a mouse model of stroke [54,55]. These are attractive compounds that may be beneficial for therapeutic intervention in HD and should therefore be tested in future experiments.

It is also important to clarify whether hyperoxidized DJ-1 in the brains of HD patients can contribute to disease progression. Assuming that upregulation of DJ-1 is beneficial, as shown in yeast and fly models, DJ-1 could exert a neuroprotective role as a redox-chaperone in the initial stages of the disease, which is lost with the progression

of neurodegeneration and consequent increase in oxidative stress. We, however, cannot formally exclude the possibility that DJ-1 is modulating mutant Htt toxicity and aggregation by other functions aside from its chaperone activity, as DJ-1 has been shown to have several other functions.

Altogether, our results show a potential novel role for DJ-1 in modulating Htt aggregation and toxicity, but whether the interaction between these two proteins is protective or not needs to be further explored, as DJ-1 may indeed contribute to HD pathology. Our findings provide the basis for future studies in understanding the role of DJ-1 in HD and other human pathologies involving protein misfolding and aggregation.

CONCLUSION

The increase of life expectancy, especially in developed countries, is leading to an increase in the incidence and prevalence of neurodegenerative diseases - as ageing is the main risk factor for the majority of these diseases. These are devastating diseases without a cure or effective treatment, causing a social and economic burden for society. Therefore, it is urgent to elucidate the molecular mechanisms that underlie these neurodegenerative diseases and find novel therapeutic targets.

The work presented in this thesis shows that translational dysfunction is implicated in the pathogenesis of HD. The impairment of this mechanism has recently been associated with other misfolding diseases, strongly suggesting that translation is a pathogenic mechanism shared by several diseases. Importantly, we identified several novel suppressors of Htt toxicity, including many proteins involved in translation. These are attractive potential therapeutic targets for HD that will be further validated in the future.

We also provide novel clues into the role of the yeast members of the DJ-1 superfamily. These proteins are required to mount a stress response and change yeast metabolism at diauxic-shift, likely through TORC1. TORC1 is a highly conserved pathway that is implicated in several diseases because it controls several fundamental mechanisms, including autophagy. This work provides the basis for future studies to understand the function of the human protein DJ-1 that may bring not only novel insights into the pathogenesis of PD but also of other diseases.

Finally, we propose a novel role for DJ-1 in modulating the toxicity and aggregation of Htt, possibly acting as a redox-chaperone. We observed that the yeast and fly homologues suppress Htt toxicity, suggesting that DJ-1 has a protective role,

however, in mammalian cells DJ-1 enhances Htt toxicity in a redox dependent manner. DJ-1 was found upregulated and irreversibly oxidized in the brains of patients with HD, as it is found in the brains of AD and PD patients. The increase in oxidative stress associated to protein misfolding diseases may lead to DJ-1 hyperoxidation and consequently to its inactivation, which in turn may contribute to the pathogenesis of these disorders. Whether DJ-1 is beneficial or deleterious at early stages of the pathology is still unclear. Nevertheless, these findings provide clues for the general role of DJ-1 in these disorders and therefore it may have implications in treating not only HD and idiopathic PD, but also other disorders that are associated with oxidative stress and protein misfolding.

References

1. Wexler, N. S. et al. Venezuelan kindreds reveal that genetic and environmental factors modulate Huntington's disease age of onset. Proc. Natl. Acad. Sci. U.S.A. 101, 3498–503 (2004).
2. Miller-Fleming, L., Giorgini, F. & Outeiro, T. F. Yeast as a model for studying human neurodegenerative disorders. Biotechnol J 3, 325–38 (2008).
3. Marshall, L., Kenneth, N. S. & White, R. J. Elevated tRNA(iMet) synthesis can drive cell proliferation and oncogenic transformation. Cell 133, 78–89 (2008).
4. Pavon-Eternod, M. et al. tRNA over-expression in breast cancer and functional consequences. Nucleic Acids Res. 37, 7268–80 (2009).
5. Brito, M. et al. Polyglycine expansions in eRF3/GSPT1 are associated with gastric cancer susceptibility. Carcinogenesis 26, 2046–9 (2005).
6. Garber, K. B., Visootsak, J. & Warren, S. T. Fragile X syndrome. Eur. J. Hum. Genet. 16, 666–72 (2008).
7. Shi, Y. When Translation Meets Metabolism: Multiple Links to Diabetes. Endocrine Reviews 24, 91–101 (2003).
8. Lee, J. W. et al. Editing-defective tRNA synthetase causes protein misfolding and neurodegeneration. Nature 443, 50–5 (2006).
9. Tuller, T. The Effect of Dysregulation of tRNA Genes and Translation Efficiency Mutations in Cancer and Neurodegeneration. Frontiers in genetics 3, 201 (2012).
10. Lempiäinen, H. & Shore, D. Growth control and ribosome biogenesis. Curr. Opin. Cell Biol. 21, 855–63 (2009).
11. Lempiäinen, H. & Shore, D. Growth control and ribosome biogenesis. Curr. Opin. Cell Biol. 21, 855–63 (2009).
12. Holcik, M. & Sonenberg, N. Translational control in stress and apoptosis. Nat. Rev. Mol. Cell Biol. 6, 318–27 (2005).
13. Moreno, J. a et al. Sustained translational repression by eIF2α-P mediates prion neurodegeneration. Nature 485, 507–11 (2012).
14. Hoozemans, J. J. M. et al. The unfolded protein response is activated in pretangle neurons in Alzheimer's disease hippocampus. Am. J. Pathol. 174, 1241–51 (2009).
15. Holtz, W. A. & O'Malley, K. L. Parkinsonian mimetics induce aspects of unfolded protein response in death of dopaminergic neurons. J. Biol. Chem. 278, 19367–77 (2003).
16. Stern, E., Chinnakkaruppan, A., David, O., Sonenberg, N. & Rosenblum, K. Blocking the eIF2α kinase (PKR) enhances positive and negative forms of cortex-dependent taste memory. J. Neurosci. 33, 2517–25 (2013).
17. Huang, Y.-C., Tseng, S.-F., Tsai, H.-J., Lenzmeier, B. A. & Teng, S.-C. Direct interaction between Utp8p and Utp9p contributes to rRNA processing in budding yeast. Biochem. Biophys. Res. Commun. 393, 297–302 (2010).
18. Zhang, L., Lin, J. & Ye, K. Structural and functional analysis of the U3 snoRNA binding protein Rrp9. RNA 19, 701–11 (2013).

19. Culver, B. P. et al. Proteomic analysis of wild-type and mutant huntingtin-associated proteins in mouse brains identifies unique interactions and involvement in protein synthesis. J. Biol. Chem. 287, 21599–614 (2012).
20. Takemaru, K., Harashima, S., Ueda, H. & Hirose, S. Yeast coactivator MBF1 mediates GCN4-dependent transcriptional activation. Mol. Cell. Biol. 18, 4971–6 (1998).
21. Ingolia, N. T., Brar, G. a, Rouskin, S., McGeachy, A. M. & Weissman, J. S. The ribosome profiling strategy for monitoring translation in vivo by deep sequencing of ribosome-protected mRNA fragments. Nat Protoc 7, 1534–50 (2012).
22. Thomas, B. & Beal, M. F. Parkinson's disease. Hum. Mol. Genet. 16 Spec No, R183–94 (2007).
23. Bonifati, V. et al. Mutations in the DJ-1 gene associated with autosomal recessive early-onset parkinsonism. Science 299, 256–9 (2003).
24. Abou-Sleiman, P. M., Healy, D. G., Quinn, N., Lees, A. J. & Wood, N. W. The role of pathogenic DJ-1 mutations in Parkinson's disease. Ann. Neurol. 54, 283–6 (2003).
25. Powers, R. W., Kaeberlein, M., Caldwell, S. D., Kennedy, B. K. & Fields, S. Extension of chronological life span in yeast by decreased TOR pathway signaling. Genes Dev. 20, 174–84 (2006).
26. Zaragoza, D., Ghavidel, a, Heitman, J. & Schultz, M. C. Rapamycin induces the G0 program of transcriptional repression in yeast by interfering with the TOR signaling pathway. Mol. Cell. Biol. 18, 4463–70 (1998).
27. Galdieri, L., Mehrotra, S., Yu, S. & Vancura, A. Transcriptional regulation in yeast during diauxic shift and stationary phase. OMICS 14, 629–38 (2010).
28. Gray, J. V et al. " Sleeping Beauty ": Quiescence in Saccharomyces cerevisiae †. 68, 187–206 (2004).
29. Laplante, M. & Sabatini, D. M. mTOR signaling in growth control and disease. Cell 149, 274–93 (2012).
30. Lynch-Day, M. A., Mao, K., Wang, K., Zhao, M. & Klionsky, D. J. The role of autophagy in Parkinson's disease. Cold Spring Harbor perspectives in medicine 2, a009357 (2012).
31. Hara, T. et al. Suppression of basal autophagy in neural cells causes neurodegenerative disease in mice. Nature 441, 885–9 (2006).
32. Komatsu, M. et al. Loss of autophagy in the central nervous system causes neurodegeneration in mice. Nature 441, 880–4 (2006).
33. Xilouri, M., Brekk, O. R. & Stefanis, L. Alpha-synuclein and protein degradation systems: a reciprocal relationship. Mol. Neurobiol. 47, 537–51 (2013).
34. Vincow, E. S. et al. The PINK1-Parkin pathway promotes both mitophagy and selective respiratory chain turnover in vivo. Proc. Natl. Acad. Sci. U.S.A. 110, 6400–5 (2013).
35. Krebiehl, G. et al. Reduced basal autophagy and impaired mitochondrial dynamics due to loss of Parkinson's disease-associated protein DJ-1. PLoS ONE 5, e9367 (2010).
36. Irrcher, I. et al. Loss of the Parkinson's disease-linked gene DJ-1 perturbs mitochondrial dynamics. Hum. Mol. Genet. 19, 3734–46 (2010).
37. Ren, H. et al. DJ-1, a cancer and Parkinson's disease associated protein, regulates autophagy through JNK pathway in cancer cells. Cancer Lett. 297, 101–8 (2010).
38. Ravikumar, B. et al. Inhibition of mTOR induces autophagy and reduces toxicity of polyglutamine expansions in fly and mouse models of Huntington disease. Nat. Genet. 36, 585–95 (2004).
39. Sarkar, S., Ravikumar, B., Floto, R. A. & Rubinsztein, D. C. Rapamycin and mTOR-independent autophagy inducers ameliorate toxicity of polyglutamine-expanded huntingtin and related proteinopathies. Cell Death Differ. 16, 46–56 (2009).
40. Tain, L. S. et al. Rapamycin activation of 4E-BP prevents parkinsonian dopaminergic neuron loss. Nat. Neurosci. 12, 1129–35 (2009).
41. Malagelada, C., Jin, Z. H., Jackson-Lewis, V., Przedborski, S. & Greene, L. A. Rapamycin protects against neuron death in in vitro and in vivo models of Parkinson's disease. J. Neurosci. 30, 1166–75 (2010).
42. Bové, J., Martínez-Vicente, M. & Vila, M. Fighting neurodegeneration with rapamycin: mechanistic insights. Nat. Rev. Neurosci. 12, 437–52 (2011).
43. Groth, C. G. et al. Sirolimus (rapamycin)-based therapy in human renal transplantation: similar efficacy and different toxicity compared with cyclosporine. Sirolimus European Renal Transplant Study Group. Transplantation 67, 1036–42 (1999).
44. Meric-Bernstam, F. & Gonzalez-Angulo, A. M. Targeting the mTOR signaling network for cancer therapy. J. Clin. Oncol. 27, 2278–87 (2009).
45. Vasseur, S. et al. DJ-1/PARK7 is an important mediator of hypoxia-induced cellular responses. Proc. Natl. Acad. Sci. U.S.A. 106, 1111–6 (2009).
46. Das, F. et al. High glucose upregulation of early-onset Parkinson's disease protein DJ-1 integrates the PRAS40/TORC1 axis to mesangial cell hypertrophy. Cell. Signal. 23, 1311–9 (2011).
47. De Virgilio, C. & Loewith, R. The TOR signalling network from yeast to man. Int. J. Biochem. Cell Biol. 38, 1476–81 (2006).

48. Moruno, F., Pérez-Jiménez, E. & Knecht, E. Regulation of Autophagy by Glucose in Mammalian Cells. Cells 1, 372–395 (2012).
49. Choi, J. et al. Oxidative damage of DJ-1 is linked to sporadic Parkinson and Alzheimer diseases. J. Biol. Chem. 281, 10816–24 (2006).
50. Zhou, W., Zhu, M., Wilson, M. A., Petsko, G. A. & Fink, A. L. The oxidation state of DJ-1 regulates its chaperone activity toward alpha-synuclein. J. Mol. Biol. 356, 1036–48 (2006).
51. Waak, J. et al. Oxidizable residues mediating protein stability and cytoprotective interaction of DJ-1 with apoptosis signal-regulating kinase 1. J. Biol. Chem. 284, 14245–57 (2009).
52. Miyazaki, S. et al. DJ-1-binding compounds prevent oxidative stress-induced cell death and movement defect in Parkinson's disease model rats. J. Neurochem. 105, 2418–34 (2008).
53. Yamane, K. et al. Oxidative neurodegeneration is prevented by UCP0045037, an allosteric modulator for the reduced form of DJ-1, a wild-type of familial Parkinson's disease-linked PARK7. Int J Mol Sci 10, 4789–804 (2009).
54. Kitamura, Y. et al. Neuroprotective effect of a new DJ-1-binding compound against neurodegeneration in Parkinson's disease and stroke model rats. Mol Neurodegener 6, 48 (2011).
55. Inden, M. et al. Protection against dopaminergic neurodegeneration in Parkinson's disease-model animals by a modulator of the oxidized form of DJ-1, a wild-type of familial Parkinson's disease-linked PARK7. J. Pharmacol. Sci. 117, 189–203 (2011).
56. Kitamura, Y. et al. Neuroprotective effect of a new DJ-1-binding compound against neurodegeneration in Parkinson's disease and stroke model rats. Mol Neurodegener 6, 48 (2011).

Chapter 6

Appendix

This chapter contains results published in the following articles:

Tauber E*, Miller-Fleming L*, Mason RP*, Kwan W, Clapp J, Butler NJ, Outeiro TF, Muchowski PJ and Giorgini F. Functional gene expression profiling in yeast implicates translational dysfunction in mutant huntingtin toxicity. J. Biol. Chem. 2011 Jan 7;286(1):410–9.
* equal contribution

Chapter 6. Appendix

Appendix 2.1. Validation of differentially expressed genes identified via microarray analysis by QPCR

Gene	Fold Change Microarray	Fold Change QPCR	P-value	Expression
AQR1*	-10.22	-2.19	0.002	Down
BAG7*	13.68	2.19	< 0.001	Up
DAK2*	25.27	1.86	< 0.001	Up
HSP26	5.80	0.57	0.102	No change
HXT2	-5.52	1.55	0.008	Up
PHM6	-9.53	1.31	0.676	No change
PHO84	-4.80	1.22	0.261	No change
PRM7	-5.71	-1.31	0.238	No change
SPL2*	-4.74	-1.52	0.021	Down
SRX1*	8.58	2.51	0.001	Up
TMA10*	9.76	2.01	< 0.001	Up
YDR034W-B*	11.72	3.61	0.001	Up
YGR079W	-5.03	1.00	0.964	No change
YLR194C*	15.02	3.07	< 0.001	Up
YOR338W	-6.02	1.54	0.055	No change
YPK2	4.28	1.27	0.223	No change
YPR077C*	4.17	8.73	< 0.001	Up

The majority of DEGs identified by microarray analysis were validated by QPCR (9/17; 53%, indicated by astericks). An additional 3 genes were found to be differentially expressed via QPCR analysis in the same direction as observed by mRNA profiling, but failed to reach statistical significance.

Appendix 2.2. Gene ontology groups significantly upregulated in Htt103Q versus Htt25Q expressing yeast cells

Gene Ontology Group	Count	%	P-value	Enrichment
response to unfolded protein	11	5.0	6.2E-06	6.3
response to stimulus	42	18.9	1.9E-04	1.7
response to stress	31	14.0	2.1E-04	2.0
response to chemical stimulus	27	12.2	2.9E-04	2.1
protein folding	13	5.9	7.8E-04	3.1
ubiquitin cycle	12	5.4	1.7E-03	3.1
cell wall organization and biogenesis	15	6.8	2.1E-03	2.5
protein metabolic process	58	26.1	2.9E-03	1.4
protein ubiquitination	8	3.6	3.0E-03	4.1
cellular macromolecule metabolic process	58	26.1	3.2E-03	1.4
cellular protein metabolic process	55	24.8	6.2E-03	1.4
post-translational protein modification	24	10.8	6.5E-03	1.8
chitin- and beta-glucan-cell wall biogenesis	6	2.7	8.6E-03	4.6
protein modification by small protein conjugation	8	3.6	1.1E-02	3.2
cellular carbohydrate metabolic process	14	6.3	2.2E-02	2.0
catabolic process	23	10.4	2.4E-02	1.6
protein refolding	3	1.4	2.9E-02	10.9
cotranslational protein targeting to membrane	3	1.4	3.5E-02	9.9
hexose metabolic process	8	3.6	3.7E-02	2.5
glucose metabolic process	7	3.2	3.7E-02	2.8
carbohydrate metabolic process	15	6.8	3.9E-02	1.8
signal transduction	14	6.3	4.0E-02	1.8
vacuolar protein catabolic process	3	1.4	4.1E-02	9.1
monosaccharide metabolic process	8	3.6	4.8E-02	2.4

Gene ontology groups determined by the DAVID Functional Annotation tool. Count refers to number of genes within input gene list that fall into the specified GO group. % denotes what percentage of the total input genes analysed fall within the specific GO group. P-value represents the threshold of EASE Score, a modified Fisher Exact P-value, for gene-enrichment analysis. Enrichment category denotes the overall enrichment of the particular GO group over background.

Appendix 2.3. Gene ontology groups significantly downregulated in Htt103Q versus Htt25Q expressing expressing yeast cells

Gene Ontology Group	Count	%	P-value	Enrichment
ribosome biogenesis and assembly	74	31.2	7.5E-40	5.9
ribonucleoprotein complex biogenesis	75	31.7	3.6E-35	5.0
rRNA metabolic process	42	17.7	2.2E-21	5.9
rRNA processing	41	17.3	5.1E-21	6.0
RNA processing	54	22.8	6.9E-16	3.3
organelle organization and biogenesis	95	40.1	5.0E-13	1.9
ribosomal large subunit biogenesis and assembly	19	8.0	2.2E-12	8.5
RNA metabolic process	73	30.8	6.4E-08	1.8
ribosome assembly	14	5.9	2.9E-07	6.1
maturation of 5.8S rRNA from tricistronic rRNA	10	4.2	1.0E-06	8.8
maturation of SSU-rRNA from tricistronic rRNA	11	4.6	1.2E-06	7.4
maturation of SSU-rRNA	12	5.1	1.5E-06	6.4
maturation of 5.8S rRNA	10	4.2	1.7E-06	8.3
cellular component organization and biogenesis	109	46.0	8.2E-06	1.4
ribosomal large subunit assembly	9	3.8	7.1E-05	6.2
ribosomal subunit assembly	10	4.2	1.2E-04	5.1
protein-RNA complex assembly	15	6.3	3.7E-04	3.0
cleavages during rRNA processing	6	2.5	5.8E-04	8.3
nucleobase, nucleoside, nucleotide metabolism	85	35.9	8.2E-04	1.3
maturation of LSU-rRNA	5	2.1	1.0E-03	10.4
gene expression	73	30.8	1.1E-03	1.4
endonucleolytic cleavage mature 5'-end of SSU-rRNA	5	2.1	2.8E-03	8.1
establishment of organelle localization	8	3.4	3.4E-03	4.0
endonucleolytic cleavage of tricistronic rRNA	5	2.1	3.5E-03	7.6
RNA modification	9	3.8	3.5E-03	3.5
transcription from RNA polymerase I promoter	6	2.5	6.3E-03	5.0
positive regulation of RNA pol I transcription	3	1.3	6.7E-03	21.8
tRNA processing	10	4.2	6.9E-03	2.9
processing of 27S pre-rRNA	4	1.7	8.8E-03	8.9
biopolymer metabolic process	96	40.5	9.4E-03	1.2
tRNA modification	7	3.0	1.2E-02	3.6
tRNA methylation	4	1.7	1.3E-02	7.7
biopolymer methylation	6	2.5	1.5E-02	4.0
ribosome export from nucleus	5	2.1	1.8E-02	4.8
endonucleolytic cleavage 5'-ETS of tricistronic rRNA	4	1.7	1.9E-02	6.8
RNA methylation	4	1.7	2.2E-02	6.4
tRNA metabolic process	11	4.6	3.0E-02	2.2
organelle localization	8	3.4	3.2E-02	2.6

Gene ontology groups determined by the DAVID Functional Annotation tool. Count refers to number of genes within input gene list that fall into the specified GO group. % denotes what percentage of the total input genes analysed fall within the specific GO group. P-value represents the threshold of EASE Score, a modified Fisher Exact P-value, for gene-enrichment analysis. Enrichment category denotes the overall enrichment of the particular GO group over background.

Appendix 2.4. Gene ontology groups significantly differentially expressed in bna4Δ Htt103Q-expressing yeast versus wild-type Htt103Q expressing cell

Gene Ontology Group	Count	%	P-value	Enrichment
carboxylic acid metabolic process	23	11.7	2.6E-05	2.7
translational elongation	8	4.1	3.1E-04	6.0
amino acid catabolic process	6	3.1	3.2E-04	9.6
nitrogen compound metabolic process	18	9.2	3.3E-04	2.6
amino acid and derivative metabolism	16	8.2	3.6E-04	2.9
organic acid transport	8	4.1	4.1E-04	5.7
amine catabolic process	6	3.1	5.9E-04	8.5
amino acid metabolic process	15	7.7	6.0E-04	2.9
amine metabolic process	16	8.2	1.1E-03	2.6
carboxylic acid transport	7	3.6	2.2E-03	5.1
glutamine family amino acid metabolism	6	3.1	6.4E-03	5.0
monocarboxylic acid metabolic process	10	5.1	6.5E-03	2.9
biopolymer biosynthetic process	8	4.1	8.6E-03	3.4
water-soluble vitamin metabolic process	7	3.6	2.2E-02	3.2
water-soluble vitamin biosynthesis	5	2.6	3.1E-02	4.2
alcohol metabolic process	10	5.1	3.2E-02	2.2
urea cycle intermediate metabolism	3	1.5	3.9E-02	9.3
sterol transport	3	1.5	3.9E-02	9.3
arginine metabolic process	3	1.5	3.9E-02	9.3
tyrosine catabolic process	2	1.0	4.2E-02	46.5
L-phenylalanine catabolic process	2	1.0	4.2E-02	46.5
vesicle organization and biogenesis	3	1.5	4.4E-02	8.7
cellular biosynthetic process	27	13.8	4.5E-02	1.4
catabolic process	18	9.2	4.7E-02	1.6

Gene ontology groups determined by the DAVID Functional Annotation tool. Count refers to number of genes within input gene list that fall into the specified GO group. % denotes what percentage of the total input genes analysed fall within the specific GO group. P-value represents the threshold of EASE Score, a modified Fisher Exact P-value, for gene-enrichment analysis. Enrichment category denotes the overall enrichment of the particular GO group over background.

Appendix 2.5. Gene ontology groups significantly differentially expressed in mbf1Δ Htt103Q-expressing yeast versus wild-type Htt103Q expressing cells

Gene Ontology Group	Count	%	P-value	Enrichment
amino acid metabolic process	28	14.0	2.7E-12	5.0
nitrogen compound metabolic process	29	14.5	2.4E-10	4.0
lysine metabolic process	8	4.0	3.1E-10	34.7
lysine biosynthetic process via aminoadipic acid	7	3.5	3.4E-09	38.0
carboxylic acid metabolic process	30	15.0	1.2E-08	3.3
aspartate family amino acid biosynthesis	10	5.0	3.0E-07	10.3
aspartate family amino acid metabolic process	11	5.5	6.5E-07	8.1
amine biosynthetic process	16	8.0	1.6E-06	4.5
amine catabolic process	8	4.0	7.1E-06	12.0
urea cycle intermediate metabolic process	6	3.0	1.4E-05	17.4
nonprotein amino acid metabolic process	5	2.5	4.9E-05	21.7
glutamine family amino acid metabolic process	8	4.0	2.5E-04	6.2
ornithine metabolic process	4	2.0	3.8E-04	24.8
cellular biosynthetic process	36	18.0	4.1E-04	1.8
arginine biosynthetic process	4	2.0	1.2E-03	17.4
translational elongation	7	3.5	2.7E-03	4.9
carboxylic acid transport	7	3.5	3.2E-03	4.7
serine family amino acid catabolic process	3	1.5	7.3E-03	21.7
amine transport	6	3.0	8.0E-03	4.7
serine family amino acid metabolic process	5	2.5	1.5E-02	5.2
glutamine family amino acid catabolic process	3	1.5	2.1E-02	13.0
glycine metabolic process	3	1.5	2.1E-02	13.0
amino acid transport	5	2.5	2.2E-02	4.6
biosynthetic process	37	18.5	2.3E-02	1.4
polyamine transport	3	1.5	2.9E-02	10.8
glutamine family amino acid biosynthesis	4	2.0	3.3E-02	5.6
biopolymer biosynthetic process	7	3.5	3.9E-02	2.8
tyrosine catabolic process	2	1.0	4.5E-02	43.4
L-phenylalanine catabolic process	2	1.0	4.5E-02	43.4
arginine catabolic process	2	1.0	4.5E-02	43.4
Translation	17	8.5	4.9E-02	1.6

Gene ontology groups determined by the DAVID Functional Annotation tool. Count refers to number of genes within input gene list that fall into the specified GO group. % denotes what percentage of the total input genes analysed fall within the specific GO group. P-value represents the threshold of EASE Score, a modified Fisher Exact P-value, for gene-enrichment analysis. Enrichment category denotes the overall enrichment of the particular GO group over background.

Appendix 2.6. Gene ontology groups significantly differentially expressed in ume1Δ Htt103Q-expressing yeast versus wild-type Htt103Q expressing cells

Gene Ontology Group	Count	%	P-value	Enrichment
water-soluble vitamin biosynthetic process	8	4.0	1.2E-03	4.8
NAD biosynthetic process	4	2.0	1.9E-03	14.8
nitrogen compound metabolic process	20	10.1	2.6E-03	2.1
monocarboxylic acid metabolic process	13	6.5	2.6E-03	2.7
response to pheromone	10	5.0	3.9E-03	3.2
G-protein coupled receptor protein signaling	6	3.0	5.0E-03	5.3
response to chemical stimulus	25	12.6	5.2E-03	1.8
pyridine nucleotide biosynthetic process	4	2.0	7.4E-03	9.5
response to pheromone / conjugation	7	3.5	8.5E-03	3.9
regulation of catalytic activity	7	3.5	8.5E-03	3.9
water-soluble vitamin metabolic process	9	4.5	1.1E-02	2.9
signal transduction during conjugation	5	2.5	1.1E-02	5.6
carboxylic acid transport	7	3.5	1.2E-02	3.6
ammonium transport	3	1.5	1.2E-02	16.7
glutamate metabolic process	4	2.0	1.3E-02	7.8
regulation of conjugation with cellular fusion	5	2.5	1.4E-02	5.2
carboxylic acid metabolic process	21	10.6	1.5E-02	1.7
regulation of cyclin-dependent protein kinases	4	2.0	1.5E-02	7.4
Transport	49	24.6	1.6E-02	1.3
amine transport	6	3.0	2.3E-02	3.6
Localization	50	25.1	2.4E-02	1.3
amine metabolic process	16	8.0	2.5E-02	1.8
NAD metabolic process	4	2.0	2.6E-02	6.1
cell surface receptor linked signal transduction	6	3.0	2.7E-02	3.5
tricarboxylic acid cycle metabolism	4	2.0	3.0E-02	5.8
conjugation with cellular fusion	9	4.5	3.4E-02	2.4
glyoxylate cycle	3	1.5	3.4E-02	10.0
response to unfolded protein	6	3.0	3.9E-02	3.2
glyoxylate metabolic process	3	1.5	4.1E-02	9.1

Gene ontology groups determined by the DAVID Functional Annotation tool. Count refers to number of genes within input gene list that fall into the specified GO group. % denotes what percentage of the total input genes analysed fall within the specific GO group. P-value represents the threshold of EASE Score, a modified Fisher Exact p-value, for gene-enrichment analysis. Enrichment category denotes the overall enrichment of the particular GO group over background.

Appendix 2.7. Validation of differentially expressed genes identified via microarray analysis in suppressor strains by QPCR.

	*bna4*Δ103Q vs WT103Q			*mbf1*Δ103Q vs WT103Q			*ume1*Δ103Q vs WT103Q		
Gene	Microarray	Fold Change	P-value	Microarray	Fold Change	P-value	Microarray	Fold Change	P-value
AQR1	Up*	7.86	<0.001	Up	-3.04	0.088	Up*	2.216	0.002
DAK2	Down	1.984	0.097	Down*	-2.72	0.024	Down	1.606	0.01
YGR035C	Up*	6.543	0.008	Up†	3.087	0.197	Up*	5.044	<0.001
YMC2	Up†	1.974	0.099	Up*	2.83	0.031	Up*	4.31	<0.001

Four DEGs (*AQR1*, *DAK2*, *YGR035C*, and *YMC2*) that were identified by microarray comparison of the three deletion suppressor strains (*bna4*Δ *mbf1*Δ *ume1*Δ expressing Htt103Q versus WT expressing Htt103Q were validated by QPCR. Of the 12 comparisons, 7 were significantly confirmed by QPCR analysis (7/12; 58%, indicated by astericks). An additional 2 genes were found to be differentially expressed via QPCR analysis in the same direction as observed by mRNA profiling, but failed to reach statistical significance (indicated by †). Fold changes and P-values refer to QPCR data.

Appendix 3.1. Validation of microarrays by real-time quantitative PCR

	***hsp31Δ* vs WT**			***hsp32Δ* vs WT**			***hsp33Δ* vs WT**		
	Microarrays	**qPCR**		**Microarrays**	**qPCR**		**Microarrays**	**qPCR**	
	Fold-change	**Fold-change**	***p*-value**	**Fold-change**	**Fold-change**	***p*-value**	**Fold-change**	**Fold-change**	***p*-value**
SOL4	0.14	0.13	0.02	0.04	0.07	0.02	0.12	0.09	0.02
SSA3	0.12	0.11	0.00	0.14	0.11	0.01	0.12	0.10	0.01
GTT1	0.24	0.18	0.00	0.08	0.08	0.01	0.15	0.15	0.01
TRX3	0.42	0.48	0.03	0.41	0.37	0.01	0.33	0.35	0.01
OM45	n.c.	0.24	0.01	0.26	0.09	0.01	0.36	0.16	0.00
POT1	0.15	0.20	0.01	0.04	0.05	0.02	0.08	0.07	0.01
HXK2	5.46	7.31	0.00	6.08	6.58	0.00	6.66	20.23	0.12
MIG2	6.49	4.50	0.26	8.38	2.84	0.00	7.94	6.27	0.29
HXT4	5.74	9.10	0.02	5.70	5.94	0.01	4.97	7.80	0.01
RPS24A	2.91	3.02	0.00	3.42	3.77	0.05	3.02	1.90	0.03
HEM13	n.c.	6.73	0.01	7.25	25.21	n.s.	4.43	7.42	n.s.

11 DEGs found in both the gene expression microarrays of *hsp32*Δ and *hsp33*Δ strains were validated by QPCR. Among these 11 genes, 9 were also differentially expressed in *hsp31*Δ cells. The table indicates the fold change obtained by microarray and QPCR analyses. In addition, it shows the standard deviation and p-value obtained by QPCR. (n.c. – genes that were not changed and n.s. – statistically not significant)

Appendix 3.2. Gene ontology groups significantly upregulated in *hsp31*Δ, *hsp32*Δ and *hsp33*Δ vs wild-type cells

	No. of genes		Frequency (%)					
Gene ontology process	**List**	**Genome**	**List**	**Genome**	**Total DEG**	**Pop Total**	**p-value**	**Benjamini**
Translation and ribosomal biogenesis								
endonucleolytic cleavage of tricistronic rRNA transcript	7	38	5,00	0,78	127	4870	0,000	0,013
rRNA export from nucleus	8	42	5,71	0,86	127	4870	0,000	0,003
maturation of 5.8S rRNA from tricistronic rRNA transcript	8	69	5,71	1,42	127	4870	0,002	0,045
ribosome assembly	11	69	7,86	1,42	127	4870	0,000	0,001
ribonucleoprotein complex assembly	11	117	7,86	2,40	127	4870	0,001	0,022
maturation of SSU-rRNA from tricistronic rRNA transcript	15	83	10,71	1,70	127	4870	0,000	0,000
regulation of translation	18	180	12,86	3,70	127	4870	0,000	0,000
rRNA processing	21	239	15,00	4,91	127	4870	0,000	0,000
ribosomal subunit assembly	23	335	16,43	6,88	127	4870	0,000	0,002
ncRNA metabolic process	26	393	18,57	8,07	127	4870	0,000	0,001
ribosome biogenesis	38	351	27,14	7,21	127	4870	0,000	0,000
translation	60	677	42,86	13,90	127	4870	0,000	0,000
Cellular metabolic processes								
cellular amino acid biosynthetic process	11	134	7,86	2,75	127	4870	0,002	0,050
organic acid biosynthetic process	14	172	10,00	3,53	127	4870	0,000	0,015
sulfur amino acid metabolic process	7	47	5,00	0,97	127	4870	0,001	0,031
ergosterol biosynthetic process	6	24	4,29	0,49	127	4870	0,000	0,012

Number of overlapping genes that have a known ontology term associated - downregulated: 286; upregulated: 127

Number of yeast genes with an ontology term associated - 4870

Appendix 3.3. Gene ontology groups significantly downregulated in *hsp31*Δ, *hsp32*Δ and *hsp33*Δ vs wild-type cells

	No. of genes		Frequency (%)					
Gene ontology process	**List**	**Genome**	**List**	**Genome**	**Total DEG**	**Pop Total**	**p-value**	**Benjamini**
Stress response								
response to temperature stimulus	65	217	17,71	4,46	286	4870	0,000	0,000
response to abiotic stimulus	74	344	20,16	7,06	286	4870	0,000	0,000
response to oxidative stress	25	82	6,81	1,68	286	4870	0,000	0,000
cellular response to stress	66	562	17,98	11,54	286	4870	0,000	0,000
Aerobic respiration								
aerobic respiration	15	102	4,09	2,09	286	4870	0,002	0,047
tricarboxylic acid cycle	9	30	2,45	0,62	286	4870	0,000	0,006
acetyl-CoA metabolic process	10	34	2,72	0,70	286	4870	0,000	0,003
coenzyme metabolic process	25	149	6,81	3,06	286	4870	0,000	0,000
Cellular metabolic processes								
glycogen biosynthetic process	6	12	1,63	0,25	286	4870	0,000	0,010
generation of precursor metabolites and energy	42	264	11,44	5,42	286	4870	0,000	0,000
oxidation reduction	57	353	15,53	7,25	286	4870	0,000	0,000
disaccharide metabolic process	7	24	1,91	0,49	286	4870	0,002	0,046
trehalose metabolic process (biosynthesis)	7	11	1,91	0,23	286	4870	0,000	0,001
glycoside metabolic process	7	12	1,91	0,25	286	4870	0,000	0,001
glucose metabolic process	22	100	5,99	2,05	286	4870	0,000	0,000
hexose metabolic process	26	122	7,08	2,51	286	4870	0,000	0,000
pentose metabolic process	8	19	2,18	0,39	286	4870	0,000	0,002
monosaccharide metabolic process	30	136	8,17	2,79	286	4870	0,000	0,000
alcohol catabolic process	18	65	4,90	1,33	286	4870	0,000	0,000
energy reserve metabolic process	13	42	3,54	0,86	286	4870	0,000	0,000
carbohydrate biosynthetic process	17	94	4,63	1,93	286	4870	0,000	0,003
carbohydrate catabolic process	25	84	6,81	1,72	286	4870	0,000	0,000
Others								
vacuolar protein catabolic process	54	117	14,71	2,40	286	4870	0,000	0,000
autophagy	20	143	5,45	2,94	286	4870	0,001	0,015
ascospore formation/sexual sporulation	16	113	4,36	2,32	286	4870	0,002	0,047

Appendix 3.4. Genotypes of the strains used in this study

Strain	Genotype	Reference
BY4741	MATa his3Δ0 leu2Δ0 met15Δ0 ura3Δ0	Open Biosystems
BY4742	MATα his3Δ1 leu2Δ0 lys2Δ0 ura3Δ0	Open Biosystems
*hsp32*Δ 2n	MATas3Δ1 leu2Δ0 ura3Δ0 lys2Δ0/*LYS2* met15Δ0/*MET15* can1Δ::*LEU2*-MFA1pr-HIS3/CAN1+ *hsp32*::URA3MX/*HSP32*	Open Biosystems
*hsp31*Δ	MATa his3Δ1 leu2Δ0 met15Δ0 ura3Δ0 *hsp31*::kanMX4	Marek Skoneczny lab
*hsp32*Δ	MATa ura3Δ0 leu2Δ0 his3Δ1 lys2Δ0 met15Δ0 can1Δ::*LEU2*+-MFA1pr-*HIS3 hsp32*::*URA3*MX	This study
*hsp33*Δ	MATα his3Δ1 leu2Δ0 lys2Δ0 ura3Δ0 *hsp33*::NatMX	This study
*hsp34*Δ	MATα his3Δ1 leu2Δ0 lys2Δ0 ura3Δ0 *hsp34*::HygMX	This study
Lx Wild-type	MATa ura3Δ0 leu2Δ0 lys2Δ0 his3Δ1 can1Δ::*LEU2*-MFA1pr-*HIS3*	This study
Lx1 (*hsp31*Δ)	MATa his3Δ1 leu2Δ0 lys2Δ0 ura3Δ0 can1Δ::*LEU2*-MFA1pr-*HIS3* *hsp31*::kanMX4	This study
Lx2 (*hsp32*Δ)	MATa his3Δ1 leu2Δ0 lys2Δ0 ura3Δ0 can1Δ::*LEU2*-MFA1pr-*HIS3* *hsp32*::URA3MX	This study
Lx3 (*hsp33*Δ)	MATα his3Δ1 leu2Δ0 lys2Δ0 met15Δ ura3Δ0 can1Δ::*LEU2*-MFA1pr-*HIS3* *hsp33*::NatMX	This study
Lx4 (*hsp34*Δ)	MATa his3Δ1 leu2Δ0 lys2Δ0 ura3Δ0 can1Δ::*LEU2*-MFA1pr-*HIS3* *hsp34*::HygMX	This study
*gis1*Δ	MATa his3Δ0 leu2Δ0 met15Δ0 ura3Δ0 gis1::kanMX4	Open Biosystems
*sod1*Δ	MATa his3Δ0 leu2Δ0 met15Δ0 ura3Δ0 sod1::kanMX4	Open Biosystems
*yap1*Δ	MATa his3Δ0 leu2Δ0 met15Δ0 ura3Δ0 yap1::kanMX4	Open Biosystems

Appendix 3.5. Primers used in this study

Primer	Forward sequence (5' to 3')	Reverse sequence (5' to 3')	Comments
HSP33 flanking regions	ACACTTTTCTCCTTCATTCAAAAAG AAAACTGGCCTTGCACGTACGCTG CAGGTCGAC	CATTAGAAGCCTCCCCTTCAACAAT TCCCTTGTCTTTTGTTATCGATGAA TTCGAGCTCG	Excision of *HSP33* or *HSP34*
GIS1	TAACACCTCTGCAGCCGCATCTAT	TTGTCATCGTTATCGCCGCCTAGA	QPCR
HSP31	ATCTGCAGGCCACGGTACCTTATT	TGCGACAACACCACCGTTAGCATA	QPCR
HSP32	TTTTGCGGTCGTTCGATACT	GGTCCATGACAGATGGCA	QPCR
HSP33	ATTTTGCGATCGTTCGATACA	GGTCCATGACAGATGGCA	QPCR
TAF10	ATATTCCAGGATCAGGTCTTCCGTA GC	GTAGTCTTCTCATTCTGTTGATGTT GTTGTTG	QPCR – control
UBC6	AGCAGGCTCACAAGAGATTGACGA	TACCGTGATATTGACCGCCCTTGT	QPCR – control
GTT1	TGGCAGACAAGATCAGTCAGGCAT	CCTCTGGTGCGGCAAACTTTCTTT	QPCR - validate microarrays
HEM13	AAACTTGGTGGTTTGGTGGTGGTG	GCATCCTTGTGCAGTTGGTGGAAT	QPCR - validate microarrays
HXK2	GGCCGATGTGCCAAAGGAATTGAT	TACCACCCTTCTTGGACAAACCCT	QPCR - validate microarrays
HXT4	TAGGTCTAGGTTTCGCTTGGGCTT	TGGATCGTCTGCGCTGACCTTATT	QPCR - validate microarrays
MIG2	CATTCATGCCTCCGCTGCATCTTT	TTGGCACAGAGCGTGGAGTGTTTA	QPCR - validate microarrays
OM45	AAACAGCCGCTCAACTTTCCAAGG	ACTGTTTCAAGTCCTCCTTCGCCT	QPCR - validate microarrays

POT1	CTTTCAAGCATCAGGCCTGCCTTT	AGCGACCTAGCACAGGCAGATTTA	QPCR - validate microarrays
RPS24A	TGTTGGCCAGAAAGCAATTCGTCG	ACCGAAACCAACAGACTTACCACC	QPCR - validate microarrays
SOL4	AGGATCGATGAACCAAGCGCTGTA	AATTGGTTGCCCTGATGCACTAGC	QPCR - validate microarrays
SSA3	TTGCTTATGGTGCAGCCGTTCAAG	TATGCCGCCTGCAGTTTCAATTCC	QPCR - validate microarrays
TRX3	TTGTCAAGTGCGACGTGGACGAAT	GCCATCCTTGCCAAGAACAAAGGT	QPCR - validate microarrays
HSP32/33 R		CATGGTGCAACGTGGTAAAA	Verify cassette integration
HSP32/33 /34 F	AAGATGGTGCGAAAACAGGC		Verify cassette integration
HSP34 R		GTAGAGACTCAAGAATGTCG	Verify cassette integration
MX4 F	TGGTCGCTATACTGCTGTCG		Verify cassette integration